The Geochemistry and Textures of the Grevillea Gossan, Northwest Queensland

Veryan Hann
Bachelor of Science

UNIVERSITY OF TASMANIA

A research thesis submitted in partial fulfilment for the requirements of the Degree of Bachelor of Science with Honours

CODES SRC

Centre for Ore Deposits and Exploration Studies
School of Earth Sciences, University of Tasmania
December, 1999

Notice in foreground the excellent 'termite's impression of the gossan'.

To my artistic family I would like to comment;

There cannot be art without fact ,
As there cannot be science without imagination.

Abstract

The Grevillea deposit is a newly discovered Pb-Zn-Ag stratabound sediment-hosted deposit in the Lawn Hill Region of NNW Queensland. It lies in part of the Mount Isa Inlier which has been described as one of the richest mineral provinces in the world.

The study undertook varied geochemical analyses for determining element variations and the relationships, and elemental partitions in the regolith units. It was found that Tl, Pb, Si, Fe are surface indicators of mineralisation for the Grevillea deposit. Two types of rock units dominated the regolith, which overlies the massive pyrite zone: the jarosite limonites and the hematite limonites, and both act as sponges for metals derived from the ore. The jarosite types in the area are likely plumbojarosite and argentojarosite.

Textures were also studied in outcrop, on a handspecimen scale, and on microscopic scales to search for evidence of primary sulfides. Sections of ore sample were studied and some links were made to surface textures. These included sedimentary features, bladed and platey hematite, and framboidal structures. Light rare earth minerals (monazites) in the core were an unexpected unusual find as they are not normally associated with sedex style deposits. The monazites may have useful application in dating the deposit or gossan formation.

Contents

List of Figures

List of Tables

List of Plates

Acknowledgements

I would like to thank Dr Peter McGoldrick my supervisor for practical advice, direction and patience, throughout the year.

North Limited have supported this project and I am appreciative of the exploration mining camp experience, and being able to do all the analyses I have done for the project.
Thank you to my family and partner for support, Dad for buying me a fancy colour printer, and most recently, Cherie, Kev and Paul for being wonderful practical friends in times of panic.

I would also like to acknowledge some of the geology/CODES staff, including Simon Stephens for patience and teaching me how to make thin sections, Dr David Steele for ideas, conversation and technical help on the ESEM, Kathi Stait for her assistance, Peter Cornish for packing everything for the field trip, Andrew Rae and Dr Graham Rowbottom for help with FTIR analyses, Dr Dave Cooke for a mid-year pep talk and Steve Bodon for computer support.

Chapter 1 Introduction

1.1 Introduction

Gossans are the conspicuous surface expression of sulfide mineralisation at depth, and are a special case in regolith formation over an oxidising sulfide ore. Interpretation of leached outcrop has been used, since ancient times, in the search for base-metal sulfide deposits.

Prominent gossan formation is favoured particularly in arid terrains (Blanchard, 1968). Weathering of a base-metal sulfide body produces a gossan peculiar to the composition of the parent ore, and as a function of the conditions during weathering. Gossanous product can be summarised as an oxidised, hydrated mixture of impure hematite, goethite, jarosite and silica.. The term gossan is derived from the Cornish term for wig, as a gossan forms an identifiable cap over sulfide mineralisation.

The Grevillea Gossan outcrops approximately 250 km NNW of Mount Isa, [lat 19 34′ S, long 138 34′ N], northwest Queensland, in the Lawn Hill region.. The position of the Lawn Hill Region within the Mount Isa Inlier is highlighted in figures 1.1. The gossan was recognised following stream geochemistry surveying in 1993. Subsequent drilling revealed significant a Pb-Zn-Ba-Ag sulfide deposit beneath the gossan (Jenkins et al., 1998).

1.2 Aim

The aims of this study are to:

- Document the mineralogy, geochemistry and textures of the surface rocks in the vicinity of the gossan, comparing with core sections where available.
- Investigate geochemical/mineralogical/textural trends from primary sulfide through to the gossan and also the secondary dispersion at surface.
- To use this information to constrain likely gossan forming processes, and conditions of formation of the gossan.
- To propose a model for the evolution of the gossan

Regional Distribution of Major Tectonic Units

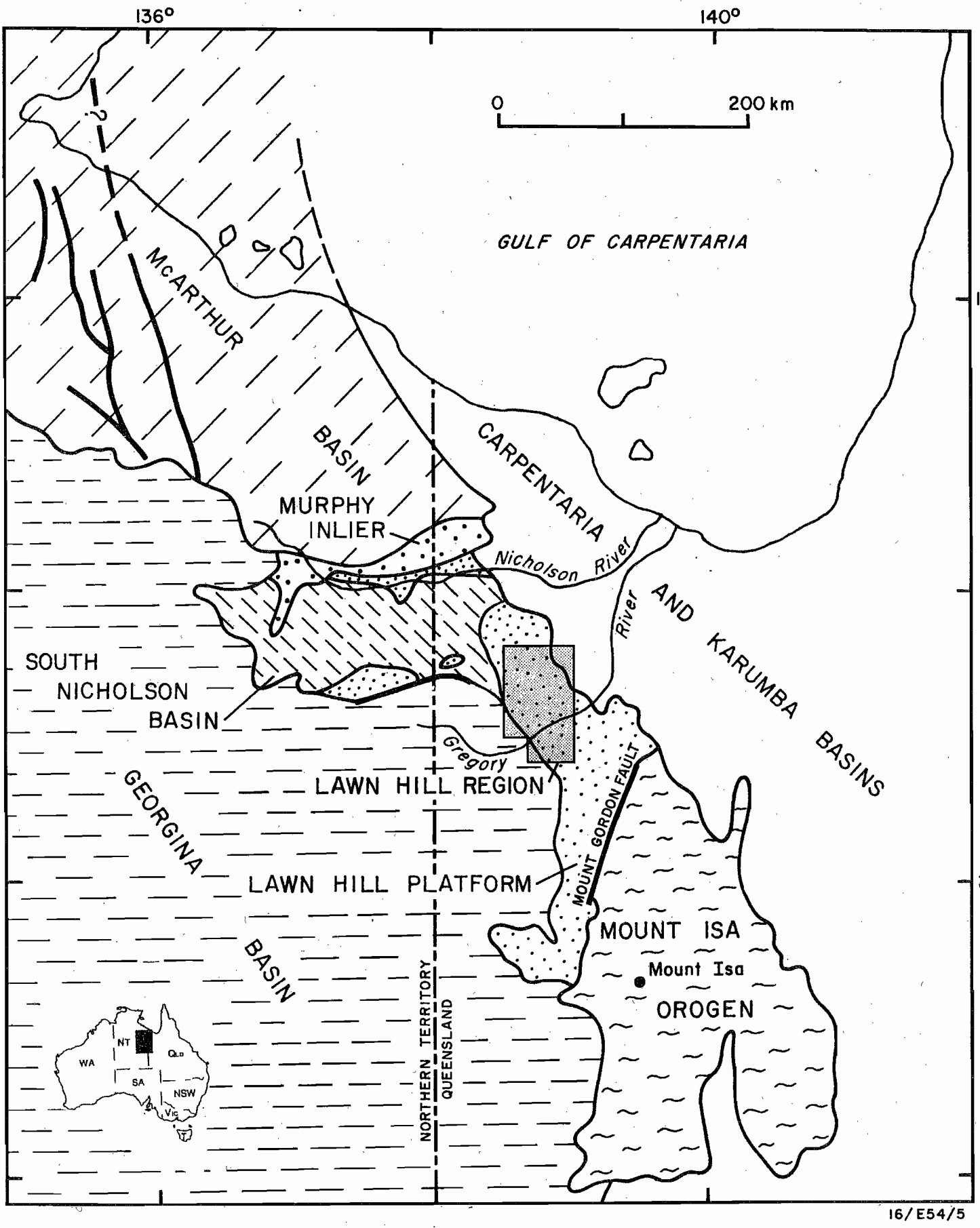

Figure 1.1 Position of the Lawn Hill Region in the Mount Isa Inlier. (Inset shows position in Australia) (after Sweet and Hutton, 1982).

1.3 Methodology

- Mapping of an area including all parts of the outcropping gossan (250x350m) to produce a 1:1000 map, and a 1:200 and 1:100 map of the main gossanous outcrops. Mapping was referenced to the local Terra Search grid (055mN), a 50x50m grid monumented by stakes. The grid positions have been named by the differential GPS file names (Global Positioning System) and used as site reference points despite the GPS data being omitted. These reference points have labels RDXX where XX is a number.
- Two cross-sections intersecting the massive sulfide zone were made using drillhole data and surfaces transects, and were compiled at 1:500.
- Various techniques (ESEM, XRD, ICP-MS, XRF, Electron Microprobe and PIMA) were used to investigate the mineralogy, geochemistry and microscopic texture of ke samples (these were selected on the basis of mapping classification).

Chapter 2 Geology of the Grevillea Area

2.1 Geological Setting

The Riversleigh Siltstone member of the McNamara Group hosts the Grevillea Deposit. The Riversleigh Siltstone is dominantly a quartzose, dolomitic and carbonaceous siltstone with minor sandstone.

The Grevillea Deposit is part of late Paleoproterozoic sag-phase sediments of the Western Succession of the Mount Isa Inlier. The Inlier is part of a diverse and 'globally significant base-metals dominated minerals province' (Williams, 1998). These rocks host numerous sedex deposits including Century and Lady Loretta of the McNamara Group and Mount Isa Hilton and George Fisher of the Mount Isa Group. The stratigraphy of the McNamara Group is shown in figure 2.1. The McNamara Group is estimated to span 1660-1595 6 Ma based on recent SHRIMP dating. The lower age is based on tuff beds in the Mount Isa Group, and the upper age is calculated b tuffs in the Lawn Hill Formation (Sweet and Hutton, 1998).

The Grevillea Deposit occurs in the lower 300+m of the Riversleigh Siltstone and the transition from Shady Bore Quartzite to Riversleigh Siltstone occurs just out of the field area about 400m to the east. The lower Riversleigh Siltstone passes from a dominantl sandy unit to dolomitic shales and carbonaceous siltstones to the northeast. The calcareous and carbonaceous siltstones form the host to the deposit, and the deposit is estimated to be between 200-800m thick (see figure 2.2 showing the stratigraphy of Grevillea sulfide body). This sequence is followed by a fine grained sandstone package less than 100m thick towards the northwest in the hanging wall of the deposit (Jenkins, *et al,* 1998).

2.2 Structure – Nature of Folding and Faulting

Structurally, the folding in the Lawn Hill Platform is strong but open, and faulting is predominantly northeast and less commonly northwest (Blake, 1987). Regionally dome and basin structures dominate the Riversleigh area. The Shady Bore Quartzite to the northeast of the filed area forms a core of one on these structures (Jenkins et al., 1998).

Figure 2.1 Stratigraphy of the McNamara Group.

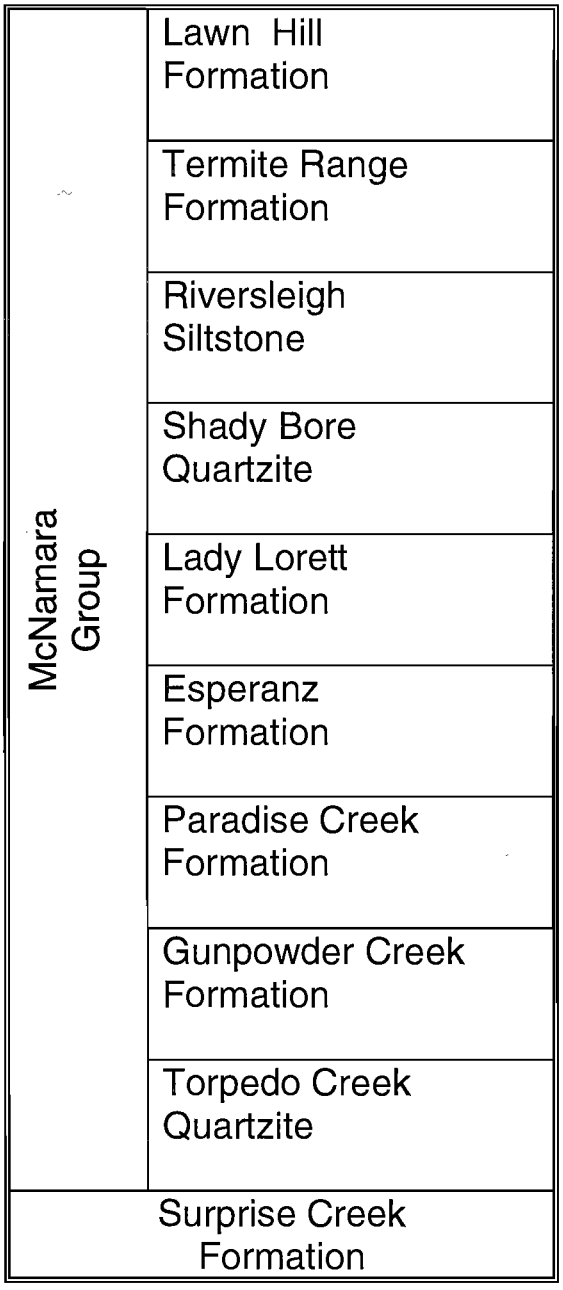

After Sweet & Hutton, 1982

Units of the Lower Riversleigh Siltstone in the Grevillea area with stratigraphy of the sulphide body expanded.

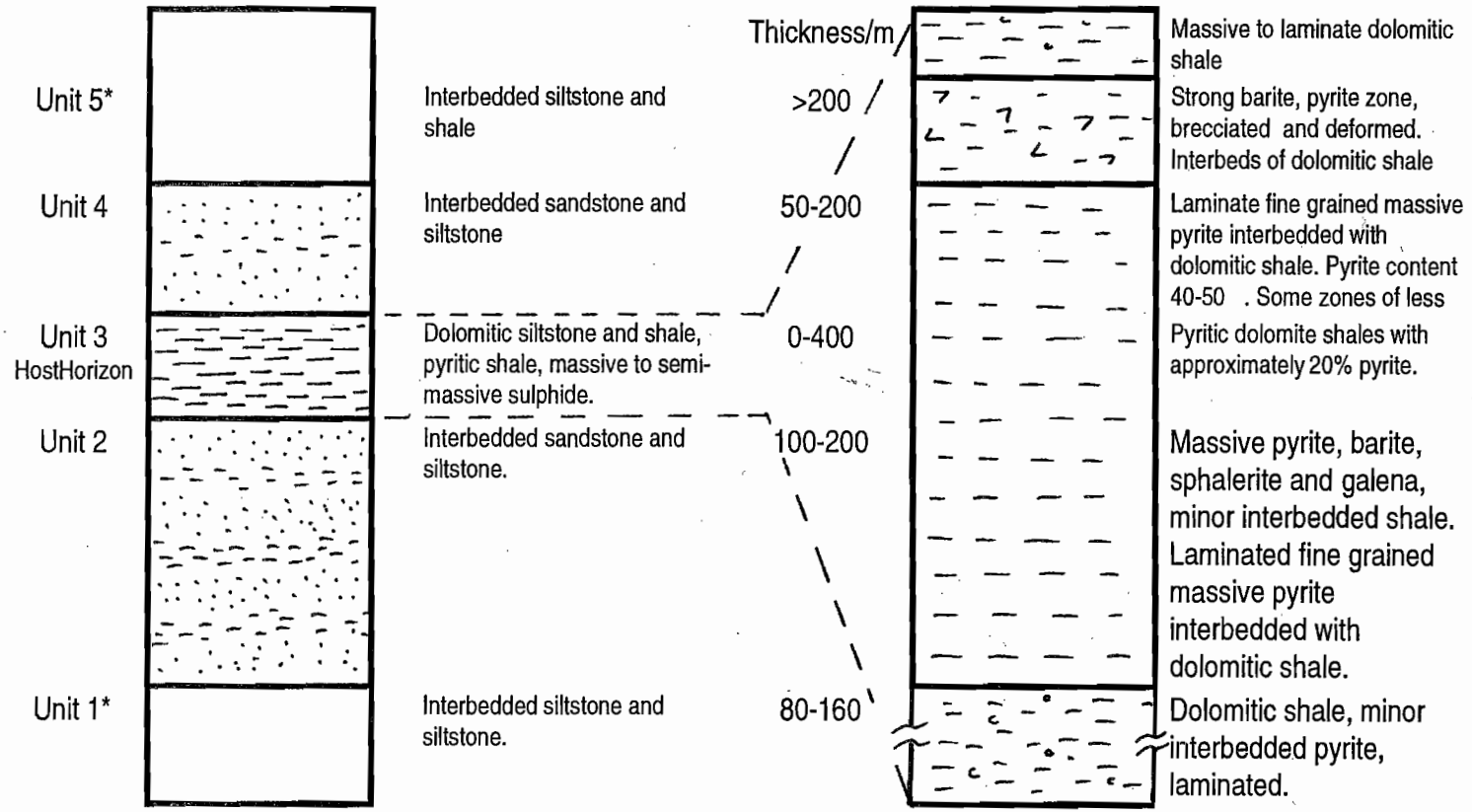

Figure 2.2 Lower Riversleigh Siltstone Stratigraph (After Jenkins et al, 1998)

*** Outside field area**

The mineralisation in the immediate vicinity Grevillea is fault bound. Numerous faults pass though the area. The gossan is offset by two main faults, both trending NE.

Folding appears open and moderately strong in the region occupying Grevillea, evidenced at surface and from core. Surface samples show folding ranging from tens of centimetres to at least two metre wavelength on the northeast end of the southern gossan. More spectacular folds are interpreted as soft sediment deformation due to slumping associated with synsedimentary faulting. Preconsolidational slumping (and plastic flow in the ore horizon) was also noted for the Lady Loretta deposit which is in the same region (L *et al.*, 1975).

2.2.1 Faults:

The outcropping parts of the gossan are offset by about 25m, with this section fault-bound. The covered gossan (northern block) has moved north relative to the ridge by about 80m. The northern and southern bounding fault zones are about 200m apart and all outcropping gossan is within these zones. Part of the northern gossan is offset 25m to the east forms the ridge. The ridge is mainly leached shales and fine-grained sandstones but a narrow 1m bed is gossanous and continuous along strike for at least 10m and is considered a minor part of the gossan.

The north gossan fault offsets the 'north gossan' to the NE by about 70m. The strike direction is indicated by a two metre zone of brecciated siltstones and is about 50°NE. The facies changes sharply from siltstones to sandstones across the fault to the north. The sandstone does not outcrop immediately, and sandy rubble obscures the siltstone and gossanous outcrop. Sandstones and interbedded siltstones outcrop on the hill immediatel to the north (the covered gossan). Siltstones associated with the gossan do not occur north of the 'north gossan fault'. A small gossanous outcrop lies on the fault (northern edge of the ridge) and siltstone beds within this outcrop are displaced by about half a meter. The area has been interpreted by Jenkins *et al* (1998) to be the start of a 200m wide fault zone.

The southern bounding fault is the other major fault, all gossanous material outcrops to the north of this. This is also interpreted to be a narrow shear zone, truncating the mineralisation and being important in the formation of a local depositional basin (Jenkins,

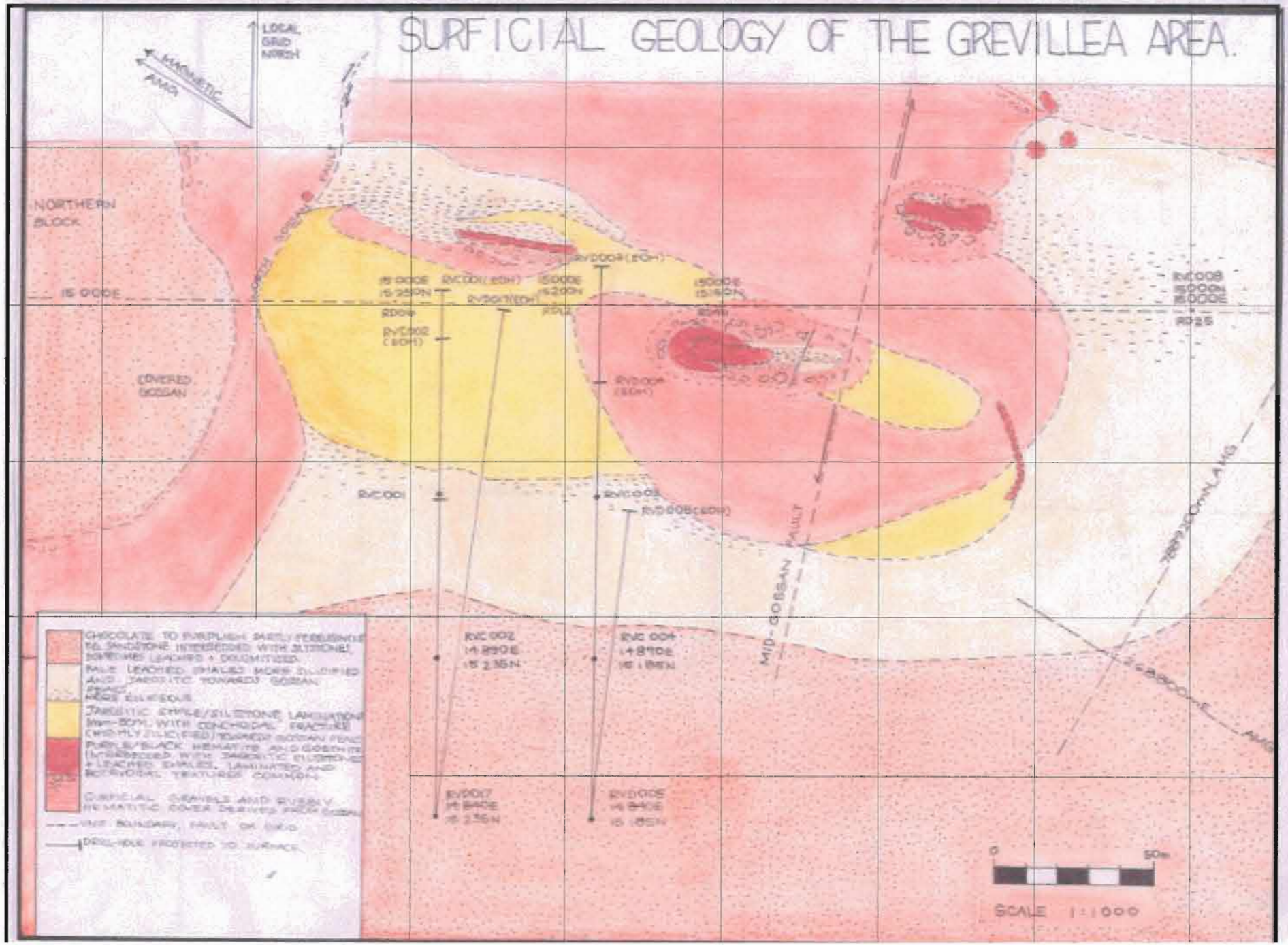
SURFICIAL GEOLOGY OF THE GREVILLEA AREA.
LOCAL GRID NORTH
MAGNETIC AMG
NORTHERN BLOCK
15 000E
COVERED GOSSAN
MID-GOSSAN FAULT
RVC001
RVC002 (EOH)
RVC003 (EOH)
RVC004 (EOH)
RVC005 (EOH)
RVC006 (EOH)
RVC007 (EOH)
RVC008 (EOH)
RVC 002 14 890E 15 235N
RVC 004 14 870E 15 185N
RVC007 14 840E 15 235N
RVC005 14 840E 15 185N
0
50m
SCALE 1:1000

PLATE 2.2

NORTHERN GOSSAN

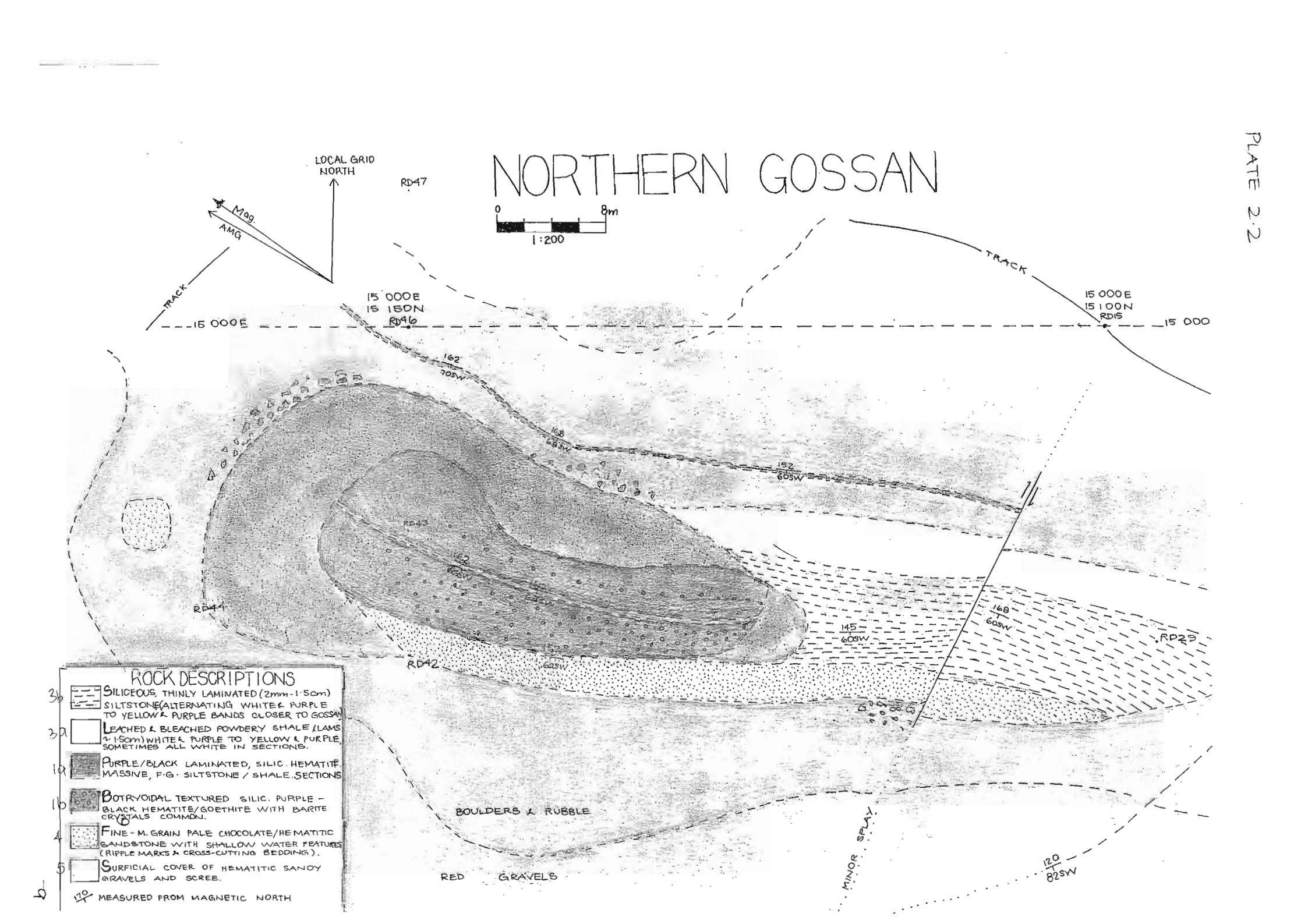

ROCK DESCRIPTIONS

3b SILICEOUS, THINLY LAMINATED (2mm-1·5cm) SILTSTONE/ALTERNATING WHITE & PURPLE TO YELLOW & PURPLE BANDS CLOSER TO GOSSAN

3a LEACHED & BLEACHED POWDERY SHALE/LAMS ~1·5cm) WHITE & PURPLE TO YELLOW & PURPLE, SOMETIMES ALL WHITE IN SECTIONS.

1a PURPLE/BLACK LAMINATED, SILIC. HEMATITE MASSIVE, F·G· SILTSTONE / SHALE SECTIONS

1b BOTRYOIDAL TEXTURED SILIC. PURPLE - BLACK HEMATITE/GOETHITE WITH BARITE CRYSTALS COMMON.

4 FINE - M. GRAIN PALE CHOCOLATE/HEMATITIC SANDSTONE WITH SHALLOW WATER FEATURES (RIPPLE MARKS & CROSS-CUTTING BEDDING).

5 SURFICIAL COVER OF HEMATITIC SANDY GRAVELS AND SCREE.

170 MEASURED FROM MAGNETIC NORTH

PLATE 2.3

SOUTHERN GOSSAN

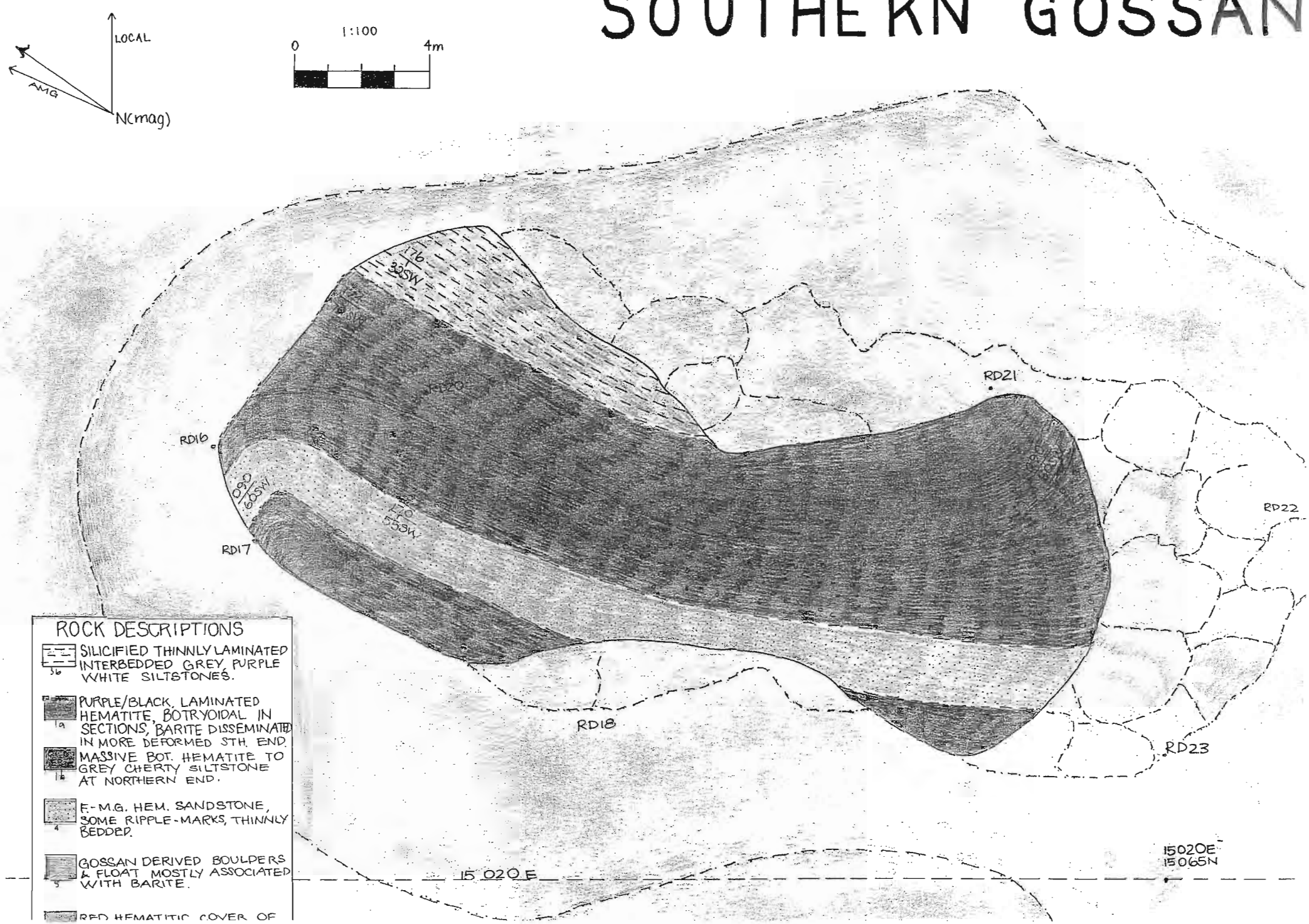

et al., 1998). 'Ironstone' outcrops are displaced in three positions, as seen on the map, and the dominant fracture set or cleavage direction is 120/82S, the other two are 172/42SW and 146/85SW. A line along approximately [15040N, 15020E]-[15025N, 15010E] has sandstone boulders and a small sandstone outcrop. The sudden facies change from the previous siltstone unit is evidence for synsedimentary faulting. The brecciation within boulders and thin (mm scale) quartz veins also indicate fault activity.

The mid gossan fault is roughly parallel to the strike of the two shear zones and offset a slice of the main gossan 25m to the east. The midgossan fault is probably a splay from the southern bounding fault zone (Jenkins *et al*, 1998).

The resulting geometry subsurface is complex because of cumulative superimposed displacements of the faults and smaller splays. This caused the scattered geometry of small ironstones from originally stratigraphically controlled ironstone striking about 155°. Minor faults in the area have a variable but northerly dip. The southern bounding fault and north gossan fault positions and orientations in cross-sections by Jenkins *et al.*, (1998), were used in this study.

2.2.2 Discussion: Stratigraphy and Depositional Environment, and Faulting

Stratigraphy and Depositional Environment

Regionally, the Riversleigh siltstone member reaches its thickest and deepest (3200m) toward the northwest in the Lawn Hill region map, (about 10km north of the Gregory and O'Shannassy River junction). The sedimentation of this siltstone formation represents an *overall* basin subsidence from the underlying Shady Bore Quartzite formation (Sweet and Hutton, 1982). The marine transgression is mainly due to the sagging and deepening of the depositional environment.

The deposit is likely to be in a shallow part of a basin, and the environment fluctuated, though grades into low energy sequences overall. Deepening occurs from the Shady Bore Quartzite, followed by locally shallowing into a fine grained sandstone sequence less than 100m thick towards the northwest. Jenkins *et al.*, interpreted that the host horizon was deposited in a sub-basin which is bound by a fault to the south of the deposit.

Faulting

The three significant features to faulting are 1) the change in facies across the faults, indicating a changing environment and synsedimentary faulting 2) the provision of fractures for remobilising oxidised ore fluids, and 3) the geometry of the MSZ and gossan is fault controlled in the area.

1) At the ridge soft sediment slumping occurs. This is probably triggered by slope instability caused by minor but continuing faulting movements in the mid gossan fault. Drillhole RVD017 intersects numerous sections of locally deformed beds and brecciation in the MSZ. Faulting is synsedimentary as the effects are on soft sediments, there is a plastic-type movement of many siltstone beds, or styolitic microfaults in the silicified but essentially barren unit is common in outcrop.
2) Faulting complicates the dispersion of elements. Continuity of trends showing anomalous element values from the gossan are disrupted by the faulting, and it introduces elevated concentrations of Ag and Fe and Cu. Elevated copper values are intersected in faults, and this vaguely conforms at surface taking into account secondar dispersion. Geochemical dispersion is based on affinities for two mineral types predominant in the gossan and nearb ; jarosites and goethites. Faulting pulls the anomalies away from the gossan for some elements (North's ICP-OES rock sample geochemistry records elevated copper values at distances from the gossan, and copper is commonly associated with faulting).
3) The provision of conduits for oxidised fluids. This is ubiquitous, seen in particular contrast with the leached bleached shales at the base of southern and northern gossans. (refer to plate 3.7 which shows an example of iron oxide remobilisation through small fractures). Slickensides are common at the midgossan fault (see plate3.6 a). Barite and quartzite veins are common in the massive pyrite zone at surface as with core (plate 3.5). Strike and position of fault zones are difficult to interpret from the outcrop which is rubbly, highly deformed and weathered with limited outcrop, but despite this it is likely that the faults are minor conjugate faults.

2.2.3 Folding

Folding is often obscured in the gossan areas as bedding is obscured by secondary textures of remobilised iron oxides. Here small isolated beds survive showing fluid–like folding. The biggest local fold is the 2.5m antiform on the southern gossan. It is part of the NE face of the southern gossan and is a barren coarse-grained siltstone to fine-grained sandstone bed 1.5m thick. Some units respond in a brittle way while others in a ductile manner to deformation. Folding is most pronounced in the jarositic unit, thick wavy beds of wavelength 1 to 1.5m amplitude at least 50cm. These beds have responded to compression in a more ductile manner than sandstones and barren siltstones within the surface expression of the MSZ, this is recorded in the RVD017 drill core log, (refer to appendix 2). The sediments at Grevillea are unmetamorphosed, and folding is broad and localised with very convolute beds formed while soft due to the ductile type of folding, as seen in the photo of the dolomitic siltstone sample S1 at the southern gossan. This type of folding clearly matches with what is observed in the core.

2.2.4 Surface Expression versus the Sulfide body at Depth

Comparing core lithologies with regolith lithologies. Referring to cross-section 15 235 N, (plate 2.6), the unit at [15 235N, 14 840E], corresponds with the collar position of RVD017 marked on the (map) plates 2.1and 2.4). This is an interbedded sandstone and siltstone unit which is weathered and ferruginous at surface and in core, becoming fresher with depth. Before RVC002 this grades into khaki coloured siltstones, very chopped and outcropping in a 2.5m section interbedded with sandstones 5-20cm thick showing pinch and swell structures indicating an environment below fair weather wave base and above storm weather wave base.

The unit grades into the dolomitic pyrite zone at 54m in RVC002. In core the shales and siltstones grade from black to grey to whitish, with the colour indicating the intensity of dolomitisation. White shales are highly dolomitic. The resulting regolith material at surface corresponds to leached and bleached shales, which are soft, crumbly and 'desilicified'. The surface shows pale leached and bleached shales overlying the dolomitic and pyritic shales in subsurface. The shales become a pink colour toward the gossan, indicating an increased iron content. It was found that finely ground hematitic/gossanous

material finely ground in with silica replicated the colour found in the field. This is possible where to a large extent, hematite, silica and goethite are not intimately co-precipitated but exist as a mixture.

Jarosite outcrops for 40m from about 15m after RVC001. It is more resistant and elevated compared to the recessive dolomitic shales. The unit lies between the dolomitic shales and gossanous material, and for the most part is the non-gossanous expression of the MSZ. The MSZ is defined as a zone of 30% or more pyrite and the jarosite outcrops over a moderately pyritic envelope which is slightly below 30% in the area of transition as indicated by cross-section 15 235N. The jarosite, an impure basic K sulfate formed from the oxidation of sulfides, and precipitated in the dolomitic shales because of the carbonate buffering providing a relatively more basic environment than other parts of the oxide zone. Stratigraphically below this is the botryoidal textured goethite of the gossan, formed in an acidic environment.

At the gossan [15 235N, 15010E], there are layers over a metre thick of massive botryoidal and hematite and thinner beds (~10cm) of laminated hematite containing primar laminations and strings of tiny (<1mm) voids vacated by pyrite. Sometimes the voids are filled with barite crystals in leached dolomitic interbeds. The photo of this disseminated type of boxwork associated with the (neutralising) dolomitic shales is shown in plate3.1a. Generally boxworks are of a cellular sponge type, not displaying a neat honeycomb of preferred cleavage directions but a mass of sponge like 'fluffy limonite'. In core RVC001 (75-118m) the pyrite is coarse grained (and 50-90% total core), with subordinate galena and sphalerite. The MPZ for RVC002 (75-163m), and RVD017 (115-192.3m) contains fine-grained pyrite in laminated bands, some dolomitic shales, and the coarse grained pyrite is in the lower portion of the zone and is associated with barite and coarse-grained sphalerite and galena.

In the gossan, coarse-grained barite in veins (1mm-3cm thick) has specular hematite around the barite crystals and in cleavage planes and small cracks, and in core (RVD017 @ 102-146m and 154-180m) fracturing and deformation is associated with barite veinlets and baritic breccia. The botryoidal texture of the gossanous material falls into two modal sizes, the 'beds' may be masses of mushed nodules 1-3mm or 5mm. The coarseness of the

secondary textures may reflect the primary grain size. Where the texture is larger it is also associated with larger barite crystals, as with the core. Comparison of surface to core for section 15 185 is identical to 15 235 in terms of regolith lithologies.

2.2.5 Discussion

The cross-sections reveal that the gossan conforms to the MPZ of a fluctuating pyrite grainsize generally in lenses which are massive. Some interbeds of barren sediment, also observed at surface, and late stage barite veins of barite at a low angle to bedding, and a possibly earlier stage of barite which is more deformed. The barite is also disseminated and veins are deformed in goethitic/hematitic botryoidal beds.

The sandstones to the left of the cross-sections have thin primary laminations and crossbedding. The surface and core weather identically, becoming fresher with depth and increasing presence of the interbedded siltstones and shales. The calcareous nature of the shales increases towards the *Massive Pyrite Zone* (MPZ) overlying recessive and leached shales mark an area derived from 30% or less pyrite in core. The *Massive Sulfide Zone* (MSZ) is a zone of <30% pyrite, and areas at surface which lie above this are referred to as being derived from the massive sulfide zone. The host unit for the deposit trends towards increasing hardness and siliceousness in the surface expression of the MSZ. Jarosite fringes the MPZ and is within the MSZ envelope, with 30-70% pyrite common (Drill Logs appendix 2). Therefore, the MPZ is delineated by gossanous material and the jarosite.

In summary, 15 185N and 15 235N sections are consistent in showing regolith type from sulfide poor to sulfide rich zones in subsurface. The gossan, with goethitic and hematitic nodular texture formed in a fluctuating MPZ of variable pyrite grain size. FeS was sacrificed from this area and accumulated in the gossan zone by supergene processes. The low pyrite zone adjacent is the boundary of the dolomitised host unit, and shows pale shales at surface. The sandstone unit more than 100m from the gossan is ferruginous and is stable at surface conditions due to the lack of sulfide mineralogy. The minerals in core are extremely unstable under surface conditions, but the weathering products are as resistant as the sandstone.

2.3 Regolith Units of the Grevillea Deposit

The surface expression of the ore sequence is 35x15m wide resistant ridge elevated 10-15m above the surrounding gently northwest sloping terrain. The predominant lithologies in the area are siliceous and weathered dolomitic, ferruginous siltstones and shales, with rarer interbedded sandstones.

The gossanous outcrop is the siliceous, ferruginised, dark, heavy, resistant rocks which consist of impure mixtures of hematite and goethite and jarosite interbedded with silicified and ferruginised siltstones and minor fine grained sandstones. General surface gravels show no outcrop at all and the oxidised products of the gossan drape over and conceal underlying lithologies.

The same units are used for maps and cross-sections, though the units have been sub-divided for the 1:200 and 1:100 maps. For mapping, the regolith units were distinguished by colour, texture, hardness and specific gravity. Assumptions were made in the field about the differences of the units based on iron content and silica content, which were verified later by applying geochemistry to key samples. It was clear that rock types could be divided into end-members of either dark, hard and heavy or alternatively pale, soft, and lightweight. The dark, hard, heavy type represents the gossanous material, iron-rich and siliceous, a site of secondary of accumulation. At the other end of the spectrum, pale and soft and crumbly siltstones are leached of iron and other metals derived from the metal sulfide zone and leached of silica (desilicified), leaving a porous amorphous silica framework.

The regolith units:

Five main surficial units were recognised in the area and are outlined below;

2.3.1 UNIT 1a

Gossanous material: (Limonitic Jasper)

Hematite-goethite: -laminated texture

Finely laminated, silicified hematitic and goethitic siltstones. Primary laminations remain, and often better preserved on the silicified, exposed coating than on fresh surfaces.

Laminations are typical of the siltstone sequence, varying from 0.1mm to 2mm apart, occasionally up to 4-5cm apart. Thin lines of voids parallel with bedding are left b vacated strings of pyrite crystals.

Exposed surfaces appear black with a silverish lustre or 'desert varnish'. Fresh surfaces shows blue-purple specular hematite, especially if near a barite vein or associated with disseminated barite in abundance (~15%). Alternatively where extremely weathered it is earthy dark brown to purple bluish, probably containing more goethite. The specular hematite is fine-grained grains (<0.1mm) but are noticeably bigger when associated with barite in abundance. Slickenside surfaces have microscopic spheres (in the order of magnitude of 0.01mm) of hematite, and in hand specimen lend a dark metallic lustre to the friction-polished surface.

Quartz grains are euhedral and seen in thin section, dispersed and compose less than 15% content of this type of silica. The remaining quartz is intimately intergrown with the hematite and goethite as the ESEM Xray spectra found Si in the iron oxides without recognising silica separately. The gossanous material commonly holds 30wt% silica (see XRF data appendix 5).

Barite veining is commonly 2mm-1cm and sub-parallel to bedding, it is prominent in the gossan and observed less in other areas. Veins range in width from fine wispy veins of on a millimetre scale to 30cm wide (for example, the northwest facing side of the southern gossan, plate 3.5 b). A background level of barite, keeping away from obvious veins and sampling hematitic and goethitic material with no noticeable barite ranged from 0.1wt% to more than 3wt% Ba (from XRF data on representative grab samples near the gossan). This unit is in the lower 20% of the massive sulfide zone. Barite is disseminated throughout unit 1b but is rarer in unit 1a.

2.3.2 UNIT 1b

Gossanous material: (Limonitic Jasper)

Hematite-goethite: -botryoidal texture

Heterogeneous fine-grained silicified impure goethite and hematite, with variable and subordinate jarosite and clays, and minor quartz and barite crystals. Signs of previous

boxworks are deformed due to the remobilisation textures, they survive from pseudomorphing by iron oxides and by silicified jarosite (plate 3.1 a). Thin growths of silicified jarosite on surface sometimes have a dendritic appearance. The jarosite also pseudomorphs secondary textures such as bladed hematite. This rock type has a dark, dullish-metallic lustre on exposed surface, and has a botryoidal or nodular texture. The mineralogy is more heterogeneous than Unit 1a.

2.3.3 UNIT 2

Jarositic Jasper

Yellow silicified siltstones and shales. Laminations are 0.1mm-2cm, in beds 2cm-15cm. More resistant/siliceous towards gossan ridge. Crumbly, soft, leached and paler in colour away from the gossan and into the shaley unit. Folded beds of ~1.5m wavelength, and amplitude ~50cm. Some pale, cherty, red/hematitic interbeds 5mm thick every 20cm. There some dispersed pockets or pods 1x5cm of weathered brick-red botryoidal textured hematite from 5-15% in distribution. These bulge out of bedding but are parallel to it, associated with interbedded hematitic beds. The jarosite has a resistant exterior, and softer and more crumbly interior, with increasing silicification closer to gossan. Near the northern and mid gossan fault zone, samples showing quartz and barite veins, and it has a brecciated texture.

Mineralogy of the jarositic jasper is estimated to be 70% $KFe_3(SO_4)_2.H_2O$ and a mixture of quartz and opaline silica. The remaining 10% comprise water and 'impurities'. Hematite and goethite represent up to 20% in some samples.

2.3.4 UNIT 3a

Leached and bleached shales

Pale coloured (usually white-buff-yellowish-pale purple) soft crumbly shales. Fine primar laminations preserved 0.1mm-3mm in beds ~7mm thick. Interbedded with ferruginous fine grained sandstones at gossan. Dominant presence interbedding with unit 1a to east of the northern gossan. Massive and without texture (laminations usually common) in some sections, especially south and SE of the Southern gossan.

The mineralogy of the samples was determined as amorphous silica by XRD and FTIR.

Key samples show mineralogy from FTIR to be high purity amorphous silica, extremel leached and bleached. The siliceous jacket is 2-3mm thick. This unit is part of and fringes the massive sulfide zone, and the minor pyrite zone.

2.3.5 UNIT 3b

Leached, bleached and silicified shales

Pale coloured, yellow and buff, grey and most commonly cream and white. It is white east and SE of the ridge, and also at the base of the northern gossan. It grades from unit 3a into the jarositic unit. Primary laminations are in a very good state of preservation in comparison to the unit 3a rock types. The north-eastern end of the southern gossan represents the darkest type of rock for this unit, a dark, fine and crinkly laminated dark gre bands alternating pale pink and yellow layers. Rare bedding parallel hematitic beds exist in the unit, with no signs of alteration. The mineralogy is dominated by silica and geochemical techniques were limited to FTIR and PIMA.

2.3.6 UNIT4

Ferruginous sandstone

Fine-grained ferruginous sandstone, honey coloured to purplish brown. Truncated laminations at a gentle angle. Pinch and swell structures in SW of field area. The laminations and other sedimentary features have fine dark grey lines marking the tops of the laminations.

2.3.7 UNIT 5

Cover:- Surface gravels

Gravels and rubbly brick-red hematitic cover derived from gossan. The gravels are a heterogeneous mixture of final stage weathering or complex soil forming processes.

2.3.8 Discussion

Unit 1b formed from supergene silicification superimposed apon the massive pyrite zone (MPZ) The supergene silicification preserved the secondary textures. Secondary textures have been infilled by remobilised goethite occurring at and above the water table in the

lowest zone of oxidation, in the gossan forming profile. Erosion and time have then exposed the present day gossan as ferruginous resistant ridges.

Extreme leaching of Unit 3a over a long period of time may have contributed to the silica and metal content to different parts of the profile. An increase in silica content is noted as approaching the gossans, a single bed on the northern gossan can be followed from relatively silica poor to silica rich *along strike* towards the gossan peaks.

The presence of a ferruginous sandstone layer 50cm-1.5m thick stratigraphically above the gossan may have acted as a permeable filter and the siltstones below as a barrier to percolating fluids, so that accumulation was enhanced at the site which is now the present gossan level, (see northern and southern gossan plates).

PLATE 2.4 SAMPLE SITES AND TRANSECT 15 150N POSITION

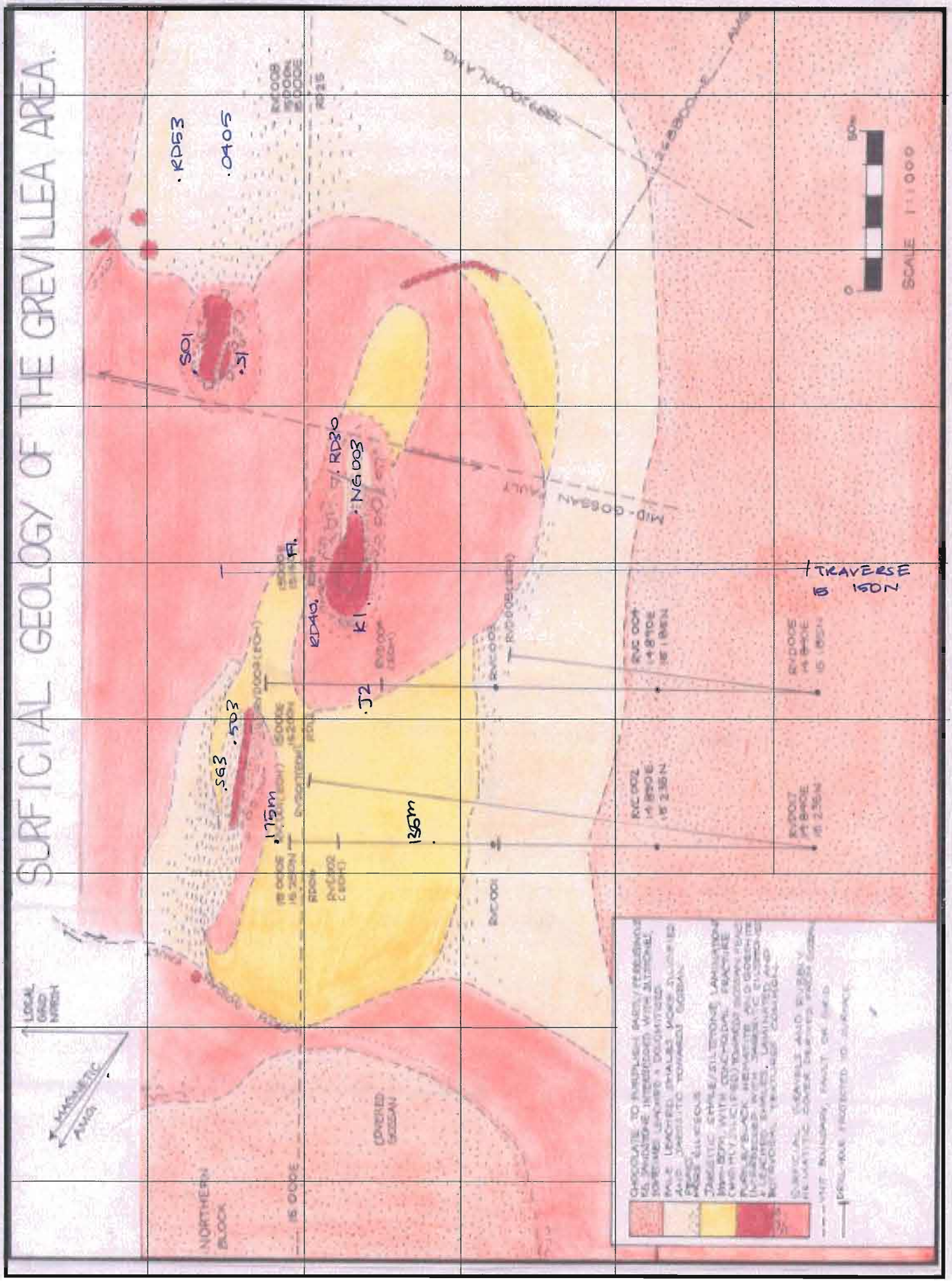

PLATE 2.5

CROSS SECTION ON GRID NORTHING 15 185 N, LOOKING NORTH.

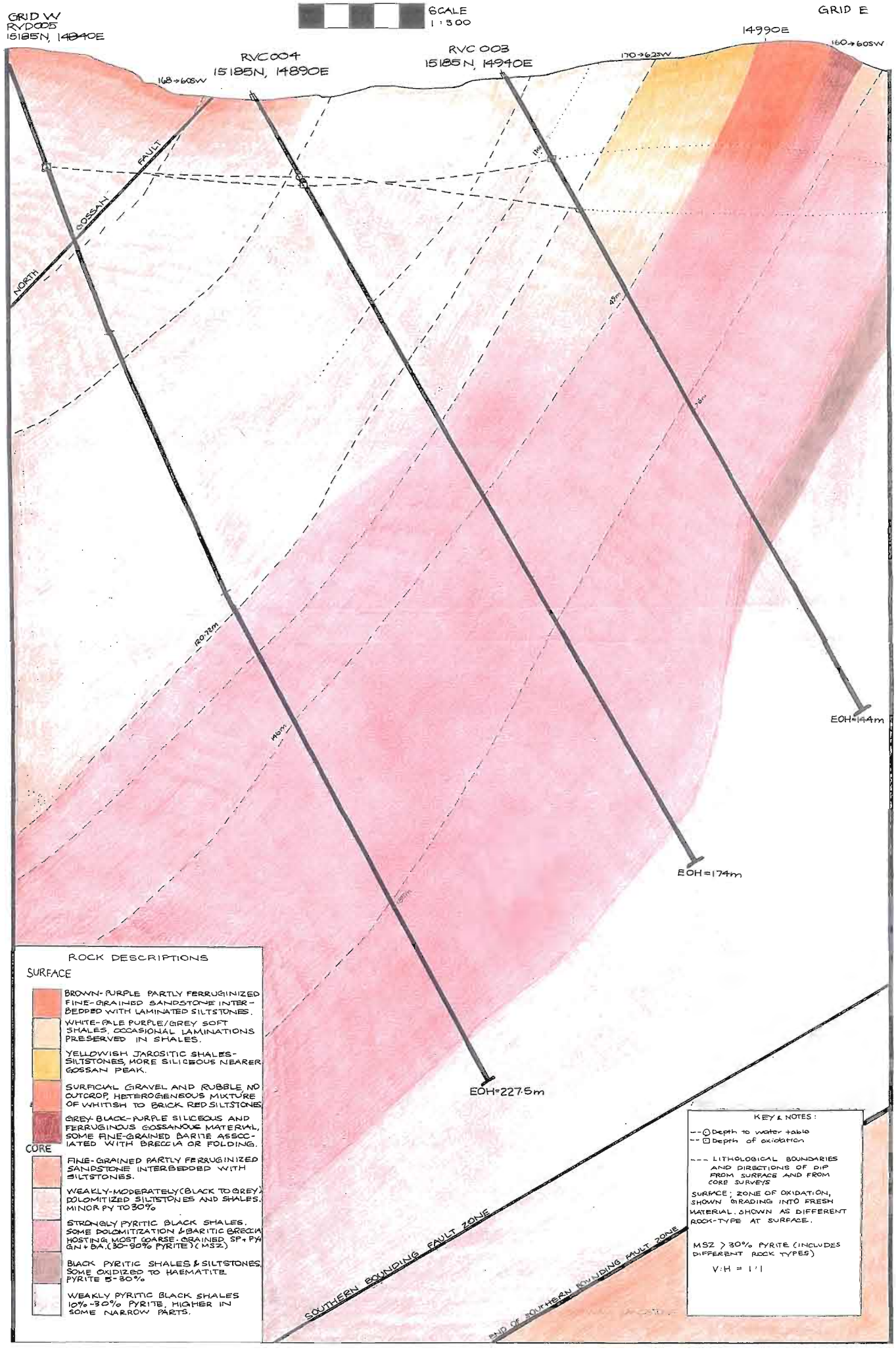

CROSS-SECTION ON GRID NORTHING 15235N, LOOKING NORTH

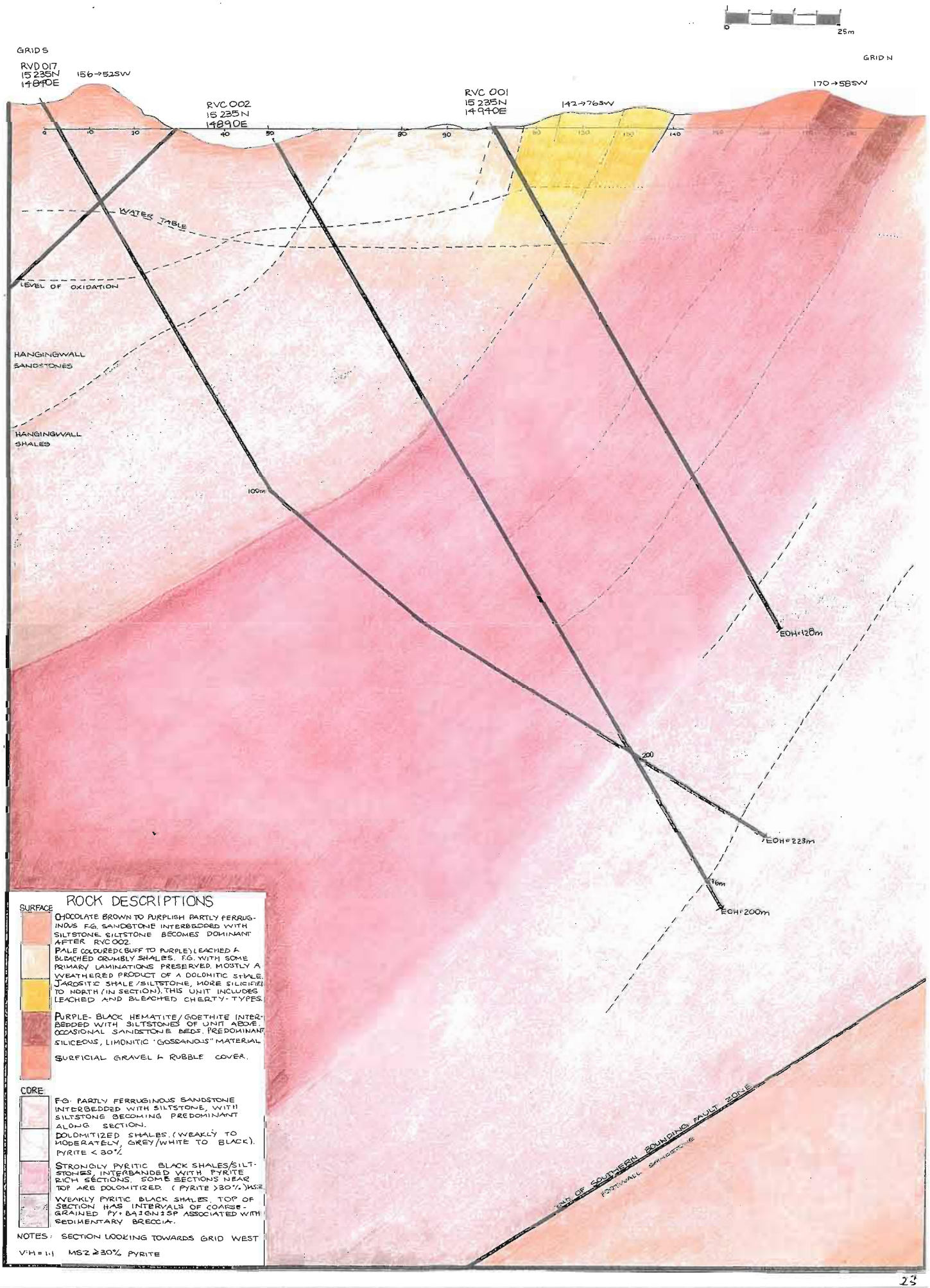

Chapter 3 Macro and Hand-specimen Scale Textures and Mineralogy

3.1 Introduction

It is important to state clearly that a gossan *is an exposed zone of supergene enrichment or depletion.* Gossans form just above the water table in the zone of oxidised enrichment, which subsequently is exposed by time and erosion.

The *idea of supergene enrichment* had just become accepted by the end of the 19th century, and what followed was a window of only about 70 years of close attention to 'leached outcrop interpretation' as a guide to ore. By the time the most comprehensive book on the subject, *Interpretation of Leached outcrops* Blanchard (1968) was published, it was argued that 'the day of leached outcrop interpretation has passed' essentially because 'the earth had been sufficiently combed over' in regards to gossans, and that other methods had been developed to locate deposits (Scheild, 1968).

By the 1940's in the United States and in Australia the study of limonite textures in handspecimen had become the most successful device to

a) distinguish sulfide-ore derived outcrops from those developed over barren areas,
b) estimate the proportions of ore minerals in subsurface and
c) to estimate deposit grade (Blanchard, 1968).

3.2 Formation of Ore-related Textures in Outcrop

Blanchard (1968) outlined the key textures in gossans arising from pyrite, sphalerite, galena and other common ore minerals. The key boxwork patterns are based on: 1) angularity of cells, 2) thickness of cell walls and 3) features such as internal growths off the cell walls.

The co-precipitation of iron and silica carried in circulation groundwaters creates siliceous replicas of the cleavage and sulfide grains at the water table, though the boxworks will appear ragged where the water table has only been briefly at the one level (Blanchard, 1968). Sponge textured limonites like those formed at the Grevillea gossan (see plate 3.1

a) are formed when the water table drops leaving residuals in the boxworks and with an intermittent supply of silica, irregular patterns result.

Blanchard (1968) terms all gossanous product as *limonitic jasper.* Limonitic jasper is an impure mixture of goethite, hematite, jarosite and variable amounts of silica, which co-precipitates with the iron. The oxidation of the sulfide ore body yields sulfuric acid and silicates, and a proportion breaks down to $SiO_{2\,(aq)}$. For stable groundwater conditions layers form which are high-iron and low-silica alternating with high-silica and low-iron (Blanchard, 1968). Layering of this kind is observed at Grevillea in the repetition of red crumbly layers and harder pale layers at the SE base of the northern gossan, seen in bottom of photo (Plate 3.8 c).

3.3 Ideal Textures for Galena and Sphalerite

The following descriptions classify textural differences of boxworks in galena and sphalerite;

3.3.1 Galena

The galena key textures are (i) ridged parallel cell walls, Blanchard describes these as 'ribs', and (ii) angular, often triangular internal boxworks. This was very hard to find at Grevillea, though specimen G2 may have these features after galena, and the colour a deeper red-purple which is a typical galena-derived colour compared to the redder (hematite)-derived pyrite. The example of galena boxwork in plate 3.14 b, is a specimen derived from the same region as the Grevillea deposit (Lawn Hill).

A tiny section of the jarosite in the middle of G2 is probably after galena, it shows a highly angular to triangular boxwork.

3.3.2 Sphalerite Textures

Ideally, the boxwork for sphalerite is an open honeycomb structure. Crinkly cell walls are also a key for identification. Plate 3.11 c is an example of hieroglyphic sphalerite from Mount Isa. This is also recognised as a key texture. Sphalerite textures were extremely difficult to identify from the gossan at Grevillea. Textures would be quickly distinguished for a section of gossan representing coarse-grained disseminated sphalerite. Even so, for a

fine grained, highly pyritic ore and a gossan dominated by secondary textures, small patches may survive showing sphalerite boxworks, interpreted shapes after sphalerite in specimen G2 are marked on the transparency of plate 3.1.

3.4 Ore-derived Textures at Grevillea

Ore derived textures found at the gossan broadly fall within two classes:

a) Primary textures reflecting the sulfide-ore mineralogy and are a boxwork or sponge type.

b) Secondary textures which are solution deposition textures.

Macro and handspecimen scale textures at the gossan relating to the ore have been:

Primary-

1. Voids from leaching of pyrite in laminated, non-botryoidal goethite/hematite, and in leached shales.

Secondary-

2. Botryoidal goethite/hematite mixture (small or large type) Precipitation and 'zonation' from remobilised hematite in fractures and thin veins in leached shales from thin hematitic bearing veins (as seen in Plate 3.7, figures (a) and (c))

3. Range of gossan minerals-including grainy specular hematite, and hydrated and silicified jarosite laths

Texture types are only diagnostic of particular sulfide minerals in the ore *at* the gossan. In the vicinity of the gossan, primary sulfide-ore related textures are rarely observed, however, the textures are a surface indication of a form of sulfide oxidation.

Textures observed at Grevillea vary with unit types as outlined below;

3.4.1 Unit 1a

This unit is a laminated ferruginous, gossanous unit, as previously discussed and is represented by plate 3.3 b. The texture is simple, laminated with no hints of sulfide-derived texture on weathered surfaces.

3.4.2 Unit 1b

This unit comprises the main textural type at the gossan. The texture is a nodular, botryoidal form. On weathered surfaces, the rock appears dark coloured and hard, often with a semi-metallic luster. Specimen G2, representative of this unit is a 'cellular sponge' of pyrite and galena. The textural type is described as a botryoidal boxwork *sponge*, because primary boxworks are lacking. The sponge has indefinite patterns of irregular cell shapes, and the parent rock is more likely to be granular than massive (Blanchard, 1968). The product is highly porous, with an etched and eaten away effect. The specimen contains small sections of boxworks of galena, pyrite and sphalerite. The sample is 86wt% iron oxides (by XRF), the cells in hematite and goethite are irregular but they are angular in sections preserved by siliceous jarosite.

The cut surface on plate 3.1a, shows specimen G2, typical of the textures seen in this unit. The surface reveals, at closer inspection, a squarish honey-comb texture in center of the specimen. This siliceous jarosite rich boxwork has the characteristics of a sphalerite boxwork, equi-dimensional cells, though some of the section has angular cells joined to a ridge and this may be a galena derivative. Generally sponge textured boxworks are not diagnostic, but may retain some structures.

3.4.3 Unit 2

Unit 2 is a jarositic shale, and in most cases it is laminated, though it is 'fluffy'/ powdery textured in the area next to the leached dolomitic shale unit 3a. An example of the fluffy type is specimen 175m (plate 3.2). The fluffy-type has no distinct textures that link to specific sulfides, though the laminated type contains textures from pyrite these are seen in thin section.

Unit 3a

Specimen 005.110 is from this category (plate 3.9 c). Disseminations of voids after pyrite grains in leached shale seen clearly in the photo (plate 3.1, figure (b)). This type of texture may indicate sulfides.

Unit 3b

This unit is similar to the unit above in terms of the inapplicability of this unit in understanding the regolith in terms of parent sulfides. No relevant textures preserved.

Unit 4 and Unit 5 are the ferruginous sandstone and surfical gravels, which may have geochemical use, but not textural.

In summary, only the rocks at the gossan are useful in terms of textural interpretation of a parent sulfide in the ore.

Discussion

Solution deposited textures are common and easily recognised. Primary textures after galena or sphalerite were not recognised in outcrop. The fine-grained boxworks after pyrite and galena are deformed and crushed by infilling of goethite.

3.5 Non-ore related Textures

Sedimentary features present prior to gossan formation, including laminations are primary. Veining, brecciation and preconsolidational slumping are categorised as secondary. An angular breccia of siltstone clasts (<5mm) in a barite-quartz matrix is common in rubble in the mid-gossan fault zone located at the base (north-eastern side) of the southern gossan. This secondary fault/vein associated texture is only found between the two gossan peaks.

3.6 Interpretation

The sulfide minerals and silica are discussed, and an interpretation of major units is given;

Pyrite:

An effect of pyrite weathering seen at the gossan and described by Blanchard (1968) is 'desert varnish' which is a thin polished film on weathered rock surfaces. Moisture from the ground is drawn up in the rocks to the surface and the solutions are evaporated leaving iron and silica. Desert varnish is very common at Grevillea and thin enough so that laminations could be seen. It is a common effect in arid to semi-arid terrains.

Silica

Case hardening also described by Blanchard (1968) was also very common at Grevillea. Almost all rocks at Grevillea have a hard surface and were softer inside. The effect was seen clearly on pale samples where a zone of silica concentrates at the surface which

protects the surface textures. This effect is common in arid environments (Blanchard, 1968).

Interpretation on the formation of textures for Unit 3a

Specimen RD43 (plate 3.1 b) is an example of the unit-type is discussed in terms of possible mechanisms of formation;

At surface, voids vacated by pyrite and replaced by barite are preserved in a neutralising/ dolomitic shale matrix (corresponding to a fringe of the MPZ).

In a zone of aeration and oxidation due to the falling water table, boxworks form. As the water table fell, the oxidation of the disseminated pyrite released acid, which was neutralised by the dolomitic gangue. The iron precipitated nearby, probably fringing the leached cells (Balnchard, 1968).

Specimen RD43 shows that some of the cells have been infilled by barite. This is either a grain for grain replacement or later infilling. Pore fluids rich in Ba^{2+} from contemporaneous barite veining and fluid circulation, facilitated barite precipitation in the convenient euhedral spaces (vacated by pyrite).

Later, extensive leaching (or continued leaching) removed most barite into solution and a pale, leached shale remains, with craggy pyritic holes, a few containing barite, and having an amorphous silica (ie leached) signature with FTIR.

Interpretation of the formation of Unit 1b

The weathering products of pyrite are common, as the source is highly pyritic. The sulfide body oxidised, releasing iron and sulfuric acid which destroyed most textures in this part of the profile. The precipitation and solution of iron oxides is pH-Eh dependent (Garrels, 1953), hematite precipitates in less acidic conditions that goethite. It is expected that the texture of G2, a solution derived texture, is produced in acidic conditions.

Interpretation on the formation of Unit2

Specimen 175m is a jarositic *fluffy limonite* which is a light porous limonite. It is produced in conditions of high porosity, free oxidation and low silica in the zone of aeration with a

neutralising gangue (dolomitic in the case of Grevillea) forming the powdery/fluffy effect (Blanchard, 1968). Carbonate or bicarbonate reacting with $FeSO_4$ foams and 'fluffs' up the limonite particles in forming limonite. This type of limonite is commonly expressed at regolith as an indication of unidentified sulfide minerals.

Plate 3.1 Common Primary and Secondary Textures from the Surface Expression of the MSZ

(a) Specimen G2

Specimen G2 shows typical sponge texture from oxidising pyrite. Yellow siliceous jarosite in middle shows triangular boxwork from galena.

Overall, a solution infilled texture with rare primary boxworks.

(b) Specimen RD43

Craggy voids from disseminated pyrite in a neutalising dolomitised gangue. Some crystals of barite have infilled. Note cubic and euhedral shapes, and the 'case hardening' effect of the silica concentrated at the surface (from top left to bottom right).

Plate 3.2 Common Secondary Textures at Grevillea, from the Surface Expression of the MSZ

(a) Specimen RD46

Bladed hematite weathered to goethite (centre), nodular solution deposited goethite (bottom left).

(b) Specimen 175m

Fluffy limonite.
Dolomitic leached shale (left), leached hematitic (middle) and leached jarosite (right).

Preserves no primary textures, but possible relict late bladed hematite (left, top right).

Plate 3.3 Common Primary Textures from the Gossan

(a) Specimen G3

Hematite and goethite showing remnant craggy voids after fine grained pyrite, in bands parallel to bedding.

Solution-deposited textures (more clearly seen on left side of specimen).

(b) Specimen NG003

Massive, laminated siliceous hematite.

Laminations at surface sealed by *desert varnish*.

Plate 3.4 Sedimentary Features

(a) Specimen S1

Near RD52.
Laminated siltstone/shale,
showing plastic deformation, with beds behaving individually; note s -folding (centre),
opposed to gentle curving of bed above (top).

Poor boxworks after sulfide grains (<1mm) (top and left side).

(b) Specimen SG1

Ductile-like microfaults prior to silicification due to gossan forming processes, flame structures (bottom left).

Black layers were carbonaceous (and pyritic), pale pink are barren and siliceous interbeds. Yellow jarositic staining formed in pink (K rich) layers with iron from the carbonaceous bands. This rock type commonly shows wriggly microbial (dark) laminations. (not this specimen).

(c) Specimen SG002

Laminations showing ductile behaviour. This represents an early post-depostional stage.

Plate 3.5 Barite Veining at the Gossan

(b) Barite vein Rd16 (NE base of SG)
Coarsed grained barite in vein 15cm wide, at a low angle to bedding. Layered effect, parallel to vein walls.

(c) Specimen G5

Section of gossanous material. An example of bladed hematite associated with late stage barite veinlets,common at NG and SG. Weathered patches of hematite (brick red), bladed hematite grows around barite crystals, remobilised from heat/fluid due to the barite vein. Specular hematite is often associated with barite,
disseminated or near veins..

Plate 3.6 Textures Related to Faulting

(a) Specimen 506 Slickensides

From rubble at base of Northern Gossan 10m south of RD46.

Fine-grained hematitic silt-stone. matt/dull on reverse surface, with surface facing showing 'friction-polished' hematite from mid-gossan fault.

(b) Northern part of Ridge 15m NE of RD06.

Botryoidal growths on bed-ding plane cleaved open enough to allow precipitation of goethite. Curved streaks-from movement.

Flattened tops on the nodular goethite from restricted space between the two bedding planes.

(c) In same vicinity as above.

Short parallel and curved marks from goethitic rich solutions pushed along fracture surfaces.

Plate 3.7 Veinlets and Fractures - Core to surface, Iron-oxide Remobilisation.

(a) 10m Sw RD05

Cracks and fractures in a leached and bleached zone showing hematite staining from remobilised iron oxides.

(b) Specimen 005.110m

Sample collected along RVD005 section at 130m. (Compare with cross-section).

Iron oxides remobilised from ore, contrast enhanced by pale, leached nature of host rock.

(c) Drillcore:RVD005, 108.5m

Dolomitised shale, with iron oxides infilling fractures.

Fluid infiltration containing iron oxides along fronts (smaller fractures).

Plate 3.8 Laminated Hematitic Gossanous Outcrop

(a) NG at RD29, Northern Gossan

Alternating beds of hematite anfd leached shales, to interbedded goethite and jarosite at top.

Heavy drip of hematite into porous leached shale.

(b) Northern part of Ridge 15m NE of RD06.

Immediately below figure(a). Interbedded goethitic and jarositic shales (bottom), grading into more resistant and dense hematite layers at top.

(c) Gossan outcrop

Gossanous outcrop at NG fault zone.

Bedding as for figure (b), with typical hematite gossanous capping.(black)

Plate 3.9 Regolith Material derived from MPZ and MSZ

(a) Specimen J2

Frequent outcrop, J2 rock-type near the northern gossan especially. This type of jarosite (dense and siliceous) occurs close to the gossanous outcrops.

Silicified, jarosite beds up to 30cm thick, underlain by goethite and hematite mixture. Barite in jarosite shows specular hematite clinging around it (dark grey).

(b) Specimen K1

This type of rock only found at northern end of Northern Gossan. None found in situ.
Maroon clay with white blebs of opalline silica (infusiorial earth opal). Irregular highly deformed brecciated texture.

(c) Specimen 005.110

Soft, amorphous, light/porous silica. Leached and bleached chalky textured shale.

(d) Specimen 0405

Leached and bleached silicified shale. Laminations rarely preserved.
Very low specific gravity, but hard conchoidal fracture.

Plate 3.10 Leached Regolith Material in Surface Expression of MSZ

(a) Specimen 503

Alternating beds of goethite and leached jaositic shales.

Bands of hematite parallel to bedding, limited diffusion into yellow layers. Jarosite often in spots or splotchy within goethite beds.

Yellow areas occur for locally lower in Fe, higher K and sulfate 'pockets'

(b) Specimen 135m

Freshly broken surface of jarosite most commonly outcropping at Grevillea.

Pale yellow shales with minor hematie stained bands and 'pods' of nodular secondary goethite (middle).

(c) Specimen NG001

Leached shale with alternating hematitic with opalline silica layers.

The Hematite is a disseminated microscopic platey type.

Plate 3.11 Pyrite and Sphalerite Limonite Derivatives

Figure (a)
An example of the formation of sphalerite and pyrite limonite in a dolomitised shale from Mount Isa.

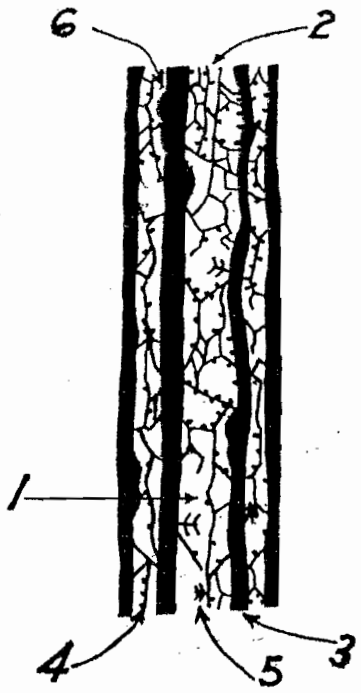

Sketch showing limonitic products formed by the leaching of sphalerite and pyrite. The host rock was a shale that contained dolomitic bands. When the rock was mineralized, medium-grained sphalerite selectively replaced the dolomitic bands, finely disseminated pyrite replaced about 25 percent of the more siliceous shale bands. When leaching later took place, the sphalerite was replaced at an early stage by cellular pseudomorphs characterisitc of that mineral, the pyrite was later replaced by massive jasper. Each oxidized pyrite grain was neutralized by one or two dolomite particles, greatly retarding the exportation of iron in solution, and thereby aiding the kaolinization and jasperization and confining it to the pyritized bands. The only iron visibly exported is that precipitated as sparse, finely nodular crusts or "blisters" on the surfaces of the jasper bands.

1. Coarse cellular boxwork derived from sphalerite.
2. Fine cellular boxwork derived from sphalerite.
3. Massive jasper derived from the oxidation of pyrite.
4. Sandy limonite grains, thinly coating the cell walls of sphalerite-derived boxwork.
5. Limonite rosettes.
6. Nodular limonite crusts.

These are the usual types of products resulting from oxidation and leaching of sphalerite-pyrite mixtures in dolomitic shale at Mount Isa, Queensland, Australia. Enlargement 3x.

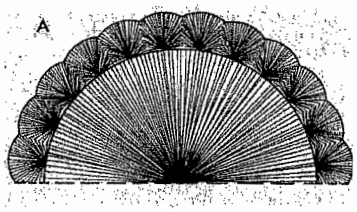

Figure (b)
Radiating fibrous limonite from pyrite. Seen faintly on specimen RD46 (plate 3.2 figure (a)), as flat radiating spokes. This type also forms spherical growths. The limonite is made up of 'mutually interfering repetitions of the unit pattern'. On weathered exteriors the limonite is 'smeary and nodules have a run together effect'. (After Blanchard, 1968)

Plate 3.12 Key Limonite Boxworks for Sphalerite

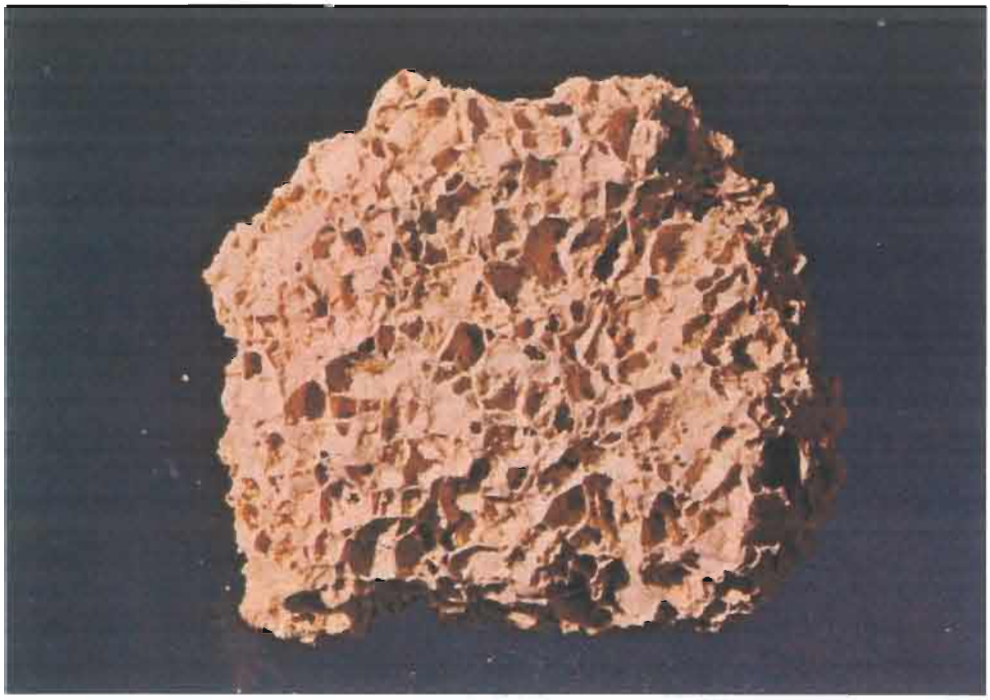

Figure (a) Cellular boxwork derived from sphalerite. From North Broken Hill.

Figure (b) Key Features

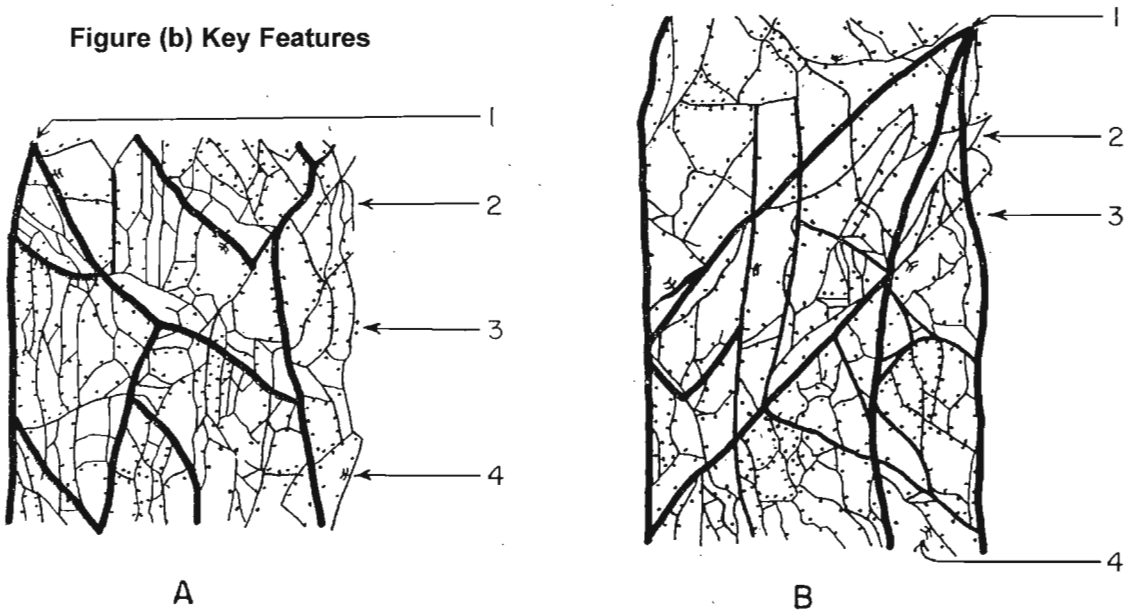

Sketches showing characteristic limonite boxworks derived from sphalerite. 1. Coarse cellular boxwork. 2. Well connected fine boxwork. 3. Sandy limonite grains, slightly coating cell walls. 4. Limonite rosettes.

A. The cell walls in this specimen are well connected and the cells themselves almost empty of material. The boxwork usually has a sharply angular form, with intersecting angles of 30° to 55°. These features constitute the "key" structure. From a shaly limestone, Spruce Mountain, Nev. Enlargement 3x.

B. In this specimen the boxwork is well connected, and is of sharply angular pattern. The angles of intersection are often about 30°, but vary somewhat. Lawn Hill, Queensland, Australia. Enlargement 3x.

Figure (a) is enlargement 2.5x. Specimen collected and Sketches by Blanchard (1968)

Plate 3.13 Galena, Cerussite and Sphalerite

Figure (a)

Sketch of Key Galena Boxworks

A

B

A. Sketch showing cleavage boxwork derived from galena, as it appears when divested of partially sintered crusts. The long, minutely thin parallel ribs and cubic boxes are replicas of galena's cleavage, proof that limonitic jasper penetrated along the galena's cleavage planes during incipient oxidation before the sulfide residuals had been converted into anglesite and cerussite from which the partially sintered crusts later were derived. A characteristic feature is the thinness of the cellular walls, often not more than 0.005 mm. thick, and the main reason that the boxwork is seldom well preserved in the outcrops. Lawn Hill, Queensland, Australia. Enlargement 3x.

B. Sketch showing diamond-mesh boxwork. Note the irregular diamond-mesh structure, with only occasional cubic boxes preserved. Note more particularly the pairs of closely spaced, rigidly parallel, minutely thin webs that constitute the structure's major ribs. Usually the boxwork is coated with partially sintered crusts, which in part obscure the diamond-mesh pattern (see fig. 56). Close conformity in pattern of the structure to certain crystallizations of cerussite suggests the pattern may be derived in some instances from cerussite rather than chiefly directly from galena. From an outcrop at Ruby Hill, Eureka, Nev. Enlargement 3x.

Figure (b)

Cellular sponge boxwork (crinkly-walled sphalerite type).
Mixed limonite boxwork of ~30% galena, ~60% sphalerite derivation.
From Northern Orebody, Broken Hill, NSW. 1.5x

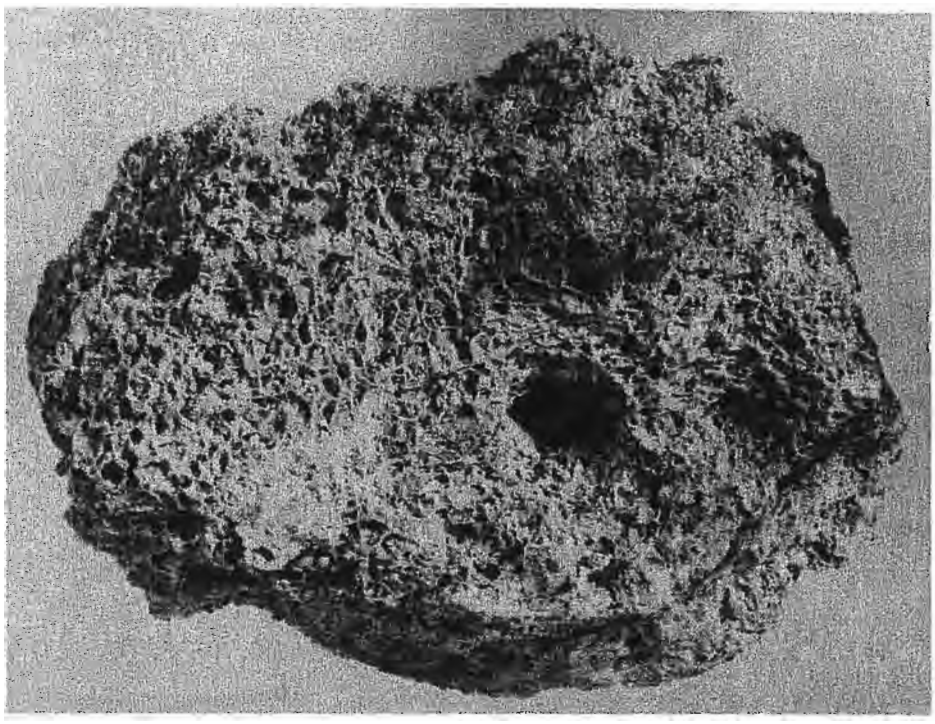

Plate 3.14 Key Boxworks Derived from Galena

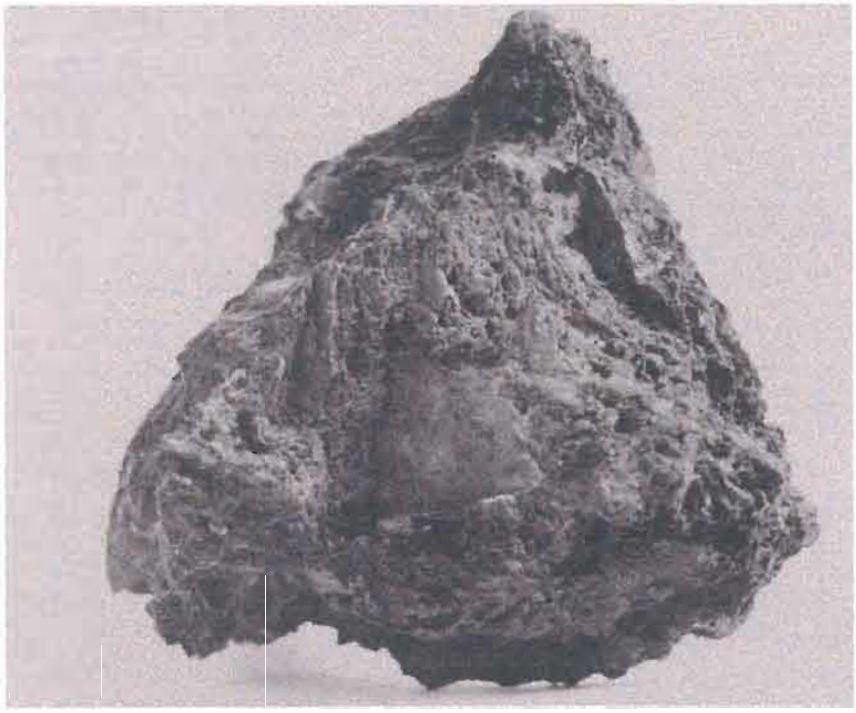

Figure (a)
Weathered surface. Cleavage boxwork of galena showing ridged parallellism of cell walls. Sample from Nevada. USA Enlargement~2.5x

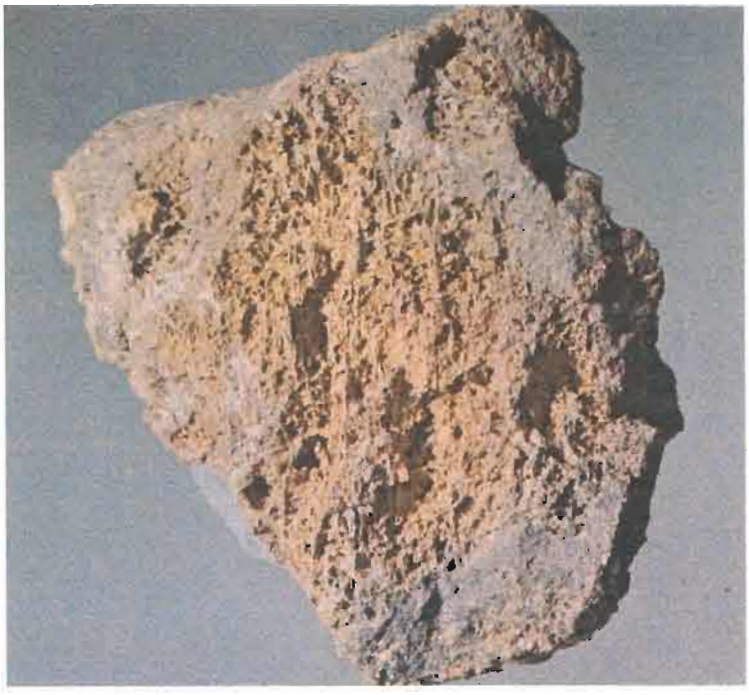

Figure (b)
Weathered surface. Cleavage boxwork derived from galena, showing thin ridgedly parallel cell walls. Sample from Lawn Hill, Queensland. 1.25x enlargement.

(After Blanchard, 1968)

Table 3.2

DESCRIPTION OF DIAGNOSTIC REPLICA OF COMMON TEXTURES IN GOSSANS

Mineral	Diagnostic Replica Textures
SULFIDES	
Pyrite (FeS_2) Isometric	-Cubic pseudomorphs or cavities -Concentric or nested cubic boxworks, commonly with octahedral modification. -Concentrically zoned webworks or anhedra
Marcasite (FeS_2)	-Radiating elongate boxworks with herringbone cross walls. -Pseudomorphs of stellate spear-head twin
Galena (PbS) Isometric	-Regular, cubic, thin walled, concentric boxwork (more regular the pyrite) -Stepped pyramidal boxwork. -Rhombic, cerussite boxwork: thick walled, multiple parallel septa with acute angle ideally 62 degrees
Sphalerite (ZnS) Isometric	-Angular boxwork: well connected, oblique (45 degrees) cross walls and continuous, parallel long walls produce triangular sub-cells.
OXIDES, HYDROXIDES	
Goethite (FeOOH) Orthorhombic	-Spherical, cellular boxworks (gel texture) -Poorly connected hieroglyphic boxworks
CARBONATES/GANGUE	
Calcite ($CaCO_3$) Hexagonal	-Highly regular, rhombohedral boxworks ideally acute angle 72 degrees
Siderite ($FeCO_3$)	-Curved, rhombohedral boxworks: ideally acute angle 73 degrees.

(After Blain and Andrew, 1977.)

Table 3.1 **Rock Types Divided On Basis Of Colour, Hardness and secondary Botryoidal textures from Pyrite Dissolution***

		Hard (silicified)	Soft**(leached)
Dominantly Darker Rocks (hematite, goethite & limonite types)	Botryoidal Texture	*Occurrence*- common at gossan peak, secondary flooding of goethite and hematite from a massive sulphide zone. Botryoidal texture in two modal sizes, nodules ~7.5mm and ~2mm.(reflecting differing primary grain size?). Dark , fine grained with specular hematite common.	*Occurrence*- Shales with small amounts of iron and remnant botryoidal texture is rarely found. It does not occur near the gossan peaks but nearby interbedded with highly weathered previously dolomitic shales.
	Laminated Texture	*Occurrence*- common at gossan peaks and near gossan interbedded with siltstones and shales. Finely laminated to massive hematite. Commonly a cherty fracture on laminated textured	*Occurrence*- Rare. Chalky textured, previously laminated but with massive appearance in parts, stained with iron or other metals but still extensively leached compared to cherty/siliceous counterparts.
Dominantly Lighter Coloured (jarosite and leached types)	Botryoidal texture	*Occurrence*- Does not exist where leached and bleached, a sample seen of weathered type A	*Occurrence*- Does not exist
	Laminated Texture	*Occurrence*- Common to north-east of both gossan peaks. Massive hematite at gossan peaks, more siliceous purple and yellow laminated cherts at northern ends of southern and northern gossan peaks.	*Occurrence*- Common especially in area near Rd 51, south-east of both gossan peaks, and Rd07, west of the northern gossan.

Note: all gossanous product at Grevillea falls within these groups * The interpretation presented in the table reflects observation (followed up by geochemistry) that rock types have end-members, which are:Fe rich and siliceous, or pale leached and bleached. ** Soft is any rock which can be scratched with a coin and commonly can be scratched with the fingernail.

Chapter 4 Fine-scale Textures and Mineralogy

This chapter describes certain key textures found at the gossan and in the ore body using reflected and transmitted light microscopy and the ESEM technique. In particular, four key mapping units are represented by the thin-sections. The sample locations are shown in plate 2.4 - *The Surficial Geology of the Grevillea Area.* Only samples that form part of the massive sulfide zone are studied in terms of textures.

Although gossan textures are focused on, textures from core samples from within the massive pyrite zone (MPZ) are looked at for comparison. The following section discusses the thin-sections from diamond drill core RDVC017.

4.1 Textures from Core

Thin-sections were available from core are dominated by pyrite, with subordinate galena and sphalerite. The following section discusses primary and secondary ore and gangue textures observed in thin sections from the gossan and in core beneath the gossan. Primary and secondary textures are not subdivided as another category but described where they occur in sulfide and gangue textures.

Gangue mineralogy is simple and so it is not covered in a section separately from the ore mineral descriptions. Gangue minerals are dominated by barite, K-feldspar and quartz. The barite is infills voids and replaces pyrite and galena, the barite is vein and breccia associated and sphalerite, galena and pyrite are noted as occurring in a coarse cubic fashion with the barite. The RVD017 drill core log records calcite as a recurring gangue mineral in the ore zone but it was not present in the thin sections available for this study.

4.1.1 Sulfide-ore Mineral textures

4.1.1.1 Pyrite:

- *Disseminated pyrite* (primary texture):

  Disseminated pyrite has euhedral grains of various sizes, ranging from 10μm to 2mm. Disseminated pyrite grains with a diameter exceeding 10μm, tend to have imperfect octahedral shapes. Smaller grains often have imperfect cubic shapes.

- *Laminated Pyrite* (primary texture)

  Pyrite commonly occurs in bands that are parallel to bedding. Laminated pyrite has a variable grain size, but in similar range to the disseminated pyrite. Grains tend to be octahedral and in clusters, with small pockets of bedding parallel framboidal pyrite.

- *Massive pyrite* (primary texture)

  Massive pyrite consists of extensive aggregates of pyrite grains of various morphologies. The most common morphology of this type is a slightly irregular euhedral shaped, equigranular mass of grains approximately 10μm in diameter. In some parts the crystals have indistinct grain boundaries, and spread over large areas (approximately 500x500μm) without interruption. The larger grains are associated with a reticulate texture (irregular shaped patchwork-quilt type) with galena and sphalerite.

- *Framboidal Pyrite (primary and secondary textures)*

  Small clusters of groups of spherical aggregates (framboids) occur in some thin sections. A framboid is a spherical aggregate of minute euhedral pyrite crystals of nearly equal size (0.5-1.0μm) (Love and Amstutz, 1966). Secondary textures occur where whole framboids are either pseudomorphed by other minerals, or have been partially replaced (Endo, 1978). Partial replacement of framboids is often as atoll structures. Atoll textures have an irregular rim of pyrite with a small part of the core comprising pyrite with infilling/replacement of the middle of the structure with another mineral, usually galena. Framboidal pyrite may only have the core replaced by another mineral with the rim remaining as pyrite, and some of these relict framboids have fibrous, acicular or needle-like hematite crystals, replacing the pyrite rim.

4.1.1.2 Galena:

- *Anhedral crystals (primary texture)*

  Crystals of galena (up to 500μm) often have a reticulate texture type with the pyrite and sphalerite. The morphology is an anhedral mass that generally has finely jagged boundaries with other minerals, this boundary has an etched or 'eaten away' appearance, this is referred to as a cell, net or mesh texture (Schwartz, (1956) and Ineson, (1989)).

- Sometimes pyrite is embedded in the galena, and the pyrite has a mottled or partially decomposed appearance within a grain of pyrite, Schwartz (1952) has described the same texture as a granule texture. For intact pyrite, a neat meeting of grain boundaries of galena and pyrite is seen, and this is classified as a mutual grain boundary texture by Schwartz (1952).
- *Replacement textures*

  Galena has been observed replacing pyrite (atoll structures are an example).

4.1.1.3 Sphalerite

Sphalerite was not well represented in the available database of thin sections. It is usually coarse grained and massive, associated with coarse-grained barite and pyrite according to Jenkins *et al* (1998) and from drill core logs (appendix 2 and3).

- *Anhedral sphalerite*

  Infilling, anhedral textured sphalerite was observed in thin section. The sphalerite is a pale honey-brown coloured variety, with faint internal reflections. Generally, the sphalerite has homogenous appearance. The texture is highly irregular, infilling around other grains and in voids and cracks. The pale colour of the sphalerite was also noted by Jenkins *et al* (1998).
- *Laminated sphalerite*

  Light brown bands of laminated sphalerite are observed in RVD017 thin section samples.

4.1.2 Descriptions of thin sections:

Thin section 175.5

This specimen consists of 80% brassy coloured pyrite in 10% (infilling) barite, and 10% sphalerite, and minor quartz. Pyrite has well formed euhedral, and subhedral crystals, 20-50μm. Framboidal textured pyrite is observed in a pod-like section (1x1mm) at bottom of the slide. The sphalerite is grey with pale brownish internal reflections, and has an infilling/xenomorphic texture.

Thin section 175.5B

Predominantly colloform textured pyrite, overall 70% pyrite, with a minor (less than 2% framboidal pyrite texture). The bottom half of the slide contains approximately 10%

Plate 4.1 Common Core Textures

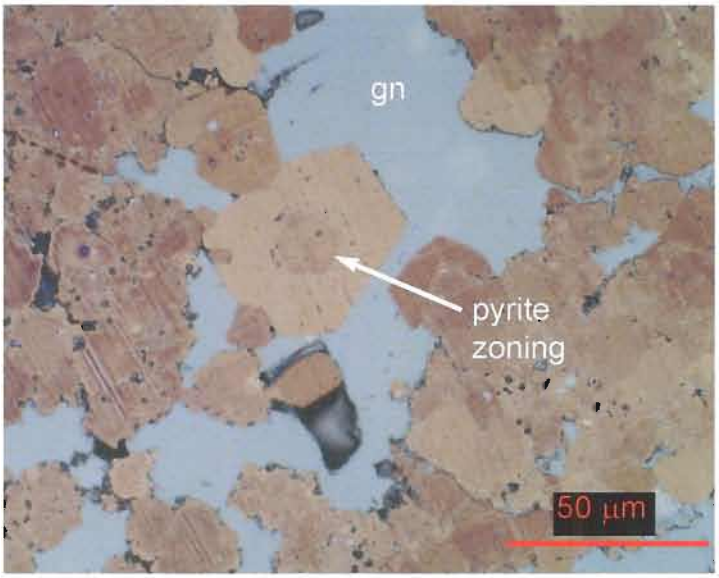

(a) Specimen 129.8B

Photomicrograph of zoned euhedral pyrite surrounded by infilling galena.

Reflected light.

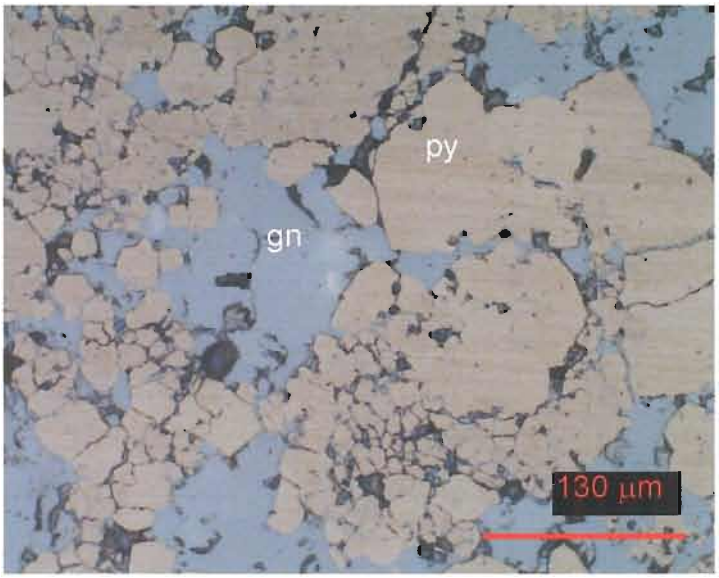

(b) Specimen 175.5B

Photomicrograph of inter-grown subhedral pyrite and galena.

Reflected light.

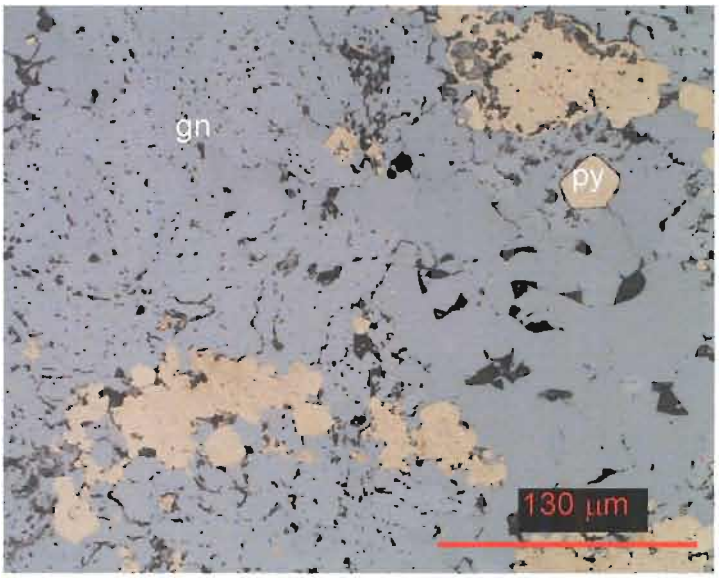

(c) Specimen 129.8B

Photomicrograph of euhedral and relict framboidal pyrite in galena.

Top right of shows atoll structure after framboid.

Pentagonal* pyrite marked.

Reflected light.

* The pyrite may have an unusual cut, although Endo (1960) mentions the existance of pentagonal pyrite, and that it has a higher sulfur supersaturation than octahedral pyrite

Plate 4.2 Framboidal Pyrite

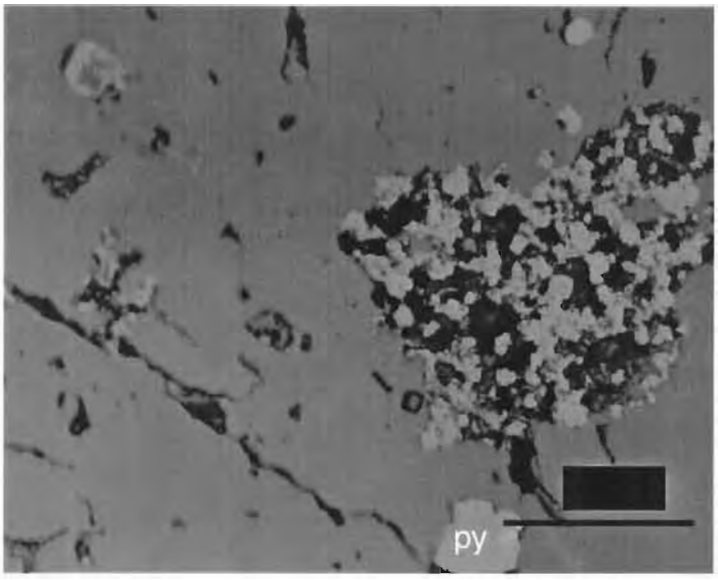

(a) Specimen 129.8B

Photomicrograph showing remnant euhedral pyrite grains embedded in galena.

Partial dissolution of grains or framboids, with etched appearance.

Reflected light.

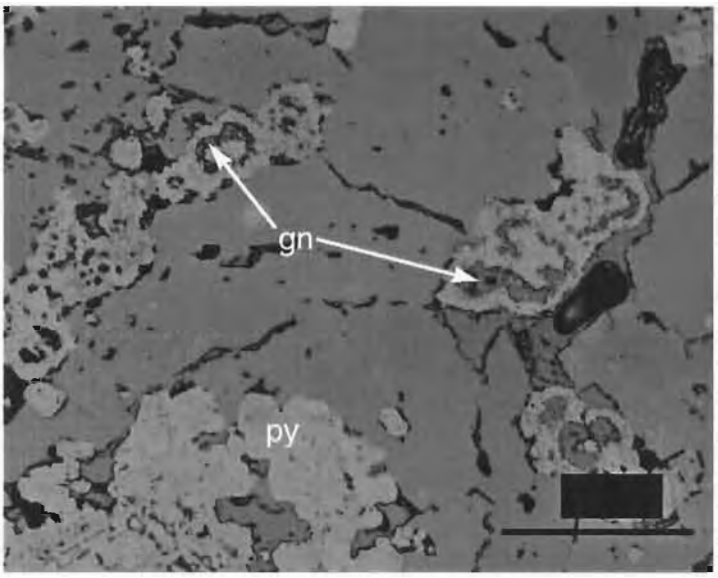

(b) Specimen 129.8B

Relict pyrite atoll structures in idiomorphic galena.

Bottom left small euhedral pyrite clusters.

Reflected light.

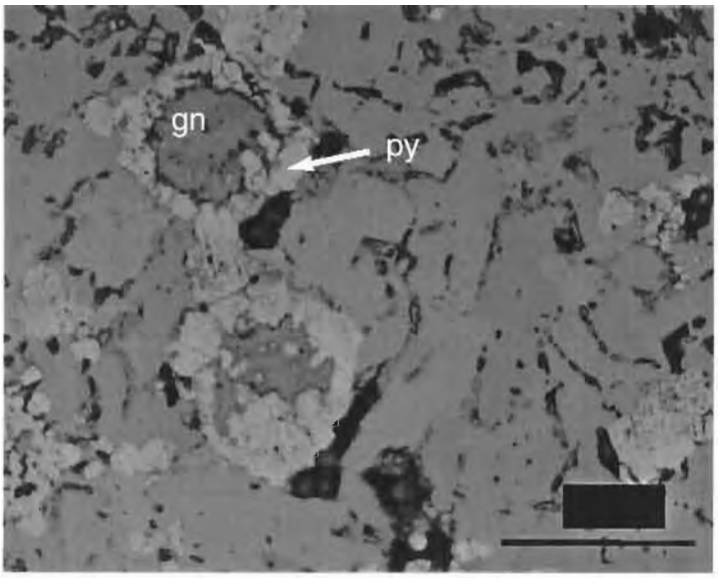

(c) Specimen 129.8B

Photomicrograph of pyrite and galena.
Relict framboids of pyrite with core replaced by galena.

Reflected light.

Plate 4.3

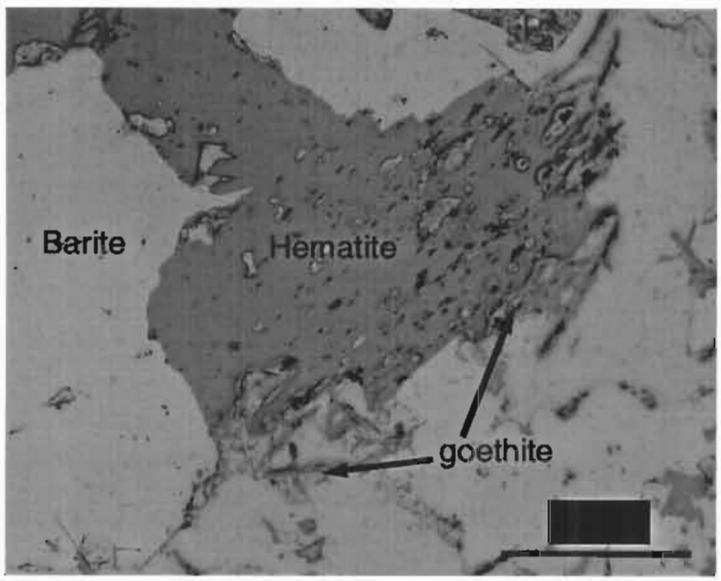

(a) Specimen G4

Photomicrograph of goethite (blue) replacing hematite (orangish-brown).

Triangular pits in hematite indicate the grain was pseudomorphed from galena.

Reflected light.

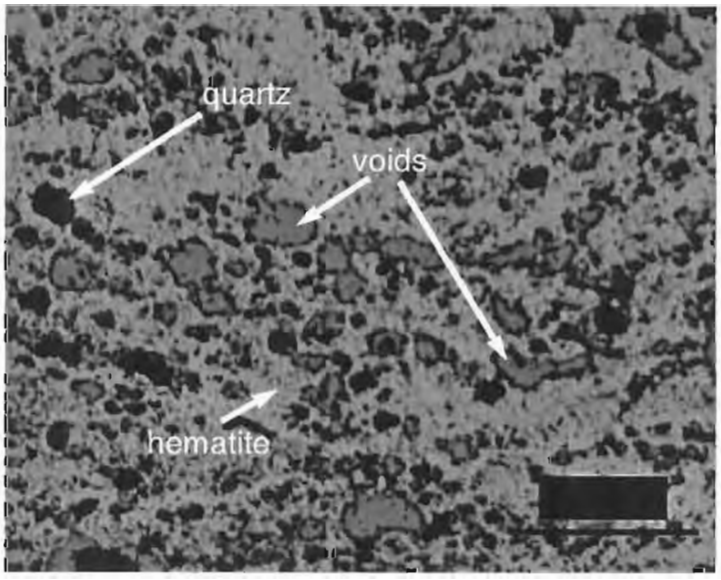

(b) Specimen G3

Photomicrograph of porous cellular-sponge textured hematite boxwork.

Quartz replaces disseminated pyrite, i.e. voids.

Reflected light.

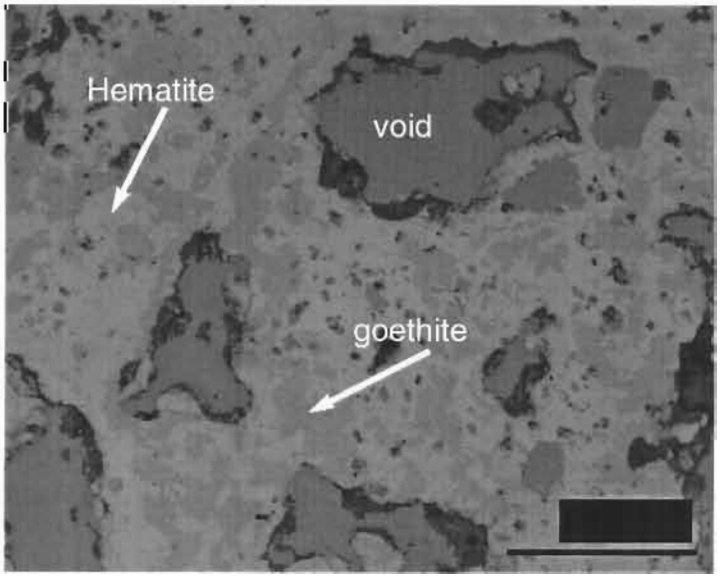

(c) Specimen G3

Etched/irregular voids after sulfide grains.

Intimately intergrown hematite (lighter colour) and goethite (darker colour).

Reflected light.

galena, 20% sphalerite, 50% pyrite and 30% gangue. Galena shows network dissolution texture, which is a texture of etching along cleavages into the host (ie galena). Pyrite also exists as cubic and euhedral masses in some bands, and mostly replaced by barite which is pale grey with a well defined cleavage.

Thin section 175.5c

This section contains various types of pyrite morphology; colloform pyrite, acicular or needle shaped pyrite, euhedral pyrite and irregular pyrite. In up to 10% of pyrite aggregates chalcopyrite disease is present. The chalcopyrite is in two forms; as dendritic meandering filaments, and as concentric zoning of pale blue and blue rings over pyrite. The pyrite containing the chalcopyrite disease is embedded in sphalerite, and is this type of pyrite is fractured and has irregular but smooth grain boundaries.

Thin section RVD017

Fine grained laminated potassium feldspar at the bottom part of the slide, passing into a pyrite rich band. The pyrite band has fine crinkly laminations at the top surface of individual laminations. Overall the section consists of 5% euhedral pyrite, 30% laminated pyrite 30% sphalerite (irregular, infilling textured), and the remainder is feldspar, and minor (less than 5%) quartz.

Thin section 129.8B

Thin section 129.8B shows a combination of varied and unusual features. This thin section contains abundant core and atoll structures of pyrite (see plate 4.2 b,c). Pyrite framboids have had the cores replaced by galena to produce the atoll structures. Zoning around cores of pyrite is a common textural feature of the larger crystals (see plate 4.1 a) as well as patchy replacement of individual crystals that make up the framboids as seen in plate 4.2 a. The gangue is predominantly irregularly shaped infilling barite. The sphalerite is a 'clean' homogenous simple type, though it has an irregular morphology.

Specimen BMR2 270

BMR 270 contains a section of black carbonaceous, thinly laminated siltstone with a speckly appearance of disseminated pyrite throughout. Pyrite consists of less than 5% of the total content of the section, with euhedral crystals less than 20μm in diameter.

4.2 Textures at Surface

Sulfide-ore derived textures observed in the field are varied and are discussed below. Gangue mineralogy is less varied and is outlined at the end of this section.

4.2.1 Pyrite

- *bladed/acicular hematite (a texture of specular hematite)*

Clusters of hematite blades range from 15-120μm long and 3-20μm thick, and occur in the gossan. The blades occur as aggregates and as isolated crystals. Isolated blades are thinner, needle like and have smaller dimensions than blades which occur in dense pockets. Usual dimensions for an isolated crystal are less than 5x15μm. The blades are often associated with barite.

- *boxwork texture*

Euhedral voids from pyrite are seen, with a minor amount (usually more than 15%) are infilled with barite or quartz. The voids are often 'craggy', having irregular/jagged perimeters.

- *framboid replacement textures*

Framboid textures are evidenced by spherical replacement rims, the rims are the remnants of pyrite after the core has been replaced and the rims have been replaced with bladed hematite, as recorded by plate 4.6.

- *platey hematite*

This texture is only noted in the gossan and does not have an analogue in the core. It is found in small aggregates (refer to plate 4.6). The 'plates' are usually of equal size (25μm) with smooth edges of varying number of sides.

4.2.2 Other minerals

Textures from other sulfide ore minerals were not identified in thin section, as generally, boxworks have not been preserved.

Gangue minerals at the surface include opaline silica, amorphous silica, quartz, barite, clays and phengite (a low aluminium muscovite, recorded by PIMA analysis on specimen K1, and white mica was also referred to by Jenkins et al, (1998)).

4.3 Thin section Descriptions of Surface Samples

Thin section G4

This specimen collected from within unit 1b

This section shows bladed hematite and platey hematite. The rock is 60-70% hematitic gossanous material with 'pods' of jarositic-type material (3x1cm). The platey hematite only occurs in the hematitic/gossanous material. The bladed hematite is common in both the hematitic and jarositic pods, and less abundant in the jarositic pods. The bladed hematite has is partly replaced by goethite, evidenced by blue tinge in reflected light. The thin sections was cut from a rock from gossan unit 1b.

Thin section J2

This specimen from unit 1a.

The slide is a section of material cut from specimen J2, on the hematitic-jarositic boundary (as seen on plate 3.9 a). The hematitic portion, shows 80% opaques in transmitted light. These opaques are made up of irregularly oriented bladed hematite as infills between colloform textured hematite. There is bladed hematite throughout with blades becoming longer and flake/platey textured in more hematitic layers, and infilling of fractures with barite. In the jarositic-rich pods, the jarosite has a thin dendritic texture that appears to replace hematite. Euhedral shaped voids after pyrite are outlined by bladed hematite which is usually parallel to void surface. When bladed hematite is growing in free space, infilling voids the texture is a radiating inwardly, as shown in plate 4.5.

Thin section NG001

This specimen from unit 2a

The specimen has alternating white and purple bands as seen in plate 3.10 (c). In reflected light the white-grey bands have a very fine-grained well-meshed, mutual grain boundary texture, with little or no porosity. White bands are almost 100% opaline silica, and the

Plate 4.4 Bladed Hematite in the Gossan

(a) Specimen G5

Photomicrograph of relict bladed hematite along a barite grain boundary within the gossan. Emulsion textures are displayed by barite.

Reflected light.

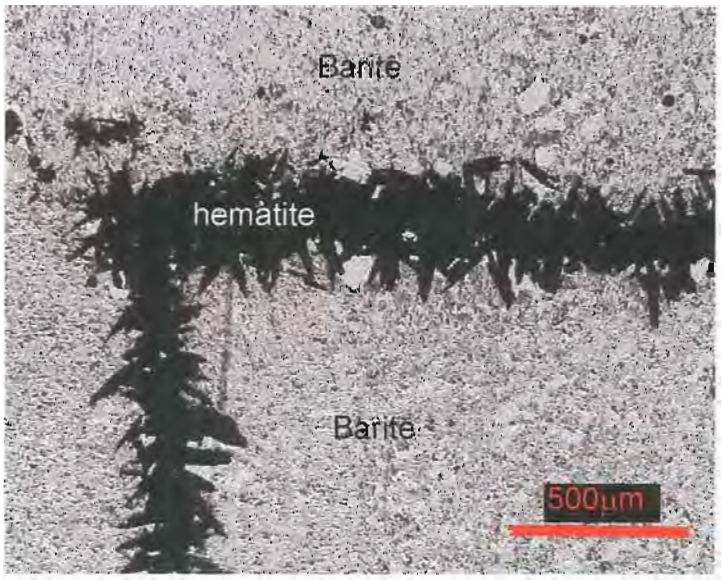

(b) Specimen G5

Bladed hematite (specularite) within barite grain boundaries. Barite shows emulsion textures (Schwartz, 1951).

Transmitted light

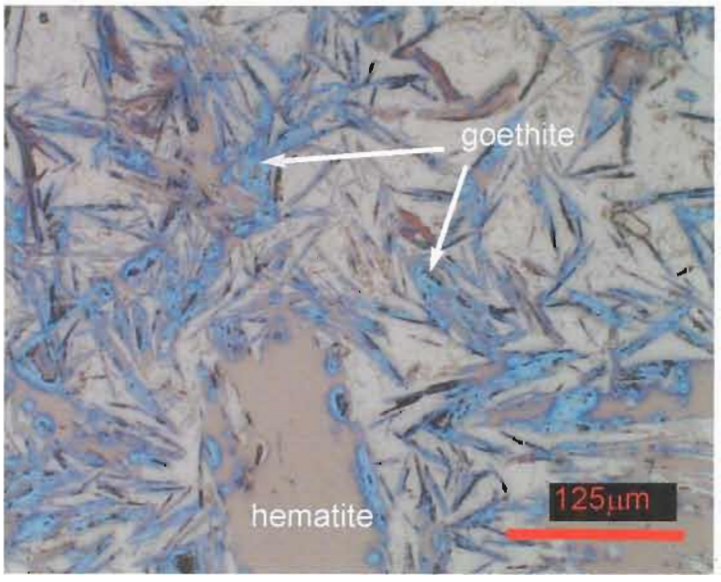

(c) Specimen G4

Acicular/bladed of hematite and goethite with randomly orientations within the gossan.

Reflected light.

Plate 4.5 Framboid Structure In Gossan

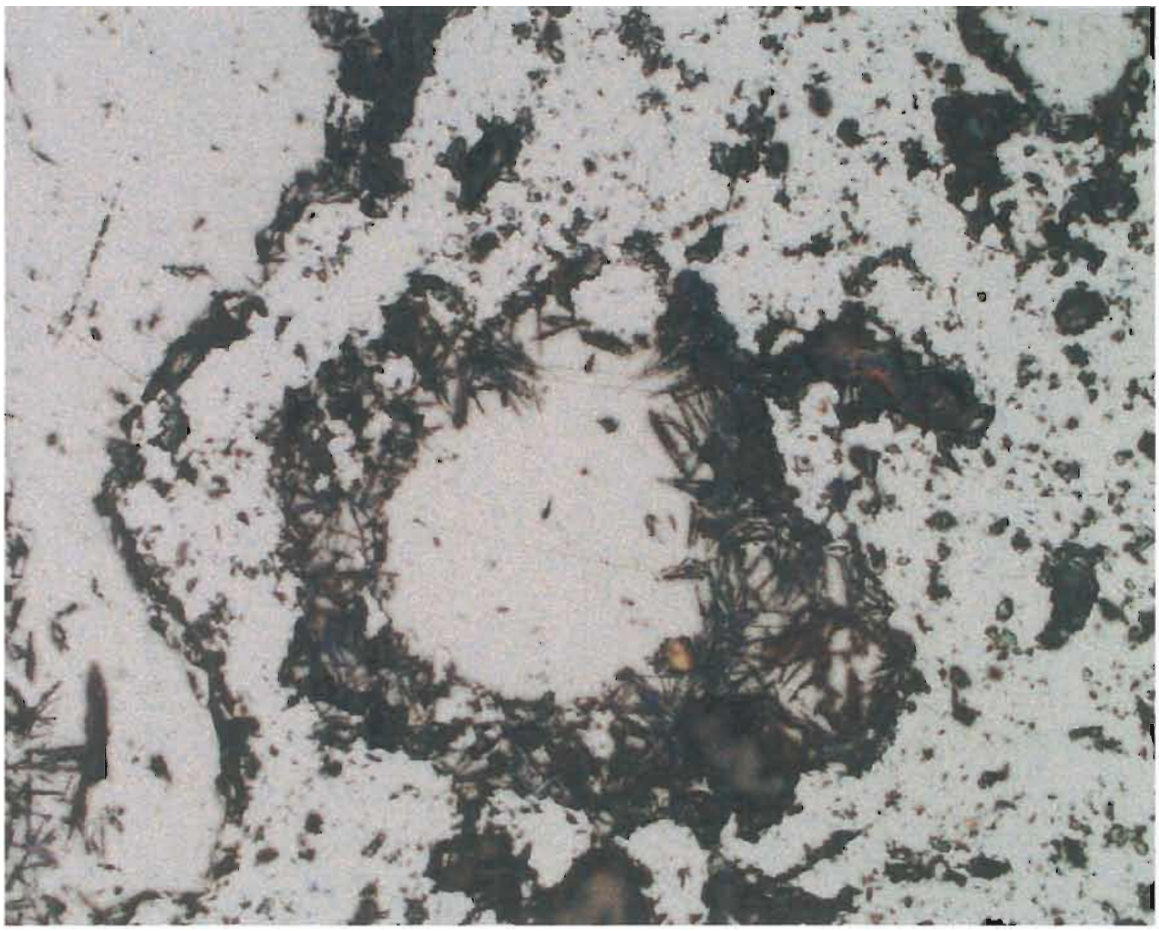

Thin section of specimen G2 showing rim and core replacement of pyrite framboid. The core is replaced with barite.

Plate 4.6 Platey Hematite

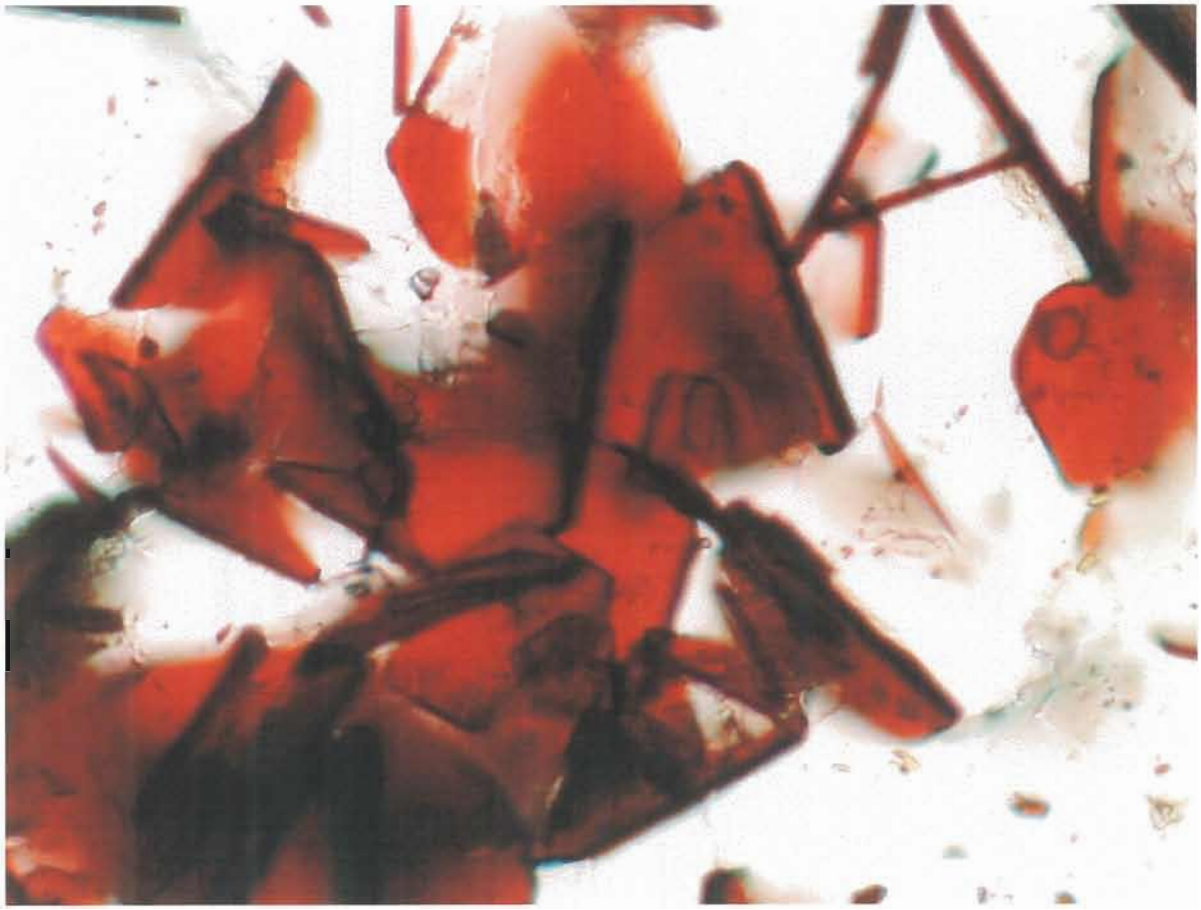

Thin Section of Specimen G4 Transmitted Light Field of view 100μm

Plate 4.7 ESEM Scale Textures

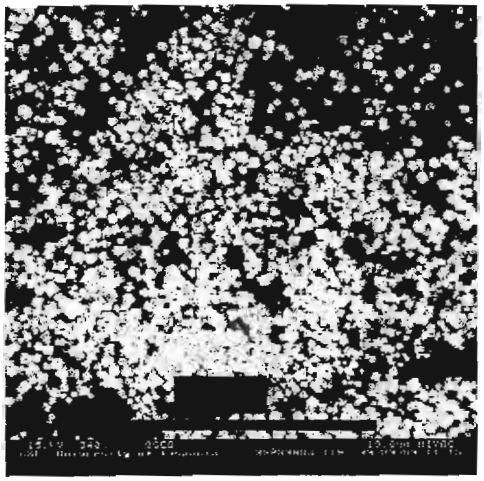

(a) Thin section 175.5B

ESEM phtomicrograph of euhedral pyrite aggregation in feldspar

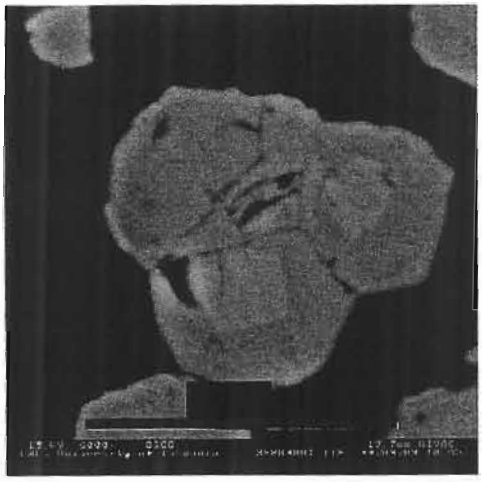

(b) Thin section 175.5b

ESEM phtomicrograph of subhedral mantling of pyrite showing thin zoning.

(c) Thin section BMR 2

ESEM phtomicrograph of crystalline carbonate (siderite) with octagonal pyrite.

Plate 4.7

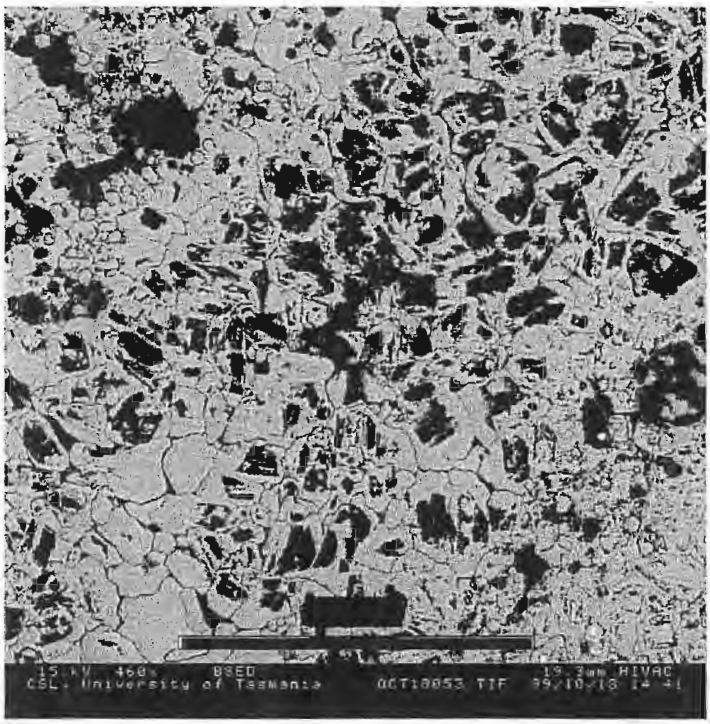

(d) Microscopic boxwork texture possibly after Pb carbonate, the cell outlines are 'ridged' or thick, and the shape is similar to the platey, mutual grain boundary type texture, pyrite (middle left).

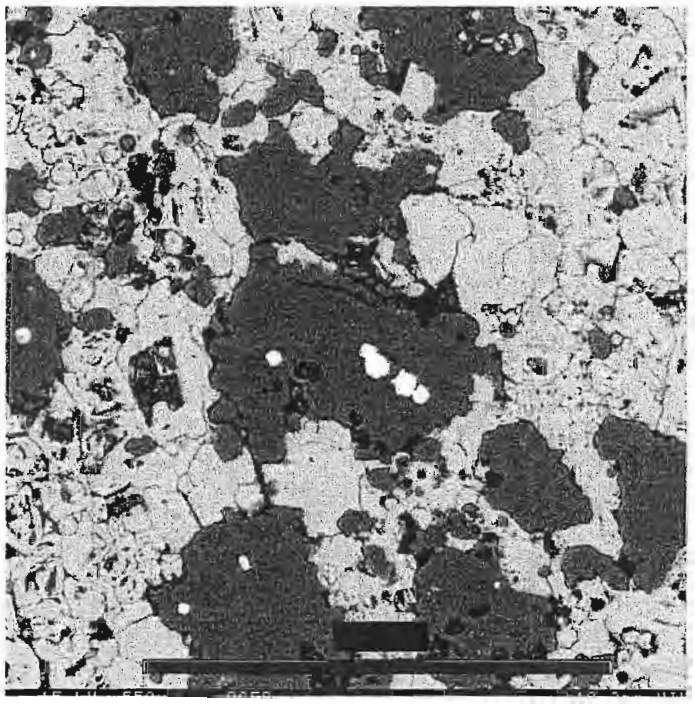

(e) Mutual grain boundaries of carbonate (pale), quartz (grey) and ferroan carbonate (Mg rich siderite).

Plate 4.7

(f) Thinsection, specimen G2

Voids encrusted with acicular hematite.

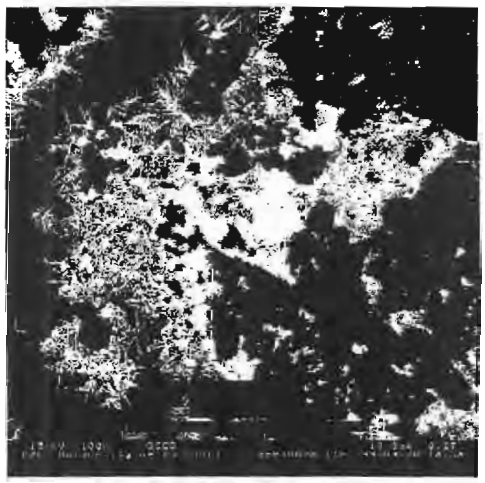

(g) Thin section, specimen G2

Acicular/bladed hematite radiating out into free space.

(h) Thin section, specimen G2

Pyrite (top right) and fibrous hematite needles.

purple bands have greater than 75% silica which is slightly more crystalline and contains (20% surface of section) specs of hematite.

4.4 Electron Microscopy

The Environmental Scanning Electron Microscope (ESEM) was used at the CSL at the University of Tasmania for very fine scale detection of textures and for qualitative geochemistry of individual minerals.

The ESEM confirmed textures seen by the microscope and brought to light additional information for barite, opal and jarosite. It was found that for sample K1, with the electron beam on a (white) opal and phengite pod (hand specimen shown plate 3.9 b), that some pyrite laths 5x1μm are disseminated in the opal.

Jarositic specimen 135m (plate 3.10 b) shows on an SEM scale that barite pseudomorphs pyrite. Much of the specimen consists of equant intergrowths, showing a mutual grain boundary texture.

Thin section BMR 2 has a band 2cm long of thinly laminated potassium feldspar determined by the electron back-scattered detector that acquired peaks for K, Al, SiO_2 and Ti. A relationship was found between K and Ba. It was observed that some quartz grains in the feldspar were mantled in zonations of alternating high K, low Ba and low K, High Ba layers. The sample also contained carbonates. Carbonate in thin sections from core was usually a high iron, high manganese carbonate, or a manganosiderite.

Textures specific to ore minerals are shown in plates 4.1, 4.2 and 4.7. These are octahedral and euhedral pyrite in core (4.7 a), showing the mantling of pyrite (4.7 b). Plate 4.7 a shows microscopic (10μm) boxworks after equant sulfide grains, and shows an infilling of voids after sulfide grains, leaving patchy irregular grain boundaries.

Plate 4.8 c shows bladed hematite on three scales. The blades are radiating into free space in the boxwork texture of plate 4.7 (f) plate 4.7 (g) is a magnification of the microphotograph before, and plate 4.7 (h) shows a detail of the blade structures, with remnant pyrite.

An unexpected find in the core material worth further investigation is the presence of a light rare earth element mineral (REE), monazite. The monozites were detected in feldspar layers in thin section BMR 2. They were detected because they appear significantly lighter coloured than pyrite and galena, and 5μm in size which is large enough for microprobe analysis. Mineral density and visual 'lightness' on the SEM screen are inversely proportional. The monozites showed up particularly luminescent, with an irregular shaped/infilling texture, and a spectra from the back scattered detector with La, Ce, Pr, Nd, Sm, Gd, P, O, and Si peaks.

4.5 Discussion

Pyrite is most texturally variable, which may be a function of its dominant presence in the ore within a range of gossan forming conditions. Pyrite morphology is commonly euhedral, with the smallest grains generally octahedral and sometimes cubic. The coarse grained cubic variety of pyrite discussed by Jenkins *et al,* (1998) is associated with coarse-grained barite, sphalerite and galena. Galena has a close association with the coarse-grained barite, pyrite and sphalerite (Jenkins *et al*, 1998). Galena associated with breccia may be replacing dolomite in a similar style to Hilton and Mt Isa deposits (Perkins and Bell, 1998), and dolomite is a common lithology within the massive sulfide zone.

Sphalerite has a laminated and anhedral texture in core. The sphalerite has been observed in two kinds; laminated and as anhedral fillings, and it is interpreted that the pale honey coloured irregular/infilling type has a low iron content and is associated with barite breccia (Jenkins *et al*, 1998). This darker coloured sphalerite occurs after the laminated sphalerite, and is probably produced by remobilisation of laminated sphalerite in the ore.

Monazites can be useful for dating purposes, as they are geochemically sensitive to changes in conditions (diagenetic or weathering processes for example), so that timing of the supergene enrichment process (gossan formation) might be dated. Monozites also evidence temperatures of formation as they are found in a narrow temperature window before breaking down (Dr D. Steele, *pers. comm.*, 1999). Monazites are not usually associated with sedex style deposits or weathering processes in particular. It is suggested that monozites are affected by pH (McLennan, 1989). The dispersion of minor and trace

elements during arid weathering (eg. leaching of Zn from upper horizons) may also be linked with REE *accumulation* in lower horizons (C R M Butt, 1999).

The most unusual texture derived from pyrite are the framboids, which are observed in core and in the gossan. These textures and styolitic laminations in silicified algal; chert (See plate 3.4 (b), although this specimen was chosen to show microfaulting, fine wriggly laminations preserved in this unit, 3b. This rock type (within unit 3b) is interpreted to closely match the core analogue. They are barren inter-sediments (within the massive sulfide zone) as noted in the drill log, and the core is carbonaceous in parts, and contains potassium feldspar. The surface expression is interpreted to be a silicified algal chert.

In summary, the core textures repeating at gossan are: *sedimentary textures* (laminations as previously mentioned), *irregular microscopic boxworks* after pyrite from voids created by dissolution of the core and replacement of the rim (as for plate 4.7 a), *whole replacement* (plate 4.7 b), by barite, iron oxides, or quartz, and *framboids*, plate 4.5.

Chapter 5 Geochemistry

5.1 Introduction

This chapter examines the geochemistry of rock types surrounding the Grevillea gossan (figure 2.6). Geochemical data previously collected by North Ltd (1994) was available for this study. The relevant drillhole geochemistry data and logs, and rock chip geochemistry of surface samples are provided in appendix 2, 3 and 4.

This study focuses on regolith rock types analysed by XRF, XRD, ICPOES, PIMA, electron microprobe and FTIR techniques. The results were compared with the data from North to examine geochemical anomalies at surface and related to the base-metal sulfide body at depth. Additionally, regolith geochemistry helped clarify relationships between rock types derived from the weathering of the ore and element affinities at surface.

5.2 Sample Preparation

5.2.1 XRF (X-ray Fluorescence)

Six samples were analysed for major elements using the Phillips XRF instrument at the Earth Sciences Department at the University of Tasmania. Half the samples were representative of material at the gossan (G3, G4, NG003), and the other half were of a jarositic rock type which is common around the gossan (135m, 175m, J1). Samples were crushed to ~0.5cm^3 chips and unrepresentative chips were removed prior to milling to talc texture (hematitic samples needed at least 3 minutes milling time whereas the jarosite material needed about 30 seconds for talc consistency). An iron-mill was used which was cleaned between samples by milling with silica followed by washing and drying.

5.2.2 XRD (X-ray Diffraction)

Ten samples were selected for XRD analysis to confirm mineralogy of the key samples of (i) gossanous hematite and goethite and (ii) jarosite and (iii) leached and bleached rock types near the gossan (containing high opaline or amorphous silica, samples 'opaline', and 'amorphous'). The gossanous/hematitic samples (G2, G3, G4, NG003) and siliceous jarositic material (130m, 135m, 175m, J1) were milled in an iron mill, and the softer

material was powdered with a pestle and mortar. The X-ray Diffractometer at the Chemistry Department was used by technician Dr Peter Traill.

5.2.3 ICP-OES

(Inductively coupled plasma-optical emission spectrometry)

This solution-based technique was used to complement XRF and XRD data. XRF was suitable for major element analysis and ICP-OES (IC587 triple acid digestion method) was used for trace element analysis. The technique has a detection limit of about 1-5ppm for most elements, with good precision (~1%). The analysis on six key samples (same samples as for XRF) was outsourced to ALS laboratories. Samples were prepared as for XRF. Ag, Cd and Tl were analysed by ICP-MS by the same laboratory. Rock chip geochemistry for surface traverses 15150 and 15200 were also analysed by the IC587 triple digestion method.

5.2.4 PIMA and FTIR Spectrometry Techniques

These techniques use MIR wavelength. PIMA measures spectra of reflected radiation in the 1300-2500nm range and the FTIR covers a much larger spectral range from 66-25000nm. A broader spectral range has potential for determining a wider range of minerals, however, FTIR has limited applicability for cation studies, as heavy cations are too broad in the spectrum to be identified precisely. Still, FTIR is useful for determining if rocks contain carbonates, sulfates, other anions, organic components, and silica crystallinity.

5.2.5 FTIR (Fourier Transform Infra-red Spectrometer)

The FTIR required pulverising and pressing into KBr to make discs about 0.5mm thick. Trial and error was used to determine the concentration of sample needed for the FTIR run. It was found that the hematitic samples were such strong absorbers and less material was needed (~50mg) compared to the jarosite samples (~150mg). FTIR was carried out using the CSL laboratory's Bruker IFS66 infrared spectrometer under the supervision of Dr G. Rowbottom.

5.2.6 PIMA (Portable Infra-red Mineral Analyser)

PIMA uses reflected (sample surface) radiation in the short wavelength infrared (SWIR) from 1300-2500nm. PIMA was ideal for light coloured samples, but could not be used on dark, opaque gossanous material. There was no sample preparation for PIMA as the instrument was applied directly to the surface of the sample. Samples analysed were NG001, NG002, NG004, RD43, RVD005a and S2.

5.3 RESULTS

5.3.1 XRF

XRF data is displayed in figure 5.1. Graphs showing relations between elements and trends within rock types are presented in figures 5.2 – 5.8. The elements plotted highlight the differences and the trends between elements and the partition of elements between the hematite-goethite mixture (gossanous material) and jarosite type minerals (adjacent to the gossan). The elements plotted are generally oxides produced from the XRF technique.

Elements Variance

Pb

The first thing to note is that there are two orders of magnitude difference between iron oxides and one of the most useful pathfinders, lead. Pb ranges from 0.03-0.05 wt% in the hematite (gossanous samples). Pb is also an order of magnitude higher in the jarosite and ranges from 0.1 to 0.38 wt%.

Zn

Zinc is present in concentrations near or below a range which can be expressed as weight percent. Two jarosite samples are below the detection limit of 0.01wt%, and all hematite samples are at the 0.01 wt% level.

Cu

Copper is below the detection limit of the XRF.

XRF ANALYSES

11/10/99 UNIVERSITY OF TASMAINIA SCHOOL OF EARTH SCIENCES ANALYST P.ROBINSON
SAMPLE AND IGNITION LOSSES RUN IN DUPLICATE

SAMPLE	SiO2	TiO2	Al2O3	Fe2O3	MnO	MgO	CaO	Na2O
135m	19.12	0.12	1.19	36.06	<0.01	0.08	<.01	0.13
175m	29.47	0.06	6.2	29.87	0.01	0.07	0.04	<0.05
J1	16.38	0.09	0.19	37.55	<0.01	0.12	<0.01	0.17
G3	28.80	0.03	0.49	86.93	<0.01	0.42	0.01	<0.05
G4	37.04	0.03	0.47	54.89	<0.01	0.02	<0.01	<0.05
NG003	24.5	0.31	0.7	71.8	<0.01	0.02	<0.01	<0.05

SAMPLE	K2O	P2O5	S	Ba	Cu	Pb	Zn	1000 Degree Loss
135m	6.92	0.07	10.09	0.12	<0.01	0.1	<0.01	32.41
175m	2.95	0.54	6.04	6.06	<0.01	0.38	0.01	19.64
J1	6.68	0.24	10.27	1.08	<0.01	0.32	<0.01	33.23
G3	0.04	0.15	0.36	0.59	0.01	0.05	0.01	7.56
G4	0.01	0.15	0.91	3.22	<0.01	0.06	0.01	1.68
NG003	0.05	0.9	0.06	0.13	0.01	0.03	0.01	2.16

Figure 5.1 **XRF Data**

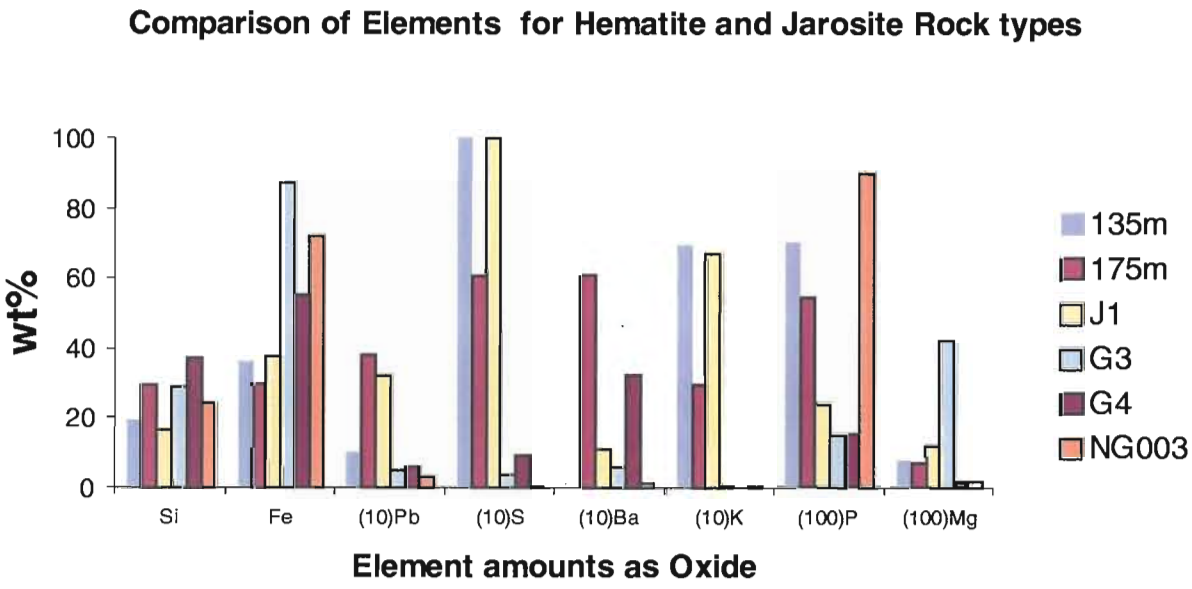

Figure 5.2 General comparison of element abundances

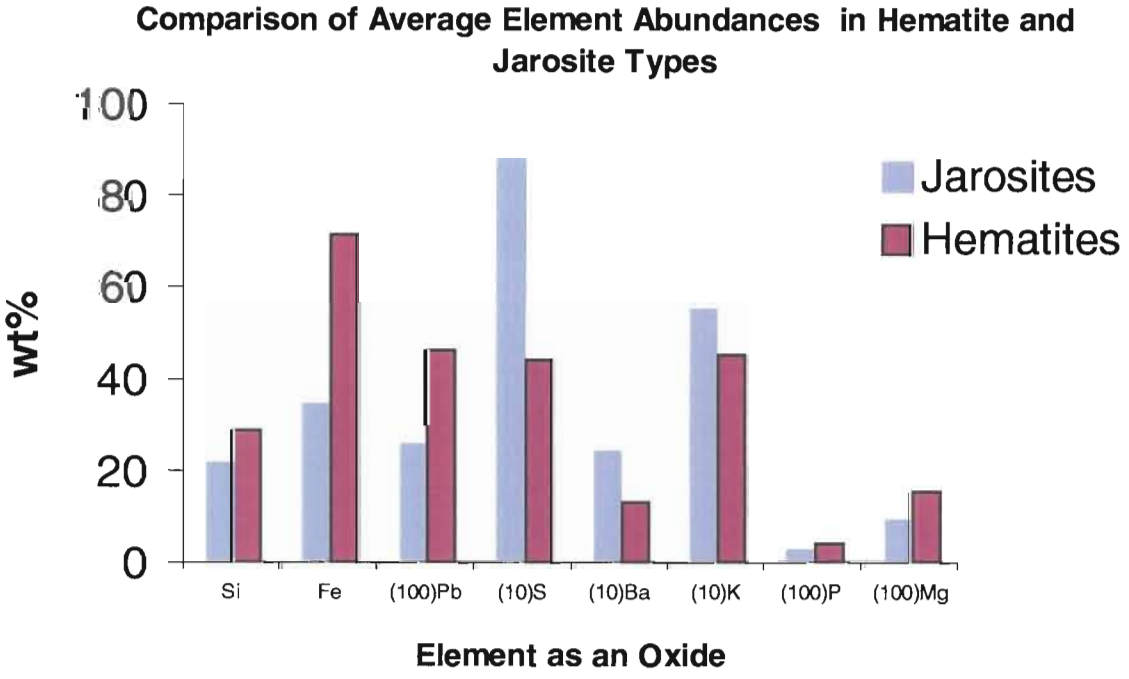

Figure 5.3 Jarosite and Hematite

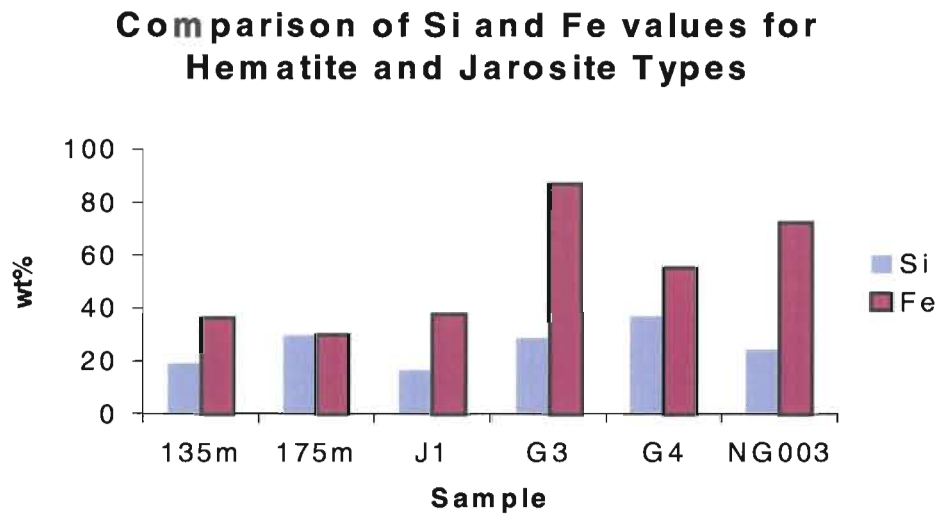

Figure 5.4 Major-elements (Si and Fe) Trends in Jarosite and Hematite-types

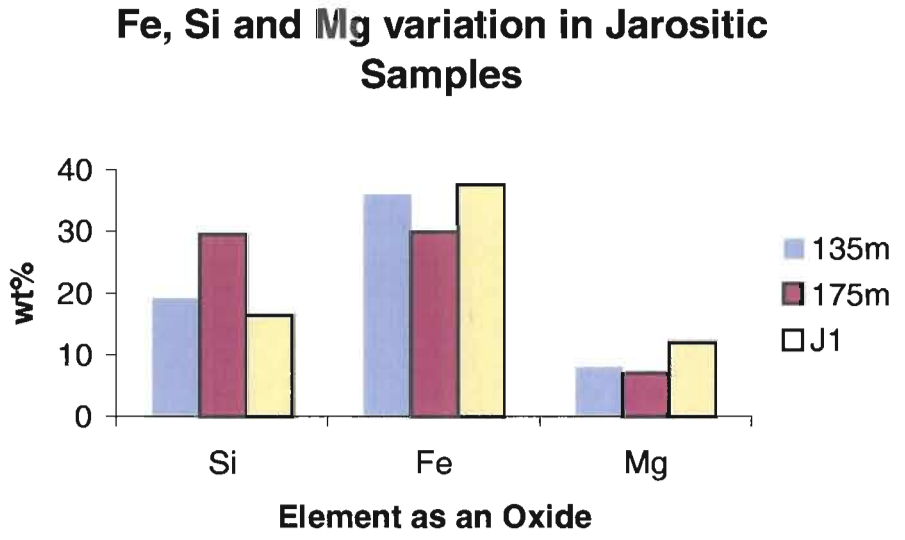

Figure 5.5 General trends of Fe, Si and Mg in Jarositic samples

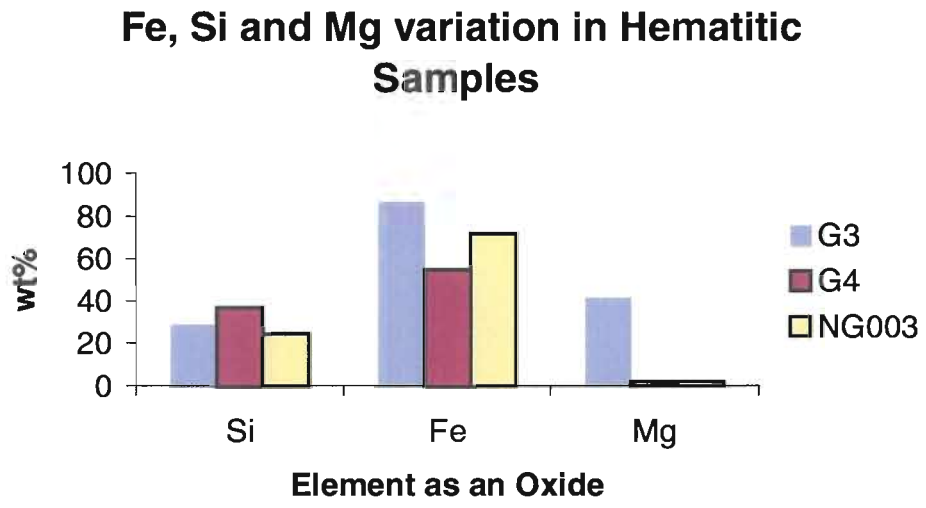

Figure 5.6 General trends of Fe, Si and Mg in Hematite type rocks

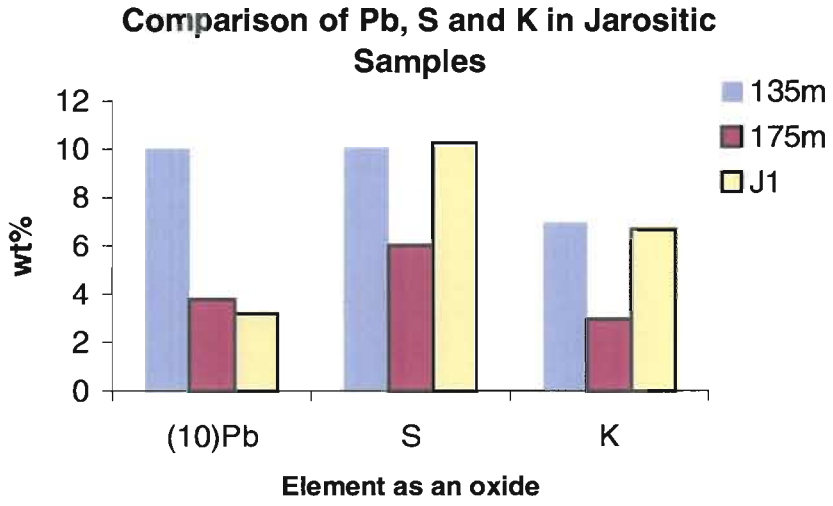

Figure 5.7 Pb, S and K variation in Jarosite type rocks

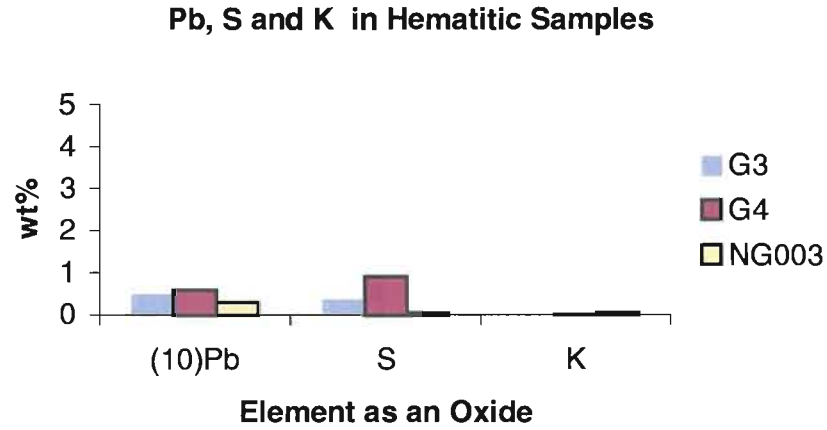

Figure 5.8 Pb, S and K variation in Hematite type rocks

Na and Ca

Sodium and calcium have higher values in the jarosites than in the hematite samples, though generally in the same order of magnitude and low overall. Ca and Na for hematite are lower than 0.05 wt%, and Ca for the jarosites range <0.01wt% to 0.04wt%, and <0.05-0.13 wt% for the sodium.

Fe and Si

Figure 5.3 shows higher concentrations of Fe in the hematite than the jarosite. The Fe-oxide ranges from 29.87-37.55 wt% in the jarosite and 53.89-71.8 wt% in the hematite. Silica varies according to the iron content, and it is higher overall for the hematite rock types. Over both rock types the silica lies between 19.12 and 37.04 wt%.
Figures 5.4 and 5.5 show the relationship between silica and iron in jarosite and hematite. Mg is also included and may be higher in the jarosite samples. Pb, S and K were grouped for plots of hematite and jarosite to show that S and K are markedly higher in the jarosite as is expected by the mineralogy but that the Pb is also significantly enriched in the jarosite. Al also appears enriched slightly in the jarosite. Ti, Mn, Ca, and Ba are inconclusive for these samples by this data alone.

Trends

Overall comparison of element variation is plotted in figure 5.2. Specifically, XRF reveals the following: -

Comparing jarosite and hematite;

- Jarosite contains significantly higher concentrations of sulfur and potassium as expected (figure 5.7 and 5.8), and hematite contains 34.5% more Fe on average than jarosite (figure 5.5 and 5.6)
- Jarosite contains significantly more lead than hematite (on average 82.5% higher in jarosite)
- Silica and iron appear to have a direct positive relationship – both are elevated in hematite, on average silica is 28% higher in hematite for the samples (figure 5.4).

Comparing jarosite samples;

Although the sample base is limited the following differences emerged:

- J1 has slightly higher Mg, S and Fe than the other jarosites (figures 5.5 and 5.7).
- Sample 175m contained more Pb than all samples, and had less S than the other jarosite types (figure 5.7).

Comparing Hematite Samples

- G3 has the highest Fe at 86.93% iron-oxide content (figure 5.4).
- There may be a correlation between S and Pb. For the hematites G4 has both the highest levels of Pb and S. (figure 5.8).

Summary and Discussion

The major element variations for gossan grab samples are

(i) K and S are higher in the jarosite and Fe oxides are enriched in the hematitic samples, reflecting the mineralogical differences between the samples

(ii) Pb is enriched in jarosite versus hematite in all samples. Jarosite acts as a sponge to Pb. Jarosite mineralogy allows 'impurities' such as P and Al to substitute into the lattice. Sample 135m is the most common type of jarosite at Grevillea, and it contains substantially higher amounts of Pb with a lower K value compared to 135m and J1. For a jarosite to convert to a plumbojarosite it needs to substitute K in the ratio K:Pb=2:1. Jarosite is $[KFe_3(SO_4)(OH)_6]$, and this has converted to a plumbojarosite $[Pb_{0.5}Fe_3(SO_4)_2(OH)_6]$. Additionally, for sample 175m may have another mineral hosting the Pb as this sample is lower in S and K needed for jarosite although it is elevated in Pb.

(iii) Pb is traditionally an indicator element of base-metal sulfide deposits, and Pb retention being favoured in jarosite may be an additional consideration in geochemical exploration to explain anomalies at a distance from the gossan.

(iv) It was not expected that the hematite would show minor enrichment in Mn which commonly accumulates gossans.

(v) There is a correlation between Fe and Si for gossanous material.

(vi) J1 which is associated with veining, and is derived from a fault zone area. It is elevated in Mg, S and Fe.

5.3.2 XRD

The traces resulting from the XRD spectra were so noisy that I enquired to Dr Graham Taylor who has done XRD studies of gossans from the Mount Isa Inlier and he kindly offered to run and confirm the spectra at CSIRO Adelaide. The original traces, though noisy were confirmed as jarosite +silica, and hematite + silica with every peak accounted for. Tables were used to compare relative count intensity of the 'unknowns' to known mineral intensities at a D-value with an error of ±0.06 dA (Dr P Traill, pers. comm., 1999) taken into account. The samples had a good correlation between theoretical peak heights and positions for the respective minerals, and the samples fall within the ±0.06 dA variance. Tables and traces are provided in appendix 5.

Hematite Samples

Samples G2, G3, G4, NG003 were run with reasonably sharp traces from G2 and G4. The three largest peaks in G3 and NG003 give a hematite signature above background noise.

Sample	XRD Mineralogy	Reference
G2	Goethite +hematite + α-quartz	Refer to figure 5.3 (a)
G3	Hematite + α-quartz	Too noisy- not presented
G4	Hematite + α-quartz + goethite + jarosite	Refer to figure 5.3 (b)
NG003	Hematite + α-quartz	Too noisy- not presented

Table 5.1 XRD mineralogy

Sample G2

The trace has sharp peaks identifying a goethite-quartz-hematite mixture.

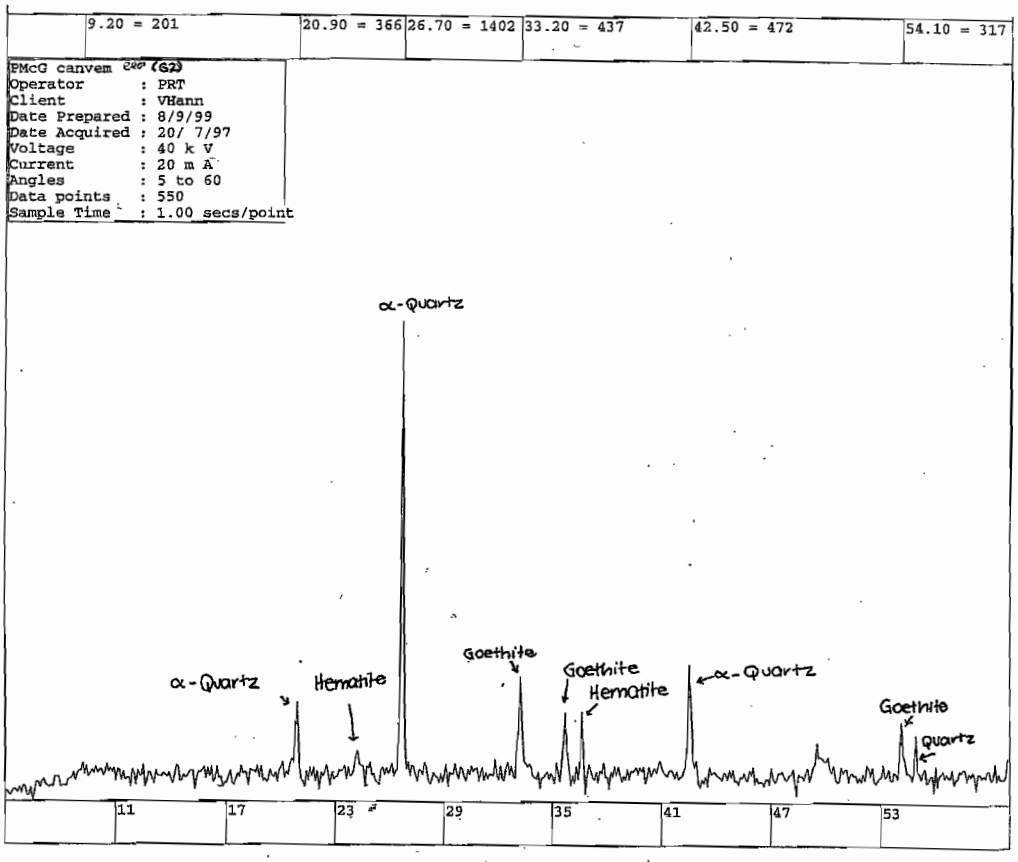

Figure 5.9 G2 XRD trace

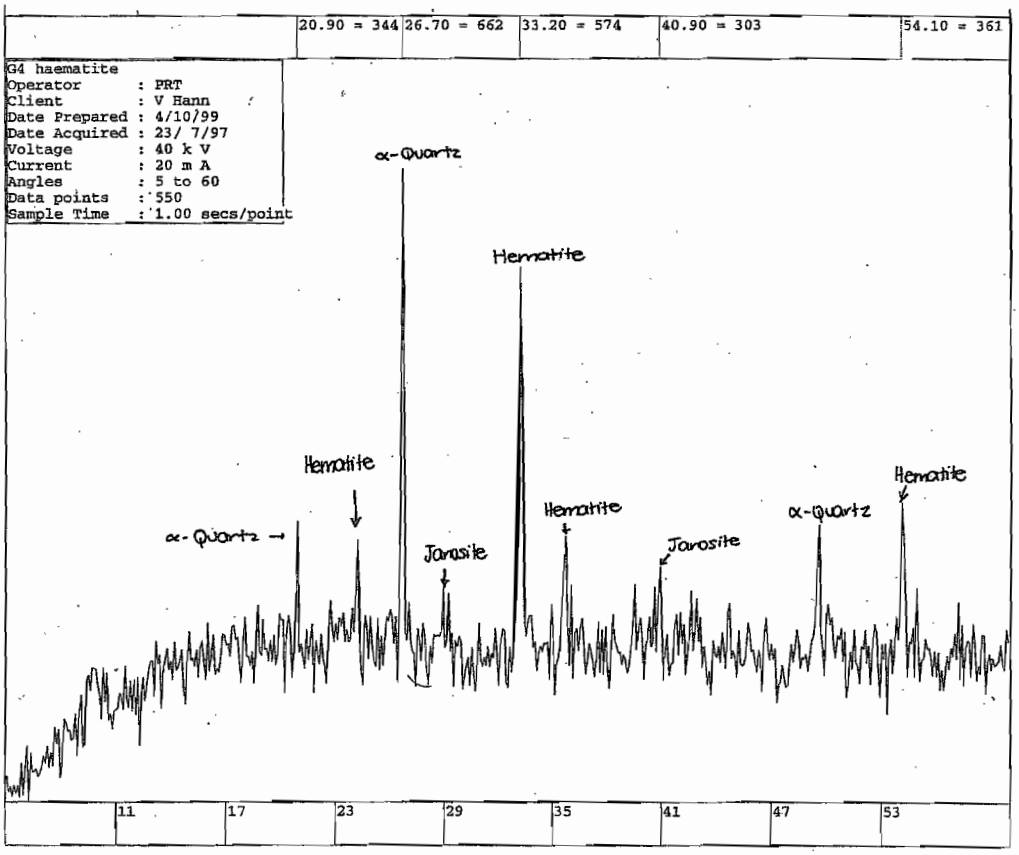

Figure 5.10 G4 XRD trace

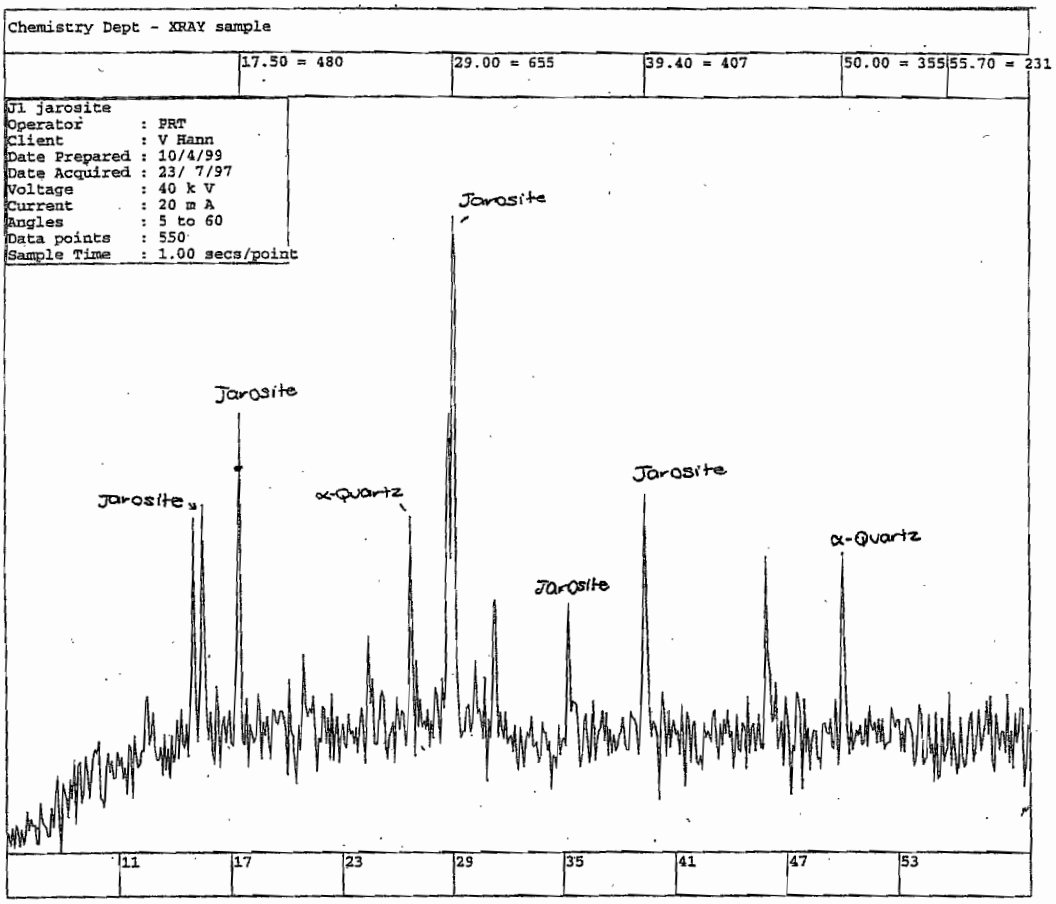

Figure 5.11 J1 XRD trace

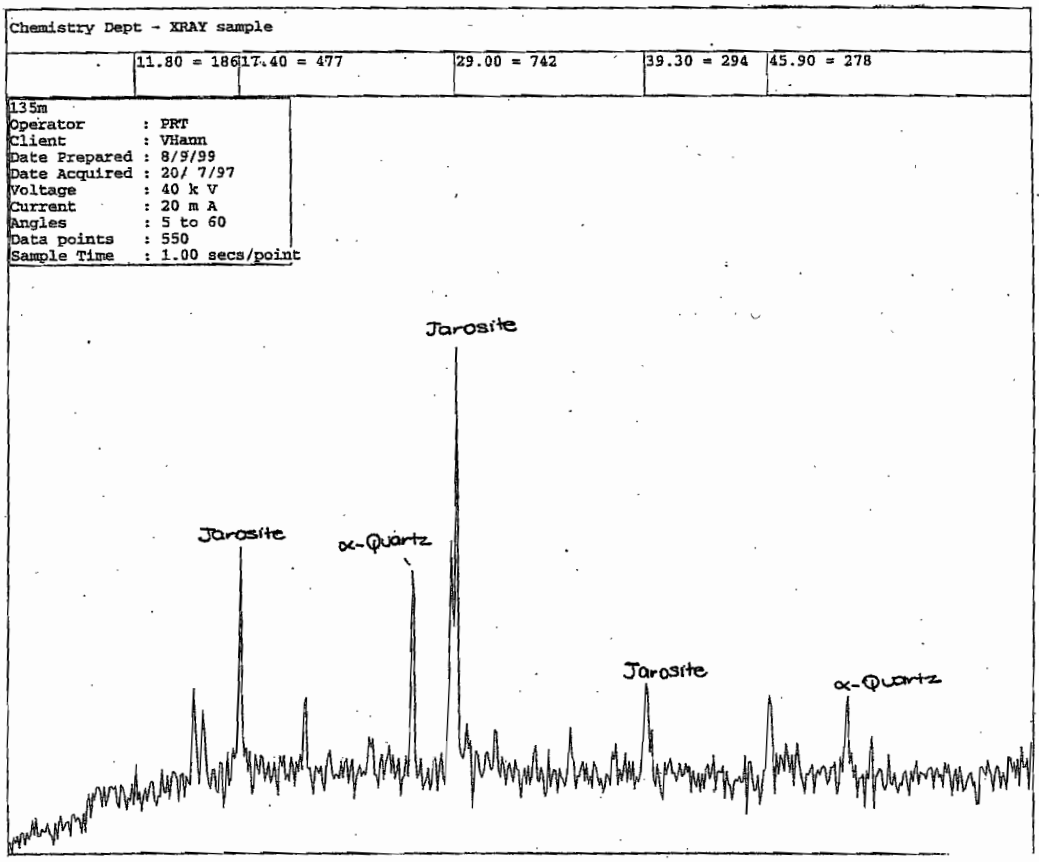

Figure 5.12 135m XRD trace.

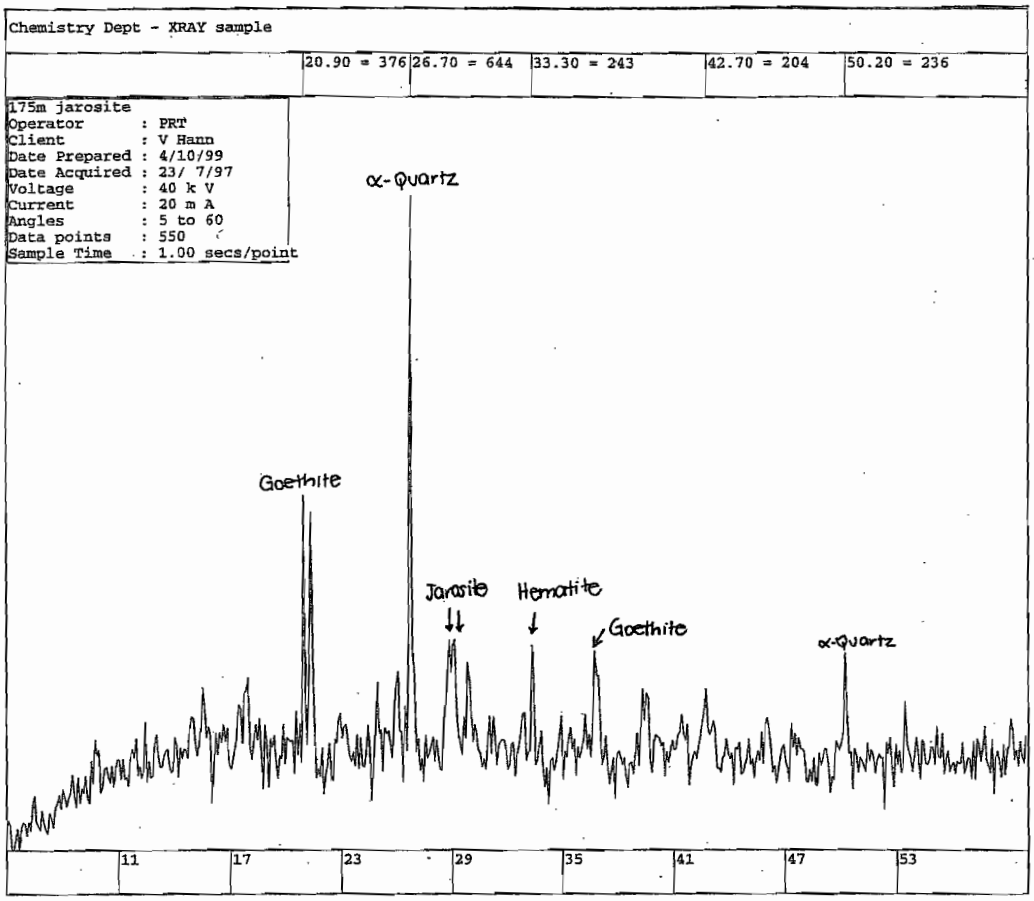

Figure 5.13 175m XRD trace

Sample G4

The trace from G4 has a trace which identifies it as hematite-quartz-goethite-jarosite mixture, confirming XRF data which shows that this hematite sample has elevated sulfur and depressed iron values (for jarosite) compared to G3 and NG003.

Jarosite Samples

Samples 175m, 135m and J1 were run. J1 and 175m samples had strongest peaks at dθ=29.00, this corresponds to dA of 3.079, and the standard for jarosite has d=3.08 which is a strong correlation.

Sample	XRD Mineralogy	Reference
J1	Jarosite + α-quartz	Refer to figure 5.3 (c)
135m	Jarosite + α-quartz	Refer to figure 5.3 (d)
175m	Goethite + α-quartz + jarosite + Hematite	Refer to figure 5.3 (e)

Table 5.2 XRD mineralogy for jarosite samples

Silica

Results were inconclusive for silica samples as the XRD did not differentiate between amorphous and opaline silica samples which in hand specimen were differentiated as cherty and supergene-silicified or leached and bleached amorphous types.

Summary and Discussion

The sharpness of the peaks in G2 indicates that the rock contains these minerals as a mixture. It is expected that hematite and quartz would exist as a mixture (not chemically bound), and that goethite and jarosite may have more variable traces because the goethite and jarosite accept other elements readily into the mineral structure, so that impurities change the trace. This probably accounts for the noise in the traces, however the peaks for goethite and hematite are in a fingerprint region and do not shift for different samples showing that they are in an un-mixed or well partitioned form.

Silica in G2 and G4 –

Comparision of XRD traces by Jones and Segtnit (1971) and the traces obtained for G2 and G4 indicate quartz, not amorphous silica or opal, as the major SiO_2 phase.
The jarosite samples may contain minor amounts of hematite, the trace 175m is a goethite-quartz-jarosite-hematite mixture, and the noise in traces J1 and 135m may also be due to small amounts of hematite.

5.3.3 ICP-OES

Traverse 15 150N

ICP-OES geochemical data of regolith samples for traverses 15 150 N and 15 200 N are provided in appendix 4. Elements that showed the strongest anomalies, and elements that showed the greatest variance between the geochemistry of the jarositic from hematitic rocks are presented in figure 5.4.

Element Variation along Traverse 15 150 N, falls into two main groups; enrichment in the gossan and enrichment in the jarosite, it is also apparent that enrichment in the gossan is predominantly base-metal (generally high atomic number elements), and enrichment in the jarosite is light-metal (lower atomic number elements): -

Enrichment in the Gossan:

The elements discussed below behave in a similar manner over the transect; accumulating between 14 970 and 14 99 N, and continuing the anomaly at lower levels to the north of the gossan.

Zinc

Zn varies from 6ppm 150m from the gossan to 57ppm at the gossan. The Zn anomaly continues to the north of the gossan but at lower values. Zn is elevated in the jarosite but is highest at the gossan.

Silver

Ag is preferentially concentrated in the gossan (16ppm) compared to the jarosite zone (0.5ppm), though is still slightly elevated to the north of the gossan.

Arsenic

As is enriched in the jarosite and hematite zones but more so in the gossan and beyond to the north. Arsenic concentrations peak at the gossan 14 970-14 990N (705-626ppm

respectively), and 14 550N (jarosite) returned samples of 700ppm. Concentrations in the hundreds of ppm continue to the north of the gossan.

Iron

Fe increases across the transect, reaching highest concentrations at 14 970-14990N at 33.81wt%, and staying at high values at least 50m north of the gossan. Iron is less than 4ppm in the section 14 812.5-14 887.5 N, in the hangingwall sandstone.

Copper

Cu is significantly enriched in the gossan at 107ppm, rising from 2.5ppm at 14 812.5 N. The anomaly continues to the north of the gossan.

Enrichment in the Jarosite

The elements listed below have anomalies affected by the mineralogy of jarosite, and are preferentially accumulated in the jarosite than in the gossan.

Lead

Pb ranges from 27 to 3320ppm over 150m. Pb is elevated though the section, the lowest return was 55ppm. The concentration lead peaks before the gossan zone, at 14 955 N (refer to map 2.6), in the jarosite. The lead is 3320ppm in the jarosite and only 15% of that in the gossan. Pb concentrations are higher to the north of the gossan than the south.

Aluminum, Potassium and Manganese

Aluminum is elevated in the jarosite especially between grid points 14 812.5 – 14 887.5N (4.68wt%) compared to the gossan which is relatively depleted (0.32 wt%). Potassium concentrations are also elevated in the same zone as Al concentrations peaking in the jarosite closest to the gossan (14 995 N). Manganese values are highest in the jarosite (242ppm) as opposed to 30ppm in the gossan.

Thallium, Antimony and Sulfur

Tl, Sb and S peaks coincide at 14 955 N. All are enriched in the gossan compared to the transect as a whole, but are one-to-two orders of magnitude higher in the jarosite.

Cadmium, Sodium, Cobalt, Molybdenum and Nickel

Cd, Na and Co are at low levels and are inconclusive, and Mo and Ni show broad and weak anomalous trends through the transect.

DISPERSION OF ELEMENTS OVER TRAVERSE 15 150N

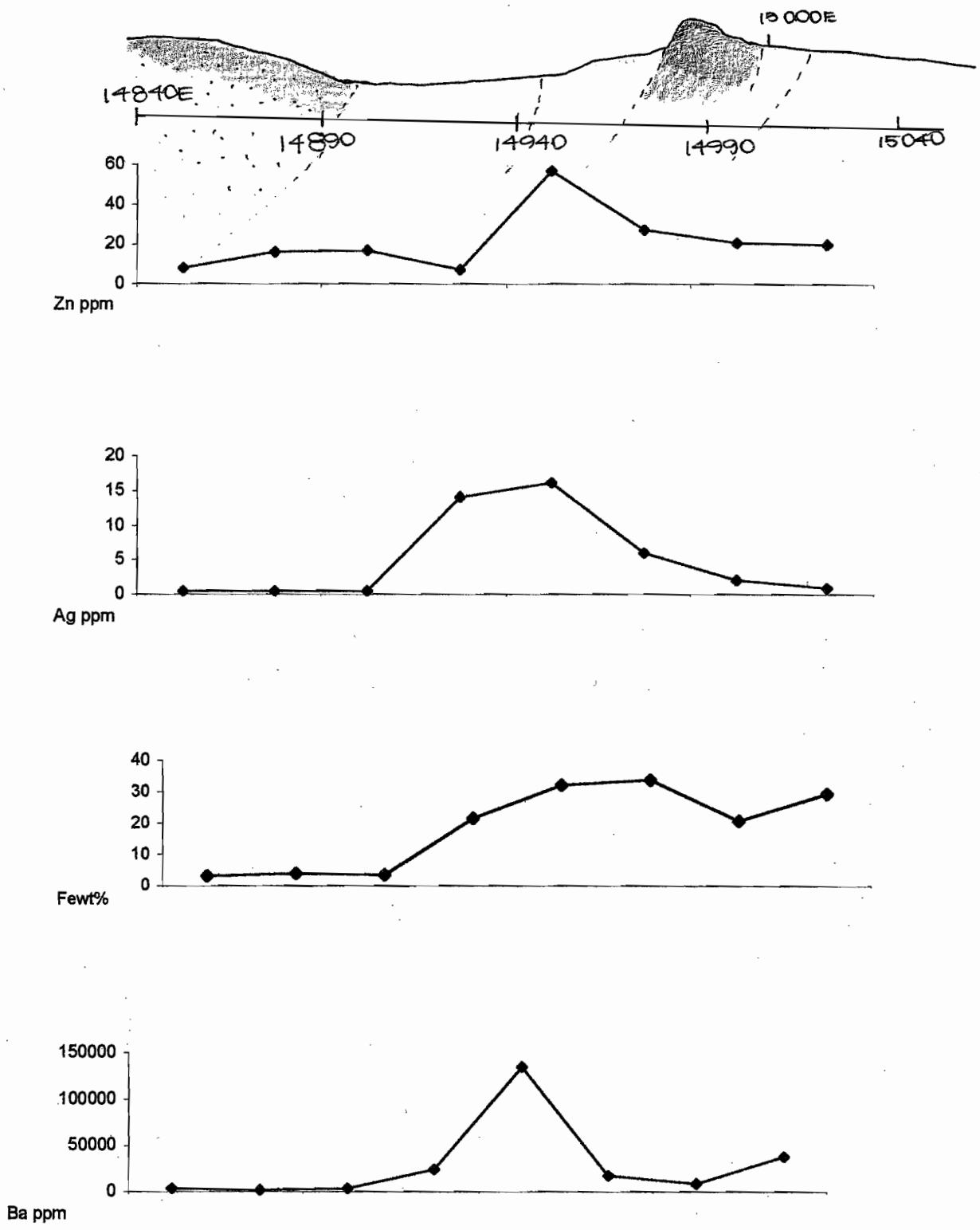

Figure 5.14 15 150N Chemical dispersion patterns over the gossan

DISPERSION OF ELEMENTS OVER TRAVERSE 15 150N

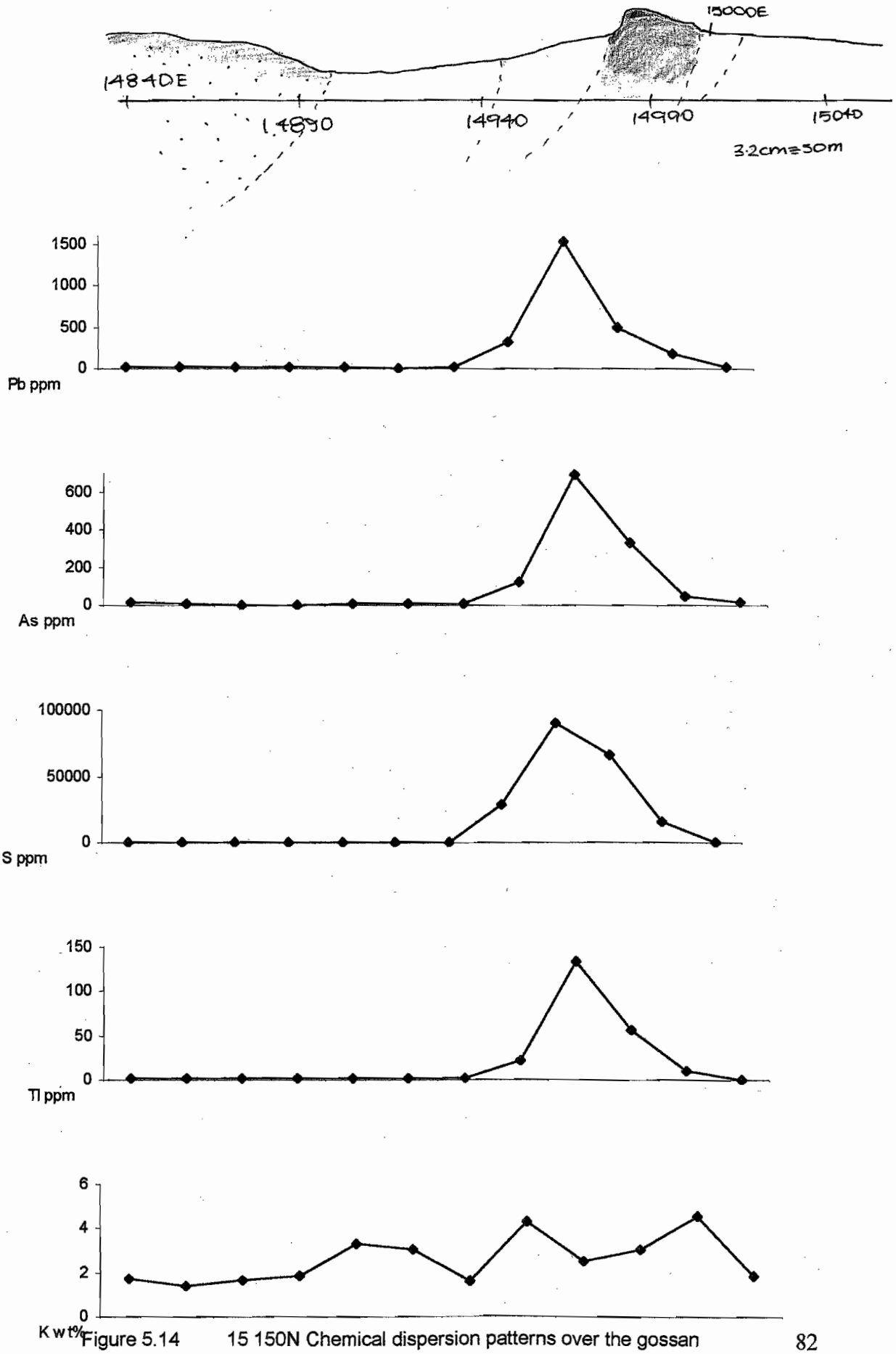

Figure 5.14 15 150N Chemical dispersion patterns over the gossan

Comparison to Traverse 15 200N

Rock-chip geochemistry of the 15 150 N traverse is mirrored in the 15 200 N. Zn, Ag, As, Fe and Cu values are elevated in the gossan, and Pb, Al, K Mn, Tl, Sb and S show sharp peaks and preferentially enriched in the jarosite. The position of peak concentrations of these elements is displaced 32m grid north relative to the 15 150 N section. Mo and Ni increase to the north of the section.

Element variation for typical hematite and jarosite

ICP-OES for selected hematite samples (G3, G4, NG003) and jarosite samples (135m, 175m, J1) returned concentrations of elements which generally follow the trends of the traverses discussed above (See appendix 4). Exceptions are Cu, Zn and Ag having higher values in the jarosite than the hematite samples. Arsenic is also particularly high in all samples, ranging from 143-9970ppm. Plots (figure 5.14) were chosen show the strongest and most obvious trends for these indicator elements.

Discussion

The geochemistry again confirms a difference in element affinities between jarosite and hematite rock types, with high target and pathfinder elements in both groups of Pb, As and Tl.

From the ICP-OES data (appendix 4) two broad geochemical trends are revealed:

(1) *Base-metal enrichment* in the gossan zone. Strong anomalies over the peaks of the gossan were returned for Pb, Zn, Ag, As, Fe, and Ni.

(2) *Light-metal enrichment* (and S and Mo enrichment) in the jarosite zone. Tl, K, Al Mg, Na enrichment defines the difference between the hematite and jarosite.

5.3.4 PIMA

Results from PIMA analyses are presented in appendix 6. PIMA analysis is limited to relatively pale coloured rocks, so hematitic/gossanous type rocks could not be tested, so the jarosite type, and the two leached and bleached shale types were tested with this technique. These correspond to units 2, 3a and 3b. The sample NG001a and NG001b are the same sample but are tested on different parts of the rock.

Opal samples

NG001, RD43 and S2 were matched to opal spectra with a reasonably good level of error, as all were below TSA=200, (see note at bottom of table 5.3). The PIMA produced a high possible error type of spectra for RD43 with gypsum as secondary mineral.

Jarosite and opal samples

Both jarosites tested, NG002 and NG004 show a good match to the jarosite that the PIMA uses as a standard and opal as a secondary mineral.

Interpretation

The sample NG001 came from a position in the outcrop, which is adjacent to a jarositic zone. The PIMA picked up hydrated silica (opal) as a primary mineral which supports a supergene silicification process acting to produce this rock type. K-Alunite is the secondary mineral and it is the aluminum analogue of jarosite, which is known to form by sulfuric acid solutions leaching through K-feldspar rich rocks (Klien and Hurlbut, 1985). The match to alunite composition is closer for the pale bands in the rock than the purple bands. The purple bands have microscopic disseminated flakes of hematite, which alters the signature, increasing the error.

Sample RD43 has a result similar to the pale bands in NG001, indicating this was also from a zone of supergene silicification. At a stage after the supergene silicification, it could have been leached again, accounting for the crumbly, lightweight and porous nature of the rock. RD43 and S2 are from a zone of extreme chemical leaching, but also a zone of supergene silicification grid east of the gossan areas. A potentially dubious result returned for sample RD43 is actually most likely, the sample was taken from an area which overlies a dolomitic lithology, and is highly weathered.

Table 5.3

Pima Results

Sample Name	Description	Description of Location	Section Pima applied to	Mineral 1	Mineral 2	TSA Error
1. NG001a	'zebra rock' sharp zones parallel to bedding of alternating purple-grey and cream coloured shale	Fringe of Gossan.5m south of RD31.	Pale cream to very pale yellow shale bands	Opal	K-Alunite	176.197
2. NG001b	as above	as above	Pale purple banding	Opal	K-Alunite	350.881 *
3 NG002	Yellow f.g powdery laminated shale	2m south of NG001a	n/a (sample homogenous)	Jarosite	Opal	69.944
4 NG004	Yellow f.g. powdery laminated shale, appearance as for (3) but a tone lighter yellow	Closer to gossan peak, same section line as previous samples	as above	Jarosite	Opal	100.878
5 RD43a	Leached , hollow sounding finely laminated shale, with a section presenting possible voids from pyrite crystals	10m mNE from RD43'Northern gossan' peak	White to very pale cream coloured layer at bottom of sample, not including the section with voids	Opal		185.042
6 RD43b	as above,	as above	Cream/very pale purple laminated section containing no replacement textures, possibly more ferruginous than previous Pima, 3cm higher in sample in right way up position	Opal	Gypsum	461.654 *
7 RDV005a	Pale soapy textured f.g shaley matrix, with x-cutting veins probably haematite, and fluid remobilisation zoning, overall appearance purple and white	In the siltstone enveloping the gossan, approximately 12m from the sulphide zone. RVD005 at 108.5m	Cream matrix only suitable	Phengite		129.054
8 S2	Generally pale purples/yellows/greys, showing ductile fluid like flow of layers. Lamination still obvious	3m along stike from RD50,	Purple and yellow bands	Opal		140.57

* Poor Spectral results for NG001b, and RD43a, spectra not printed for these. High error in spectra interpreted as due to reflective /non-absorbing nature of the minerals, absorbance not distinct.. NB. TSA Errors exceeding 200 are unreliable predictors of mineralogy.

The potential use for the PIMA in exploration and mineral identification in the field is severely limited in the search for base-metals because of the inability of the PIMA to deal with dark rocks, and therefore gossan material. Despite this, the PIMA still may have a useful application. Grevillea area has rocks outcropping which, although are leached of indicator elements for geochemistry, are likely to indicate supergene processes associated with gossan forming processes because of supergene silicification which occurs hand-in-hand with supergene processes. Therefore the presence of an 'opaline' form of silica may be used to indicate nearby sulfide mineralisation for strata bound deposits of the base-metal variety using this portable field device.

5.3.5 FTIR

Minerals containing heavy metals are conventionally not used with FTIR, which is predominantly an organic. However, others (Wilson, 1987) have successfully differentiated various morphologies of iron minerals using this method.

In the present study, the FTIR was used primarily to look at the silica-water bonding relationships, which are of interest, as described above in the PIMA section, but are also of interest because understanding supergene silicification processes are intimately linked with (base-metal) supergene processes.

Results

Hematite samples from Grevillea are compared (NG003, G2, G3 and G4). The three key, familiar jarosite samples were tested, 135m, 175m and J1. The traces are given appendix 6, and are discussed in the following section. Silica samples were also run for Si-O stretch comparisons to the jarosite and hematite types.

Hematite and the FTIR

The large broad peaks in the 3462-3421cm^{-1} indicate a significant amount of water in the structures; it is an OH stretching mode, and dominates the traces in this spectral range.

G2

This sample has the highest α-quartz peaks, with a doublet at 796.5, 778.9 cm^{-1} showing that the quartz in the sample is predominantly of the crystalline quartz variety. The two

peaks at 531.0 cm^{-1} and 455.4 cm^{-1} are indicative of a platey morphology of hematite (Wilson, 1987).

G3

G3 has less well defined peaks across the peaks compared to other hematites. The 798.4cm^{-1} peak is a broad single peak showing no crystallinity in the silica. The silica is opaline, and the 456 and 531cm^{-1} peaks again show that platey hematite is a major constituent. The hematite:silica ratio is higher in G3 than the other samples.

G4

Platey hematite peaks are higher than silica peaks, which show a mixture of amorphous and opaline silica. The quartz doublet at 796.6 cm^{-1} is small (compared to the total height of the silica peak) indicating that silica is more abundant in an opaline form rather than an amorphous form.

NG003

NG003 is characterised by platey hematite, crystalline silica (large doublet to total peak height ratio), and that the 1101.9cm-^{1} quartz peak is sharp.

Interpretation

Hematite samples have peaks which match well with a platey hematite texture. All the samples contain water in a bonded form. For free water, the FTIR peak would be broad in the 1640cm^{-1} region of the spectra. The peaks are small and sharp indicating very little H-O-H wagging (free water). The OH is deduced as being bonded to the silica.
If the OH was bonded to the iron, then the spectra would be not characteristic for hematite in the 450-750 cm^{-1} range but would be characteristic of goethite.

Jarosite and the FTIR

Jarosite traces have spectra that show sharp and small quartz peaks.

J1

The FTIR trace shows that OH is tightly bound (3383.1cm^{-1}). This is bound in the jarosite lattice (2mols OH : per 1mol jarosite). The silica doublet suggests that a small amount of quartz is present, and it is not hydrated. The 500-2550cm^{-1} range is the fingerprint range for jarosite and is consistent for all samples.

Interpretation

Hematite-rich samples have peaks which match well with a platey hematite texture. All the samples contain water in a bonded form. For free water, the FTIR peak would be broad in the 1640cm^{-1} region of the spectra. The peaks are small and sharp indicating very little H-O-H wagging (free water). The OH is deduced as being bonded to the silica.
If the OH was bonded to the iron, then the spectra would be not characteristic for hematite in the 450-750 cm^{-1} range but would be characteristic of goethite.

Summary

Element variation between the hematite and jarosite limonites

XRF shows elevated concentrations of Pb in the jarosite limonite samples J1 and 175m. These are interpreted to be plumbojarosites. Specimen 135m is elevated in Ag, defining it as argentojarosite. Jarosite acts as a 'geochemical trap for mobile elements' (Scott, 1987) Pb, Al, K, Mn, Tl, Sb and S. The gossan hematitic samples are preferentially enriched in Zn, Ag, As and Fe (figure 5.14). The FTIR indicated the platey hematite texture of specimen NG003.

Chapter 6 Conclusion

Geochemistry

Zinc is leached from the gossan and is mobile in acidic conditions.
Geochemical techniques confirmed that Jarosite is a 'geochemical trap for mobile elements' (Scott, 1987), and also Pb. The jarosite in the area is probably a plumbojarosite.

The preference of metals for each rock type is different except for iron which is a major component of both. Thallium has an anomaly in the jarositic unit and as a rare earth may be useful in defining target elements in the region. Zinc is mobile in these conditions and may not be a suitable pathfinder. Lead, a time-trusted pathfinder is one of the most important elements in distinguishing gossans in the Lawn Hill Region. Arsenic is also a key pathfinder for the Grevillea style deposits.

Barite has a tight surface anomaly in the jarositic unit, and decreases over the gossan. This is a function of faulting and associated barite veining. The barite is late stage, and serves the function of remobilising oxidised ore fluids through the thin conduits, and dispersing elements at the surface. Thin veins of barite were seen at surface, closely associated with specular hematite.

Textures

The sponge textured gossan indicates acidic conditions of formation. The highly pyritic ore generated a high amount of acid which, when neutralised with the dolomitic shales produced fluffy limonite. The gossan textures, where botryoidal, have destroyed primary textures that are diagnostic of primary sulfides.

It is concluded that for fine grained ores, and regolith over acidic conditions textures are very difficult to recognise in hand specimen. Textures at gossan are summarised as i) *sedimentary textures*, ii) *irregular microscopic boxworks* and iii) *whole replacement* or *pseudomorphing or infilling.*

Hematite and goethite are indivisibly mixed on a hand specimen scale, and microscopy reveals goethite forming from the breakdown of hematite. Bladed hematite is particularly common texture in thin section for the gossan.

The gossan formed at the onset of weathering and oxidation of the ore, and produced acid which solubilised base-metals from the profile, creating zones which are depleted and enriched, these were seen at surface. The iron oxides then percolated to a favourable Eh-pH site where the metals had conditions favourable to precipitation, in the supergene zone, now the present day gossan (In effect the gossan is an ancient supergene zone at surface).

Further study that may be of interest are

1) The monazites, these REE's have accumulated in a feldspar rich environment in a partially oxidised section of core. Monazites have the potential for dating purposes, and for constraining conditions of formation of the gossan.

2) The use of Mossbauer spectroscopy, which is more effective than XRD in determining oxy-hydroxide phases.

3) It is known that Fe and Si co-precipitate and the Fe is enormously enriched in the gossan , as is Silica. The effect of leaching , supergene enrichment and supergene silicification processes may be investigated by the use of PIMA for vectors to mineralisation.

References

Aheimer 1994 Geology and geochemistry of the Lady Loretta Formation, northwest Queensland. Unpublished honours thesis, University of Tasmania

Anand R R., and Smith R E., 1999 Use of ferruginous materials for geochemical exploration. *In* Exploration geochemistry and hydrothermal geochemistry (Regolith geology and exploration geochemistry) short course manual 11:117-123 CODES, Hobart

Bampton et al 1977 Geochemical indications of concealed copper mineralisation in Mount Isa. J Geochem. Expl. 8:169-188.

Battey 1987 Mineral associations in Mineralogy for students. Longman House, New York.

Blain C F., and Andrew R L., 1977 Sulphide evaluation and the evaluation of gossans in mineral exploration, *Minerals Sci. Engng.* 9:119-150

Blake D H., 1987 Geology of the Mount Isa Inlier and environs, Queensland and Northern Territory, BMR. *Geophys. Aust. Bull* 225.

Blake D.H., Etheridge M.A., Page R.W., Stewart A.J., Williams P.R. and Wyborn L.A.I., 1990 Mount Isa Inlier - regional geology and mineralisation, in Geology of mineral deposits of Australia and Papua New Guinea pp. 915-925.(The Australian Institute of Mining and Metallurgy: Melbourne)

Blanchard 1968 Interpretation of leached outcrops. Nevada Bureau of Mines, Nevada.

Blanchard R. and Boswell P. F., 1934 Additional limonite types of galena and sphalerite derivation. Economic Geology 29:671-690.

Broadbent G C., Russell E M., and Wright J V., 1998 Geology and origin of shale-hosted Zn-Pb-Ag mineralisation at Century deposit, Northwest Queensland, Australia. *Economic Geology* V93:1264-1295.

Brown J. S., 1936 Supergene sphalerite, galena and willemite at Balmat, N.Y. Economic Geology 31:331-354.

Butt C R M., 1999 Weathering and Regolith evolution *In* Exploration geochemistry and hydrothermal geochemistry (Regolith geology and exploration geochemistry) short course manual 11:6-14 CODES, Hobart

Conner A.G., Johnson I.R. and Muir M.D., 1990 Dugald River zinc-lead deposit, in Geology of mineral deposits in Australia and Papua New Guinea. pp. 949-953. (The Australasian Institute of Mining and Metallurgy).

Cox R. and Curtis R., 1977 The discovery of the Lady Loretta zinc-lead-silver deposit, northwest Queensland, Australia-A geochemical exploration case history. Journal of Geochemical Exploration 8:189-202.

Endo Y., 1960 Surface microtopographic study of pyrite crystals. Bull. Geol. Surv. Japan. 29:701-743.

Forrestal P.J., 1990 Mount Isa and Hilton silver-lead-zinc deposits, in Geology of mineral deposits in Australia and Papua New Guinea pp. 927-934 (The Australian Institute of Mining and Metallurgy: Melbourne)

Grondijs H.F. and Schouten C., 1937 A study of the Mount Isa ores. Economic Geology 32:407-450.

Guilbert 1986 Deposits related to weathering *in* The geology of the ore deposits, Ch17:796-818.W H Freeman and Company, New York.

Handcock M.C. and Purvis A.H., 1990 Lady Loretta silver-lead-zinc deposit in Geology of mineral deposits in Australia and Papua New Guinea. pp. 943-948. (The Australasian Institute of Mining and Metallurgy: Melbourne).

Huber N K., 1958. The environmental controls of sedimentary iron minerals. Economic Geology 53:123-141.

Jenkins D.R, J.P. Laurie and Beams S.D., 1998 Grevillea zinc-lead-silver deposit, In Geology of Australian and Papua New Guinean Mineral Deposits (Eds: D A Berkman and D H Mackenzie). Pp753-758 (The Australasian Institute of Mining and Metallurgy; Melbourne).

Jones J B, and Segnit E R., 1971 The nature of opal (I) Nomenclature and constituent phases. J. Geol. Soc. Aust., 18:57-68

Joyce A S., 1983 Ironstones and gossans ***in*** - Geochemical Exploration workshop course. Australian Mineral Foundation, Adelaide.

Kelly W C., 1958 Topical study of lead-zinc gossans State Bureau of Mines and mineral Resources, Socorro, New Mexico

Kullerud G and Yoder H S., 1959 Pyrite stability relations in the Fe-S system. Economic Geology 54:533-572.

Lewis etal 1981 Sediment-hosted stratiform deposits of copper lead zinc in Economic Geology 75th Anniversary volume

Loudon A G., Lee M K., Dowling J F., and Bourn R., 1975 Lady Loretta silver-lead-zinc deposit In Economic Geology of Austarlai and Papua New Guinea 1. Metals. Ed Knight C L. AIMM. Vic., Aust.

McGoldrick P. and Large R., 1998 Proterozoic stratiform sediment-hosted Zn-Pb-Ag deposits. AGSO Journal of Australian Geology and Geophysics. 17(4): 189-196.

McQueen K G 1999 Gossans and leached outcrops: morphology and Textures. *In* exploration Geochemistry and Hydrothermal Geochemistry (Regolith geology and exploration geology) short course manual 11:176-194 CODES, Hobart

McQueen 1999 Gossan geochemistry and regolith geochemistry, Eastern Australia. In Exploration geochemistry and hydrothermal geochemistry (Regolith geology and exploration geology) short course manual 11:200-219 CODES, Hobart

Page and Sweet, 1998 Geochronology of basin phases in the western My Isa Inlier, and correlation with the McArthur Basin. Australian Journal of Earth Sciences 45: 219-232.

Perkins W. G. and Bell T.H., 1998 Stratiform replacement of lead-zinc deposits: A comparison between Mount Isa Hilton and McArthur River. Economic Geology 93:1190-1212.

Rollinson H., 1996 Using Geochemical Data: evaluation, presentation, interpretation. Longman, UK.

Sato M., 1960 Oxidation of sulfide ore bodies, I. Geochemical environments in terms of Eh and pH. Economic Geology 55:928-961.

Sato M., 1960 Oxidation of sulfide ore bodies, II. Oxidation mechanisms of sulfide minerals at 25 C. Economic Geology 55:1202-1231.

Scott K.M., 1999 Gossan geochemistry and regolith geochemistry, Eastern Australia *In* Exploration geochemistry and Hydrothermal geochemistry

(Regolith geology and exploration geology) short course manual 11: 200-219 CODES, Hobart

Scott K.M., 1987 The mineralogical distribution of pathfinder elements in gossans derived from dolomitic shale-hosted Pb-Zn deposits, northwest Queensland, Australia. Chemical Geology 64:295-306.

Scott K.M. and Taylor G.F., 1987 The oxidized profile of BIF-associated Pb-Zn mineralisation: Pegmont, northwest Queensland, Australia. Journal of Geochemical Exploration 27:103-124.

Smith R E Campbell N A and Perdrix J L., 1982 Identification of some Western Australian Cu-Zn and Pb-Zn gossans by multi-element geochemistry. *In* Geochemical exploration in deeply weathered terrain. Ed R Smith, CSIRO, WA.

Taylor G F 1984 Gossan profiles developed above stratabound sulphide mineralisation. Journal of Chemical Exploration 22:351-352.

Taylor G F and Appleyard E C., 1983 Weathering of the lead-zinc lode, Dugald River, north-west Queensland: I. The gossan profile. Journal of Geochemical Exploration 18:87-110.

Taylor G.F. and Scott K.M., 1983 Weathering of the zinc-lead lode, Dugald River, northwest Queensland: II Surface mineralogy and geochemistry. Journal of Geochemical Exploration 18:111-130.

Taylor G.F. and Scott K.M., 1982 Evaluation of gossans in relation to lead zinc mineralisation in the Mount Isa Inlier, Queensland. (BMR) Journal of Australian Geology and Geophysics 7:159-180.

Taylor G F and Sylvester G C 1982 Analysis of a weathered profile on sulphide mineralisation at Mugga Mugga, Western Australia. Journal of Chemical Exploration 16:105-134.

Taylor G F, and Thornber M R., 1992 The mechanism of sulphide oxidation and gossan formation *in* Regolith exploration geochemistry in tropical and subtropical terrains. 4:118-137. Elsevier, Amsterdam.

Taylor G F., Wilmhurst J R, Butt C M R., and Smith R E. 1980 Elements and sample media used in geochemical exploration: definitions, descriptions and use. *In* Conceptual models in exploration geochemistry 4:27-33. Elsevier, Amsterdam.

Taylor G F Wilmhurst J R Togashi Y and Andrew A S., 1984 Geochemical and Mineralogical haloes about the Elura Zn-Pb-Ag orebody, western New South Wales. Journal of Geochemical Exploration 22:265-290.

Thornber M R., 1985 Supergene alteration VII. Distribution of elements during the gossan forming process, *Chemical Geology* 53:279-301.

Thornber M R., 1982 Weathering of sulphides. *In* Geochemical exploration in deeply weathered terrain. Ed R Smith, CSIRO, Western Australia.

Thornber M R., and Wildman J E. 1983 Supergene alteration of sulphides, VI . The binding of Cu, Ni, Zn, Co and Pb with gossan (iron-bearing) minerals, *Chemical Geology* 44:399-434

Valenta R., 1994 Deformation of host rocks and stratiform mineralisation in the Hilton Mine area, Mt Isa. Australian Journal of Earth Sciences 41:429-443.

Walker R.N., Gulson B. and Smith J., 1983 The Coxco deposit- A Proterozoic Mississippi Valley-type deposit in the McArthur River district, Northern Territory, Australia. Economic Geology 78:214-249.

Williams P.J., 1998 An introduction to the metallogeny of McArthur River-Mount Isa-Cloncurry minerals province. Economic Geology 93:1120-1131.

Appendix 1

Literature review

Gossan Forming Processes

Gossan Forming Processes; Interpretation and controlling factors

Veryan Hann
Bachelor of Science

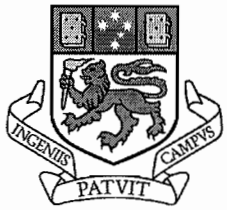

UNIVERSITY OF TASMANIA

A literature review submitted in partial fulfilment for the requirements of the Degree of Bachelor of Science with Honours

CODES SRC

Centre for Ore Deposits and Exploration Studies
School of Earth Sciences, University of Tasmania
July, 1999

Abstract

Gossan formation is the process of leaching and precipitating of metals and anions from gangue, the parent sulphide and surrounding rocks. This process of weathering which is commonly accompanied by enrichment is due to a geo-electrochemical redox weathering process.

Gossans may be colourful and conspicuous 'flag-wavers' to possible significant base-metal sulphide mineralisation and are important in exploration for metal-sulphide deposits. To maximise their utility, the objective is to be able to reconstruct the primary sulphide by working back from textures and minerals at surface, with information on processes of sulphide weathering (from comparison of progressions of known sulphide deposits through to gossan) so that a primary sulphide may be interpreted.
Evaluation can be made by careful examination of outcropping gossan using colour, textures, mineralogy and trace element geochemistry.

pH is the main factor in determining gossan textures and final mineralogy , this in turn is dependent on the primary sulphide, in particular the amount of pyrite and the type of gangue present.
Textures indicate a pH environment which indicates conditions for leaching or retaining minerals at surface. Generally, a neutral to alkaline environment is required for surviving boxworks and acidic for producing secondary textures.

Acknowledgments

A thank you to Dr Peter McGoldrick, for practical directions on this topic and also to Michael for cups of tea and encouragement.

TABLE OF CONTENTS

List of Figures

Chapter 1 Introduction

The Power of the Gossan

To understand a gossan is to understand the processes involved in its development. This review will describe gossan-forming processes. Ultimately, the aim is to be able to *read* gossanous outcrop and make informed interpretations of the nature of the fresh sulfide body *at depth*. Interpretation of leached outcrops; combining geochemistry with surface textures (where favourable) and mineralogy of a gossan provides a record and link to the pre-weathered state of the sulfides.

Gossans have long been recognised as potential indicators to base-metal mineralisation. However, the heterogeneous nature of gossans has meant that until at least the beginning of this century gossans were generally viewed as subjective as a tool in exploration and therefore of limited capacity in exploration. Chemical analysis has made gossan evaluation more comprehensive and a review by Taylor and Thornber (1992) states that the geochemical evaluation of gossans as a *"universally accepted cost-effective technique in the exploration for outcropping and near-surface mineralisation, particularly in deeply weathered terrain."* Many of Australia's significant metal-sulfide deposits resulted from gossan recognition; for example, Mt Isa and Broken Hill. The understanding of gossan forming processes aids in interpreting the nature of the sulfide body at depth from the surface outcrop.

1.1 Gossan Definition and Discrimination

A gossan is a specific form of *ironstone* as it overlies base-metal sulfide mineralisation. Gossans and other ironstones are rich in silicified, oxidised and hydrated iron oxy-hydroxides. Though gossans are a type of ironstone, the term ironstone commonly refers to uneconomic ferruginous outcrop. Ironstones generally form by the ferruginisation of barren rock (or overlying low level mineralisation), and may have enriched target or pathfinder anomalies at surface. Boxwork textures are like a skeleton of the ore minerals at surface. Finding and identifying primary sulfide boxwork textures of sphalerite and galena can identify a gossan from ironstone over and Pb-Zn deposit (as opposed to only pyrite at

depth). Using galena as an example, the mineral cleavage tends to leave an angular to triangular honeycomb texture after leaching and silicification, due to its three cleavage directions. The preservation of boxworks is favoured for i) coarse-grained ore, ii) a neutralising host eg. carbonate-rich sediments, and also iii) for ores with concentrated zones of one or two minerals so that the effects of leaching are uniform on that area (a boxwork after galena would need to have many galena crystals together to form a structure reflecting the cleavage distinct to galena and not mixed extensively with other minerals, and iv) in tectonically stable terrain, for minimal deformation and metamorphism and v) for ores with a high M:S ratio; so that for an ore 80% pyrite, texture preservation is minimal, whereas ores with higher galena and sphalerite primary textures will be better preserved.

Gossans may also be indicated by secondary textures (colloform goethite for example) and also by the presence of anomalous concentrations of target and pathfinder elements. As some kinds of ironstones may be enriched in target elements, analysis of immobile indicators such as Ba and Pb can be used and, mobile elements like zinc migrate away from the gossan and may create a halo. Lead isotopes are unaffected by oxidation and weathering and may also useful in discrimination (Gulson and Mizon 1979). Historically, different primary minerals were thought to be responsible for different colours in outcrop. Colour variations may be a way of picking the mineralogy of gossans, though it has been argued that it may only have local significance (Kelly, 1958). Even so, gossans over metal-sulfide mineralisation are characteristically colourful and variable in colour. In general, from various gossans studied in various conditions in the U.S. it was reported by Blanchard, (1968) that colours attributed to galena in (boxwork associated) outcrop are dusky reds, and for pyrite dusky browns to reddish browns, and for sphalerite and light browns to yellowish oranges for.

The (Fe+Mn) are 'limonite' metals, with the Zn as the mobile element of interest. Limonite is a general term describing any impure, hydrated iron oxides (Blanchard, 1968) which typically "scavenge" mobile elements (Joyce, 1983). In terms of distinguishing gossans by anomalous geochemistry, as an example, in the western succession of the Mount Isa Basin, gossans are distinguished by the presence of

As, Ba and Sb pathfinders with target elements Pb and Zn. The ironstones have low Pb-Zn pathfinders and higher concentrations of Cu, Zn, Co and Ni (Taylor and Scott, 1982). The ratio of mobile elements to 'limonite' is likely to indicate a true gossan rather than absolute values (Joyce, 1983). That is, for the case of lead-zinc deposits, values for the ratio of Zn/(Fe+Mn) could be used to distinguish a gossan from a barren ironstone.

1.2 Gossan recognition by textures

Sulfide boxwork textures are an important diagnostic technique in the interpretation of pseudo from true gossans. Boxworks form from sulfides and gangue, and may survive in parts of the gossan, particularly where silica has preserved the fabric. Indigenous goethite boxworks outline structures of previous minerals and the hollows being the site of the weathered out mineral, or the goethite may replace the space of the original mineral as a structural replica. Structures may remain intact though usually the casts after sulfides are infilled and obscured by "flooding by exotic goethite" (McQueen, 1999), which has a botryoidal texture typical for solution redeposition of the hydrated Fe oxide.

Chapter 2 Textures

2.1 Primary Textures

The main pre-requisites for boxwork formation and preservation at the gossan are:

- abundant sulfide ore minerals with good cleavage (pyrite, galena and sphalerite)
- strong ferruginisation at the gossan
- silicification at the gossan
- gossan derived from coarse-grained sulfides, though in the in the case of a fine grained sulfides casts may be seen microscopically.

Other contributing factors include:

- presence of neutralising gangue/host
- minimal deformation/metamorphism

Primary gossan textures, as defined by Blanchard are of two main types; cellular *boxwork* or cellular *sponge*. Boxwork type generally occurs after angular minerals with good cleavage. Spongy texture is the end-product of leaching around irregular shaped sulfide minerals.

Non-sulfide minerals may also produce strong boxworks, under certain conditions carbonate boxworks form and will be rhombohedral (Blanchard, 1968), as distinct from the principle sulfide minerals.

Pyrite, galena and sphalerite the most common sulfides have a cubic symmetry (McQueen, 1999). Generally, boxworks may reflect the cleavage more than the exterior of individual mineral grains. Most sulfides will leave proportionately more cellular sponge than boxwork but as pyrite, galena and sphalerite minerals have a 'strong tendency toward cleavage' they yield most distinct boxworks when they do form (Blanchard, 1968). **Pyrite** leaves cubic to subhedral casts when leached with neutralising gangue. Massive pyrite more readily leaves cellular sponges than boxworks. When in a strongly neutralising environment, pyrite forms 'fluffy limonite' the pyrite is oxidised and all the iron precipitates as an expanded limonite. This is an example of gangue neutralisation facilitating in situ precipitation due to neutral conditions favouring metal insolubility (Blain and Andrew, 1977).

For non-neutralising siliceous hosts, vertical acid leaching results in a discontinuous bamboo-like columnar texture. Less intense leaching may result in thin-walled sub-rounded cellular mesh style of boxwork remains after a previously formed web-work. Webwork is the initial oxidation where threads penetrate along cleavage and planes of weakness into the sulfide (Blanchard, 1968), subsequent silicification preserves the 'threads' as the pyrite is leached.

Galena can form pseudomorphs of anglesite or cerussite, often with a triangular or diamond shaped morphology. Common textures described by McQueen (1999) are two types of cubic pattern: a siliceous thin walled step pattern which has an appearance of a maze, and one of 'parallel cells with irregular cubic boxes', and three pyramidal-type textures: 1) irregular triangular texture which reflects cubic cleavage planes, 2) a diamond mesh texture and 3) a deformed version of (irregular) diamond mesh texture.

Sphalerite, typically forms a network of angular cells which are partitioned by thinner walls.

2.2 Secondary Textures

These textures post-date and obliterate primary textures. Secondary textures cannot be relied on as much for interpretation of the primary sulfide, and in terms of processes which forms them, it is known that they are mostly associated with fluids. Exotic goethite is the most common secondary texture in gossans, and is common from ores with a high pyrite content. Botryoidal habit is produced by the weathering process and "indicates solution and redeposition of iron" (Taylor, Wilmhurst, Butt and Smith, 1980). Secondary textures occur as a result of remobilisation and precipitation along faults, fractures, cleavage planes or lithological boundaries (Taylor et al, 1980).

Sphalerite has a sponge texture with thick rounded walls when replacing colloform sphalerite (McQueen, 1999). $ZnSO_4$ often forms as a first product of oxidation, and the limonite formed from this has no key features because it is soft and easily destroyed.

Chapter 3 The Gossan Profile

The mineralogical zonation through the profile varies with the type of mineralisation and conditions of weathering. Hematite and goethite will always form in the oxide zone, though the profile below will vary; the presence of zones of phosphate, arsenate, carbonate, supergene enrichment zones may or may not occur (Taylor et al, 1980). This depends on the mineralogy of the primary sulfide (Blain and Andrew, 1977)

3.1 Summary of Profiles resulting from the principle Sulfide-ore Types

Suites of profiles of massive sulfide associations were synthesised by Blain and Andrew (1977). The information on the proceeding four typical associations is gathered from this synthesis, and comprise:

3.1.1 Nickel-Copper Sulfides associated with Ultramafic rocks

- *Zonal progression*: *Ore - transitional zone - (mixed) oxide zones - jasperoidal gossan.*
- *Mineralogy*: The primary ore of pyrrhotite, pentlandite, and pyrite grades into a transitional zone of these minerals and chalcopyrite, violarite and siderite. Pentlandite and pyrrhotite are progressively replaced with violarite up-sequence into the a predominantly pyrite and nickel-rich violarite zone with pyrite, chalcopyrite and siderite.
- *Gossans* invariable contain goethite and commonly hematite, native sulphur, siderite and nickel-rich carbonates.

3.1.2 Copper-Zinc Sulfides associated with Acid Volcanics

- *Zonal progression*: *Ore - supergene enrichment - metal-oxide zone- carbonate rich oxide zone - gossan.*
- *Mineralogy*: Ore of pyrite, chalcopyrite, sphalerite converts to chalcocite and covellite in the enriched zone. The oxide zone consists of hematite, goethite. At Rio Tinto Spain, a leached pyrite zone and precious metal-oxide zone lies below the gossan and above the enriched zone. The 'precious metal layer' is associated with jarosite, goethite and chlorargyrite, and the zinc is probably

incorporated into the jarosite. At Ducktown Tennessee, ore is particularly high in pyrrhotite and the enriched zone additionally contains azurite, malachite, cuprite and bornite.

- *Gossans* are hematite-goethite rich, and for assemblages containing significant copper, malachite, azurite and kaolinite will also exhibit in the gossan.

3.1.3 Lead-Zinc Sulfides associated with Carbonate rocks

- *Zonal progression*: *Ore - carbonate-sulfide zone - enriched carbonate zone - oxide-carbonate zones - oxide-sulphate zone - gossan*
- *Mineralogy*: For an ore of pyrite, sphalerite, galena and chalcopyrite, the carbonate-sulfide zone will contain hematite, smithsonite and manganosiderite and grading into the enriched-carbonate zone cerussite and malachite become more dominant.

  The oxide-carbonate zone above commonly contains hematite, smithsonite with cerussite and hydrozincite progressively dehydrating up the profile and losing zinc in the form of hydrozincite and smithsonite. Smithsonite is replaced by cerussite into the oxide-sulphate zone with hematite still persistent, and goethite, native sulphur, plumbojarosite and calcite.
- Silica-hematite/goethite-manganese rich gossans, in places native sulphur is seen.

3.1.4 Lead-Zinc-Silver Sulfides of predominant Sphalerite-Galena ore

- *Zonal progression: Ore - enriched transition zones - oxide zone - gossan*

  The sequence is for the case of Mount Isa (Black Star), and for a Broken Hill the ore grades into additional enriched zones (chalcocite + Ag) followed by a *cerussite-smithsonite-silver halide* (oxide-carbonate) zone underlying the gossan.

  The oxide assemblage at Black Star contains pyromorphite with wedges of enriched *kaolin-cerussite-silver halide*. Cerussite and goethite are continuous in both profiles including the gossans. Strong leaching in 'deeply dissected terrain' may account for the discontinuous highly variable supergene sulfide enrichment zones for these types of profiles. Blain and Andrew (1977) suggest that ancient water tables have affected the development, leaving pockets of perched lenses of enrichment in places.

- *Mineralogy:* refer to diagram for lead-zinc mineralogy. Silver occurs as Ag halides in the oxide zone of both profiles, and as native Ag in some enriched zones/lenses. Supergene sulfides are not always present.

3.2 Effect of the Water Table on the Profile

Thornber and Taylor (1992) consider that the gossan profile development occurs during periods of falling water table. During a period of a falling water table oxygen access is gained for a greater portion of the profile, encouraging weathering, and for stable and rising water tables, oxidation is reduced and the weathering rate slowed. Seasonal changes to the water table rework and remobilise the more mobile elements through the profile so that the outcropping gossan is relatively richer in silica, iron oxyhydroxides and immobile elements such as lead.

Even if the conditions are perfect for excellent boxwork formation, they may not survive. Boxworks may be destroyed by a fluctuating water table due to seasonal variation or tectonic sagging as well as local effects of topography on the water table depth. Guilbert (1986) suggests mixed or 'partially leached, partially redeposited zones' commonly form due to a fluctuating water table. Boxwork textures will form and be preserved best in the profile and in the gossan in arid to semi-arid conditions, (In New Mexico (Kelly, 1958) and in the Yilgarn Craton in Western Australia for example). Additionally, a stable water table favours the preservation of a distinctly zoned profile and gossan, and tectonically stable areas or areas of uplift will leave primary textures intact. Taylor, Wilmhurst, Butt and Smith (1980) noted that botryoidal textures are particularly common for gossans in deeply weathered profiles.

Zones within the gossan-forming profile are positioned relative to each other and to the water table. Zone mixing and boxwork destruction may be explained by the following example of a rising water table. A leached and oxidised zone (containing boxworks) which has previously acted as an anode is encroached by a water-logged metal sulphate- rich zone. The new conditions mean that some oxidation and then redeposition is likely to occur. The effect of pH is important here in redeposition and is explained later.

Iron in the form of siderite below the water table may become remobilised due to a drop in pH from the transgressing sulphate zone and redeposit as goethite near the newly positioned water table. This precipitation of goethite occurred in the part of the profile which was previously oxidised, leached and of higher pH. In a zone where delicate boxworks may stand from previous leaching, they became infilled and flooded by the redeposition of botryoidal textured goethite.

A subsequent falling of the water table leaches this zone again, and it could be argued the most leached zones in the profile are those which for long periods of time existed just above the water table being subjected most to this fluctuation: alternatively leached and exposed to oxygen (in cracks, pores) followed by the influx of stagnant water and metal sulphates in solution.

For a seasonal (repetitive) water table variation, the formation of a gossan may be marked by the abundance of solution deposited botryoidal *post-primary* textures which would be expected to be prominent compared to classic boxwork indicators to sulfides.

Metal Zonation Profile below a Pb-Zn Sulphide derived Gossan

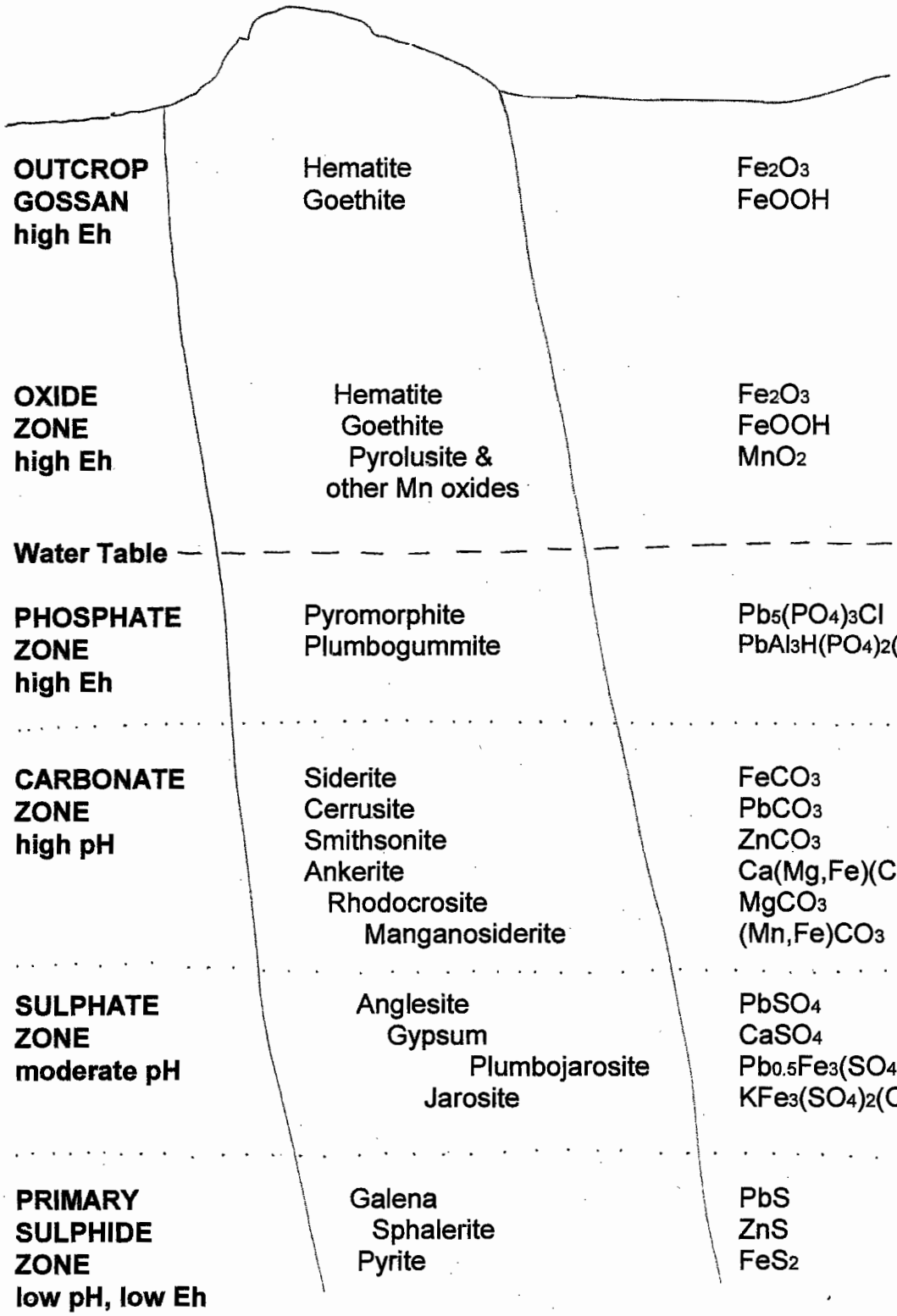

Modified after Scott (1987) and Taylor and Thornber (1992)
The above profile is for a primary ore with negligible copper. (fig. 1)

Generalised Gossan Development

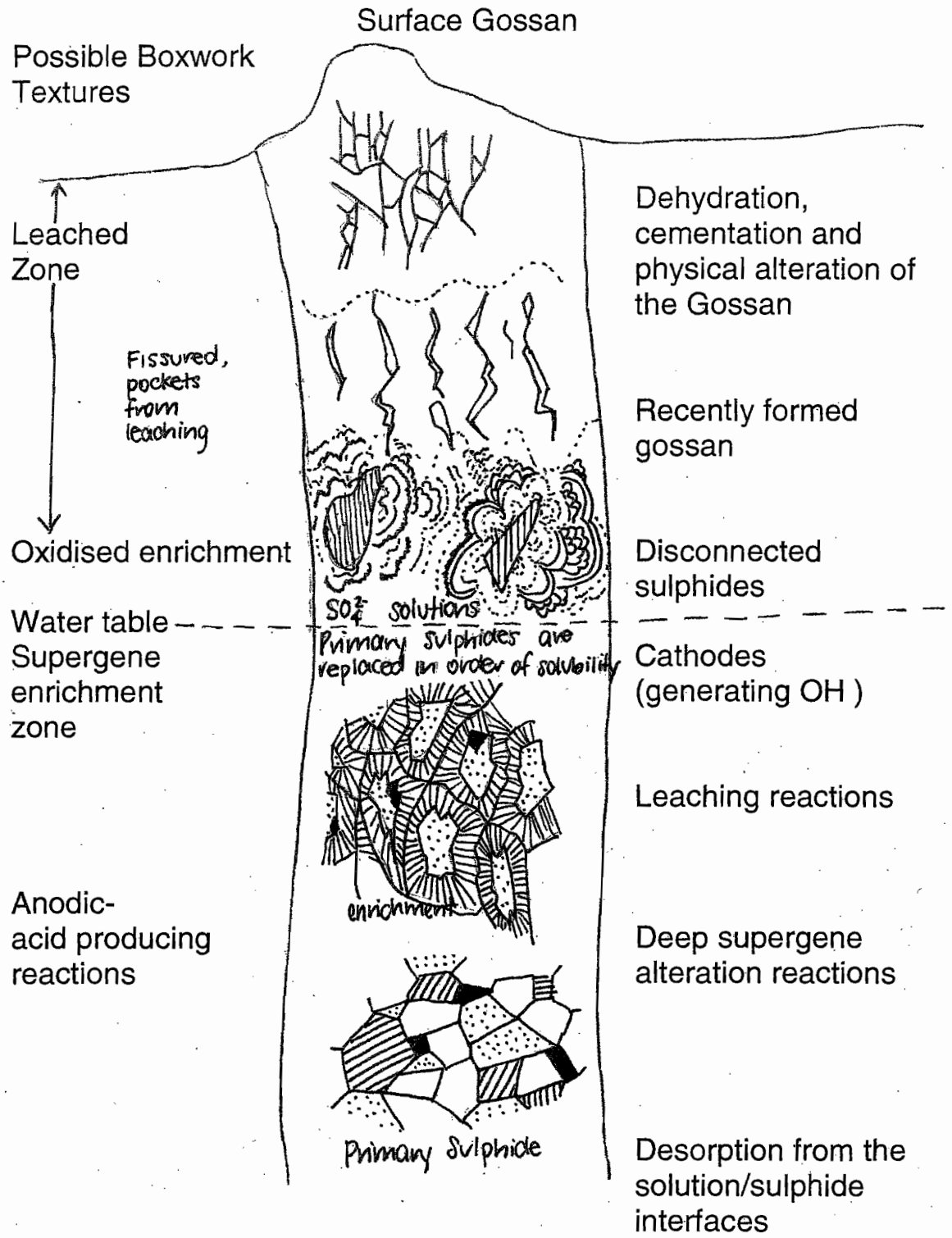

(Adapted from Taylor and Thornber (1992) and Battey (1981) (fig. 2)

Gossan 'building' can be reduced to 1) *redox* reactions in the sulfide bodies and 2) relatively high amounts of iron.

The overall redox reaction of a metal-sulfide body is the dissolution of a divalent base metal (eg. Fe^{++}), which then becomes hydrolysed, and on forming hydroxide precipitates generates acid. The presence of iron is the prime factor in determining overall acidity, and in fact, "*The whole weathering environment is dominated by the process of oxidation and hydrolysis of ferrous iron to ferric…[which] creates much acid while producing goethitic precipitates*" (Thornber, 1982).

Thornber and Taylor (1992) have found that derivatives of high iron sulfide content are good at scavenging metals which form anions, so that As, Sb Se, Te, W and Mo are retained with iron minerals. If K and Al are present they may contribute to jarosites and alunites, which adsorb or incorporate cations such as Pb, Ba, As and P.

4.2.2 The Importance Of Sulfur

It is the chemical nature of sulfur which directs the electrochemical weathering process. High sulfur to metal ratios in weathering assemblages produce more acidic conditions, which solubilise more metals. Conditions are always acidic where fresh sulfides are being weathered but the profile can be above neutral for assemblages with a low sulfide to metal ratio. Alkalinity encourages metal-carbonates and sulfates to precipitate, the oxidation products to stay in situ, and elements such as Cu, Ag and Zn are less leached.

Weathering in an electrochemical sense means that weathering rates are not slowed by depths that surface water has to percolate to enable reacting chemical species to come in contact. Even so, the cathode needs to come in contact with oxygen. O_2 may be dissolved in groundwater and derived from the atmosphere, or derived from groundwater and is necessary for the weathering process (Thornber, 1982).

4.2.3 The Importance Of Oxygen:

Oxidation Of Sulfides By Dissolved Atmospheric Oxygen Or By Groundwater

This has a huge influence on the solubility of metals and the pH (Thornber, 1985). Cathode reduction of oxygen is needed for weathering, and if there is no oxygen, weathering does not take place. However, with increasing depth (at and below the water table) dissolved atmospheric oxygen becomes less abundant, and according to Taylor and Thornber (1992) isotopic studies confirmed that oxygen is derived from the groundwater. The process of sulfide oxidation is acid generating as it is, and has generally thought to be in the from of

$MS + 2O_2 \rightarrow M^{2+} + SO_4^{2-}$

(eg. sphalerite + oxygenated groundwater $\rightarrow Zn^{2+} + SO_4^{2-}$ (in solution))

The above reaction is similar for galena and sphalerite, releasing Pb^{2+} and Zn^{2+} into solution. However, for iron (pyrite) rich occurrences FeS_2 generates a great deal of acid due to

1) the high sulfide to metal ratio, but also because
2) it is probable that the fresh pyrite is proportionately more oxidised by the groundwater compared to 'dissolved atmospheric oxygen' at depth.

Compare the following;

i) $FeS_2 + 4O_2 \rightarrow 2SO_4^{2-} + Fe^{2+}$

Anand and Smith (1999) suggest that atmospheric oxygen can gain access to rocks at depth by faults, fractures and joints, cleavage, quartz grain margins, intergranular margins and lattice voids and defects.

Even so , the reaction requires 4:1 moles of dissolved atmospheric oxygen to pyrite at depth, alternatively,

ii) $FeS_2 + H_2O \rightarrow 2SO_4^{2-} + Fe^{2+} + 2H^+$

Oxidation by groundwater generates significant quantities of acid, though acid may be buffered by neutralising gangue eg. carbonates at depth (Anand and Smith,1999). Overall, the initial weathering of pyrite is probably attributable to a combination of dissolved atmospheric O_2 and from the

ground water.

4.3 The Mechanism for Weathering: The Electrochemical Cell

Blain and Andrew (1977) elegantly explained the mechanisms of oxidation of sulfide orebodies where the gossan represents the *last* electrochemical step, as the accumulation of iron oxides at the top of the 'conducting profile'. Blain and Andrew suggest that it is useful to determine the sequences in the profile for effective gossan evaluation to track the changes in mineralogy from the ore to secondary minerals through the assemblage.

The supergene profile forms in the following way:
Sulfide minerals become chemically unstable as they come in contact with oxygenated groundwater, and on oxidising they release electrons, the orebody effectively becoming positively polarised. Above the orebody dissolved oxygen combines with acid produced by the oxidation of the sulfides, forming OH^-, which attracts an overall flow of metals to the top, and the loop completed by a flow of electrons into the orebody.

Supergene Alteration:

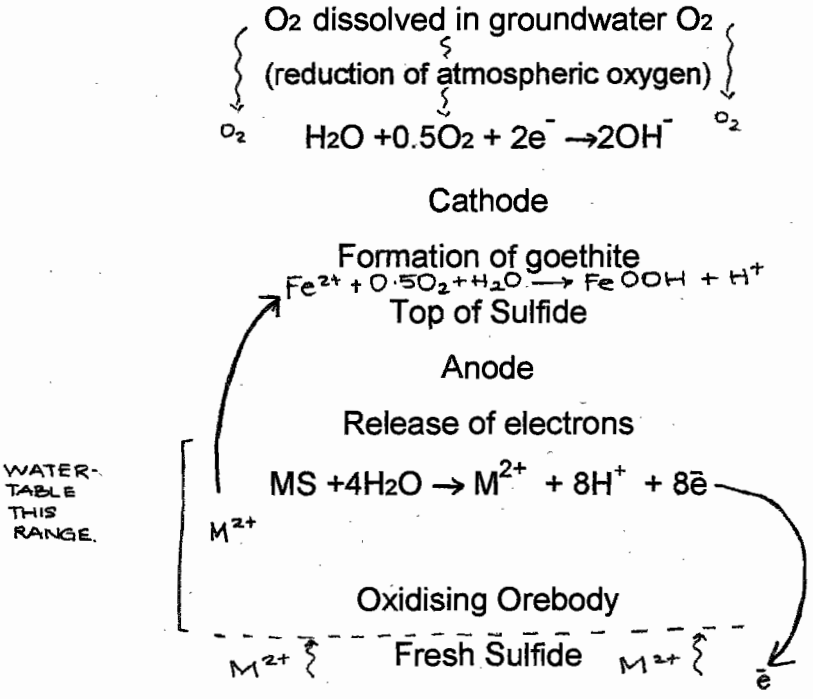

4.3.1 Cathode Reaction

For the oxygen dissolved in groundwater, the half reaction produces hydroxide in solution: $O_2 + 2H_2O + 4e \rightarrow 4OH^-$

Cathodic reactions take place at sites of relatively less reactive sulfides, and where a supply of groundwater-dissolved oxygen exist together. Relatively alkaline conditions at the cathode encourage precipitation of base metal compounds such as hematite and native elements such as silver if occurring. The supergene enrichment zone can act as a cathode as the conditions are alkaline relative to the oxidation in the above interval, and cathodic reduction also occurs higher in the profile, at young sub-surface gossan forming zones in the precipitation of goethite.

4.3.2 Anode Reactions through the Profile

Thornber (1982) divided anode reactions into four general types:

1. ***Deep Anode Reactions*** → **The oxidation of sulfides**
2. ***Shallow Anode Reactions*** → **The oxidation of Fe**
3. ***Enrichment Reactions*** → **Reactions near the water table**
4. ***Anode reactions with Dissolved Species*** → **Reactions through the profile**

4.3.2.1 Oxidation of Sulfides

Oxidation of metal sulfides at depth, this represents the initial weathering of the fresh sulfides. For somewhat oxygenated groundwater pyrite can liberate Fe(II) and very effectively reduce pH according to

$FeS_2 + 2O_2 + 4H_2O \rightarrow Fe^{2+} + 2SO_4^{2-} + 8H^+ + 6\bar{e}$

For galena,

$PbS + 2O_2 + 4H_2O \rightarrow 2Pb^{2+} + SO_4^{2+} + 4H_2O$

Similarly for sphalerite, as monosulfides show no net change in pH (Thornber and Taylor, 1992) this is conditional apon no hydrolysis of the metals in that zone.

4.3.2.2 Oxidation of Iron

$2Fe^{2+} + ½ O_2 + H_2O \rightarrow 2Fe^{2+} + + 3OH^-$

Reversible, generating alkalinity but once the Fe^{3+} forms it complexes with water generating acid.

Pyrite oxidation occurs at and above the water table,
with the reaction yielding no net change in alkalinity:

$FeS + 2O_2 \rightarrow Fe^{2+} + SO_4^{2+}$

However, acidic conditions occur for a low metal to sulfur ratio in the sulfides and alkaline conditions for a high metal to sulphur ratio.

4.3.2.3 Reactions near the Water Table

Significant metal enrichment zones below the sulfide-oxide interface occurs in a process known as *Supergene enrichment*. It is an electrolytic corrosive process. Base metals in solution can be taken up by minerals in metal-displacement reactions, normally Fe++ is the ion displaced generally exchanging for a cation of similar size and charge. Thornber (1975) gives the instance of pyrrhotite exchanging Fe^{2+} for Ni^{2+} ions to form violarite. That is ,

$Fe_7S_8 + 3Ni^{2+} \rightarrow 2Ni_{1.5}Fe_{0.5}S_4 + 4Fe^{++} + 2e$

In this case the reaction is anodic but generally enrichment reactions are only exchange or metal-displacement reactions. As there will be an abundance of iron sulfide minerals, iron will go into solution being displaced by Zn^{2+}, Pb^{2+}, Cu^{2+} and other metals. Blain and Andrew (1977) show enrichment of a *pyrite-chalcopyrite-bornite* orebody to chalcocite accompanied with the release of Fe^{2+} and electrons, and sulphuric acid. In the above oxide zone, sulfides are oxidised, promoting dissolution of metals with the decrease in pH.

For the *Nickel sulfide* body, the enrichment zone hosts pentlandite and pyrrhotite which both displace Fe^{2+} in preference for Ni^{2+} is which is removed from solution forming violarite and pyrrhotite. The displacement of Fe^{2+} from pyrrhotite forms pyrite.

The pyrite is dissolved into iron, sulphate and hydrogen ions in solution in the overlying anodic sequence. A goethite-rich gossan forms from cathodic reactions

derived from the reduction of atmospheric oxygen and the ferric ion from solution. That is, reduction of oxygen produces hydroxide which is drawn up by Fe^{3+} precipitating FeOOH at the gossan.

4.3.2.4 Anode Reactions through the profile

Metal ions (iron in particular) and sulphur anions in solution oxidise further, producing acid.

Ie. $Fe^{2+} \rightarrow Fe^{3+} + \bar{e}$

$SO_3 + H_2O \rightarrow 2H^+ + SO_4^{2-} + 2\bar{e}$

Thornber (1975) explains why galena and sphalerite near the surface remain protected from deep weathering. Galena crystals can form a jacket of $PbCO_3$ or $PbSO_4$ which acts as an inert electrochemical coating, and also the reactions of these sulfides forms SO_4 and the cations solution and instead of becoming good conductors of electrons the reactions eat up 8 electrons per mole of liberated metal cation and these sulfide grains become electrochemically 'disconnected from surface cathodes" (Thornber, 1975).

4.4 Effect of pH

The factors controlling pH in the gossan forming process are directly linked to the evaluation of gossans (Blain and Andrew, 1977), and the strongest influence on pH is metal to sulphur ratio of the ores. *Gossan formation conditions are pH dependent.*

In fact, pH is the most important factor in deciding the solubility and stability of metals and therefore where they will end up in the profile. The "*composition of the gossan minerals, the adsorption properties of minerals, the solubilities of metals, the leaching of carbonate and silicate minerals and the binding of humic materials are all pH dependent*" (Thornber, 1985).

4.4.1 Iron and acidity

Acid production the environment is increased "*if* the cation in solution is Fe^{2+}"(Scott, 1999) as it rapidly oxidises to Fe^{3+} and precipitates goethite (on hydrolysis);

$Fe^{2+} \rightarrow Fe^{3+} + \bar{e}$ followed rapidly by;

$Fe^{3+} + 2H_2O \rightarrow FeOOH_{(s)} + 3H^+$ (which produces mole-for-mole 3 times as much acid as goethite)

Thornber (1985) discusses precipitation of gossan minerals by a low and high pH mechanism. At high pH, Fe^{2+} is mostly insoluble, and likely to be precipitated as $Fe(OH)_2$ which is further oxidised to goethite;

$Fe(OH)_{2\,(s)} + OH^- \rightarrow FeOOH_{(s)} + H_2O$

At low pH, Fe^{2+} is oxidised to Fe^{3+} in solution prior to precipitation, and forms a mole of acid for every mole of goethite produced; $Fe^{2+} + H_2O \rightarrow FeOOH_{(s)} + H^+$

Goethite is dominant in the pH range 3-6 (Thornber, 1985) so it seems that the second process would be more favourable.

Thornber (1982) noted that sulfides do not always generate acidity during weathering, concluding that when the sulfur-to-metal ratio (in minerals) is greater than 1, it produces acid;

ie. **S:M>1 ⇒ acidic conditions,** and **S:M<1 ⇒ alkaline conditions**

So that for FeS_2 the pH is reduced compared to monosulfides.

It was also noted that pyrite may start out as cathodic sites for the reduction due to it's stability, however it eventually oxidises forming acid.

4.4.2 Mobility of Elements and pH

Electrochemical weathering experiments, and in particular reactions converting sulfide minerals to oxide gossan minerals were undertaken by Thornber (1985) and it was deduced that *"the interaction between the pH of the reactions and the amount of Fe in the sulfides is shown to be the dominant feature which controls the mobilities of many elements"*.

Elements are solubilised and redistributed according to the pH (Thornber and Wildman, 1983). Thornber (1985) shows that for the following adsorption sequence, there is strong adsorption on minerals, and possibly coprecipitation at higher pH by cations, and conversely for anions;

Cu>Pb>Zn>Co>Ni>Cd>Mn

Adsorption sequence (pH<7,sulfide minerals leached, pH>7 minerals retained)

Mobility is high for S, Mo, Zn and Ag in a siliceous environment (one which does not buffer acidity) from the weathering of sulfides, and the mobility for As, Pb (and As for an iron-rich environment) is low. The subsequent pattern of redistribution of the metals in the profile is occurs due to the to the prevailing pH conditions. The pH conditions, in turn, affect the solubility of the various metals present. The distribution is also dependent on the mineralogy of the host and wall rocks.

As an example of the effect of the pH on the redistribution of metals in the gossan profile is as follows; the example is for a intermittently calcareous host which has neutralising qualities, so that the pH=6, certain conditions arise. At pH=6 (at 25 C) the *maximum* concentration (mol/L) of metals in equilibrium with CO_3 for Zn, Fe and Mn is $10^{-3.3}$, 10^{-13}, and 10^{-6} respectively. Above these values they precipitate out of solution. Comparing with SO_4^{2-},(Zn, Fe, and Mn)>1; meaning that the concentration of SO_4^{2-} and metal ions can be increased by orders of magnitude and still not precipitate metal sulphates. In terms of the leaching process it is expected that carbonates will not migrate as far down the profile as sulphates, which will tend to percolate toward the bottom of the oxide zone.
This is a reason why the oxide-carbonate zone is always above the sulphate zone; as the sulphate compounds are generally more soluble in slightly acidic conditions.

Chapter 5 Summary

- Gossan formation is a complex, multi-variable process (as is usual for nature) and occurs over a long period of time.

- Primary textures can identify a handful of sulfide minerals due to the replication of cleavage or of whole mineral grains.

- The nature of secondary textures implies their limited use in seeing a link to a previous sulfide mineral, destroying indigenously formed textures and 'key' textures with them. Secondary textures indicate a low pH environment, as metals precipitate from a *solution* and metal solubility is pH dependent.

- The most common sulfide minerals associated with supergene enrichment fortuitously have the simplest boxworks (when formed in preference to cellular sponges) (Blanchard, 1968).

- Pyrite and silica are by far the most determining for prominent outcropping gossan development. Pyrite-rich systems release proportionately more acid into the profile, which is responsible for increased mobility of some (potentially pathfinder) elements, and increased production of goethite in the gossan. The zonation through the profile varies a great deal depending on the parent sulfide.

- The position of the water table is very important in the profile development (and the gossan is a part of that profile). Fluctuation of the water table destroys boxworks, and the weathering profile moves relative to the water table.

References

Anand R R., and Smith R E., 1999 Use of ferruginous materials for geochemical exploration. *In* Exploration geochemistry and hydrothermal geochemistry (Regolith geology and exploration geochemistry) short course manual 11:117-123 CODES, Hobart

Butt C R M., 1999 Weathering and Regolith evolution *In* Exploration geochemistry and hydrothermal geochemistry (Regolith geology and exploration geochemistry) short course manual 11:6-14 CODES, Hobart

Blain C F., and Andrew R L., 1977 Sulphide evaluation and the evaluation of gossans in mineral exploration, *Minerals Sci. Engng*. 9:119-150

Blanchard 1968 Interpretation of leached outcrops. Nevada Bureau of Mines, Nevada

Battey 1987 Mineral associations in Mineralogy for students. Longman house, New York.

Broadbent G C., Russell E M., and Wright J V., 1998 Geology and origin of shale-hosted Zn-Pb-Ag mineralisation at Century deposit, Northwest Queensland, Australia. Economic Geology 93:1264-1295.

Guilbert Deposits related to weathering *in* The geology of the ore deposits, Ch17:796-818. W H Freeman and Company, New York.

Joyce A S., 1983 Ironstones and gossans ***in*** workshop course- Geochemical Exploration. Australian Mineral Foundation, Adelaide.

Kelly W C., 1958 Topical study of lead-zinc gossans State Bureau of Mines and mineral Resources, Socorro, New Mexico

McQueen K G 1999 Gossans and leached outcrops: morphology and Textures. *In* exploration Geochemistry and Hydrothermal Geochemistry (Regolith geology and exploration geology) short course manual11:176-194 CODES, Hobart

McQueen 1999 Gossan geochemistry and regolith geochemistry, Eastern Australia. In Exploration geochemistry and hydrothermal geochemistry (Regolith geology and exploration geology) short course manual 11:200-219 CODES, Hobart

Scott KM 1987 The mineralogical distribution of pathfinder elements in gossans derived from dolomitic shale-hosted Pb-Zn deposits, Northwest Queensland, Australia. *Chemical Geology* 64:295-306

Scott 1999 Gossan geochemistry and regolith geochemistry, Eastern Australia *In* Exploration geochemistry and Hydrothermal geochemistry (Regolith geology and exploration geology) short course manual 11: 200-219 CODES, Hobart

Taylor G F., Wilmhurst J R, Butt C M R., and Smith R E. 1980 Elements and sample media used in geochemical exploration: definitions, descriptions and use. *In* Conceptual models in exploration geochemistry 4:27-33. Elsevier, Amsterdam.

Taylor G F., and Scott K M., 1982 Evaluation of gossans in relation to lead-zinc mineralisation in the Mount Isa Inlier, Queensland. *BMR Journal of Australian geology and Geophysics* 7:159-180.

Taylor G F, and Thornber M R., 1992 The mechanism of sulphide oxidation and gossan formation *in* Regolith exploration geochemistry in tropical and subtropical terrains. 4:118-137. Elsevier, Amsterdam.

Thornber M R., 1982 Weathering of Sulphides in Geochemical Exploration in Deeply Weathered Terrain. CSIRO, Western Australia.

Thornber M R., 1985 Supergene alteration VII. Distribution of elements during the gossan forming process, *Chemical Geology* 53:279-301.

Thornber M R., and Wildman J E. 1983 Supergene alteration of sulphides, VI . The binding of Cu, Ni, Zn, Co and Pb with gossan (iron-bearing) minerals, *Chemical Geology* 44:399-434

Appendix 2

Drill Hole Geochemistry

Drill hole data used for Cross-section 15235N

Hole ID : RVD017

Collar Survey:	(Local)	(AMG)		
	15235 N	N	Elevation:	187.00m
	14840 E	E	Inclination:	60.00

Azimuth : 89.500 59.50 Azimuth (Mag): 54.50

Precollar/Percussion metres
Open Hole :
Reverse Circulation : 117.00m of ThruHammer (11.43 cm)
Diamond Core metres : NQ (47.6mm) 117.00 to 233.80
Total Core Length : 116.80m

Final Depth : 233.80m

Purpose:
To test for mineralisation below RVC001 and RVC002.

Summary Log:
RVD017

0 -115m	Fine grained sandstone interbedded with siltstone and shale. Oxidised throughout.
115 – 192.3m	Massive sulphide zone. Fine grained, laminated pyrite bands interbedded with black shales dolomitized in places to pale white/grey shale. Bands o coarse grained sphalerite, galena, pyrite and barite interbannded with fine grained pyrite and black shales 164.7 188.66m.
192.3 233.8m	balck shales with minor fine grained pyrite bands and disseminations. Some calcareous shales and calcite veining. Sedimentary breccia present 212.2 – 212.57m, 223.6 – 223.9m. Also bands of coarse grained pyrite, calcite, and barite 205.75 – 206.68m, 207.64 – 208.47m, 211 –212m, 214.5 – 215m, 223.9 – 224.3m.
223.8m	EOH.

Water Table Details : 28.00m
Depth of Oxidation : 44.00m
Depth of Cover : .00m

Directional surveys:

Depth (downhole)	Azimuth (from Mag. N.)	Declination (from Horizon)	Survey Instrument	Survey Type
0.00	54.50	-60.00		
Compass/clinometer	Raw survey info.			
100.00	60.00	-38.00	Eastman camera	Assumed survey info.
143.80	65.00	-32.00	Eastman camera	Raw survey info.
146.80	64.50	-32.00	Eastman camera	Raw survey info.
170.00	64.50	-32.00	Eastman camera	Raw survey info.
233.80	65.00	-32.00	Eastman camera	Raw survey info.

Logged by : DRJ

Significant Intercepts:

25m @ 3.24% Zn, 0.76% Pb, 33.4 ppm Ag and 62.2 ppm Cd from 164m

incl. 6.2m @ 4.31% Zn, 1.11% Pb, 38.4 ppm Ag and 77.5 ppm Cd from 164.7m

and 11.1 m @ 4.39% Zn, 0.92% Pb, 35.9 ppm Ag and 87 ppm Cd from 177.4m.

Comments:
Diamond hole intersected the large massive sulphide body with significant widths and grade of Zn, Pb and Ag values.

HOLE ID : RVC002

Collar survey:	(local)	(AMG)		
	15235 N	N	Elevation :	176.00m
	14890 E	E	Inclination :	60.00
Azimuth: 60.00			Azimuth (Mag)	55.00

Precollar/Percussion metres

Open Hole :
Reverse Circulation : 200.00m of Hammer (13.97 cm)

Final Depth : 200.00m

Purpose :
To test for continuations of mineralisation below the intersection returned in RVC001.

Summary log :

RVC002

0 – 54m	Ferringous sandstone, fine grained, moderately weathered becoming fresher and finer grained.
54 – 68m	Grey-green siltstones/shales weak to moderately silicified becoming darker downhole.
68 – 75m	Moderately silicified balck shales, minor quartz veining and minor.
75 – 163m	Black shales with massive pyrite bands from 20 –80% weak to moderate silicification becoming strong in more pyritic zones. Coarse honey coloured sphalerite and grey-silver sulphide, galena and sphalerite? In some zones 133 –134m, 148 – 149m and 154 – 155m. probably remobilised.
163 – 168m	Balck shales, some red brown haematitic material.
168 –196m	Black shales with variable pyrite content, as disseminations and bands from <5% to 70% pyrite over individual metres.
196 – 200m	Black shale haematitic in parts, no obvious sulphide.
200m	EOH

Water Table Details : 24.00m
Depth of Oxidisation : 20.00m
Depth of Cover : 0.00m

Directional Surveys :

Depth (down hole)	Azimuth (from Mag. N.)	Declination (from Horizon.)	Survey Instrument	Survey Type
0.00	55.00	-60.00	Compass/Clinometer	Raw survey info.

Logged by DRJ

Significant Intercepts:

25m @2.5%Zn, 0.44% Pb, 18ppm Ag, and and 38.4ppm Cd – from 130m
incl
5m @ 4.5% Zn, 0.76% Pb, 29ppm Ag and 87ppm Cd – from 133m
and
7m @ 5.12% Zn, 0.75%Pb, 20ppm Ag and 61.6ppm and Cd – from 148m

Comments: A continuation of the mineralisation found in Hole RVC001 was intersected with a lower grade overall.

HOLE RVC001

Collar Survey:	(Local)	(AMG)		
	14235 N	N	Elevation:	180.00m
	14940 E	E	Inclination :	60.00
Azimuth: 60.00			Azimuth (Mag) :	55.00

Precollar/Percussion metres
Open Hole :
Reverse Circulation : 128.00m of Hammer (13.97cm)

Final Depth : 128.00m

Purpose:
To test for mineralisation below the Gossanous Zone at Grevillea which returned anomalous Pb, Ag, As geochemistry.

Summary Log:

RVC001

0 –18m	Weathered siltstone/shale, red-brown to cream, ferruginised in parts Minor fracture filling. Manganese starting 10 –11m. Fine disseminated, crystallite haematite.
18 – 30 m	Red haematitic siltstone/shale. High Haematitic content, some silver-grey crystallite haematite.
30 – 74m	Black shale with banded mostly fine pyrite. Between 30 – 50% of the total content is sulphide. Possible weak to moderate silification of shales. Minor quartz veinity noted. Some fine grey bands in shales – possibly fine clay or graphite. Trace honey brown sphalerite? Noted 49 - 50m, 54 – 55m. green blue clay fracture filling 69 – 74m.
74 –75m	Red brown haematitic siltstone.
75 – 118m	As for 30 –74m coarser pyrite present in many places. Coarse grey/silver galena and honey brown sphalerite. 81 – 91m, 92 – 94m, 98 – 99m, 103 – 104m, 105 – 107m, 109 – 111m, 113 – 114m. Total sulphide content up to 90% mostly 50%+ barite veining 101 – 102m, 11, 112m.
118 – 128m	Black shales with fine disseminated pyrite and minor pyritic bands.
128 m	EOH – very slow drilling, 4.5m/hr

Water Table Details: 24.00m
Depth of Oxidation: 16.00m

Depth of Cover: .00m

Directional Surveys:

Depth (down hole)	Azimuth (from Mag. N.)	Declination (from Horizon)	Survey Instrument	Survey Type
0.00m	55.00	-60.00	Compass/Clinometer	Raw Survey Info.

Logged by: DRJ

Significant Intercepts:

25m @ 4.7% Zn, 0.98% pb, 29 ppm Ag and 86 ppm Cd – from 89m
incl.
8m @ 8.44% Zn, 1.6% Pb, 36.5 ppm Ag and 149 ppm Cd – from 103m
and
4m @ 5.86% Zn, 1.5% Pb, 36 ppm Ag and 12 ppm Cd – from 89m

Comments: A significant intersection of Zn-Pb-Ag mineralisation was intercepted within a large highly sulphide zone.

HOLE ID RV005

Collar Survey:	(local)	(AMG)		
	15185 N	N	Elevation:	189.00m
	14840E	E	Inclination:	72.00
Azimuth: 90.00		60.00	Azimuth (Mag):	55.00

Precollar/Percussion metres
Open Hole :
Reverse Circulation : 108.00m of ThruHammer (11.43 cm)
Diamond Core metres : NQ (47.6mm) 108.00 to 227.90
Total Core Length 119.90m

Final Depth : 227.90m

Purpose:
To test for a continuation of mineralisation below the intersection in hole RVC004.

Summary Log:
RVc005

0 –120.72m	Fine grained sandstone interbedded with siltstone. Oxidised throughout but becoming less oxidised with depth.
120.72 –216m	Massive sulphide zone - fine grained laminated pyrite interbanded with black shales, some dolomitization of the black shale bands. Zones of baritic material alos with breccia textures and coarser pyrite. Coarse grained bands of honey brown sphalerite, pyrite, galena and barite subparallel to bedding and interbanded with fine grained pyrite and black shales 146.25 – 154.67m, 188.82 – 208.14m.
216 – 219.6m	Coarse grained pyrite – probable fault zone. Some core missing.
219.6m – 227.9m	Haematitic shales with interbedded kaolinitic shales – strongly oxidised possbily equivalent to pyrite zone with oxidisation die to fluids many along fault.
227.9m	EOH.

Water Table Details : 25.00m
Depth of Oxidation : 25.00m
Depth of Cover : .00m

Directional surveys:

Depth (downhole)	Azimuth (from Mag. N.)	Declination (from Horizon)	Survey Instrument	Survey Type
0.00	55.00	-72.00.	Compass/clinometer	Raw survey info.
30.00	56.50	-69.50	Eastman camera	Assumed survey info.
60.00	58.00	-66.20	Eastman camera	Assumed survey info.
117.00	61.00	-61.00	Eastman camera	Raw survey info.
162.00	61.00	-62.00	Eastman camera	Raw survey info.
226.00	60.00	-62.00	Eastman camera	Raw survey info.

Logged by : DRJ

Best intersections:

From	To	Interval	Pb	Zn	Ag	Cd
146	150	4	5.2%	2.45%	41.6%	43
188	208	20	1.5%	5.97%	56.4%	117.2
incl.						
188	198.3	10.3	2.29%	7.9%	65.4%	167.6

Comments:
Diamond hole through massive sulphide body. Significant width and grade o Zn, Pb and Ag intersected.

HOLE ID RV004

Collar Survey:	(local)	(AMG)		
	15185 N	N	Elevation:	179.00m
	14840E	E	Inclination:	60.00
Azimuth: 90.00		60.00	Azimuth (Mag):	55.00

Precollar/Percussion metres
Open Hole :
Reverse Circulation : 174.00m of Hammer (13.97 cm)

Final Depth: 174.00m

Purpose:
To test for mineralisation below the Gossanous Zone at Grevillea which returned anomalous Pb, Ag As geochemistry.

Summary Log:
RVC004

0 – 61m	Weathered becoming fresh fine grained sandstone with some grey siltstone interbeds. Ferruginised in parts 0-45m. Some silification 52-58m.
61 – 73m	Grey siltstone – partially silicified black shales minor disseminations pyrite increasing down hole to up to 30% pyrite as disseminations and bands.
73 – 156m	Pyritic black shales. Pyrite as disseminations and massive fine grained bands, also coarser veins and bands in places – possibly crosscutting and possibly remobilised, 30 – 90% pyrite. Coarse honey coloured sphalerite and grey-silver sulphides – some galena and some sphalerite 142-146m. Weak to moderate silicifaction is common with quartz veining and interstitial quartz in the more sulpidic zones.
156 – 165m	Shales/siltstones, green to brown haematitic. No obvious pyrite.
165 – 174m	Black shales with pyritic bands, strong pyrite 166-168m becoming 10% pyrite down hole. Minor haematitic crystals 171-172m.
174m	EOH.

Water Table Details : 18.00m
Depth of Oxidation : 19.00m
Depth of Cover : .00m

Directional surveys:

Depth (downhole)	Azimuth (from Mag. N.)	Declination (from Horizon)	Survey Instrument	Survey Type
0.00	55.00	-60.00.	Compass/clinometer	Raw survey info.

Logged by : DRJ

Best intersections:
4m @ 8.63% Zn, 1.12% Pb, 71.25ppm Ag and 140ppm Cd – from 142m also 30m @ 43.6ppm Ag – from 126m

Comments:
Large sulphide zone with a narrow high grade Zn-Pb-Ag zone within a broader highly anomalous Ag zone.

HOLE ID RV003

Collar Survey:	(local)	(AMG)		
	15185 N	N	Elevation:	183.00m
	14840E	E	Inclination:	60.00
Azimuth: 90.00		60.00	Azimuth (Mag):	55.00

Precollar/Percussion metres
Open Hole :
Reverse Circulation : 144.00m of Hammer (13.97 cm)

Final Depth: 144.00m

Purpose:
To test for mineralisation below the Gossanous Zone at Grevillea which returned anomalous Pb, Ag As geochemistry.

Summary Log:
RVC003

0 – 17m	Weathered red-brown siltstone mod-strongly ferruginised.
17 – 29m	Black shales disseminated pyrite, <5%.
29 – 49m	Black shales strongly pyrite 30 – 50% pyrite as bands and disseminations. Some grey laminations in parts 34-42m, possibly very fine sulphide, or a clay or graphite.
49 – 51m	Red brown haematitic clays.
57 –63m	As for 29-49m, some haematitic material.
63 – 69m	Red brown haematitic siltstone/shale with some minor pyrite chips.
69 – 100m	As for 51-63m, some very sulphidic zones with up to 80% pyrite.
110 – 116m	Black shale minor disseminated pyrite <5% with some haematitic material.
116 – 134m	Pyritic black shales some massive bands 10-30% pyrite throughout. Massive pyrite 119-121m
144m	EOH.

Water Table Details : 34.00m
Depth of Oxidation : 18.00m
Depth of Cover : .00m

Directional surveys:

Depth (downhole)	Azimuth (from Mag. N.)	Declination (from Horizon)	Survey Instrument	Survey Type
0.00	55.00	-60.00.	Compass/clinometer	Raw survey info.

Logged by : DRJ

Significant intercepts:
20m @ 29.7ppm Ag – from 76m (low Base Metals)

Comments:
Base metals values were low within a large highly sulphidic zone. High Ag zone at base of the sulphide zone correlates with the high grade zone from Holes RVC001 and 002.

RVD017 Cd variation with Depth

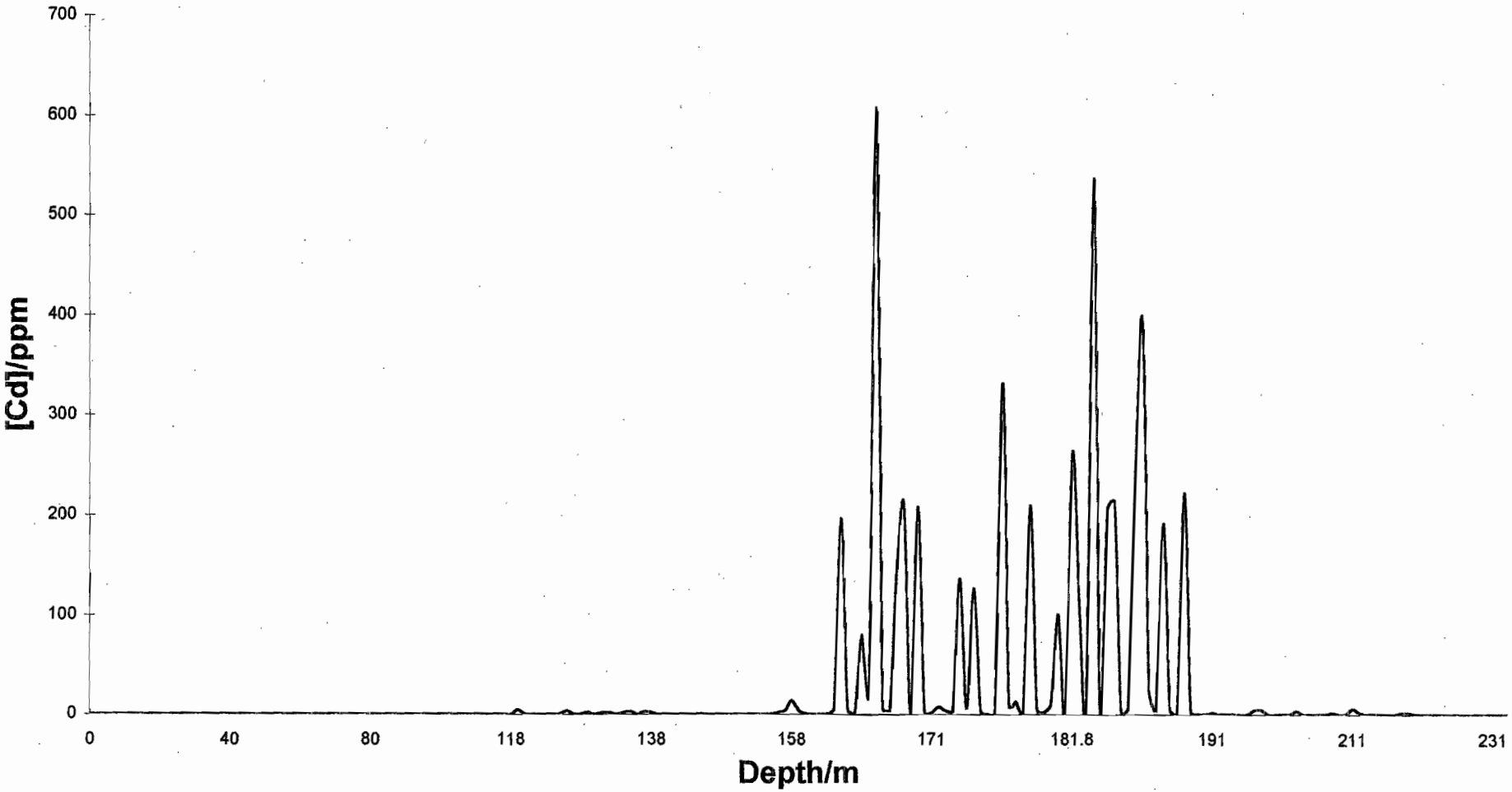

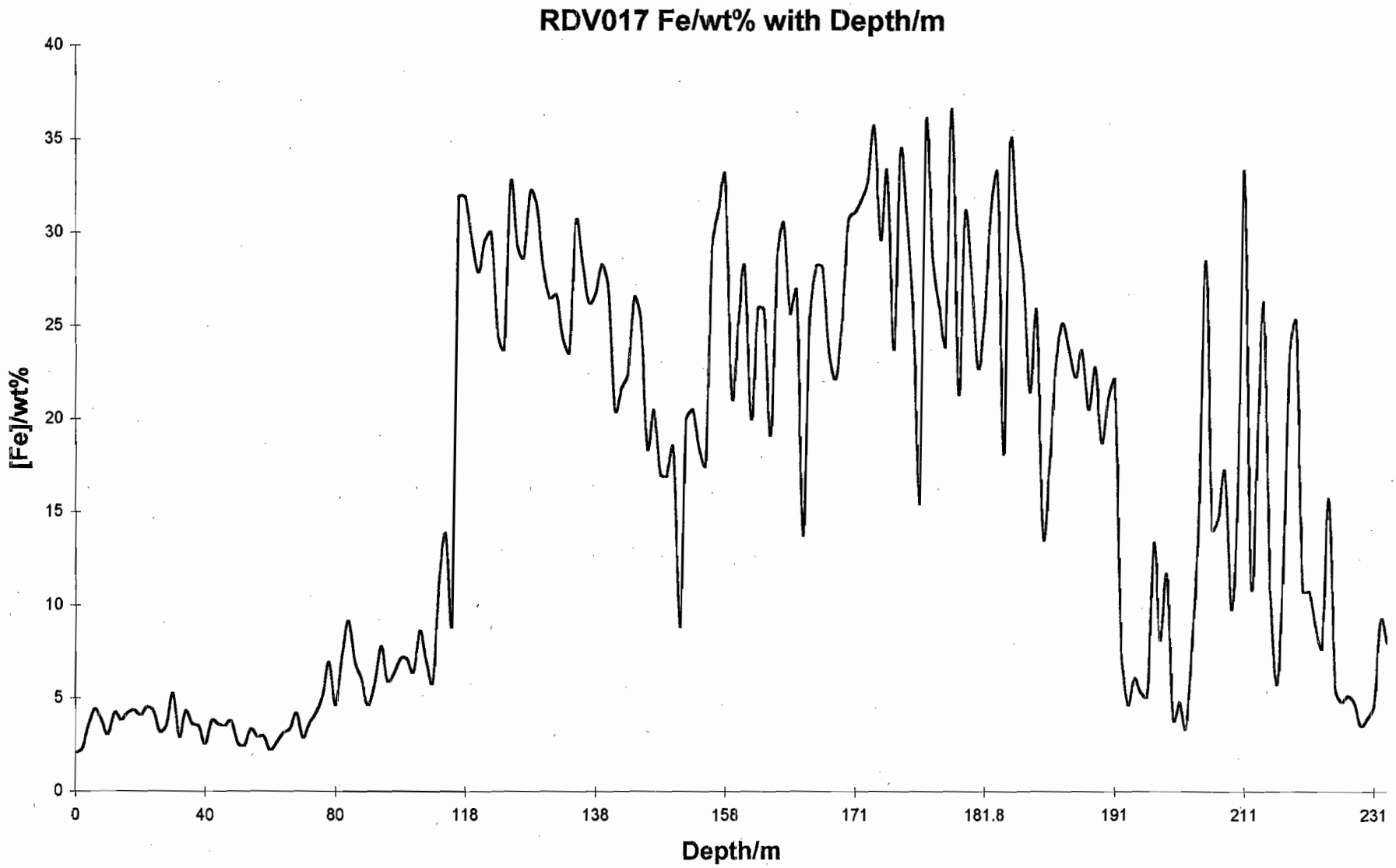
RDV017 Fe/wt% with Depth/m
[Fe]/wt%
0
5
10
15
20
25
30
35
40
0
40
80
118
138
158
171
181.8
191
211
231
Depth/m

RVD 017 As variation with Depth

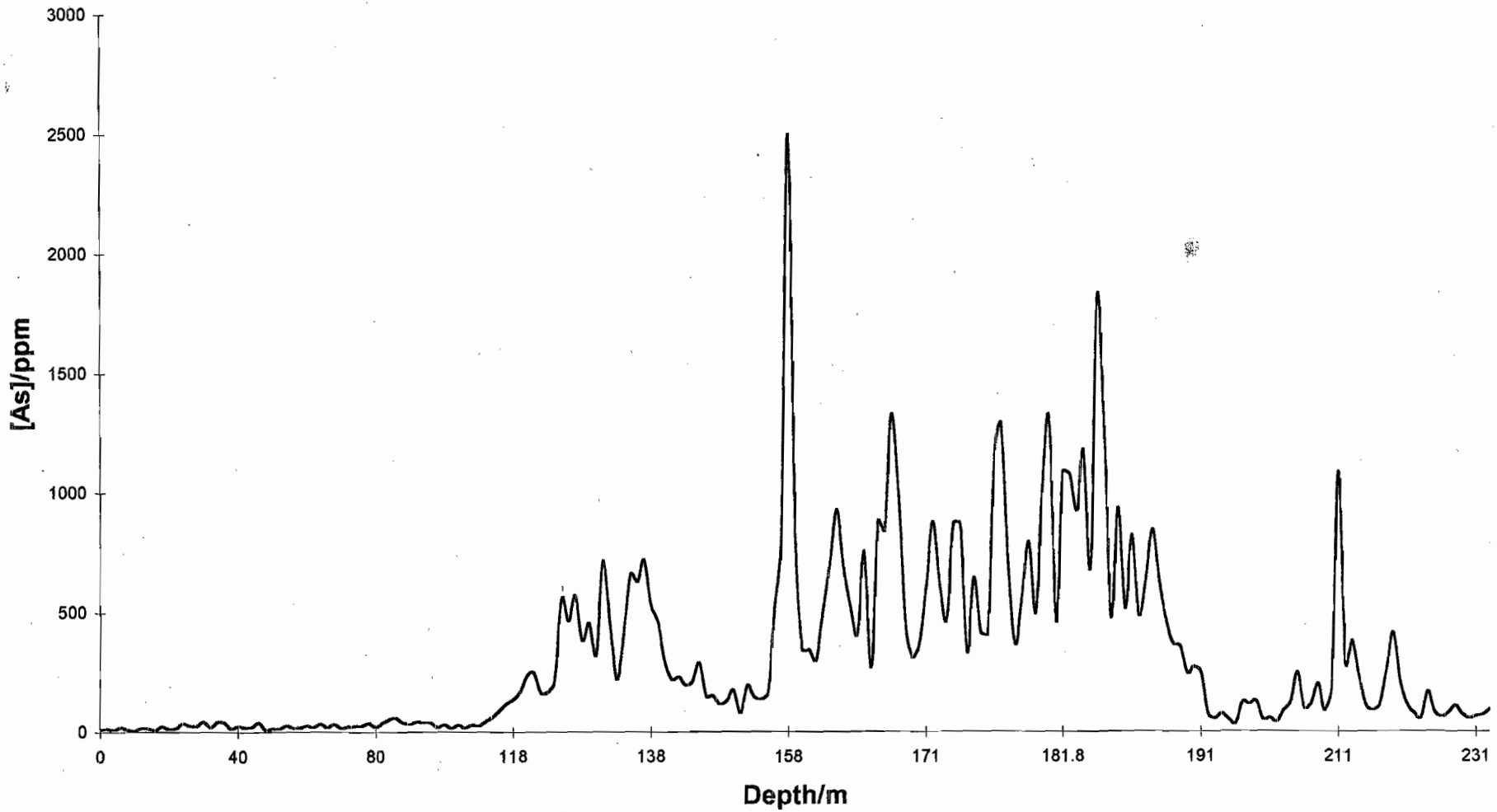

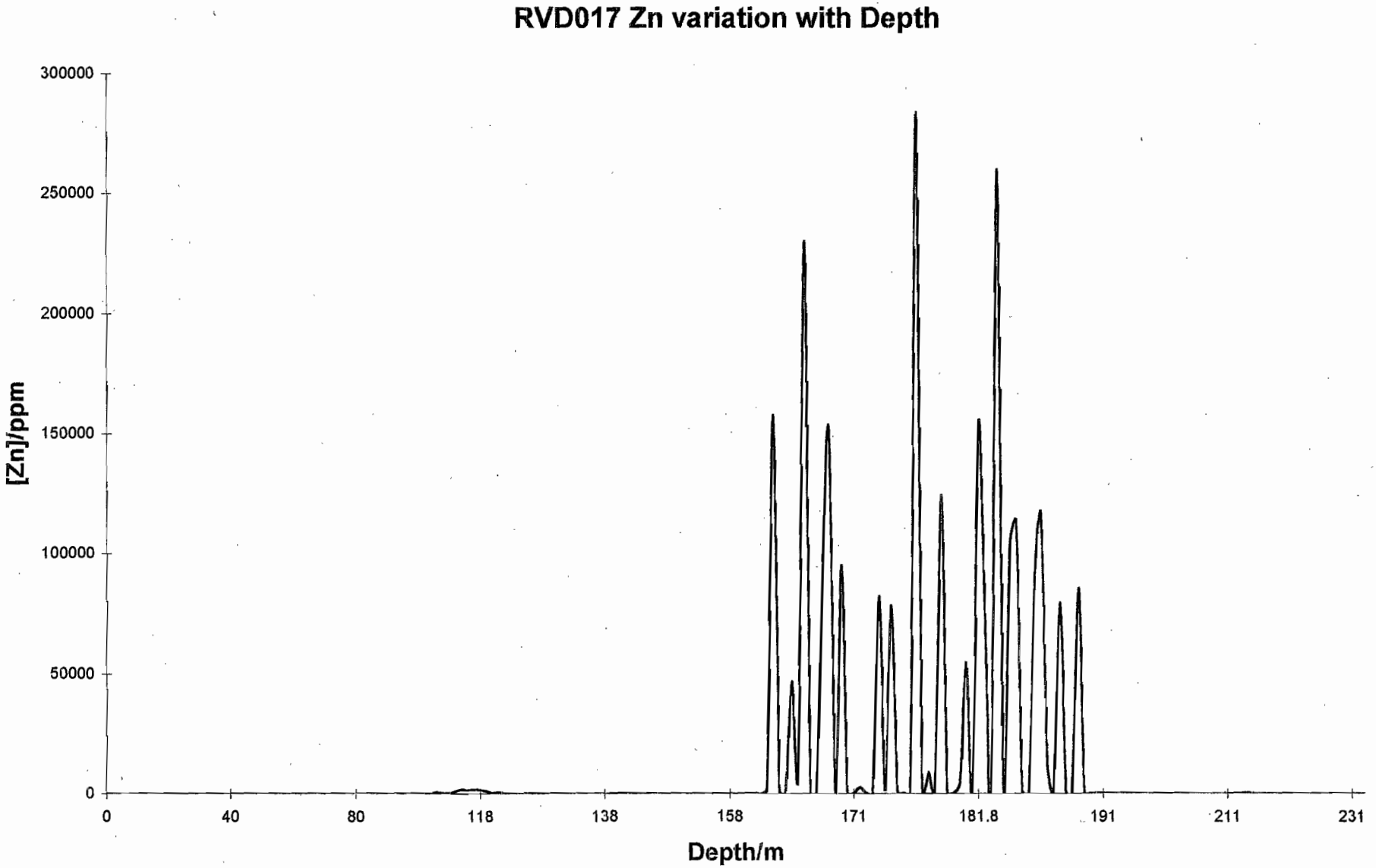
RVD017 Zn variation with Depth
[Zn]/ppm
300000
250000
200000
150000
100000
50000
0
0
40
80
118
138
158
171
181.8
191
211
231
Depth/m

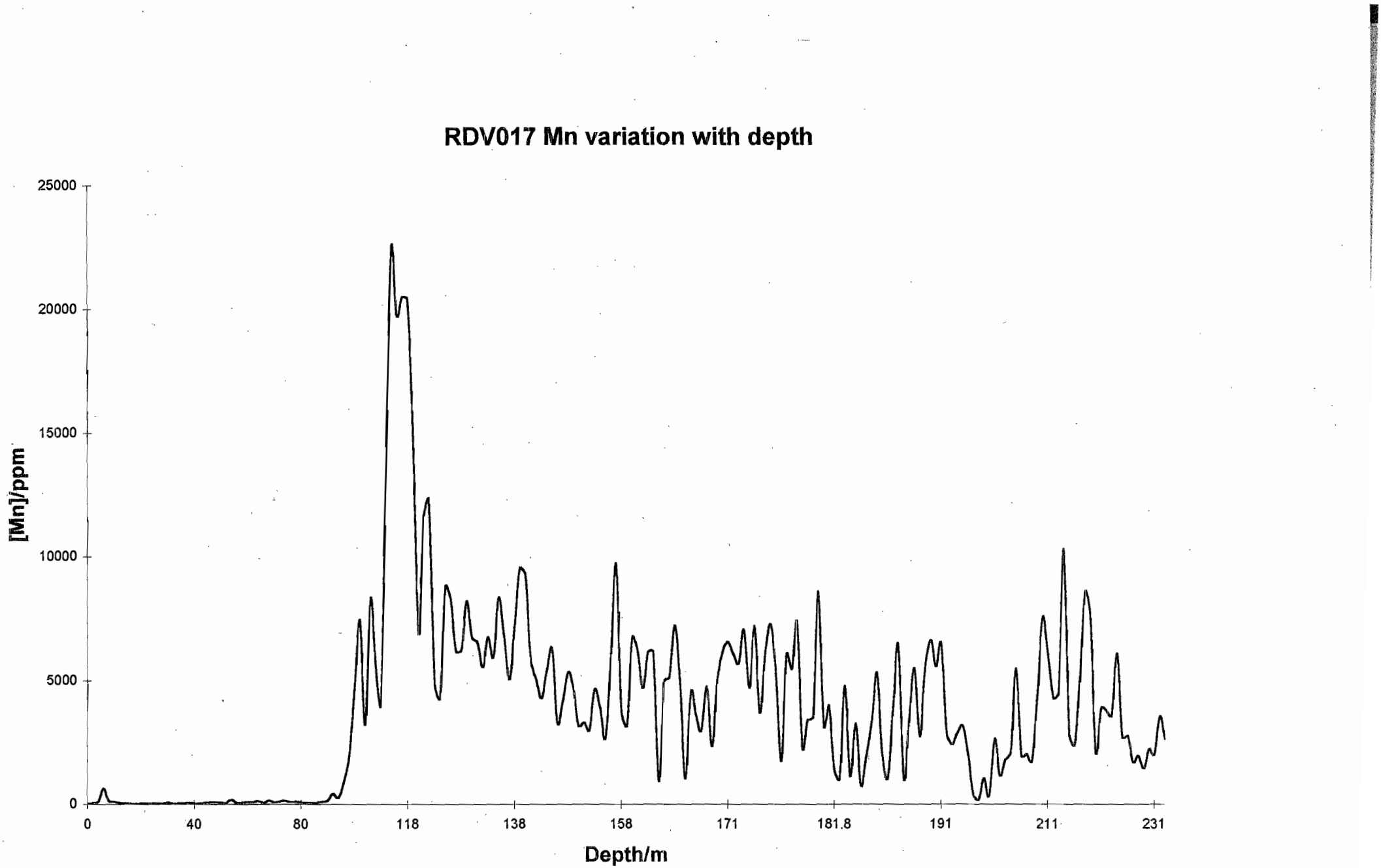
RDV017 Mn variation with depth
[Mn]/ppm
25000
20000
15000
10000
5000
0
0
40
80
118
138
158
171
181.8
191
211
231
Depth/m

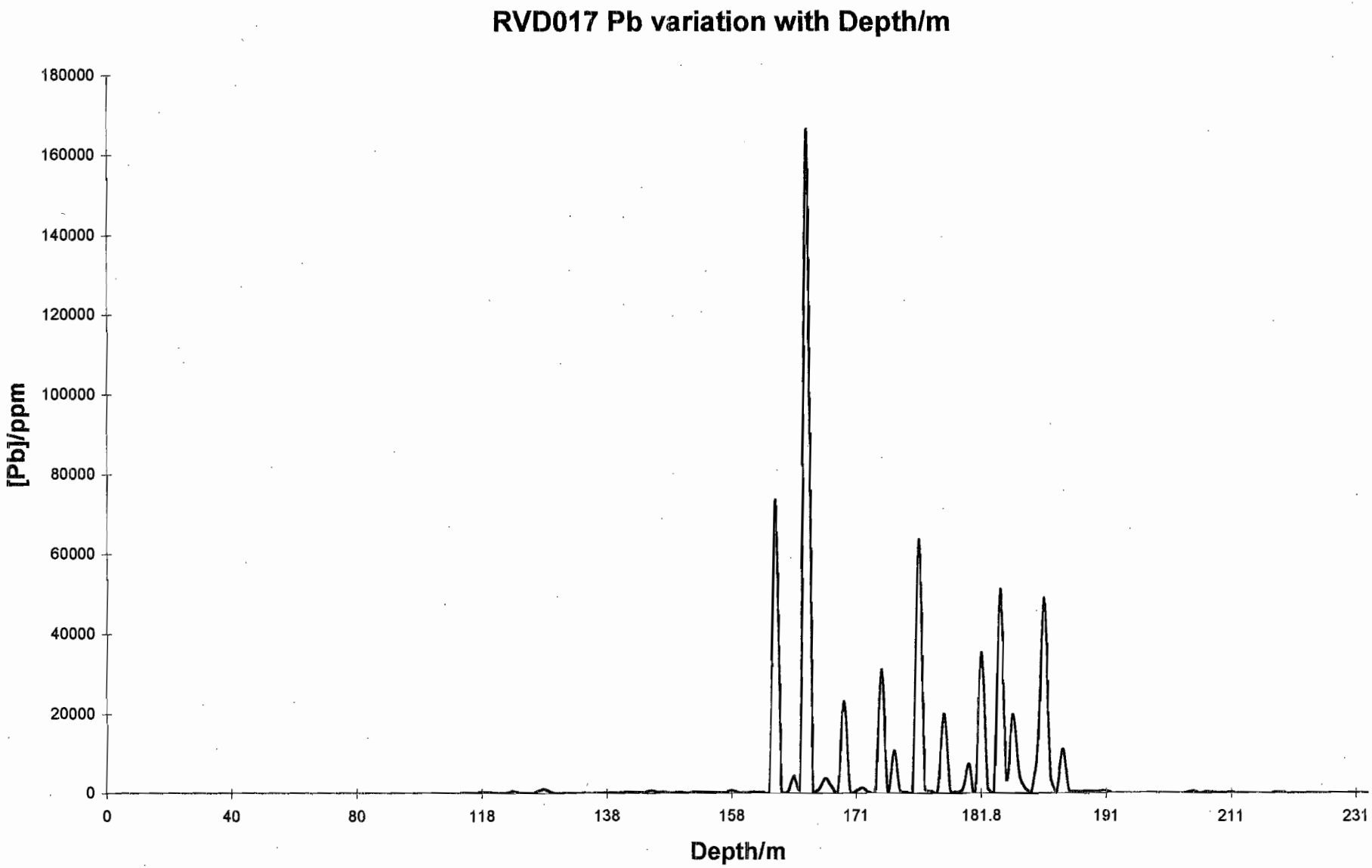
RVD017 Pb variation with Depth/m
[Pb]/ppm
180000
160000
140000
120000
100000
80000
60000
40000
20000
0
0
40
80
118
138
158
171
181.8
191
211
231
Depth/m

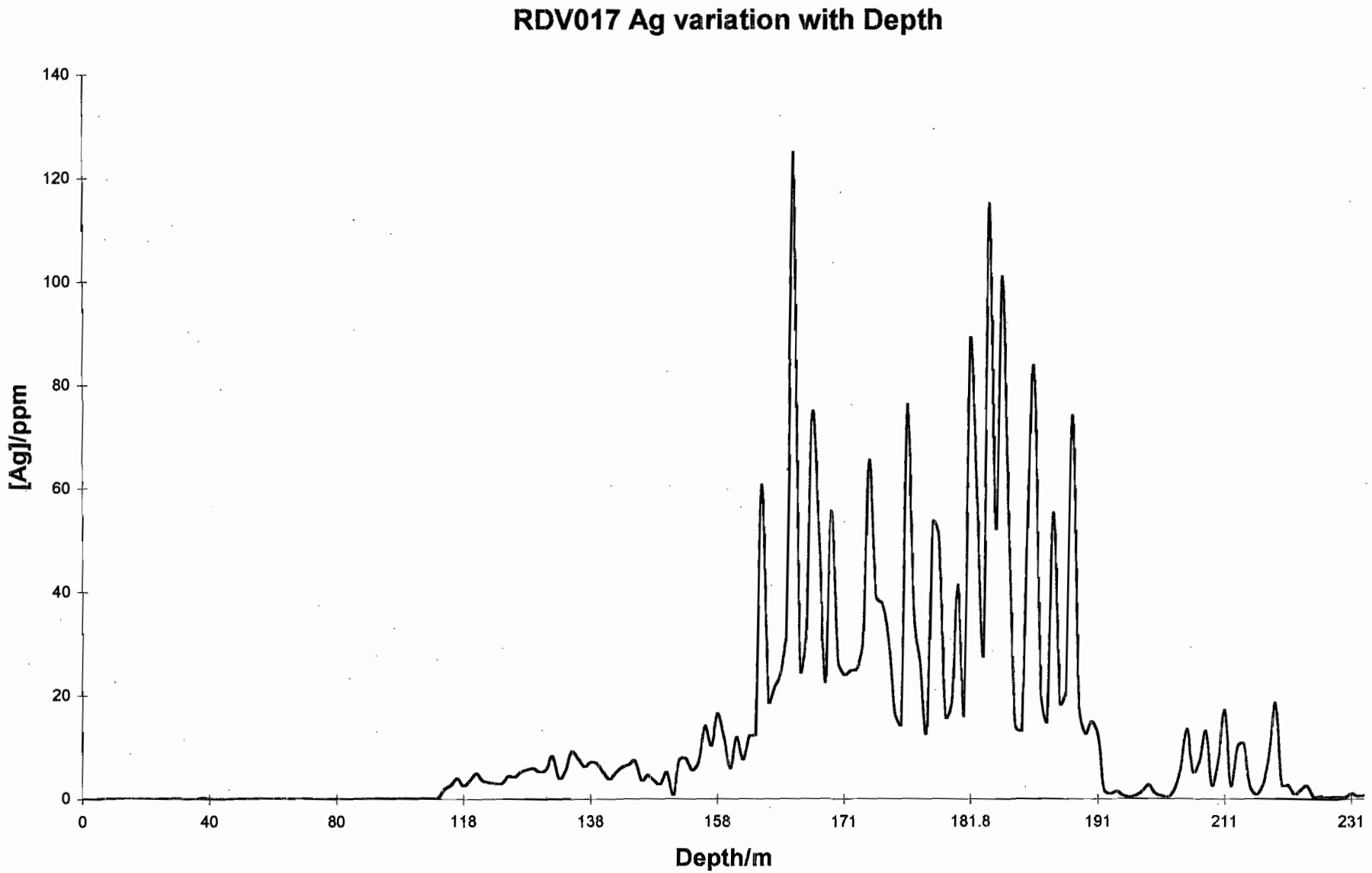
RDV017 Ag variation with Depth
[Ag]/ppm
140
120
100
80
60
40
20
0
0
40
80
118
138
158
171
181.8
191
211
231
Depth/m

RVD017 Cu variation with depth

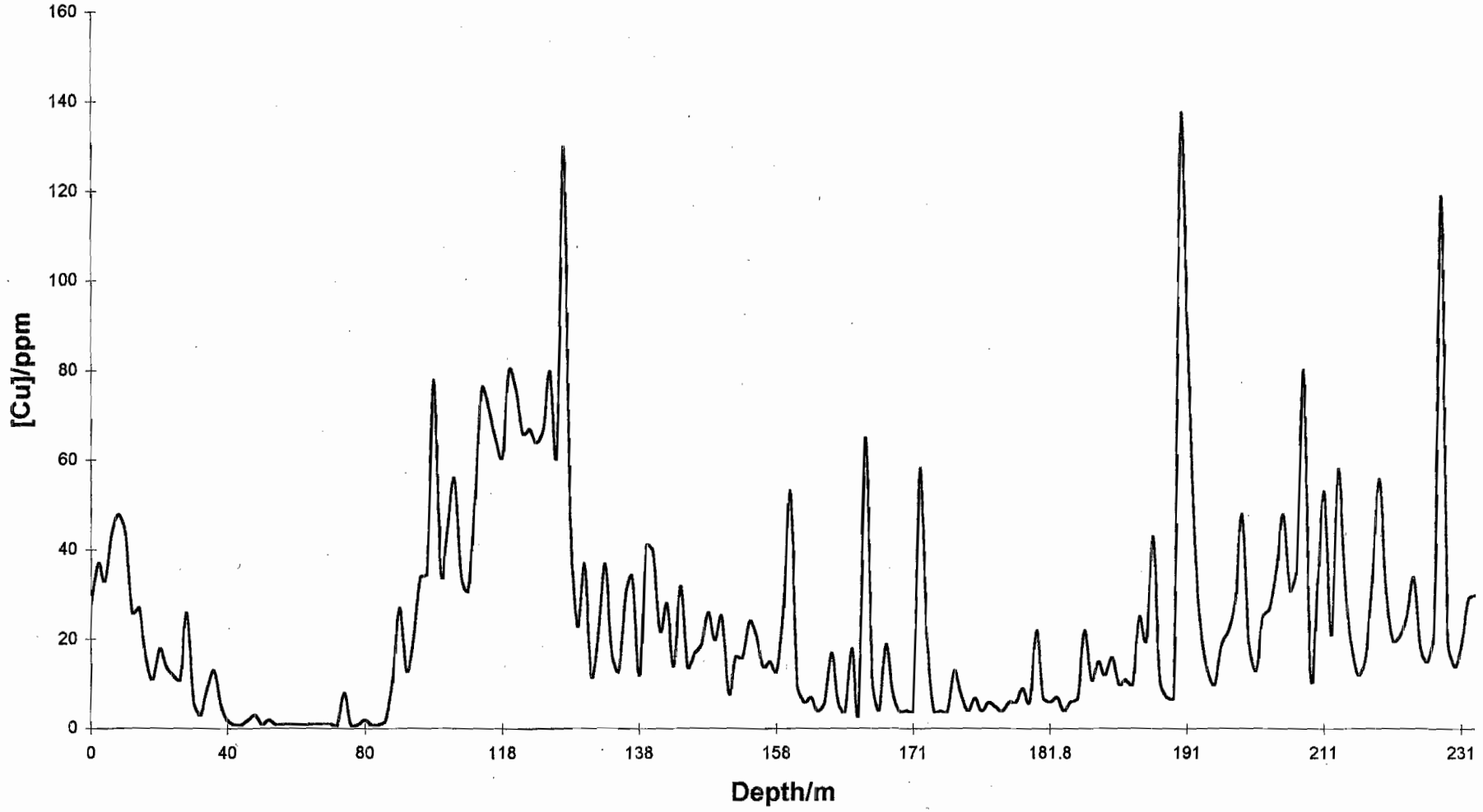

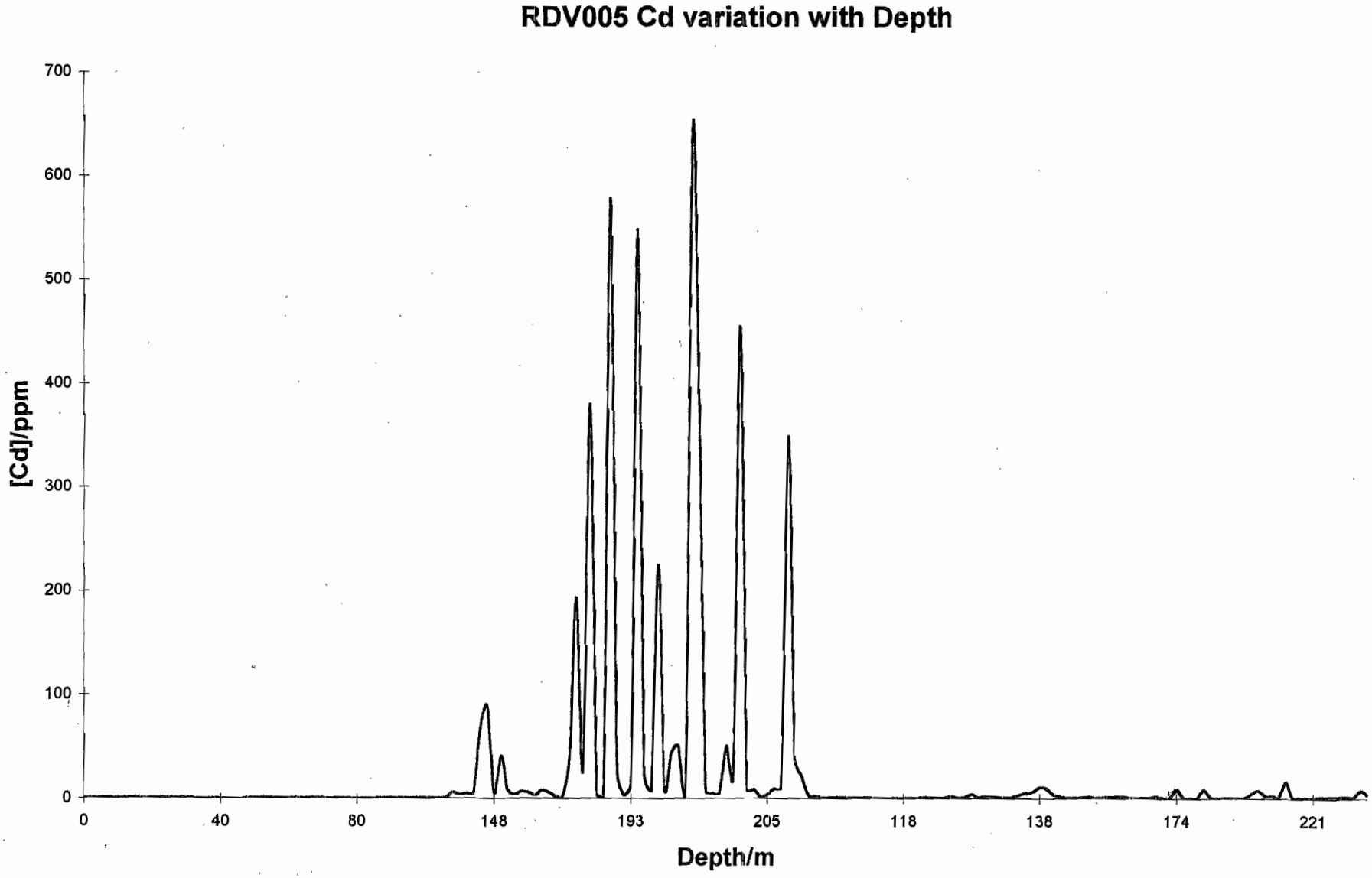
RDV005 Cd variation with Depth
[Cd]/ppm
700
600
500
400
300
200
100
0
0
40
80
148
193
205
118
138
174
221
Depth/m

Appendix 3

Drill Hole Log for RVD017

RDV017 – CORE

117.0 – 117.22m	Barite rich breccia, brecciated pyritic shales with 40-60% py, cavities within barite also present and minor calcite, core recovery ~ 100%
117.22 – 118.0m	Finely laminated black shales with fine grained pyritic bands altered to red haematite in parts. Strong dolomitization of some shale bands making them light grey. Deformed throughout with fracturing and folding with dolomitic shales deforming in a brittle manner while the black shales and the pyrite have been ductile. Breccia bands subparallel to bedding as for 117 – 117.22m. Barite veinlets common throughout with some calcite and possible qtz also associated. Brecciated bands are also barite rich. Displacement across veinlets common. Remobilisation of pyrite also common.
118 – 120m	As above strongly haematitic for most of the zone. Barite veinlets at high angle to core. Bands of dolomitic shales usually thickest (1 – 5cm thick), with pyritic bands from 2mm – 2cm thick – black shales wispy 1mm – 1cm thick fractured nature could be soft sediment deformation with late stage baritic fluids causing remob of pyrite and baritic breccia.
120 – 120.45m	Baritic, dolomitized, pyritic, "breccia" swirling veins and veinlets of barite ± qtz ± haem (silver crystalline) with associated pyrite wisps, blebs and veins, wispy particles of black shales also, pyrite content 40%.

120.45 – 121.25m Laminated black shales with finely laminated pyrite bands. Fractured dolomitic shales at 120.75m with barite and pyrite veining and plastically deformed black shales. Laminations from 1m→4cm with an overall pyritic content of ≈40%. Some bands contain barite crystals – 0.5 - 1mm size usually with associated slightly coarser grained 0.5 - 1mm pyrite. Most pyrite is very fine grained. Broken core at 121.00 but good core recovery approaching 100%.

Only minor barite veining, minor red cherty bands – 1cm max amongst shales and pyrite.

121.25 – 123.30m Mostly baritic "breccia" as above some vesicles possibly after calcite, some graphite filling these cavities at 121.25m. Graphite along fractures, also zones of laminated pyritic shales at 121.5m and 123m.

123.3 – 125.0m Laminated black shales and pyritic bands. Pyritic bands make up 60% of length from 124 - 125m. Shales vary from light grey to black, sometimes grading from the light grey to the black downhole, between pyritic bands. Light grey probably due to dolomitization.

Some bedding parallel baritic veins/layers. Bands vary from very finely laminated (<1mm) to 5cm thick for both the pyrite and the shales.

Bedding @ 170° (mag) 50°W

165° 54°W

125 – 127.8m As above with particles of fracturing/deformation with associated barite at 125.05m, 125.55m, 125.85m, 127.6m. Also pyritic bands are more irregular with veinlets joining bands and pyritic bands containing significant amounts of grey sediment. Still

from 1m→4cm with an overall pyritic content of ≈40%. Some bands contain barite crystals – 0.5 - 1mm size usually with associated slightly coarser grained 0.5 - 1mm pyrite. Most pyrite is very fine grained. Broken core at 121.00 but good core recovery approaching 100%.

Only minor barite veining, minor red cherty bands – 1cm max amongst shales and pyrite.

121.25 – 123.30m Mostly baritic "breccia" as above some vesicles possibly after calcite, some graphite filling these cavities at 121.25m. Graphite along fractures, also zones of laminated pyritic shales at 121.5m and 123m.

123.3 – 125.0m Laminated black shales and pyritic bands. Pyritic bands make up 60% of length from 124 - 125m. Shales vary from light grey to black, sometimes grading from the light grey to the black downhole, between pyritic bands. Light grey probably due to dolomitization.

Some bedding parallel baritic veins/layers. Bands vary from very finely laminated (<1mm) to 5cm thick for both the pyrite and the shales.

Bedding @ 170° (mag) 50°W

165° 54°W

125 – 127.8m As above with particles of fracturing/deformation with associated barite at 125.05m, 125.55m, 125.85m, 127.6m. Also pyritic bands are more irregular with veinlets joining bands and pyritic bands containing significant amounts of grey sediment. Still about 60% pyrite, possibly some remobilisation during deformation.

127.8 – 130m Laminated black shale and pyritic bands, 60% pyrite with zones of barite veining associated with remobilisation? Of

about 60% pyrite, possibly some remobilisation during deformation.

127.8 – 130m — Laminated black shale and pyritic bands, 60% pyrite with zones of barite veining associated with remobilisation? Of pyrite and fracturing at 128.25m, 128.95m, 129.2m, 129.8m. Core broken around 128.8m, 129.3m but ≈ 100% recovery.

130.0 – 139.0m — As above, 40% pyrite overall. Narrow more convolute beds scattered throughout commonly associated with more barite. Strongly pyritic zones 131.6 - 131.8m, 132.64 - 132.93m, 134.93 - 135.10m, 136.90 – 137.04m. Baritic and pyritic breccia present in thin subparallel bands with wider zone from 137.50m to 137.8m, 138.40 to 138.52m. Shale beds vary from black to pale grey – grading from grey to black downhole in some places between the pyrite layers minor barite veinlets.

Bedding	172° 67° W/136.4m
Bedding	156° 40° W/138.0m Near C/O
Bedding	164° 56° W/134

Local folding poss. Parasitic.

139 – 146m — As above, but with less pyrite (overall 30%) with gaps between pyrite layers of up to 29cm (at 142m).

Baritic breccia 139.15 – 139.4m, 139.55 – 139.67m, 140.9 – 141.05m, 143.7 – 143.96m, 145.0 – 145.3m. Also thin baritic (beds?) subparallel bands at 141.91m, 142.67m, 143.33m, 143.4m. Minor haematite staining 145.64m, 142.20m, sediments pale grey-black sometimes graded, grey appears to be an alteration halo around the pyrite eg. 144.13m.

	Bedding	141.2m 164° 68° W
		143.4m 148° 60° W
		144.2m 157° 66° W

146 – 154.4m Pyrite poor zone pyritic bands – finely laminated to massive within black-grey shales as above, separated by large thicknesses of black shales eg. 150.2 – 152m – almost all black shale, disseminated pyrite – only minor.

Not much baritic breccia, weakly developed, 152.2 – 152.35m, 153.8 – 153.85m.

154.4 – 154.95m Laminated pyritic shales with some baritic bands,

154.62 – 154.72m,

154.8 – 154.85m

py 40% overall

Bedding 154.55m 157° 62° W

154.95 – 155.45m Black shale with red cherty haematitic bands (possible Tuff marker Bed?) - 2mm thick – minor 1 – 3mm pyritic bands also. Micro fractured + faulting + barite veinlets.

Bedding 155.3m 150° 63° W

155.45 – 159.55m Strongly pyritic zone – some fine grained laminated pyrite and shales with some massive pyrite bands fine to medium grained and minor coarser grained pyrite – minor core loss at 157.95m in coarse pyrite bands. Barite associated with pyritic bands up to 38cm wide.

	Baritic breccia 155.55 – 155.65m, 156.2 – 156.4m, 157.05 – 157.37m, 157.50 – 157.70m.
	Bedding 156.5m 156° 56° W
159.55 – 164.5m	As above less pyritic 40% pyrite coarse pyritic band at 162.7m with barite association.
	Baritic/pyritic breccia 160.18 – 160.4m, 163.1 – 163.15m, 161.72 – 161.75m, 164.28 – 164.35m, minor barite veinlets present.
164.5 – 164.7m	Banded grey-black shale + fine grained py 1mm – 2cm bands, 40% py.
164.7 – 164.8m	Barite, pyrite + galena breccia? – coarse grained, some sp also present although galena appears dominant, 20% py, 20% gn + calcite closely associated galena 10% sp?
164.8 – 164.88m	Laminated shales + pyrite as above, 50% py.
164.88 – 164.98m	Barite and pyrite rich breccia, some galena blebs and wisps and more light honey brown sp – difficult to distinguish from sphalerite. Ba 50%, py 20%, sp 15%, gn 5%.
164.98 – 166.66m	Laminated shales and pyrite, 50% pyrite – some baritic bands 5 – 10cm thick, no obvious sp or gn.
166.66 – 167.03m	Barite 20% pyrite 70% breccia? Gn 8% sp 2% - minor calcite also.
167.03 – 167.8m	Laminated shales + py (50%).

167.8 – 167.98m	Galena and sp rich, coarse grained barite and pyrite.
167.98 – 169.54m	Laminated pyrite and shales py 50%, minor barite bands.
169.54 – 169.86m	Pyrite + barite rich zone convolute banding with sp-hon-br difficult to distinguish from barite, not much galena.
169.86 – 170.18m	Laminated silic shale and pyrite fine grained 60% py.
170.18 – 170.48m	Barite + pyrite rich zone with some sph. Hon br coarse grained amongst deformed grey sediments, fine grained siliceous shales.
170.48 – 170.65m	Banded shale and pyrite.
170.65 – 170.82m	Coarse grained galena 10% + sp 20% + py 20% + barite 20% + cc 10%.
170.82 – 173.8m	Banded shales and pyrite, 50% py. Barite veins present – some pyritic bands contain blebs/clasts of silic shales.
173.8 – 174.62m	Highly pyritic zone 80% pyrite, rest grey to black shales. Baritic veining increasing downhole.
174.62 – 175.12m	Coarse grained py, ba, gn and sp with barite veining and grey siliceous bands, 174.62 – 174.67m strong galena.

175.12 – 175.55m	Banded dolomitic shales and py 40%. Some barite veining at top of section.
175.55 – 175.73m	Medium-coarse grained sp + ba + py + gn.
175.73 – 176.51m	Banded py + shale, 60% py.
176.51 – 176.59m	Py + sp + ba + gn.
176.59 – 177.38m	Banded shales + py 40%.
177.38 – 177.90m	Sp rich zone with some gn + barite, interstitial + pyrite, sp 40% + barite veining. Coarse grained material.
177.90 – 178.26m	Banded shales + py as above, 60 % py.
178.26 – 178.32m	Medium grained sph + py + barite band, no obvious gn – top contact irregular – slightly – bottom contact gradational from fine grained py.
178.32 – 179.79m	Banded shales (silic) + pyrite 60-70%, minor barite + pyrite bands with minor sph 178.44 – 178.45m, 178.68 – 178.73m. Barite veins 178.8m, 179.55m.
179.79 – 179 89m	Medium coarse grained py + gn + sp + barite, some cavities associated with gn.

179.89 – 181.24m	Banded shales + pyrite, minor barite crystals in bands 180.6m – no obvious sph, py cont 179.89 – 180.70m – 60%, 180.7 – 181.0m – 25%, 181 – 181.24m – 40%.
181.24 – 181.30m	Medium grained sp + ba + py.
181.30 – 181.49m	Banded shale (silic) + pyrite, 80% py.
181.49 – 181.55m	Medium grained ba + py + sph zone – no obvious gn.
181.55 – 181.85m	Banded silic shale + pyrite, 40-50% py.
181.85 – 182.04m	Sp + gn + ba + py zone, top 4cm strong gn + sp coarse grained – rest medium grained sp + py + ba – no obvious gn.
182.04 – 182.28m	Banded py + shales – dolomitic, 70% py.
182.28 – 182.63m	Broadly conformable sp + gn + ba + py zone, gn wispy, ba + py interstitial , sp coarse grained, some ba veining + fine grained py bands, some cavities and minor associated calcite.
182.63 – 182.88m	Banded shale + py, 70% py.
182.88 – 183.08m	Medium grained py + sp + ba zone.
183.08 – 183.74m	Laminated shale + banded pyrite dolomitized at top and bottom of intersection where there is more pyrite. Overalll py 10-15%

	Bedding	183.3m 163° 57° W
183.74 – 183.90m	Coarse grained pyrite + barite – possible minor sph.	
183.90 – 185.06m	Banded silic shales and pyrite finely laminated, 40% py content.	
185.06 – 185.31m	Medium-coarse grained sph + gn + py + ba – conformable.	
185.31 – 185.37m	Banded shale + py + minor ba.	
185.37 – 185.41m	Medium grained sp + py + ba + gn band.	
185.41 – 185.76m	Banded shale (silic) + py, 50% py.	
185.76 – 185.84m	Bands of medium-coarse grained gn + sp + py within fine grained py bands.	
185.84 – 186.15m	Banded shale + py, 50% pyrite.	
186.15 – 186.92m	Coarse grained py + sp + gn + barite – with convolute and wispy shale + pyrite bands amongst them + shale fragments.	
186.92 – 187.68m	Banded shale + pyrite, some convolute and fractured bands, 50% py.	

187.68 – 188.14m	Banded dolomitic black shales and cherty red haematitic bands (possible TMB) – barite vein with bxd edges @ 188m 1cm thick.
188.14 – 188.35m	Pyrite and black shale (silic→grey), 60% py.
188.35 – 188.66m	Coarse grained py and ba + silic + sp + gn – sp + gn strongest near top of intersection becoming scattered downhole but still present.
188.66 – 190.23m	Banded py + shales, py 70%, barite crystals in bands 190.08 – 190.19m.
190.23 – 190.28m	Thin band of barite, py + sph.
190.28 – 190.55m	Silic black shale with some pyrite bands 20%.
190.55 – 191.90m	Banded pyrite with shale inter beds, 75% py.
191.9 – 192.3m	Transitional zone from above to below 40→20% py.
192.3 – 197.0m	Black shales, some dolomitization making them grey, in parts minor thin pyritic bands <5%. Red haematitic bands 196.6 – 197.0m.
197.0 – 199.8m	Grey-black shales with haematitic + pyritic laminations, strong haematitic zone 197.25 – 197.80m <5 py 10% hm calcite veinlets 199.40m.
199.8 – 200.00m	Pyritic shale – laminated/banded, 40% py.

200.00 – 203.80m	Grey-black shales finely laminated with some minor <0.5mm – 5mm pyrite bands <5% minor calcite veinlets.
	Bedding 201.5m 165° 61° W
203.80 – 204.73m	Grey shales with pyritic bands laminated finely. Medium grained cc rich bands ± barite ± pyrite, no obvious sp or gn 203.8 – 204.0m.
204.1 – 204.15m	Grey shale from 204.5 – 204.73m.
204.73 – 204.90m	Medium grained calcite ± barite + pyrite + minor shale.
204.9 – 205.42m	Banded shales + pyrite, 60-70% py.
205.42 – 205.7m	Massive pyrite 90% with minor cc + black shales.
205.7 – 206.12m	Mostly pyrite with interbedded shales and calcite barite, pyritic zone 205.75 – 206.02m.
206.12 – 206.55m	Banded shales + pyrite, 20% pyrite.
206.55 – 206.68m	Calcite ± barite + pyrite zone, medium grained slightly irregular contacts subparallel – cavities also present.
206.68 – 207.64m	Mostly grey-black shales – pyrite bands 206.71 – 206.79m, 206.97 – 207.03m, 207.30 – 207.34m.

207.64 – 208.47m	Pyrite + calcite ± barite + black shale bands, irregular banding local deform. No obvious sph or gn.
208 47 – 209.30m	Grey to black shales, some cc rich bands locally deformed by folding + mini faults pyritic zones + blebs associated with more deformed zones + the calcite.
209.3 – 209.84m	Grey-black shales minor pyritic bands finely laminated, 10% py.
209.84 – 210.22m	As above increasing py 20%.
210.22 – 210.80m	Irregularly banded pyrite and shales with barite crystals – minor cc + cavities in many of the shale bands, 50% py.
210.8 – 211.09m	Banded pyrite + shale 30% py.
211.09 – 212.05m	Coarse grained pyrite zone with barite blebs + veins – minor shale bands + cavities with minor associated cc. No obvious sp or gn becoming more banded down hole.
212.05 – 212.20m	Black-grey shales, minor disseminated py <2%.
212.20 – 212.57m	Black to grey shales brecciated, fractured and locally deformed – sedimentary breccia →soft sediment deformation some pyrite within the more brecciated or deformed material – grey shales from clasts with py + black shale deforming around them. Clasts of sulphide in the breccia.
212.57 – 213.40m	Mostly grey-black shales with minor <5% py in diss. + bands.

213.40 – 213.85m	As above, py increasing downhole, 25% overall.
213.85 – 214.36m	Coarse grained py + cc + ba, no obvious sp or gn, some barite vein + calcite vein (stylolitic).
214.36 – 214.48m	Banded black shales and pyrite (40%).
214.48 – 214.95m	Some zones of cc + coarse grained py + ba between grey-black shales with pyritic ands.
214.95 – 218.25m	Grey-black laminated shales with minor pyritic bands with occasional pyritic blebs, calcite rich banding around 218m.
218.25 – 220m	Black-grey shales interbedded increased py content as bands + veinlets, 20% py. Also strongly calcareous. Pyrite poor zone 219.1 – 219.4m with some sed. breccia 219.25 – 219.35m.
220 – 223.57m	Shales – minor pyrite content <5% mostly in bands. Also some calcite rich bands, good core recovery despite broken core in places.
223.57 – 223.88m	Sed. bx as for 212.20 – 212.57m.
223.88 – 224.28m	Py + cc rich zone, minor barite and shales.
224.28 – 233.8m	Grey-black shales grey from calcite content – footwall alteration some cc veinlets also scattered throughout cc bx at 226.10m.

Minor pyrite in top 0.5m. Strong cc bx/veining at 228.3 – 228.6m, no strong pyrite association, also calcite + pyrite rich band 232.9 – 233.1m. Also thin beds of sed bx 230.88 – 231.07m, 231 – 60m.

Bedding	230.6m	157°	60° W

Appendix 4

Rock Chip Geochemistry and ICP-OES Results

ICP-OES Results for Grevillea Gossan Samples

		Cu	Pb	Zn	Ag	As	Mo	Cd
UNITS		**ppm**	**ppm**	**ppm**	**ppm**	**ppm**	**ppm**	**ppm**
DETECTION LIMIT/ppm		**5**	**5**	**5**	**1**	**5**	**5**	**5**
METHOD		IC587		IC587	IC587	IC587	IC587	IC587
SAMPLE DESCRIPTION	**NAME**							
Powdery , yellow jarosite	**175m**	15	856	<5	4	279	<5	<5
Brecciated Jarosite associated with fault	**J1**	29	2860	<5	14	1510	8	<5
Most frequent jarosite at Grevillea	**135m**	26	3150	97	4	143	25	<5
Densely massive, finely laminated hematite	**NG003**	<5	165	20	2	366	7	<5

	NAME	Cu ppm	Pb ppm	Zn ppm	Ag ppm	As ppm	Mo ppm	Cd Ppm
Dense, partly laminated partly botryoidal textured hematite	**G3**	9	399	59	6	9970	17	<5
Hematite replaced in part by jarositic pods	**G4**	8	507	17	3	155	6	<5

	Co ppm **5** **IC587**	Bi ppm **5** **IC587**	Sb ppm **5** **IC587**	Ni ppm **5** **IC587**	Ag* ppm **0.2** **MS587**	Cd* ppm **0.1** **MS587**	Tl* ppm **0.1** **MS587**
135M	<5	8	<5	<5	2.5	<0.1	52.9
J1	<5	<5	32	<5	13.9	<0.1	216
175M	<5	<5	32	11	3.7	<0.1	21
NG003	<5	<5	27	<5	1.1	<0.1	2.3
G3	<5	<5	127	<5	5.6	<0.1	2.2
G4	<5	<5	<5	6	3.3	<0.1	1.3

Note: Ag*, Cd* and Tl* were analysed by ICP-MS

Rock-chip data for Traverse 15150N

East	Cu(IC587)	Pb(IC587)	Zn(IC587)	Ag(IC587)	As(IC587)	Fe%(IC587)	Mn(IC587)	Mo(IC587)	Cd(IC587)
14812.5	2.5	55	6	0.5	12	2.7	69	6	2.5
14837.5	8	27	8	0.5	13	3.08	218	2.5	2.5
14862.5	7	30	16	0.5	14	3.91	242	12	2.5
14887.5	2.5	34	17	0.5	11	3.47	174	2.5	2.5
14955	30	3320	7	14	700	21.61	26	14	2.5
14970	107	531	57	16	705	32.12	17	2.5	2.5
14990	66	259	27	6	626	33.81	30	14	2.5
15012.5	70	455	21	2	233	20.77	59	11	2.5
15037.5	51	108	20	1	268	29.42	95	7	2.5

East	Co(IC587)	Bi(IC587)	Sb(IC587)	Al%(IC587)	Ba(IC587)	%(IC587)	K%(IC587)	Mg%(IC587)	Na%(IC587)
14812.5	2.5	2.5	2.5	4.67	2570	0.04	1.85	0.08	0.07
14837.5	2.5	2.5	2.5	4.68	3680	0.04	2.14	0.12	0.06
14862.5	2.5	2.5	2.5	4.19	2520	0.07	2.18	0.12	0.06
14887.5	2.5	2.5	2.5	4.25	1900	0.04	2.05	0.1	0.06
14955	2.5	2.5	33	0.33	51	0.01	2.96	0.03	0.39
14970	5	2.5	9	0.32	183	0.04	0.37	0.01	0.02
14990	2.5	2.5	13	0.38	183	0.02	0.5	0.01	0.02
15012.5	2.5	2.5	10	1.49	147	0.06	0.75	0.03	0.02
15037.5	2.5	2.5	2.5	0.49	152	0.06	0.42	0.02	0.01

Rock-chip data for Traverse 15150N

East	Ni(IC587)	S(IC587)	Ba(XRF1)	Ag(MS587)	Cd(MS587)	Tl(MS587)
14812.5	9	1260	2790	0.4	0.05	5.5
14837.5	7	795	4110	0.3	0.05	1
14862.5	17	588	2040	0.4	0.05	1.5
14887.5	8	350	2730	0.2	0.05	1.7
14955	2.5	50700	23300	14.2	0.05	181
14970	10	7270	135200	17.2	0.05	23.8
14990	11	7510	16600	6.7	0.05	9.4
15012.5	7	9250	9050	3	0.05	3.4
15037.5	7	6320	37600	1.4	0.05	5.8

Rock-chip geochemistry for Traverse 15200N

East	Cu(IC587)	Pb(IC587)	Zn(IC587)	Ag(IC587)	As(IC587)	Fe%(IC587)	Mn(IC587)	Mo(IC587)	Cd(IC587)
14612.5	9	10	32	0.5	7	2.95	1100	2.5	2.5
14637.5	28	11	7	0.5	18	1.59	975	2.5	2.5
14662.5	24	15	15	0.5	9	2.51	1430	8	2.5
14687.5	23	13	22	0.5	2.5	2.55	1300	2.5	2.5
14712.5	30	9	29	0.5	2.5	2.76	799	2.5	2.5
14812.5	2.5	10	7	0.5	6	1.96	157	2.5	2.5
14862.5	2.5	8	6	0.5	7	1.34	407	7	2.5
14887.5	2.5	17	6	0.5	11	2.54	59	2.5	2.5
14962.5	73	325	18	6	126	7.63	53	6	2.5
14987.5	8	1530	2.5	9	693	27.24	9	13	2.5
15012.5	9	500	2.5	4	331	17.34	49	17	2.5
15037.5	14	181	12	2	43	2.66	41	6	2.5
15437.5	23	11	8	0.5	13	4.65	187	10	2.5

East	Co(IC587)	Bi(IC587)	Sb(IC587)	Al%(IC587)	Ba(IC587)	Ca(IC587)	K%(IC587)	Mg%(IC587)	Na%(IC587)
14612.5	12	2.5	2.5	6.42	2600	0.86	2.39	1.07	0.08
14637.5	12	2.5	2.5	4.44	1310	0.09	1.73	0.08	0.08
14662.5	10	2.5	2.5	5.76	1330	0.5	1.39	0.39	0.09
14687.5	9	2.5	2.5	6.71	1640	0.64	1.63	0.72	0.09
14712.5	11	2.5	2.5	7.32	1800	1.51	1.86	1.47	0.07
14812.5	2.5	2.5	2.5	5.63	2860	0.1	3.31	0.19	0.08
14862.5	2.5	2.5	2.5	4.4	3460	0.03	3.03	0.1	0.06
14887.5	2.5	2.5	2.5	6.37	2690	0.02	1.61	0.27	0.06
14962.5	2.5	6	13	8.02	119	0.04	4.26	0.36	0.07
14987.5	2.5	2.5	17	0.37	35	0.03	2.53	0.005	0.06
15012.5	2.5	7	8	4.19	37	0.04	3.03	0.02	0.1
15037.5	2.5	2.5	14	7.48	141	0.03	4.54	0.35	0.03
15437.5	5	2.5	2.5	2.16	449	0.06	1.83	0.13	0.02

Rock-chip geochemistry for Traverse 15200N

East	Ni(IC587)	S(IC587)	Ba(XRF1)	Ag(MS587)	Cd(MS587)	Tl(MS587)
14612.5	20	595	2890	0.1	0.05	1.1
14637.5	6	499	1420	0.1	0.05	1
14662.5	15	381	1390	0.1	0.05	1.2
14687.5	10	371	1720	0.2	0.05	1.2
14712.5	14	383	1950	0.1	0.05	1.1
14812.5	2.5	469	3010	0.1	0.05	1
14862.5	11	523	3690	0.2	0.05	0.9
14887.5	6	425	3010	0.6	0.05	1.6
14962.5	7	28500	4990	5.1	0.05	21
14987.5	2.5	90000	9410	8.7	0.05	134
15012.5	9	66000	8160	3.5	0.05	56
15037.5	2.5	15300	8220	1.7	0.05	9.1
15437.5	17	438	523	0.1	0.05	0.7

Appendix 5

XRD Traces and Tables,

FTIR Traces

13-534

d	2.69	1.69	2.51	3.66	α-Fe_2O_3
I/I_1	100	60	50	25	ALPHA IRON OXIDE HEMATITE

Rad. CoKα λ 1.7902 Filter - Dia. 114.6MM
Cut off I/I_1 MOLL RECORDING MICROPHOTOMETER
Ref. ARAVINDAKSHAN AND ALI, COUNCIL OF SCI. AND INDUST. RES., CENTRAL FUEL RESEARCH INSTITUTE, BIHAT, INDIA.

Sys. RHOMBOHEDRAL* S.G. $R\bar{3}c$ (167)
a_o 5.4228 b_o c_o A C
α $55^o17'$ β γ Z 2 Dx 5.287
Ref. ARAVINDAKSHAN AND ALI, SCIENTIFIC AND INDUSTRIAL RESEARCH (INDIA), TO BE PUBLISHED.

ε α 2.94 n ω β 3.22 ε γ Sign -
2V D 5.26 mp 1350-1360 Color DEEP-BROWN
Ref. IBID., D_7

*INDEXING BASED ON HEXAGONAL CELL DERIVED FROM THE OBVERSE RHOMBOHEDRON: a_H=5.0317, c_H=13.737

d Å	I/I_1	hkl	d Å	I/I_1	hkl
3.66	25	012	1.102	14	226
2.69	100	104	1.076	2	042
2.51	50	110	1.055	18	2$\underline{1}$10
2.285	2	006	1.042	2	11$\underline{2}$12
2.201	30	113	1.038	2	4$\underline{0}$4
2.070	2	202	0.9890	10	232,318
1.838	40	024	.9715	2	229
1.690	60	116	.9601	18	324
1.634	4	211	.9578	6	01$\underline{1}$4
1.596	16	018	.9512	12	140,02$\underline{1}$3
1.484	35	214	.9314	6	413
1.452	35	300	.9204	6	048
1.349	4	208	.9080	25	13$\underline{1}$0
1.310	20	10$\underline{1}$0,119			
1.258	8	220			
1.226	2	036			
1.213	4	223			
1.189	8	128			
1.162	10	02$\underline{1}$0			
1.141	12	134			

Error = ±0.06 dÅ

17-536

most important peaks & positions

d	4.18	2.69	2.45	4.98	FeO(OH) alpha form $1/2Fe_2O_3.H_2O$
I/I_1	100	30	25	10	Iron Oxide Hydrate (alpha form) Goethite

Rad. Co λ Filter Fe Dia. 19cm.
Cut off I/I_1
Ref. G. Brown, X-ray Ident. and Cryst. Struct. Clay Minerals, p. 386 London 1961 *

Sys. Orthorhombic S.G. Pbnm (62)
a_o 4.596 b_o 9.957 c_o 3.021 A 0.462 C 0.303
α β γ Z 4 Dx 4.264
Ref. Peacock, Trans. Roy. Soc. Canada 36 IV, 116 (1942)

ε α 2.260 n ω β 2.393 ε γ 2.398(Na) Sign
2V D 4.26 mp Color Black
Ref. Posnjak and Merwin, Am. J. Sci. 47 311 (1919)

Peacock records a weak line at 2.09, 5, 220.
* Cited by Harrison and Peterson, Am. Min. 50 704-712 (1965)

d Å	I/I_1	hkl	d Å	I/I_1	hkl
4.98	10	020	1.467	4	320
4.18	100	110	1.453	10	061
3.38	10	120	1.418	2	112
2.69	30	130	1.392	8	330
2.58	8	021	1.357	8	311
2.520	4	101	1.317	8	321
2.490	16	040	1.264	2	331
2.452	25	111	1.241	2	142
2.252	10	121	1.198	2	341
2.192	20	140			
2.009	2	131			
1.920	6	041			
1.799	8	211			
1.770	2	141			
1.721	20	221			
1.694	10	240			
1.661	4	060			
1.606	6	231			
1.564	16	151,160			
1.509	10	250,002			

B

dÅ = position, I/I_1 = relative intensity; measured to highest peak = 100.

10-443

d	3.08	3.11	2.29	5.94
I/I_1	100	60	50	30

$KFe_3(SO_4)_2(OH)_6$ $1/2(K_2O.3Fe_2O_3.4SO_3.6H_2O)$

BASIC POTASSIUM IRON (III) SULFATE JAROSITE

Rad. CuKα λ 1.5418 Filter Ni Dia. 114.6MM
Cut off I/I_1 VISUAL ESTIMATE
Ref. WARSHAW, AM. MIN. 41 288-296 (1956)

Sys. HEXAGONAL * S.G. C_{3v}^5 - R3M
a_o 7.29 b_o c_o 17.22 A C 2.36
α β γ Z 3 Dx 3.25
Ref. IBID. *RHOMBOHEDRAL: A_O=7.12, α=61°35'

ε α 1.715 n ω β 1.820 ε γ Sign -
2V D 2.9-3.26 mp Color YELLOW TO BROWN
Ref. D_7 (UTAH, ANOMALOUSLY BIAXIAL)

SAMPLE FROM MEADOW VALLEY MINE, PIOCHE, NEVADA (USNM R6299)

d Å	I/I_1	hkl	d Å	I/I_1	hkl
5.94	30	101			
5.74	20	003			
5.09	40	012			
3.65	10	110			
3.11	60	021			
3.08	100	113			
2.97	10	202			
2.870	20	006			
2.547	30	024			
2.292	50	107			
1.978	50	033,303			
1.941	20	027			
1.913	10	009			
1.823	50	220			
SEVERAL WEAK LINES					
1.539	30	226			
1.512	30	0.2.10			
1.484	10	404			

22-827

d	3.08	3.11	5.09	5.93
I/I_1	100	75	70	45

$KFe_3(SO_4)_2(OH)_6$ ★

Potassium Iron Sulfate Hydroxide (Jarosite)

Rad. CoKα λ 1.7902 Filter Dia. Guinier
Cut off I/I_1 Photometer
Ref. Smith, Plessey Co. Ltd., Caswell, Towcaster, Northants, U.K.

Sys. Hexagonal (Rhombo.) S.G.
a_0 7.29 b_0 c_0 17.16 A C 2.35
α β γ Z Dx
Ref. Ibid.

ε α n ω β ε γ Sign
2V D mp Color
Ref.

$Fe_2(SO_4)_3+K_2SO_4+H_2SO_4$.
Heated 170°C for 24 hours in sealed tube.

d A	I/I_1	hkl	d A	I/I_1	hkl
5.93	45	101	1.717	6	312,217
5.72	25	003	1.690	2	119
5.09	70	012	1.656	2	10$\bar{1}$0
3.65	40	110	1.621	6	1$\bar{3}$4
3.55	4	104	1.595	6	128
3.11	75	021	1.572	4	401
3.08	100	113	1.560	6	315
3.02	6	015	1.552	6	042
2.965	15	202	1.536	20	226
2.861	30	006	1.507	20	02$\bar{1}$0
2.542	30	024	1.480	8	404
2.368	4	211	1.442	4	321
2.302	12	122	1.432	4	045
2.287	40	107	1.428	4	232
1.977	45	033	1.423	4	137
1.937	10	027	1.412	4	039
1.909	8	009	1.399	4	20$\bar{1}$1
1.825	45	220	1.379	4	410,324
1.776	6	208	1.338	12	413
1.738	6	223	Plus 3 lines to 1.287.		

FORM T-2

B

11-252 * β-Quartz in no samples

d	3.40	4.34	1.84	4.34
I/I_1	100	20	10	20

SiO_2 — SILICON DI OXIDE

SiO_2 — β-QUARTZ (HIGH QUARTZ)

Rad. λ Filter Dia.
Cut off I/I_1 G-C DIFFRACTOMETER
Ref. BASSETT AND LAPHAM, AM. MIN. 42 548 (1957)

Sys. HEXAGONAL S.G.
a_o 5.002 b_o c_o 5.454 A C 1.09
α β γ Z 3 Dx 2.19
Ref. IBID.

ε α n ω β ε γ Sign
2V D mp Color
Ref.

SAMPLE FROM ARKANSAS, AT 625°C.

d Å	I/I_1	hkl	d Å	I/I_1	hkl
4.34	20	100			
3.40	100	101			
2.50	2	110			
2.31	2	102			
2.17	4	200			
2.01	4	201			
1.837	10	112			
1.696	2	202			
1.673	2	103			
1.624	2	210			
1.566	4	211			
1.477	2	113			
1.433	2	300			
1.347	2	104			
1.276	2	302			
1.249	2	220			
1.216	2	213			
1.172	2	303			

288

5-0490

d	3.34	4.26	1.82	4.26
I/I_1	100	35	17	35

SiO_2

SILICON DI OXIDE — ALPHA QUARTZ

Rad. Cu λ 1.5405 Filter
Dia. Cut off Coll.
I/I_1 d corr. abs.?
Ref. SWANSON AND FUYAT, NBS CIRCULAR 539, VOL. III (1953)

Sys. HEXAGONAL S.G. $D_3^4 - C3_12$
a_o 4.913 b_o c_o 5.405 A C 1.10
α β γ Z 3
Ref. IBID.

ε α n ω β 1.544ε γ 1.553 Sign +
2V D_x 2.647 mp Color
Ref. IBID.

MINERAL FROM LAKE TOXAWAY, N.C. SPECT. ANAL.: <0.01% AL; <0.001% CA,CU,FE,MG.
X-RAY PATTERN AT 25°C.

REPLACES 1-0649, 2-0458, 2-0459, 2-0471, 3-0419, 3-0427, 3-0444

d Å	I/I_1	hkl	d Å	I/I_1	hkl
4.26	35	100	1.228	2	220
3.343	100	101	1.1997	5	213
2.458	12	110	1.1973	2	221
2.282	12	102	1.1838	4	114
2.237	6	111	1.1802	4	310
2.128	9	200	1.1530	2	311
1.980	6	201	1.1408	<1	204
1.817	17	112	1.1144	<1	303
1.801	<1	003	1.0816	4	312
1.672	7	202	1.0636	1	400
1.659	3	103	1.0477	2	105
1.608	<1	210	1.0437	2	401
1.541	15	211	1.0346	2	214
1.453	3	113	1.0149	2	223
1.418	<1	300	0.9896	2	402,115
1.382	7	212	.9872	2	313
1.375	11	203	.9781	<1	304
1.372	9	301	.9762	1	320
1.288	3	104	.9607	2	321
1.256	4	302	.9285	<1	410

G4 haematite
Operator : PRT
Client : V Hann
Date Prepared : 4/10/99
Date Acquired : 23/ 7/97
Voltage : 40 k V
Current : 20 m A
Angles : 5 to 60
Data points : 550
Sample Time : 1.00 secs/point

Element	2*Angle	Count	D-Value
137	18.700	268	4.746
159	20.900	344	4.251
177	22.700	272	3.918
192	24.200	327	3.678
217	26.700	662	3.339
220	27.000	271	3.303
239	28.900	283	3.090
242	29.200	279	3.059
282	33.200	574	2.699
299	34.900	269	2.571
307	35.700	331	2.515
310	36.000	286	2.495
345	39.500	287	2.282
356	40.600	285	2.222
359	40.900	303	2.207
376	42.600	281	2.122
379	42.900	274	2.108
397	44.700	270	2.028
446	49.600	341	1.838
451	50.100	269	1.821
491	54.100	361	1.695
499	54.900	284	1.673
522	57.200	271	1.611

2.69 α Haem 100
50 (2.51)
60 1.69

Mixture of 100 α-quartz, hematite, goethite

PMcG canvem
Operator : PRT
Client : VHann
Date Prepared : 8/9/99
Date Acquired : 20/ 7/97
Voltage : 40 k V
Current : 20 m A
Angles : 5 to 60
Data points : 550
Sample Time : 1.00 secs/point

Element	2*Angle	Count	D-Value
159	20.900	366	4.251
192	24.200	236	3.678
217	26.700	1402	3.339
282	33.200	437	2.699
307	35.700	341	2.515
316	36.600	344	2.455
375	42.500	472	2.127
445	49.500	260	1.842
447	49.700	222	1.835
451	50.100	222	1.821
491	54.100	317	1.695
499	54.900	283	1.673

1402 ≡ 100

Fitting a spectra: compare unknown count intensity to known mineral count intensities at a D-value & error ±0.0% (?) taken into account

↑ silica, goethite and hematite

Yellow – Jarosite

135m

Operator	:	PRT
Client	:	VHann
Date Prepared	:	8/9/99
Date Acquired	:	20/ 7/97
Voltage	:	40 k V
Current	:	20 m A
Angles	:	5 to 60
Data points	:	550
Sample Time	:	1.00 secs/point

Element	2*Angle	Count	D-Value
99	14.900	288	5.946
104	15.400	259	5.754
120	17.000	209	5.216
124	17.400	477	5.097
127	17.700	209	5.011
~~159~~	~~20.900~~	275	~~4.251~~
193	24.300	223	3.663
195	24.500	220	3.634
204	25.400	211	3.507
216	26.600	444	3.351
237	28.700	485	3.111
240	29.000	742	3.079
246	29.600	240	3.018
248	29.800	218	2.998
261	31.100	232	2.876
283	33.300	211	2.693
302	35.200	235	2.550
327	37.700	213	2.386
343	39.300	294	2.293
346	39.600	232	2.276
409	45.900	278	1.977
418	46.800	214	1.941
424	47.400	214	1.918
451	50.100	277	1.821
464	51.400	223	1.778
544	59.400	211	1.556

J. 5.93
Jar. 5.09
3.66

311 Jarosite
308 Jarosite – strongest peak for J
3.02 – maybe

2.69 hematite
2.547
1.978
1.823
1.776

Jarosite, 412

Peter Trail

amount, error?
10.06

$2\lambda \sin\theta \; (\pm 0.1^\circ) = D$

$2\lambda \sin 0.1 = 0.006$

J1 jarosite

Operator	:	PRT
Client	:	V Hann
Date Prepared	:	10/4/99
Date Acquired	:	23/ 7/97
Voltage	:	40 k V
Current	:	20 m A
Angles	:	5 to 60
Data points	:	550
Sample Time	:	1.00 secs/point

Element	2*Angle	Count	D-Value
100	15.000	386	5.907
105	15.500	398	5.717
112	16.200	237	5.472
125	17.500	480	5.068
151	20.100	243	4.418
159	20.900	265	4.251
194	24.400	282	3.648
196	24.600	243	3.619
217	26.700	388	3.339
220	27.000	260	3.303
230	28.000	236	3.187
234	28.400	244	3.143
238	28.800	480	3.100
240	29.000	655	3.079
252	30.200	260	2.960
257	30.700	245	2.913
263	31.300	314	2.858
303	35.300	311	2.543
344	39.400	407	2.287
409	45.900	352	1.977
414	46.400	239	1.957
450	50.000	355	1.824

"Talc silica"

Element	2*Angle	Count	D-Value
31	8.100	71	10.917
33	8.300	85	10.654
38	8.800	121	10.050
44	9.400	88	9.409
47	9.700	78	9.119
50	10.000	80	8.846
52	10.200	73	8.673
55	10.500	72	8.426
57	10.700	70	8.269
60	11.000	75	8.044
64	11.400	81	7.763
69	11.900	67	7.438
74	12.400	78	7.139
77	12.700	68	6.971
89	13.900	76	6.372
99	14.900	75	5.946
101	15.100	69	5.868
104	15.400	81	5.754
122	17.200	66	5.156
128	17.800	115	4.984
132	18.200	69	4.875
135	18.500	70	4.796
141	19.100	73	4.647
143	19.300	81	4.599
146	19.600	110	4.530
148	19.800	106	4.484
154	20.400	84	4.354
158	20.800	295	4.271
163	21.300	79	4.172
165	21.500	82	4.134
167	21.700	93	4.096
169	21.900	76	4.059
171	22.100	90	4.023
176	22.600	81	3.935
179	22.900	93	3.884
184	23.400	88	3.802
188	23.800	92	3.739
190	24.000	78	3.708
193	24.300	79	3.663
204	25.400	122	3.507
208	25.800	164	3.454
215	26.500	1081	3.364
221	27.100	72	3.291
223	27.300	72	3.267
238	28.800	78	3.100
241	29.100	77	3.069
244	29.400	70	3.038
248	29.800	150	2.998
295	34.500	80	2.600
298	34.800	92	2.578
315	36.500	96	2.462
344	39.400	118	2.287
352	40.200	91	2.243
374	42.400	91	2.132

opaline silica
Operator : PRT
Client : V Hann
Date Prepared : 14/10/99
Date Acquired : 24/ 7/97
Voltage : 40 k V
Current : 20 m A
Angles : 5 to 60
Data points : 550
Sample Time : 1.00 secs/point

50.10 = 127

αQtz . 1350's
4.26

3.34 = (100%) αSiO2.

2.998 - α.

2.282 αQtz, 12%.

Element	2*Angle	Count	D-Value
29	7.900	67	11.192
35	8.500	67	10.404
37	8.700	80	10.165
40	9.000	88	9.827
42	9.200	75	9.614
44	9.400	67	9.409
46	9.600	73	9.214
48	9.800	79	9.026
51	10.100	67	8.759
60	11.000	64	8.044
62	11.200	70	7.901
64	11.400	65	7.763
67	11.700	64	7.564
70	12.000	71	7.376
78	12.800	62	6.917
81	13.100	70	6.759
83	13.300	65	6.658
90	14.000	64	6.326
97	14.700	62	6.027
119	16.900	67	5.247
123	17.300	77	5.126
130	18.000	94	4.929
132	18.200	69	4.875
138	18.800	66	4.721
148	19.800	112	4.484
152	20.200	90	4.397
155	20.500	77	4.333
160	21.000	280	4.231
162	21.200	94	4.191
168	21.800	80	4.077
172	22.200	79	4.005
174	22.400	81	3.969
176	22.600	72	3.935
178	22.800	78	3.901
180	23.000	80	3.867
183	23.300	76	3.818
185	23.500	66	3.786
187	23.700	79	3.755
191	24.100	72	3.693
193	24.300	78	3.663
200	25.000	73	3.562
204	25.400	104	3.507
206	25.600	102	3.480
209	25.900	86	3.440
217	26.700	1126	3.339
225	27.500	73	3.244
230	28.000	68	3.187
232	28.200	64	3.165
240	29.000	77	3.079
243	29.300	76	3.048
250	30.000	136	2.979
285	33.500	148	2.675
297	34.700	73	2.585
300	35.000	85	2.564
			2.498

RVD005 130m
Operator : PRT
Client : VHann
Date Prepared : 8/9/99
Date Acquired : 20/ 7/97
Voltage : 40 k V
Current : 20 m A
Angles : 5 to 60
Data points : 550
Sample Time : 1.00 secs/point

4.26 - silica

3.66 hematite 25%

αQtz 3.34 100%

2.69 hematite

Silica

175m jarosite	
Operator	: PRT
Client	: V Hann
Date Prepared	: 4/10/99
Date Acquired	: 23/ 7/97
Voltage	: 40 k V
Current	: 20 m A
Angles	: 5 to 60
Data points	: 550
Sample Time	: 1.00 secs/point

Element	2*Angle	Count	D-Value
99	14.900	179	5.946
105	15.500	205	5.717
124	17.400	190	5.097
129	17.900	214	4.956
155	20.500	184	4.333
159	20.900	376	4.251
163	21.300	361	4.172
179	22.900	182	3.884
199	24.900	210	3.576
210	26.000	219	3.427
214	26.400	189	3.376
217	26.700	644	3.339
238	28.800	248	3.100
241	29.100	248	3.069
246	29.600	179	3.018
248	29.800	227	2.998
260	31.000	180	2.885
262	31.200	179	2.867
279	32.900	183	2.723
283	33.300	243	2.691
299	34.900	180	2.571
312	36.200	181	2.482
317	36.700	238	2.449
343	39.300	204	2.293
345	39.500	200	2.282
364	41.400	181	2.181
377	42.700	204	2.118
410	46.000	178	1.973
452	50.200	236	1.818
484	53.400	192	1.716

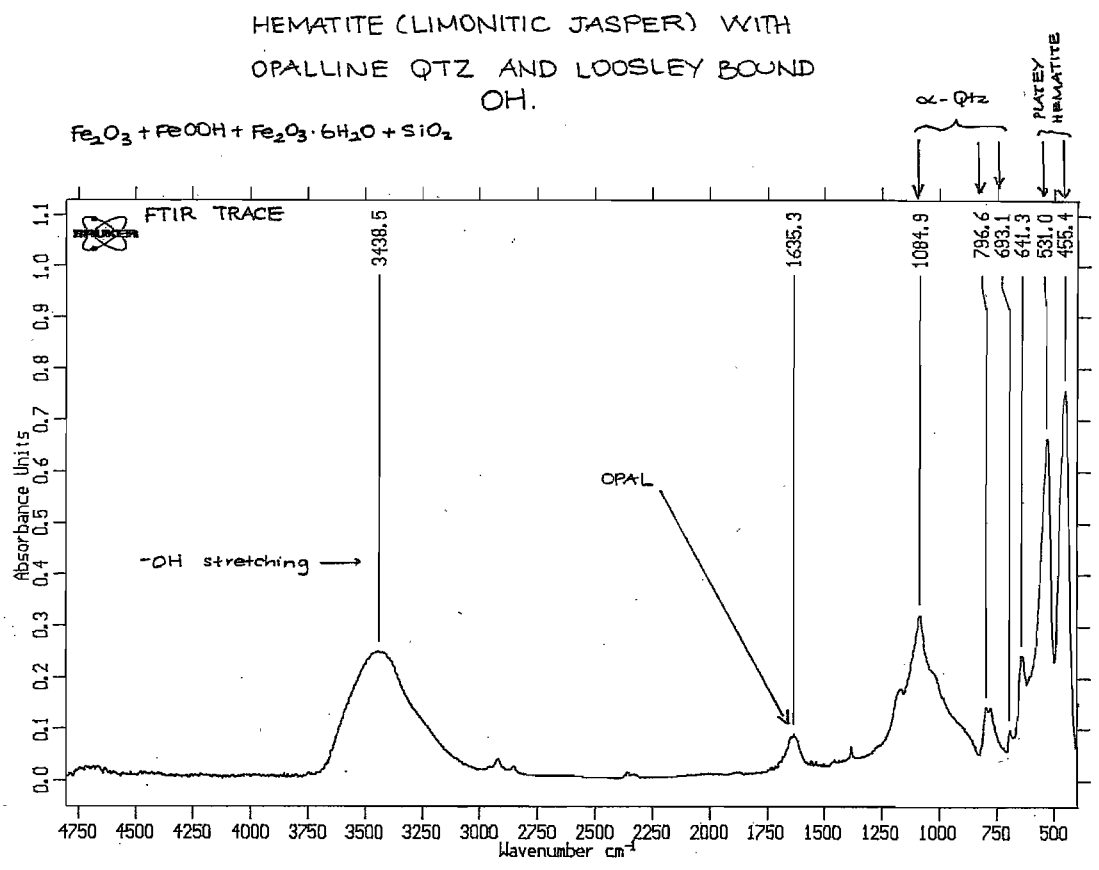

NG003

Specimen G4

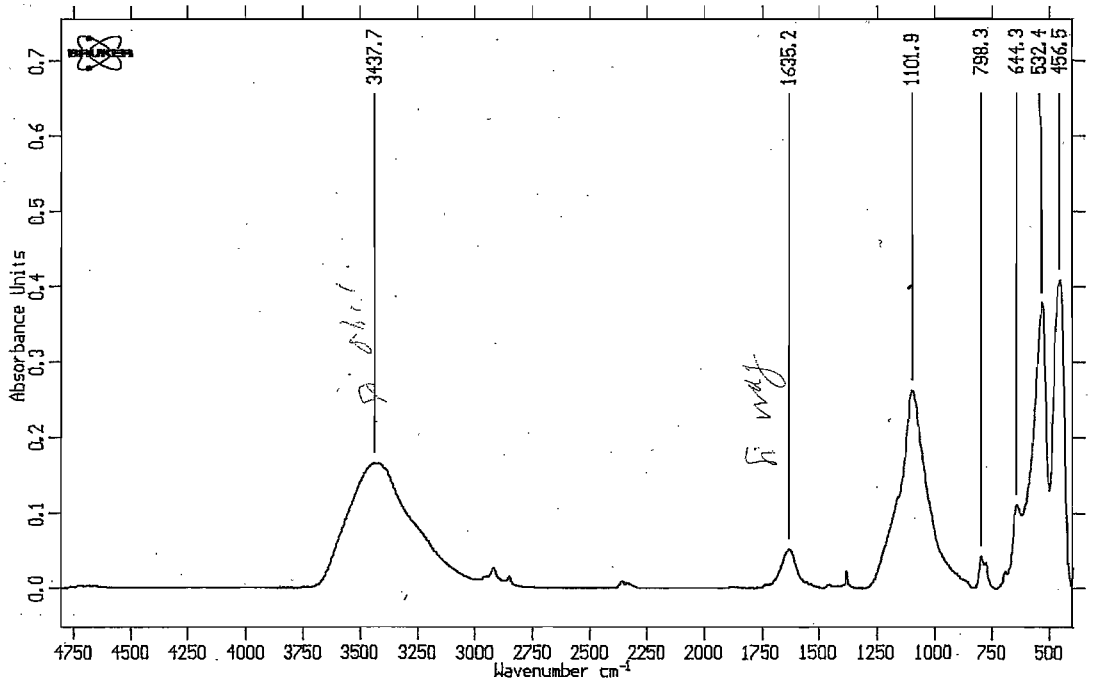

Specimen NG003

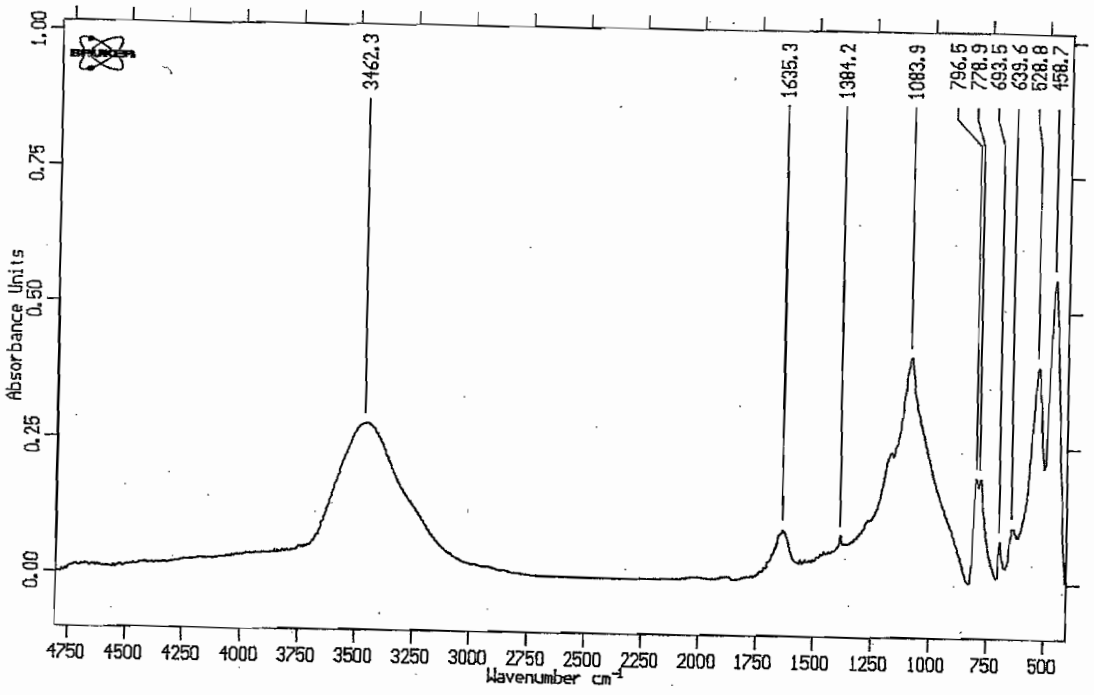

Specimen G2

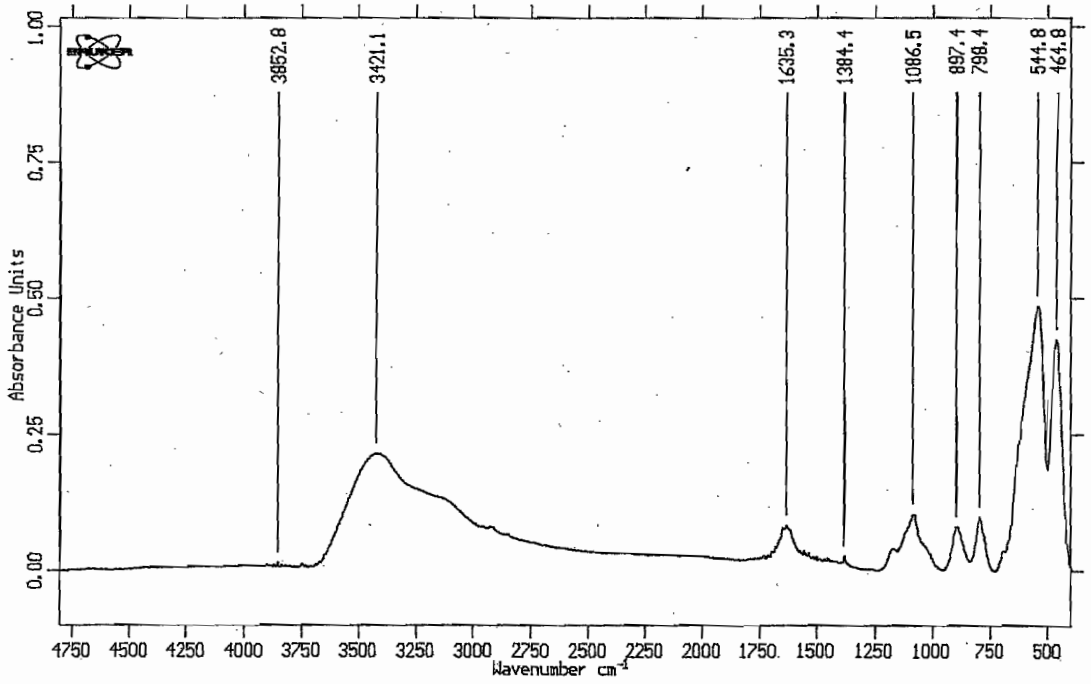

Specimen G3

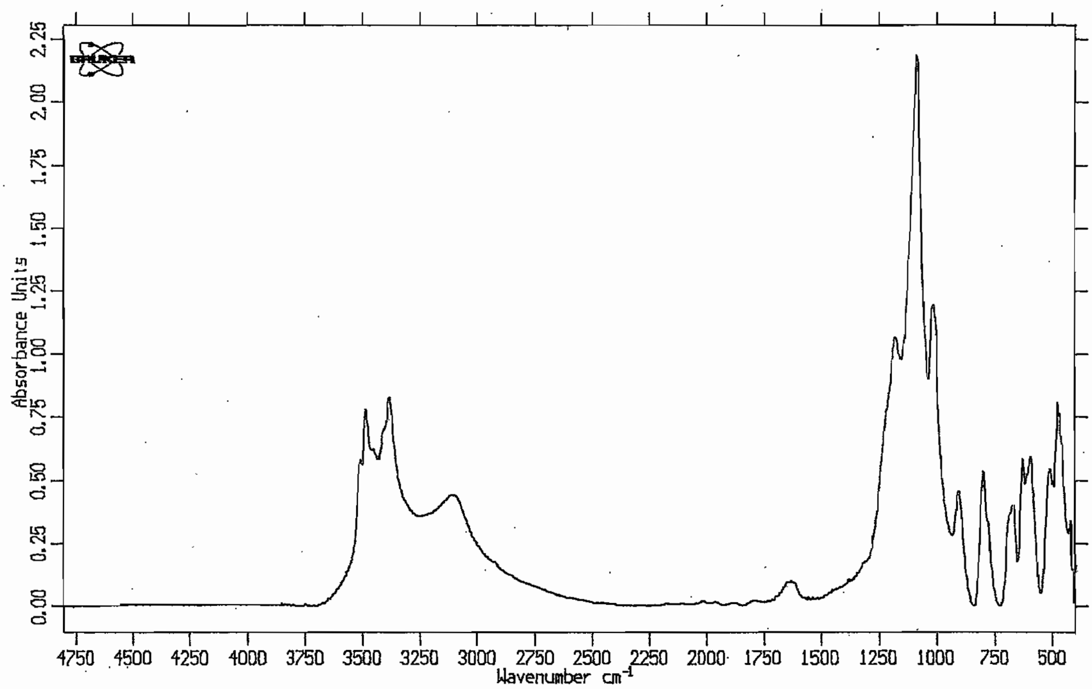

RVD00 **Specimen 175m**

yellow laminated,
soft (H<2)

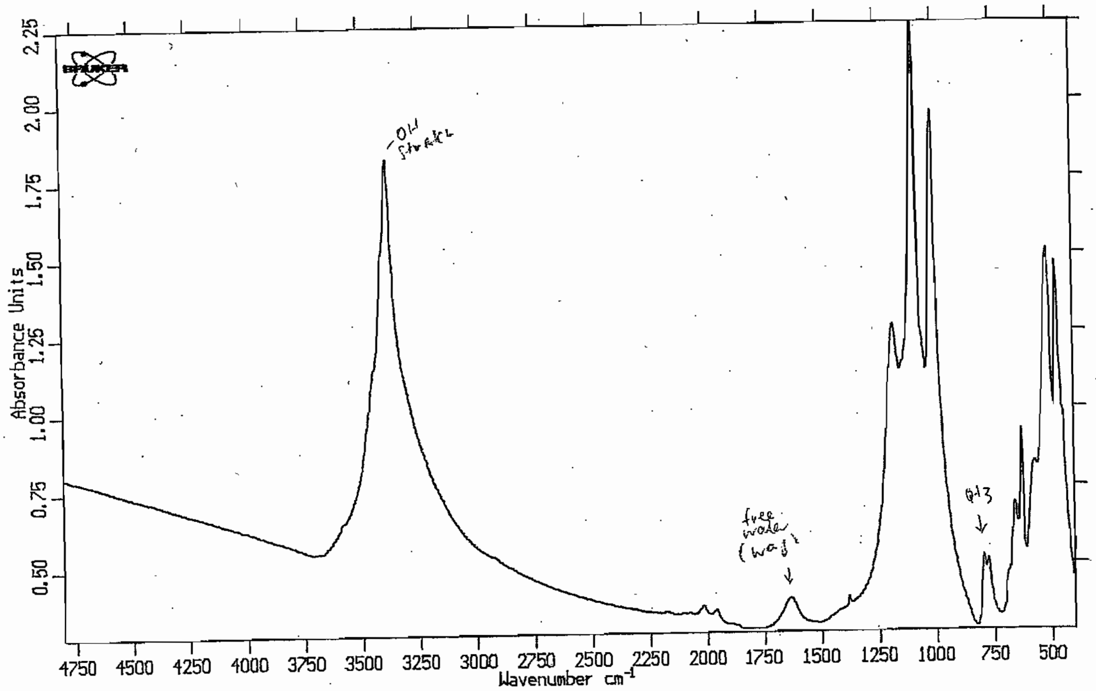

Specimen 135m

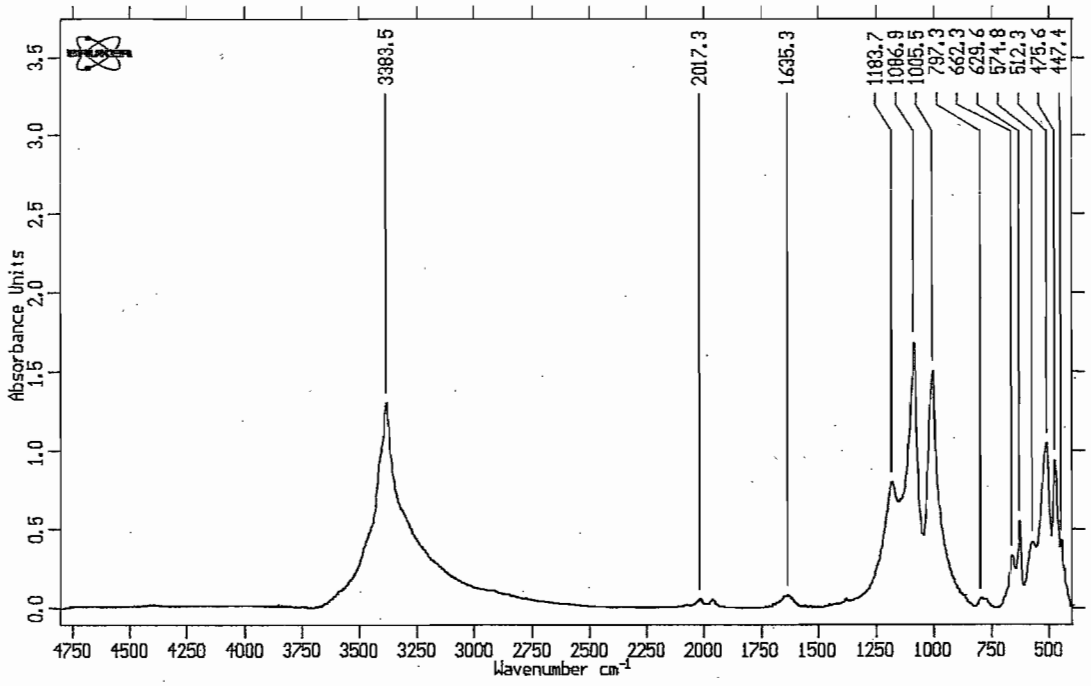
3383.5
2017.3
1635.3
1183.7
1086.9
1005.5
797.3
662.3
629.6
574.8
512.3
475.6
447.4
Absorbance Units
Wavenumber cm-1

Specimen J1

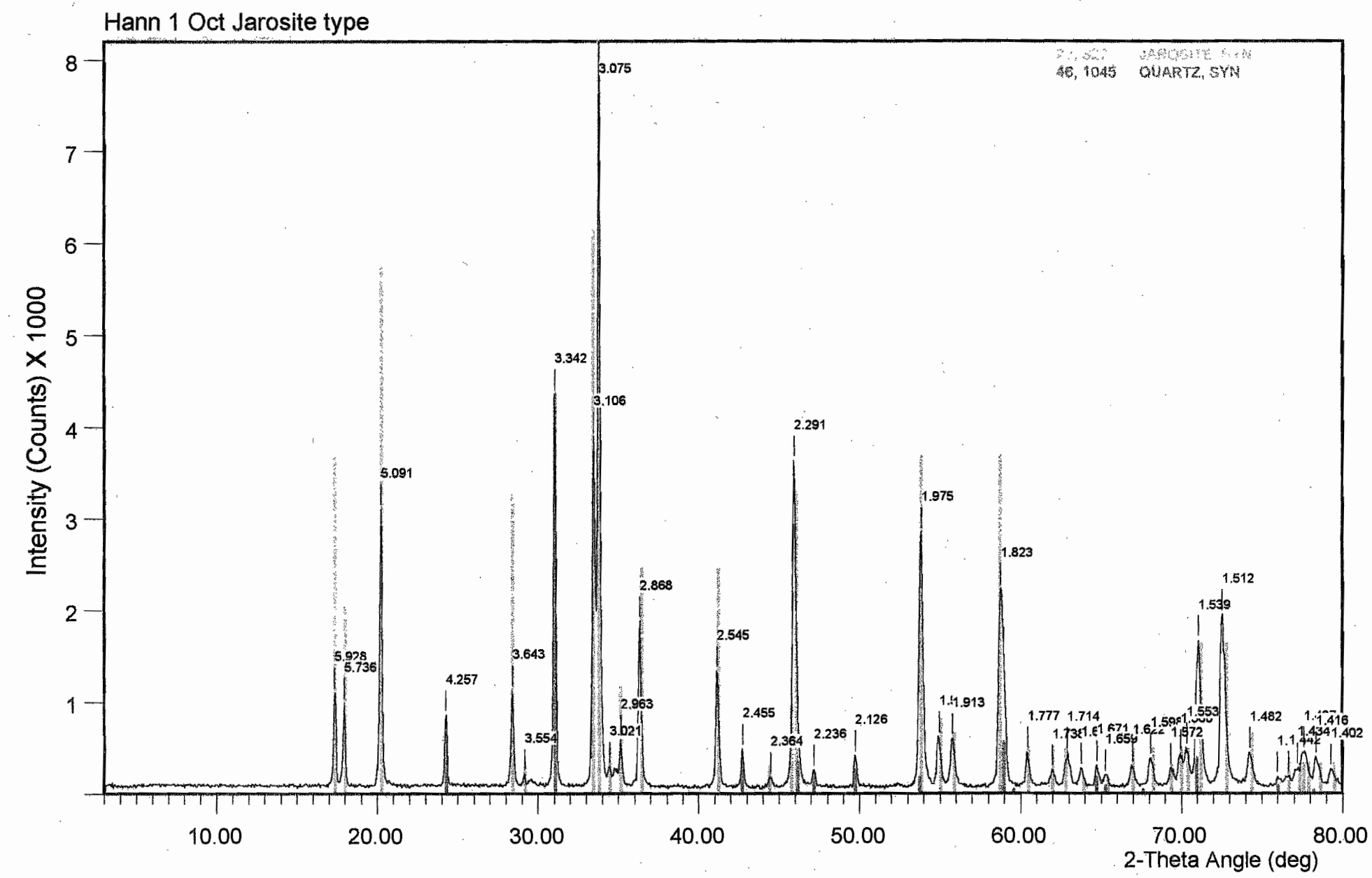

File Name: c:\...\gates\jarosblk.201

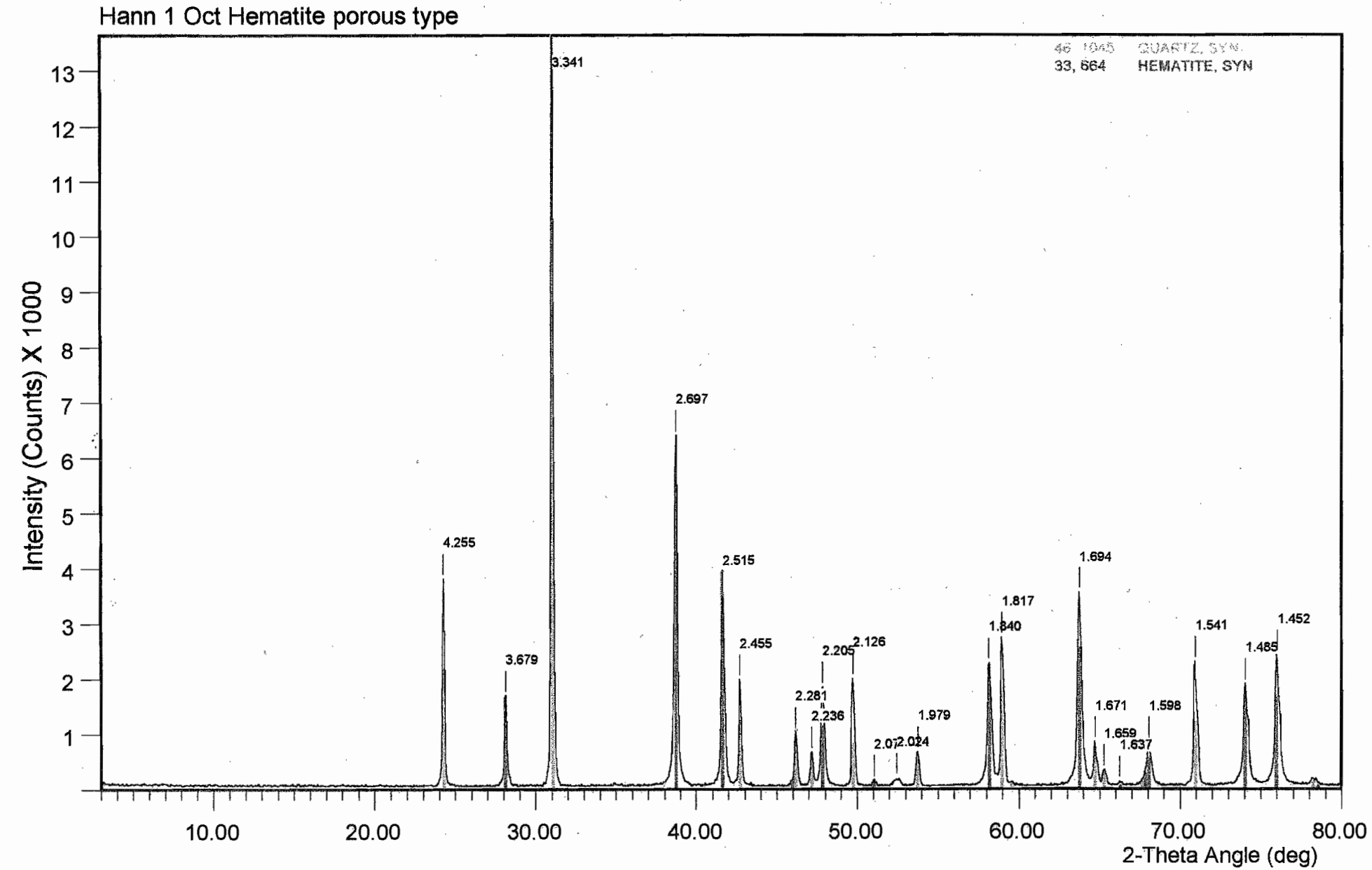

File Name: c:\...\gates\hematblk.202

Appendix 6

PIMA and FTIR Traces Geochemical Techniques for Gossan Analysis

Camorphous SiO2

File: opal.1
Background: ABG.6

FTIR Trace of Opal

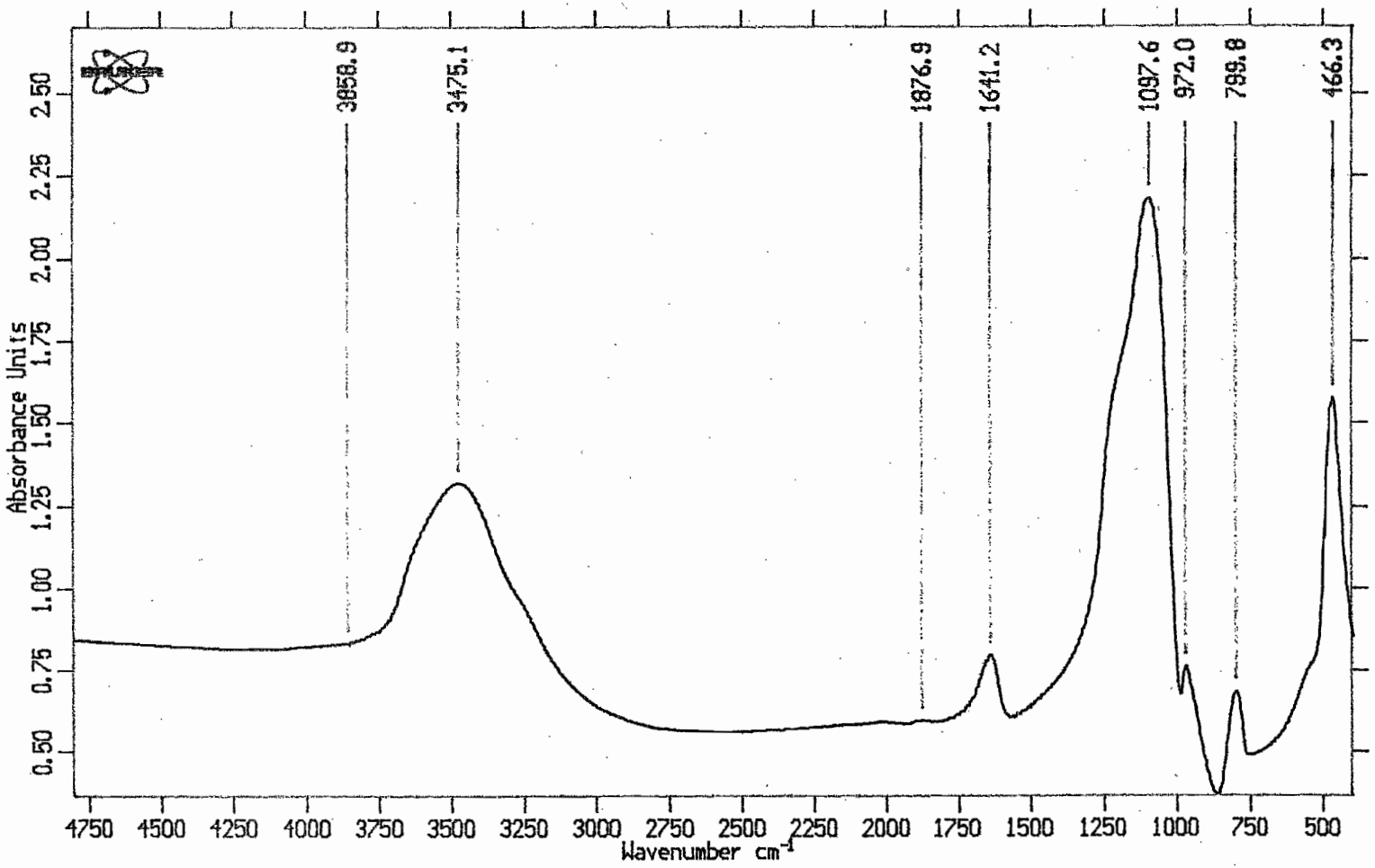

FTIR Trace of Quartz

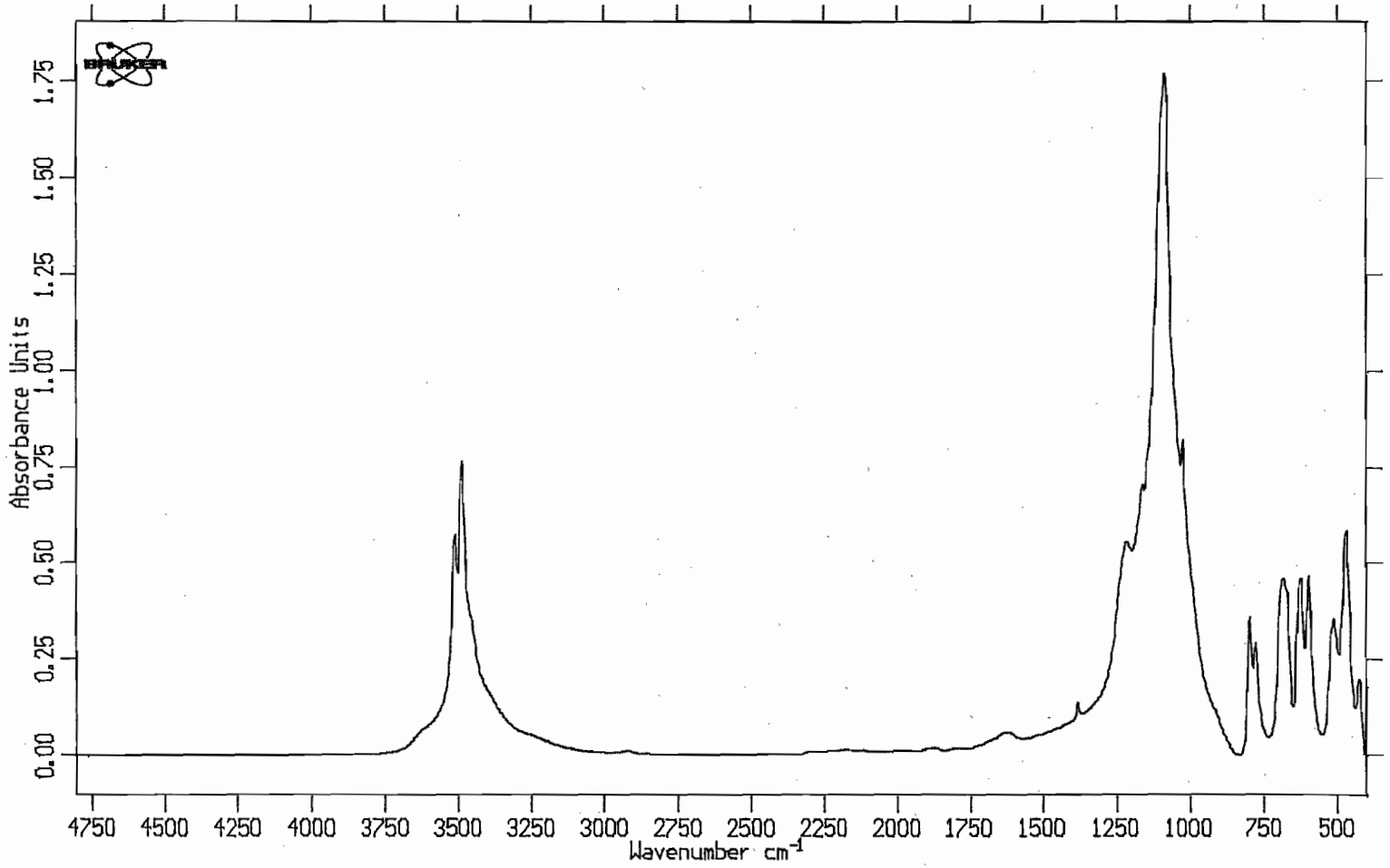

FTIR Trace of Sample 005.110 (leached and bleached shale)

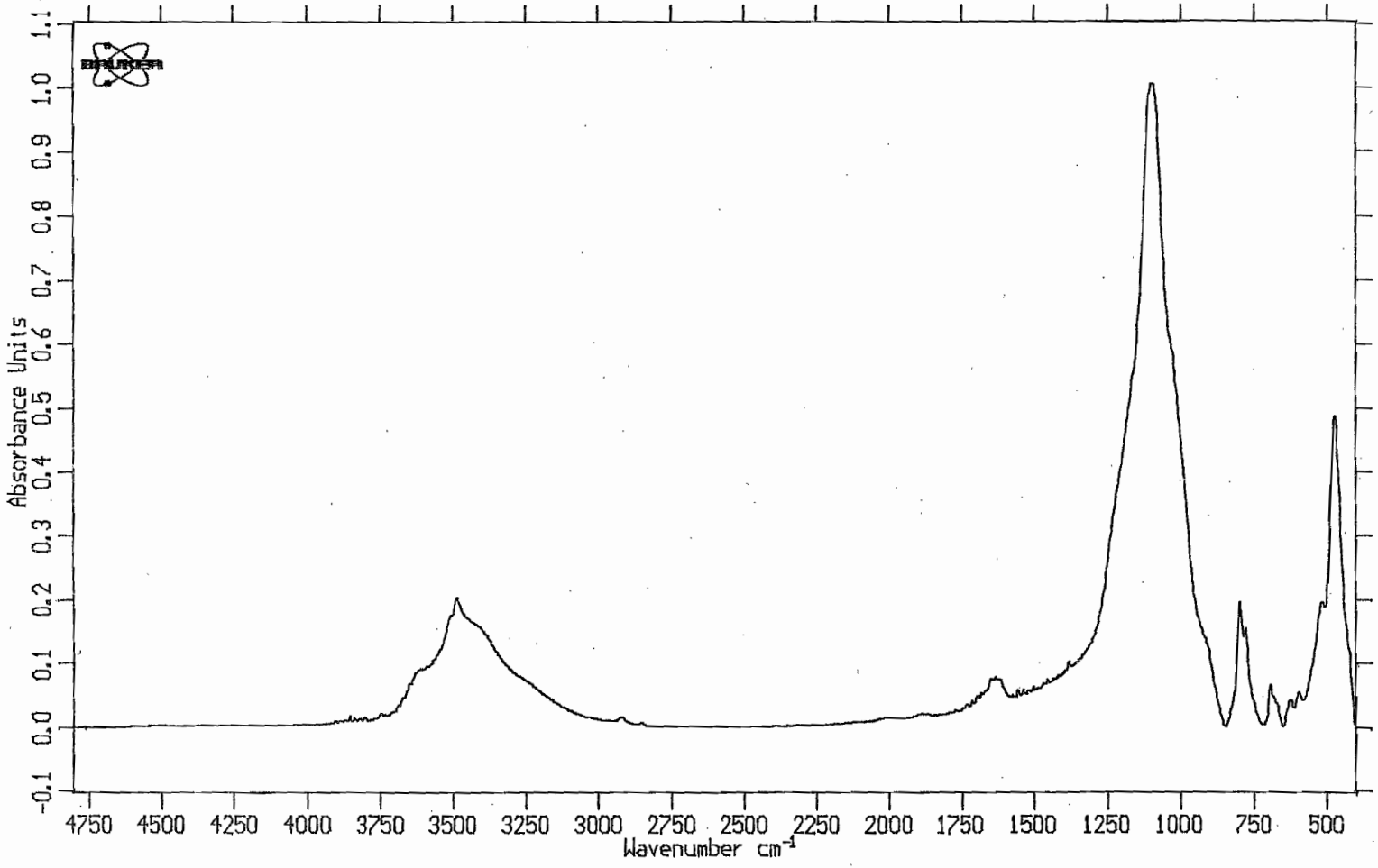

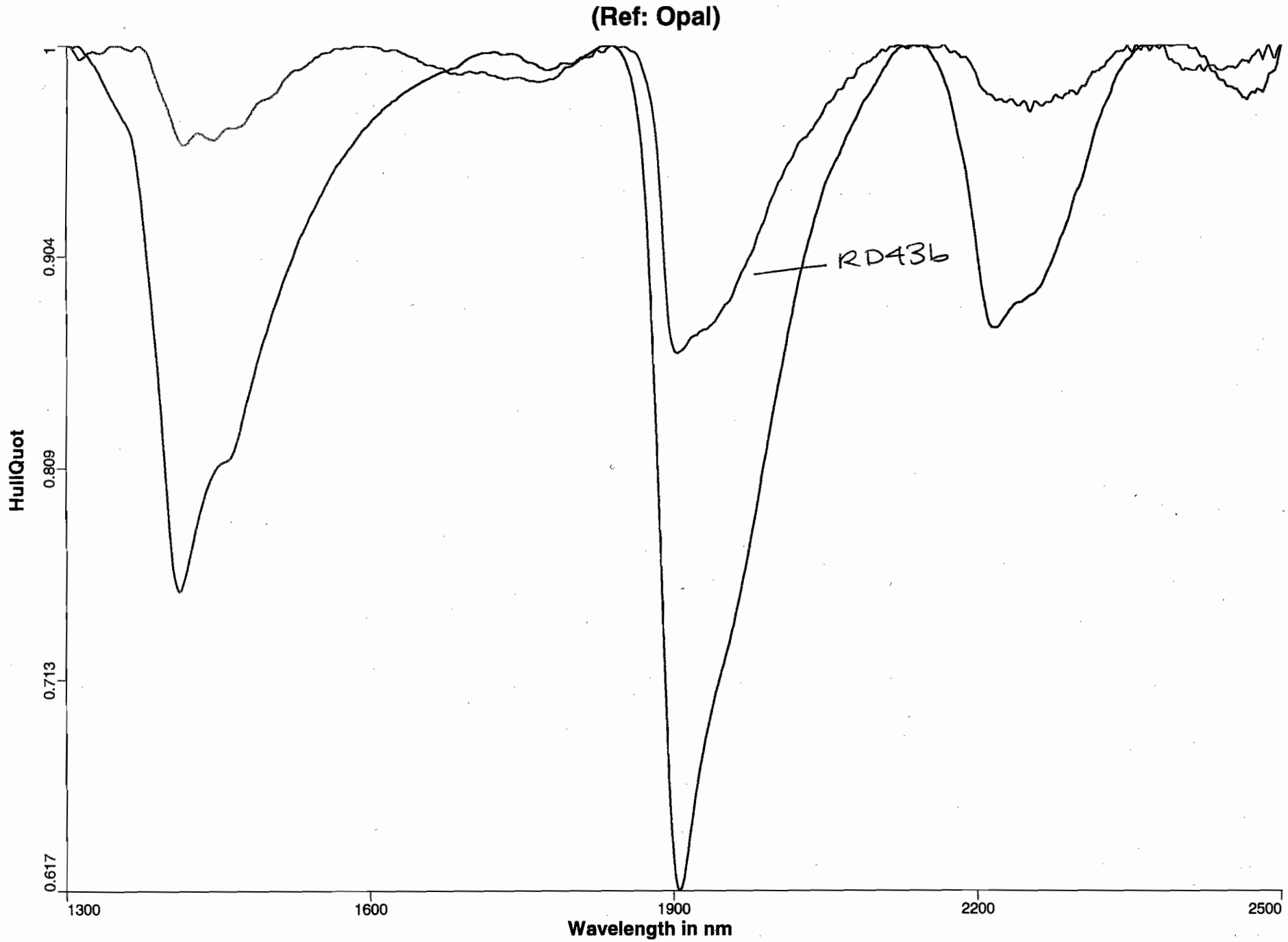
(Ref: Opal)
RD436
HullQuot
1
0.904
0.809
0.713
0.617
1300
1600
1900
2200
2500
Wavelength in nm

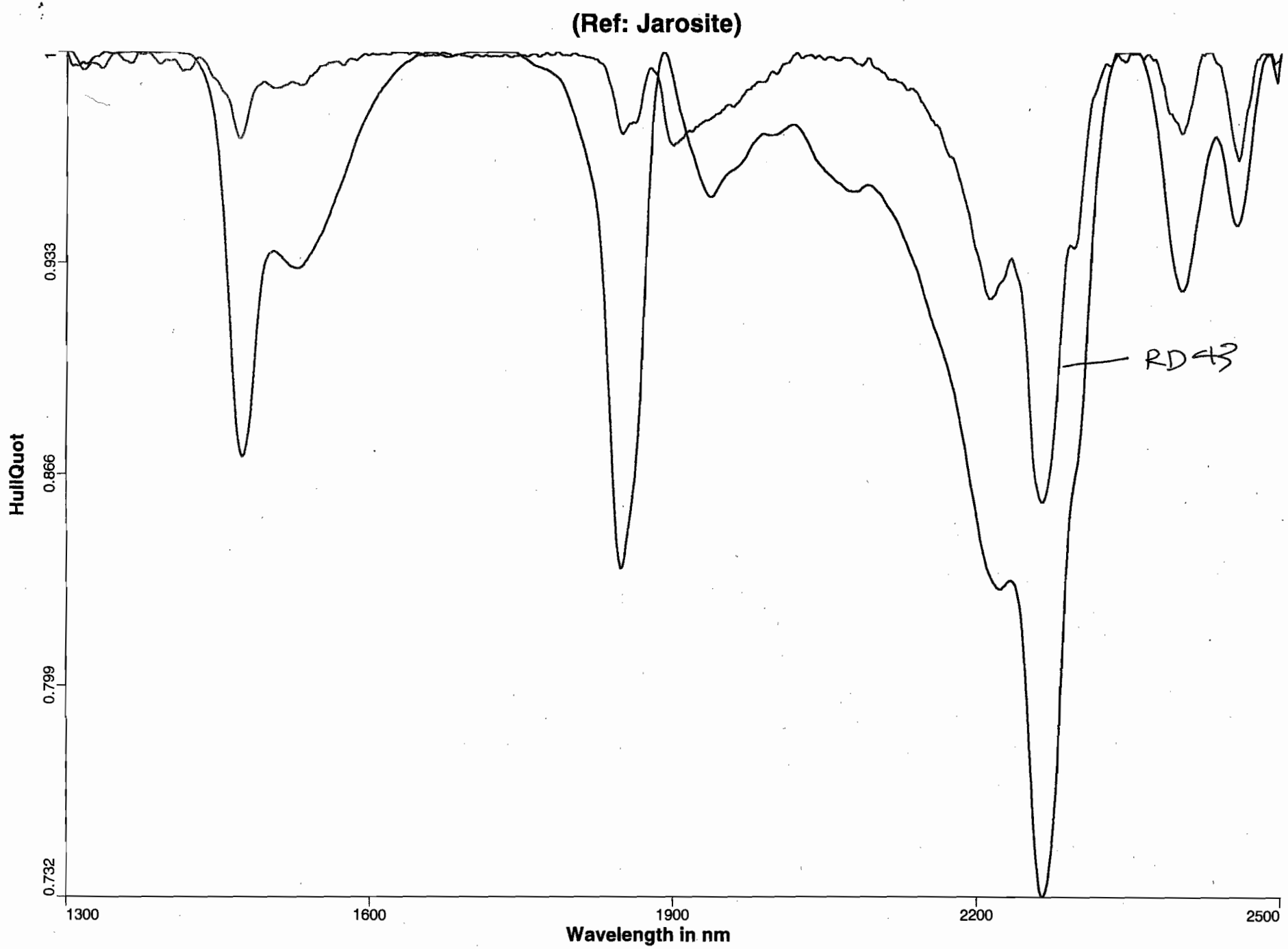
(Ref: Jarosite)
HullQuot
1
0.933
0.866
0.799
0.732
1300
1600
1900
2200
2500
Wavelength in nm
RD43

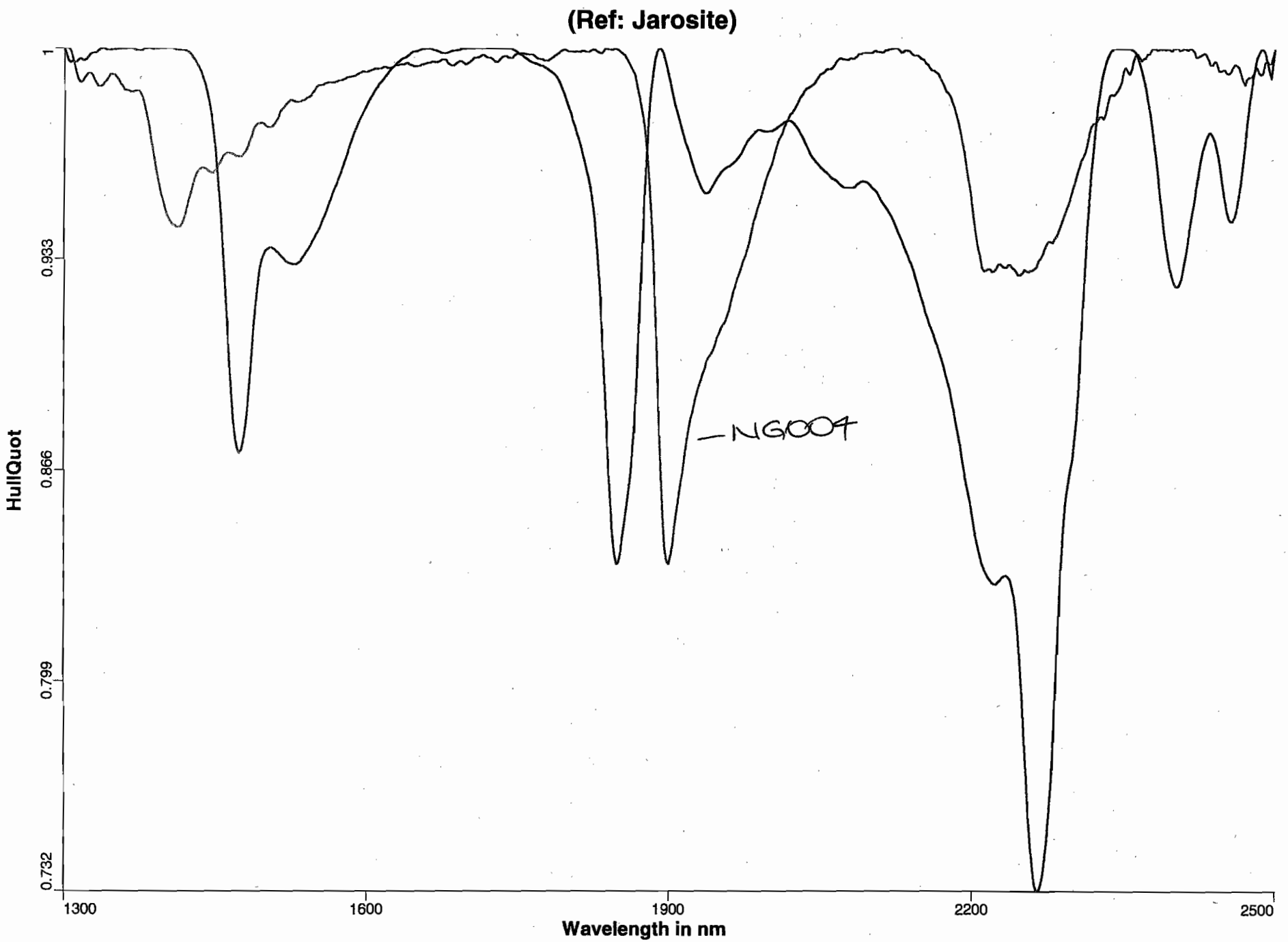
(Ref: Jarosite)
HullQuot
1
0.933
0.866
0.799
0.732
1300
1600
1900
2200
2500
Wavelength in nm
-NG004

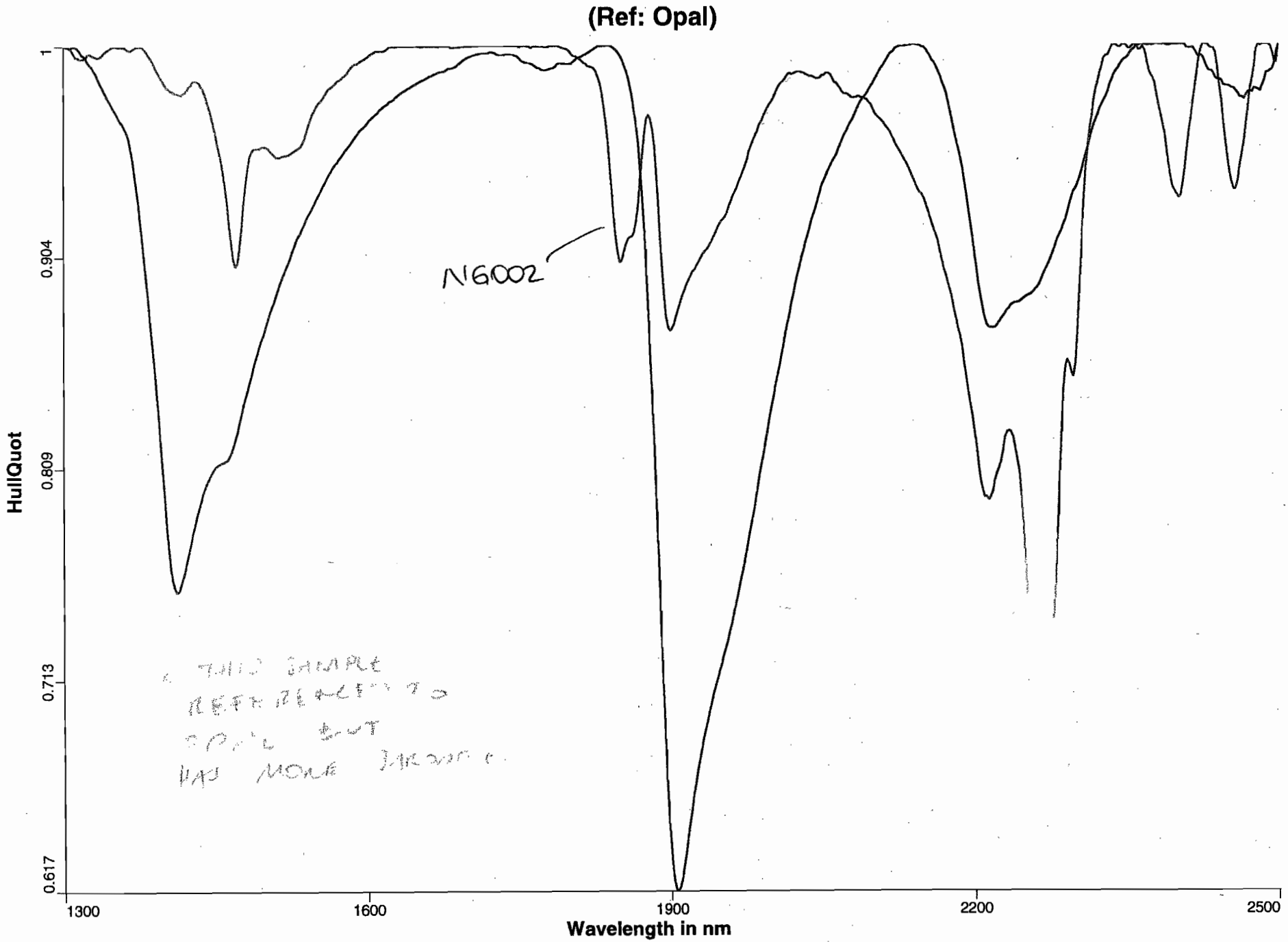
(Ref: Opal)
HullQuot
1
0.904
0.809
0.713
0.617
1300
1600
1900
2200
2500
Wavelength in nm
N6002

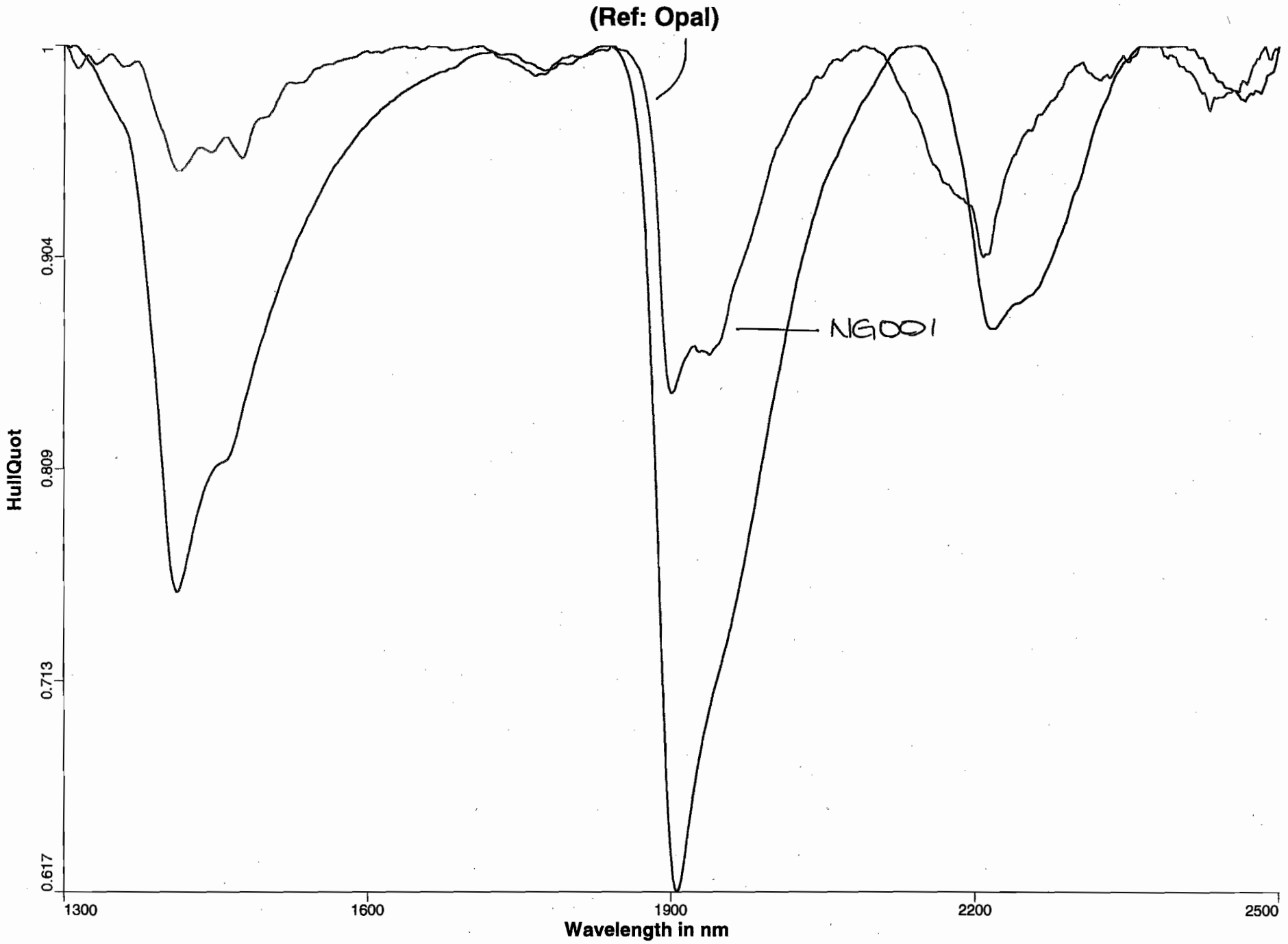
(Ref: Opal)
NG001
HullQuot
1
0.904
0.809
0.713
0.617
1300
1600
1900
2200
2500
Wavelength in nm

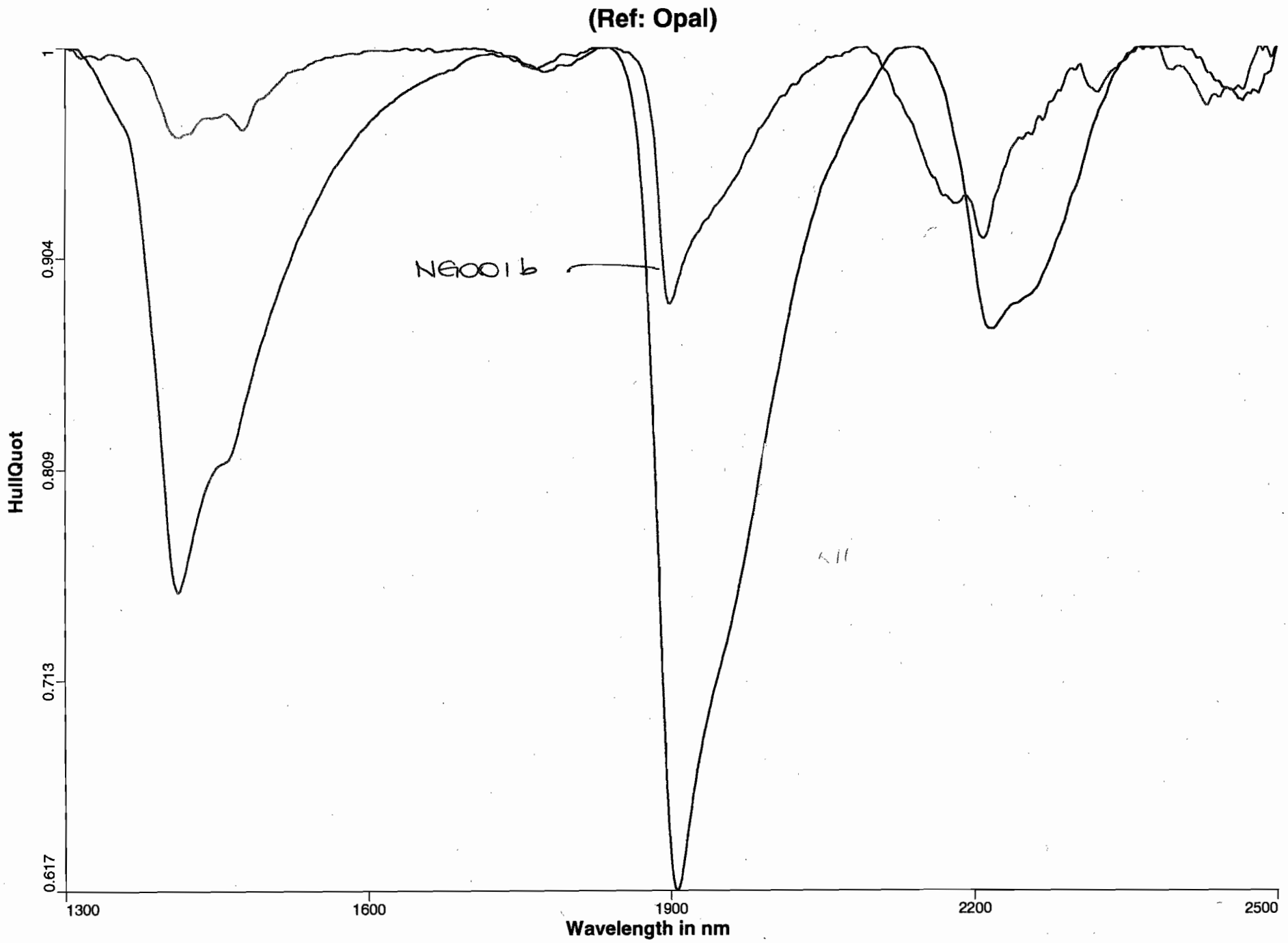
(Ref: Opal)
NE0016
HullQuot
1
0.904
0.809
0.713
0.617
1300
1600
1900
2200
2500
Wavelength in nm

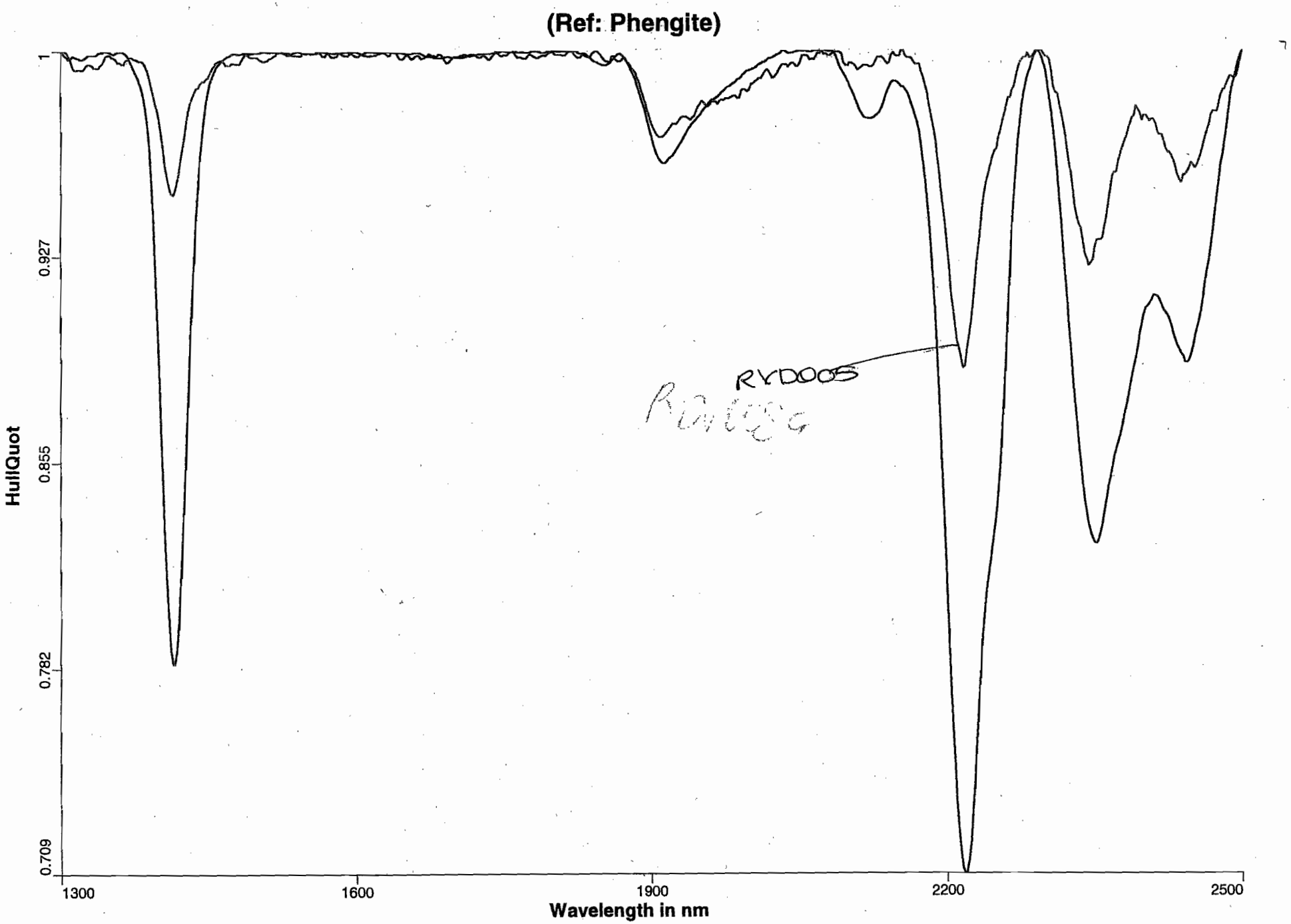
(Ref: Phengite)
HullQuot
1
0.927
0.855
0.782
0.709
1300
1600
1900
2200
2500
Wavelength in nm
RYD005
Ryd05

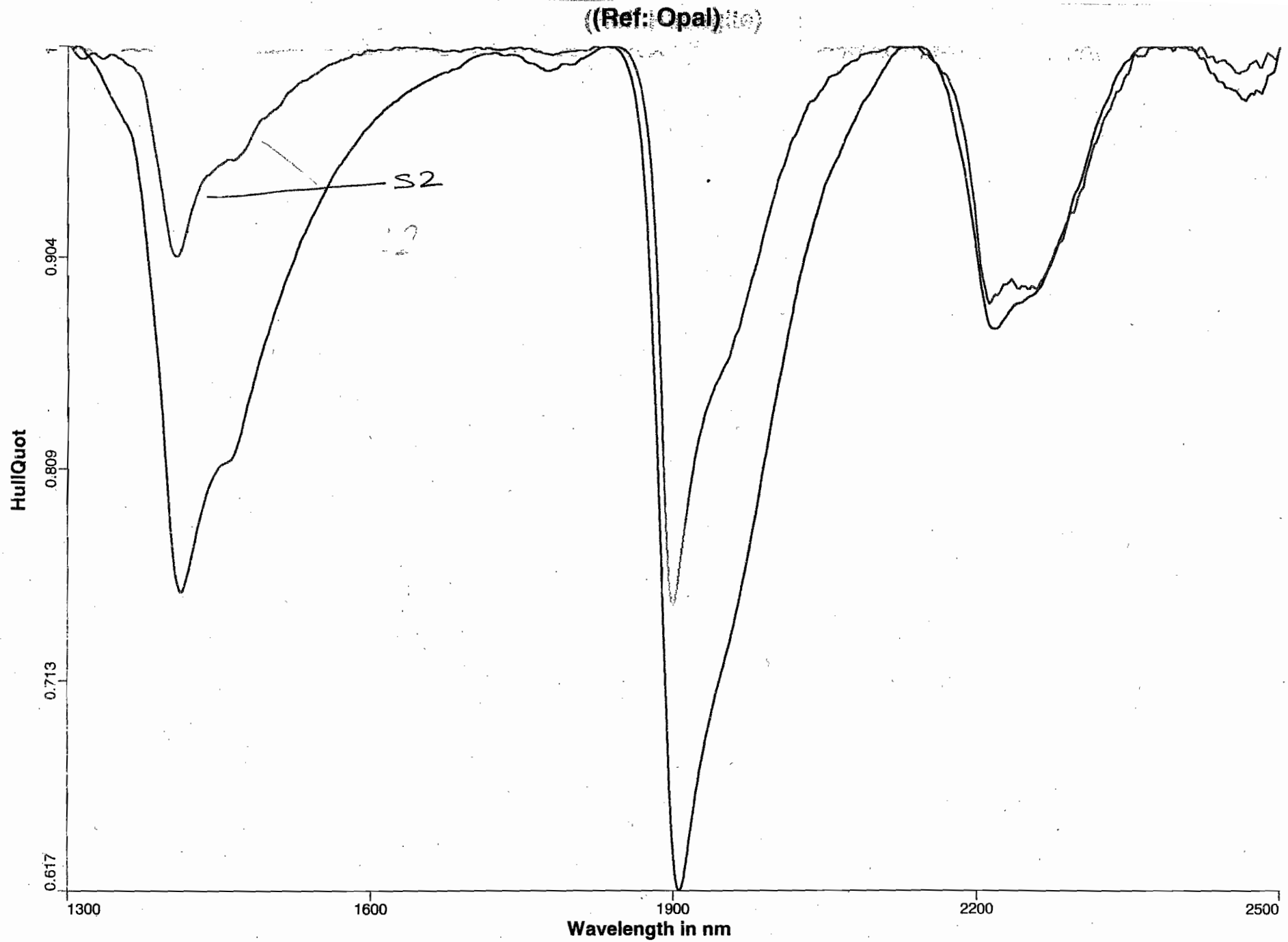
(Ref: Opal)
S2
HullQuot
1
0.904
0.809
0.713
0.617
1300
1600
1900
2200
2500
Wavelength in nm

Geochemical Analysis for Gossan Material

The Applicability and Limitations of ESEM, FTIR, XRD, ICP-MS techniques for Gossan Analysis.

Various methods were tailor-made to suit and get the most out of gossan analysis. As would be expected for complex gossanous material it is preferable to use more than one suitable method to yield the most useful information. All techniques have their advantages and limitations, and these are outlined.

Basis for Choice of Methods

The available techniques which are most useful for gossan analysis, and have been commonly used in the past are X-ray diffraction for mineralogy, XRF for major elements, optical mineralogy AAS, ICP-MS or ICP-OES, and the Electron Microprobe.

XRD

XRD is of particular use for mineralogy when the grain size is small (Taylor, 1973), and optical microscopy becomes superseded by ESEM, so that small grain size is no longer a hindrance. . XRD is a mineralogical technique, which can ' unambiguousl identify every mineral phase'.

The ESEM

The ESEM-EDS combines textural information from scanned electron imaging with a semi-quantitative spectra of elements and abundances present using an X-Ray detector simultaneously with the ESEM. The peaks of elements are proportional when the peaks are close together but comparing ends of the spectrum will be not proportional because the scale is not linear, the efficiency of the signal is not constant but has a weaker signal at low energies.

The technique is limited from directly distinguishing goethite from hematite because hydrogen is too light to be detected , however because the ratio of Fe to O is greater in hematite to goethite it is indicated by the ratios, and that Al is preferentiall incorporated into goethite rather than hematite.

ESEM-EDS gives more qualitative chemistry than the Electron Microprobe, however the ESEM can pin-point smaller areas than the probe and subtle differences in zoning

and structure can be seen which cannot be seen by the probe. The Laser Ablation technique creates 'craters' 5um across, which is as fine as the resolution allows, whereas the ESEM clearly detects subtle zoning in pyrite less than 0.5um. Certainly, as far as texture and geochemistry of mineral grains less than 5um the ESEM can distinguish and analyse reliably as compared to Laser Ablation and the Electron Microprobe.

PIMA

The PIMA is a relatively new device which has been in use widely in exploration in the last few years. The PIMA identifies unknown mineralogy of samples in the field in under a minute. It contains a library of over 2000 minerals, and will estimate a level of probability to determining a sample correctly by comparing the spectra of the unknown to the reference spectra. The infra-red spectral range used is truncated and it will not apply to dark rocks or rocks containing water. Since gossans are characterised by dark iron oxy-hydroxides, it is not applicable to these. The PIMA is worth trying on light coloured minerals.

FTIR

FTIR is a technique commonly used in the life sciences. It covers a greater spectral range than the PIMA and can deal adequately with dark coloured rocks with free water. The FTIR is not used often for mineral samples as is evidenced by the limited mineral samples used as standards. This technique is suited to targeting anions in a sample, because the FTIR detects the lighter elements. Anions such as carbonates , sulphates which commonly occur as products of weathering in gossans can be easil detected, and the amount of free water compared to hydroxide in a sample is determined which is important in determining mineralogy and level of dehydration in a sample.

A technique which has not been applied to gossan studies widely is Mossbauer Spectroscopy. The beauty of this non-destructive technique is the ability to determine the different oxy-hydroxides of iron, goethite from hematite. It is a technique which is used in chemistry and has application in the earth sciences.

Different elements had to be treated differently, in particular there is a substantial amount of barite in the area and XRF is suited to analysing it, which was applied as the 'normal' ICP-MS digestions do not fully dissolve barium.

Appendix 7

Rock Catalogue

Rock catalogue

*All rocks are the weathered surface expression of the lead-zinc-silver sulfide Grevillea Deposit.
**See comments field for full rock description when above 55 characters.

Catalog#	Field#	Rock Name	Rock description	Metamorphism	Associated with	AMG Northing	AMG Easting	Full Map Title	Map Scale
	(25 characters)	(25 characters)	(55 characters)	(20 characters)	(30 characters)	(16 characters)	(18 characters)	(75 characters)	(10 characters)
142956	G2	hem+goeth goss	Hem+ goeth+ barite, botryoidal gossanous product	sub-greenschist	host horizon	7889400N	268800E	in house North Ltd	1:1000
142957	RD43	shale	Leached dolomitic shale, voids from pyrite	sub-greenschist	host horizon	7889400N	268800E	in house North Ltd	1:1000
142958	S1	leached siltstone	Barren siltstone -plastic-type folding	sub-greenschist	host horizon	7889400N	268800E	in house North Ltd	1:1000
142959	SG1	Silicified siltston	Silicified carbonaceous siltstone, microfaulting	sub-greenschist	host horizon	7889400N	268800E	in house North Ltd	1:1000
142960	SG002	Silicified siltston	Silicified barren siltstone, hematitic, ductile folding	sub-greenschist	host horizon	7889400N	268800E	in house North Ltd	1:1000
142961	G5	Barite vien + her	Barite vein (+specularite) cutting lamninated hem	sub-greenschist	host horizon	7889400N	268800E	in house North Ltd	1:1000
142962	RD30	Sandwich of hea	Hematitic layers with jarositic siltstone layer	sub-greenschist	host horizon	7889400N	268800E	in house North Ltd	1:1000
142963	503	shale from MSZ	goethitic + jarositic leached shale	sub-greenschist	host horizon	7889400N	268800E	in house North Ltd	1:1000
142964	135m	shale from MSZ	jarositic laminated shale	sub-greenschist	host horizon	7889400N	268800E	in house North Ltd	1:1000
142965	NG001	leached shale fr	purple/white bands,leached shale (see comments)	sub-greenschist	host horizon	7889400N	268800E	in house North Ltd	1:1000
142966	O405	shale	white silicified shale with conchoidal fracture	sub-greenschist	host horizon	7889400N	268800E	in house North Ltd	1:1000
142967	OO5110m	shale	leached powdery shale, see comments	sub-greenschist	host horizon	7889400N	268800E	in house North Ltd	1:1000
142968	F1	shale	pale silicified shale, thinly laminated, cut with quartz	sub-greenschist	host horizon	7889400N	268800E	in house North Ltd	1:1000
142969	175m	shale	brown, yellow, white jarositic/hematitic powdery	sub-greenschist	host horizon	7889400N	268800E	in house North Ltd	1:1000
142970	RD46	shale/vein conta	specular hematite and textures on barite veinlet	sub-greenschist	host horizon	7889400N	268800E	in house North Ltd	1:1000
142971	G3	gossanous siltst	hematitic gossanous product with boxworks	sub-greenschist	host horizon	7889400N	268800E	in house North Ltd	1:1000
142972	NG003	laminated hem s	lam. Hematitic gossanous product	sub-greenschist	host horizon	7889400N	268800E	in house North Ltd	1:1000
142973	506	silickensides	fg hematitic siltstone, friction polished surface	sub-greenschist	host horizon	7889400N	268800E	in house North Ltd	1:1000
142974	RVD005 108.5m	shale with hem	leached dolomitic shale, Xcutting hematitic fractures	sub-greenschist	host horizon	7889400N	268800E	in house North Ltd	1:1000
142975	J2	jarosite/hematite	jarositic layer with underlying hematitic band	sub-greenschist	host horizon	7889400N	268800E	in house North Ltd	1:1000
142976	K1	clay and white m	brecciated white clay in maroon clay.	sub-greenschist	host horizon	7889400N	268800E	in house North Ltd	1:1000
142977	OO5110	leached shale fr	leached crumbly shale with fine hematitic lams	sub-greenschist	host horizon	7889400N	268800E	in house North Ltd	1:1000
142978	J1	brecciated arger	brecciated argentojarositefrom mid gossan fault zone	sub-greenschist	host horizon	7889400N	268800E	in house North Ltd	1:1000
142979	130	white shale	leached and bleached white shale	sub-greenschist	host horizon	7889400N	268800E	in house North Ltd	1:1000
142980	G4	gossanous siltst	Siliceous hematitic siltstone with jarositic 'pods'	sub-greenschist	host horizon	7889400N	268800E	in house North Ltd	1:1000
142981	Thinsection 129.8	Ba+ py breccia	barite and remobilised pyrite	sub-greenschist	host horizon	7889400N	268800E	in house North Ltd	1:1000
142982	Thinsection 129.8	Ba+ py breccia	barite and remobilised pyrite	sub-greenschist	host horizon	7889400N	268800E	in house North Ltd	1:1000
142983	Thinsection 144.8	Laminated gn, p	Thinly lam K-feldspar, with galena and pyrite	sub-greenschist	ore zone	7889400N	268800E	in house North Ltd	1:1000
142984	Thinsection 154.3	Laminated gn, p	Thinly lam K-feldspar, with remob galena and pyrite	sub-greenschist	ore zone	7889400N	268800E	in house North Ltd	1:1000
142985	insection 270 BM	Laminated gn, p	Thinly lam K-feldspar, with galena and pyrite	sub-greenschist	ore zone	7889400N	268800E	in house North Ltd	1:1000
142986	Thinsection 175.5	laminated/remob	remobilised pyrite and barite	sub-greenschist	ore zone	7889400N	268800E	in house North Ltd	1:1000
142987	Thinsection 175.5	laminated/remob	remobilised pyrite and barite	sub-greenschist	ore zone	7889400N	268800E	in house North Ltd	1:1000
142988	Thinsection 175.5	laminated feldsp	Laminated siliceous jarositic feld and pyrite	sub-greenschist	ore zone	7889400N	268800E	in house North Ltd	1:1000
142989	Thinsection 211	remob py	Remobilised textures of fg pyrite and barite	sub-greenschist	ore zone	7889400N	268800E	in house North Ltd	1:1000

Map comments (unlimited)	Mine Northing (8 characters)	Mine Easting (8 characters)	DDH (25 characters)	Depth (m) 10 characters	Relative Level 10 characters	Azimuth 10 characters	Inclination 10 characters	Position 35 characters	Area 25 characters	State (20 characters)	Country (15 characters)	Biostratigraphy (30 characters)
									Riversleigh	Queensland	Australia	
									Riversleigh	Queensland	Australia	
									Riversleigh	Queensland	Australia	
									Riversleigh	Queensland	Australia	
									Riversleigh	Queensland	Australia	
									Riversleigh	Queensland	Australia	
									Riversleigh	Queensland	Australia	
									Riversleigh	Queensland	Australia	
									Riversleigh	Queensland	Australia	
									Riversleigh	Queensland	Australia	
									Riversleigh	Queensland	Australia	
									Riversleigh	Queensland	Australia	
									Riversleigh	Queensland	Australia	
									Riversleigh	Queensland	Australia	
									Riversleigh	Queensland	Australia	
									Riversleigh	Queensland	Australia	
									Riversleigh	Queensland	Australia	
									Riversleigh	Queensland	Australia	
									Riversleigh	Queensland	Australia	
									Riversleigh	Queensland	Australia	
									Riversleigh	Queensland	Australia	
									Riversleigh	Queensland	Australia	
									Riversleigh	Queensland	Australia	
									Riversleigh	Queensland	Australia	
									Riversleigh	Queensland	Australia	
									Riversleigh	Queensland	Australia	
									Riversleigh	Queensland	Australia	
									Riversleigh	Queensland	Australia	
									Riversleigh	Queensland	Australia	
									Riversleigh	Queensland	Australia	
									Riversleigh	Queensland	Australia	
									Riversleigh	Queensland	Australia	
									Riversleigh	Queensland	Australia	
									Riversleigh	Queensland	Australia	

Stage (25 characters)	Series (25 characters)	System (25 characters)	Era (20 characters)	Eon (20 characters)	Lithostratigraphy (50 characters)	Supergroup (40 characters)	Group (35 characters)	Subgroup (25 characters)	Formation (30 characters)	Member (25 characters)	Depositional environment (30 characters)	Basin (50 characters)
Statherian			Paleoproterozoic		Pmr3, Riversleigh Siltstone	Lawn Hill Platfor	McNamara	Riverlseigh Siltstone		Pmr3	deep marine	Mount Isa Inlier, L
Statherian			Paleoproterozoic		Pmr3, Riversleigh Siltstone	Lawn Hill Platfor	McNamara	Riverlseigh Siltstone		Pmr3	deep marine	Mount Isa Inlier, L
Statherian			Paleoproterozoic		Pmr3, Riversleigh Siltstone	Lawn Hill Platfor	McNamara	Riverlseigh Siltstone		Pmr3	deep marine	Mount Isa Inlier, L
Statherian			Paleoproterozoic		Pmr3, Riversleigh Siltstone	Lawn Hill Platfor	McNamara	Riverlseigh Siltstone		Pmr3	deep marine	Mount Isa Inlier, L
Statherian			Paleoproterozoic		Pmr3, Riversleigh Siltstone	Lawn Hill Platfor	McNamara	Riverlseigh Siltstone		Pmr3	deep marine	Mount Isa Inlier, L
Statherian			Paleoproterozoic		Pmr3, Riversleigh Siltstone	Lawn Hill Platfor	McNamara	Riverlseigh Siltstone		Pmr3	deep marine	Mount Isa Inlier, L
Statherian			Paleoproterozoic		Pmr3, Riversleigh Siltstone	Lawn Hill Platfor	McNamara	Riverlseigh Siltstone		Pmr3	deep marine	Mount Isa Inlier, L
Statherian			Paleoproterozoic		Pmr3, Riversleigh Siltstone	Lawn Hill Platfor	McNamara	Riverlseigh Siltstone		Pmr3	deep marine	Mount Isa Inlier, L
Statherian			Paleoproterozoic		Pmr3, Riversleigh Siltstone	Lawn Hill Platfor	McNamara	Riverlseigh Siltstone		Pmr3	deep marine	Mount Isa Inlier, L
Statherian			Paleoproterozoic		Pmr3, Riversleigh Siltstone	Lawn Hill Platfor	McNamara	Riverlseigh Siltstone		Pmr3	deep marine	Mount Isa Inlier, L
Statherian			Paleoproterozoic		Pmr3, Riversleigh Siltstone	Lawn Hill Platfor	McNamara	Riverlseigh Siltstone		Pmr3	deep marine	Mount Isa Inlier, L
Statherian			Paleoproterozoic		Pmr3, Riversleigh Siltstone	Lawn Hill Platfor	McNamara	Riverlseigh Siltstone		Pmr3	deep marine	Mount Isa Inlier, L
Statherian			Paleoproterozoic		Pmr3, Riversleigh Siltstone	Lawn Hill Platfor	McNamara	Riverlseigh Siltstone		Pmr3	deep marine	Mount Isa Inlier, L
Statherian			Paleoproterozoic		Pmr3, Riversleigh Siltstone	Lawn Hill Platfor	McNamara	Riverlseigh Siltstone		Pmr3	deep marine	Mount Isa Inlier, L
Statherian			Paleoproterozoic		Pmr3, Riversleigh Siltstone	Lawn Hill Platfor	McNamara	Riverlseigh Siltstone		Pmr3	deep marine	Mount Isa Inlier, L
Statherian			Paleoproterozoic		Pmr3, Riversleigh Siltstone	Lawn Hill Platfor	McNamara	Riverlseigh Siltstone		Pmr3	deep marine	Mount Isa Inlier, L
Statherian			Paleoproterozoic		Pmr3, Riversleigh Siltstone	Lawn Hill Platfor	McNamara	Riverlseigh Siltstone		Pmr3	deep marine	Mount Isa Inlier, L
Statherian			Paleoproterozoic		Pmr3, Riversleigh Siltstone	Lawn Hill Platfor	McNamara	Riverlseigh Siltstone		Pmr3	deep marine	Mount Isa Inlier, L
Statherian			Paleoproterozoic		Pmr3, Riversleigh Siltstone	Lawn Hill Platfor	McNamara	Riverlseigh Siltstone		Pmr3	deep marine	Mount Isa Inlier, L
Statherian			Paleoproterozoic		Pmr3, Riversleigh Siltstone	Lawn Hill Platfor	McNamara	Riverlseigh Siltstone		Pmr3	deep marine	Mount Isa Inlier, L
Statherian			Paleoproterozoic		Pmr3, Riversleigh Siltstone	Lawn Hill Platfor	McNamara	Riverlseigh Siltstone		Pmr3	deep marine	Mount Isa Inlier, L
Statherian			Paleoproterozoic		Pmr3, Riversleigh Siltstone	Lawn Hill Platfor	McNamara	Riverlseigh Siltstone		Pmr3	deep marine	Mount Isa Inlier, L
Statherian			Paleoproterozoic		Pmr3, Riversleigh Siltstone	Lawn Hill Platfor	McNamara	Riverlseigh Siltstone		Pmr3	deep marine	Mount Isa Inlier, L
Statherian			Paleoproterozoic		Pmr3, Riversleigh Siltstone	Lawn Hill Platfor	McNamara	Riverlseigh Siltstone		Pmr3	deep marine	Mount Isa Inlier, L
Statherian			Paleoproterozoic		Pmr3, Riversleigh Siltstone	Lawn Hill Platfor	McNamara	Riverlseigh Siltstone		Pmr3	deep marine	Mount Isa Inlier, L
Statherian			Paleoproterozoic		Pmr3, Riversleigh Siltstone	Lawn Hill Platfor	McNamara	Riverlseigh Siltstone		Pmr3	deep marine	Mount Isa Inlier, L
Statherian			Paleoproterozoic		Pmr3, Riversleigh Siltstone	Lawn Hill Platfor	McNamara	Riverlseigh Siltstone		Pmr3	deep marine	Mount Isa Inlier, L
Statherian			Paleoproterozoic		Pmr3, Riversleigh Siltstone	Lawn Hill Platfor	McNamara	Riverlseigh Siltstone		Pmr3	deep marine	Mount Isa Inlier, L
Statherian			Paleoproterozoic		Pmr3, Riversleigh Siltstone	Lawn Hill Platfor	McNamara	Riverlseigh Siltstone		Pmr3	deep marine	Mount Isa Inlier, L
Statherian			Paleoproterozoic		Pmr3, Riversleigh Siltstone	Lawn Hill Platfor	McNamara	Riverlseigh Siltstone		Pmr3	deep marine	Mount Isa Inlier, L
Statherian			Paleoproterozoic		Pmr3, Riversleigh Siltstone	Lawn Hill Platfor	McNamara	Riverlseigh Siltstone		Pmr3	deep marine	Mount Isa Inlier, L
Statherian			Paleoproterozoic		Pmr3, Riversleigh Siltstone	Lawn Hill Platfor	McNamara	Riverlseigh Siltstone		Pmr3	deep marine	Mount Isa Inlier, L
Statherian			Paleoproterozoic		Pmr3, Riversleigh Siltstone	Lawn Hill Platfor	McNamara	Riverlseigh Siltstone		Pmr3	deep marine	Mount Isa Inlier, L
Statherian			Paleoproterozoic		Pmr3, Riversleigh Siltstone	Lawn Hill Platfor	McNamara	Riverlseigh Siltstone		Pmr3	deep marine	Mount Isa Inlier, L

NB: See also entries at end of catalogue (below)

Preps	Comments	Authors	Year Published	Title	Degree	Journal	Volume	Part	Pages	Editor	publisher, place	confidential unitl	book title
(25 characters)	(unlimited length)	(75 characters)	(4 characters)	(200 chara	(30 charac	(100 chara	(10 charac	(10 charac	(10 charac	(15 charac	75 characters	15 characters	unlimited
XRD, XRF, ICP-OES, ESEM, FTIR, Thin sect		V. Hann		The geochemistry and textures of the Grevillea Gossan					89				
PIMA													
nil													
ESEM, thin section													
nil													
ESEM, thin section													
ESEM, thin section													
nil													
XRD, XRF, ICP-OES, ESEM, FTIR, Thin sect													
ESEM, thin section	alternating purple/white bands,leached and bleached shale with minor microscopic platey hematite in purple bands												
PIMA													
nil	leached white powdery shale, some laminations with hematite staining												
nil													
XRD, XRF, ICP-OES, FTIR													
nil													
XRD, XRF, ICP-OES, FTIR, thin section, ESEM													
XRD, XRF, ICP-OES, FTIR.													
nil													
nil													
Thin Section, ESEM, PIMA													
Thin Section, ESEM, PIMA	PIMA suggets Opalline silica and phengite in white blebs.												
PIMA													
ICP-OES, XRD, XRF, FTIR													
XRD, FTIR, PIMA													
XRF, XRD, FTIR, ICP-OES, Thinsection, ESEM													
Thin Section, ESEM													
Thin Section, ESEM													
Thin Section, ESEM													
Thin Section, ESEM													
Thin Section, ESEM													
Thin Section, ESEM													
Thin Section, ESEM													
Thin Section, ESEM													
Thin Section													

SECTION PARALLEL TO GRID NORTHING. ROCK-CHIP GEOCHEMISTRY FOR 15200N, DRILL-HOLE CHEMISTRY 15185N, GRAB SAMPLES ON 15186N.